



University
of Glasgow

Naseer, Asif (2015) *Gammaretrovirus replication in human cells: implications for experimental xenografts and risk of zoonosis*. PhD thesis.

<http://theses.gla.ac.uk/6279/>

Copyright and moral rights for this thesis are retained by the author

A copy can be downloaded for personal non-commercial research or study, without prior permission or charge

This thesis cannot be reproduced or quoted extensively from without first obtaining permission in writing from the Author

The content must not be changed in any way or sold commercially in any format or medium without the formal permission of the Author

When referring to this work, full bibliographic details including the author, title, awarding institution and date of the thesis must be given

Gammaretrovirus replication in human cells: Implications for experimental xenografts and risk of zoonosis

Submitted to the University of Glasgow
In fulfilment of the requirements of the degree of
PhD

November 2014

Dr. Asif Naseer, M.B.B.S., PgDip Evidence Based Medicine & HPE.

Molecular Oncology Lab
Centre for Virus Research
Institute of Infection, Immunity and Inflammation
College of Medical, Veterinary and Life Sciences

Acknowledgement

Thank You God for being so merciful and giving me the strength and inspiration required.

I would like to thank my supervisors Ewan Cameron and James Neil for giving me the opportunity to undertake this project and for providing me their continuous unlimited support, encouragement, guidance and advice throughout the whole time. I really feel words cannot do justice in expressing my sincere gratitude. I am really grateful to my laboratory supervisor Anne Terry, for her continued assistance and encouragement whenever I needed. By working in the Molecular Oncology Lab, I really feel I had the best colleagues one can ever have. Anna Kilbey was always there to provide all sorts of academic and moral support through all the tough times of PhD. Nancy Mackay was always ready to provide guidance in the lab, and assistance in molecular biology procedures. I would like to thank Margaret Bell for her help in collecting samples, Alma for all sorts of assistance and Kathryn for helping me to interpret the expression analysis experiments. I would also like to thank Gillian Borland for her help in flow cytometry and for all the cakes that always kept me energized while working late hours. I really feel I was really very lucky to find such a friendly place to work. I would also like to thank Karen Blyth and Susan Mason (Beatson) for their regular help in xenograft experiments and Pamela Kearns (University of Birmingham) for kindly providing me precious primary samples and Sam Wilson for his advice in different experiments.

I am grateful to the Khyber Medical University for funding my PhD program and Prof Hafiz Ullah for his support and interest in my project.

Finally I will like to thank all my friends; Jaffer, Hamid, Inayat, Asif, Yassar, Ahsen, Shahzad, Zia and especially Dr Omar Malik for their moral and spiritual support. Last but not least I will like to thank my family (both in Glasgow and back home in Peshawar) for their patience and support, especially my father Naseer Ahmad and my mother Khalida Khanum who always believed in me and have always encourage me to work hard and my aunt Jameela and uncle Haroon Khan for their support when I needed it the most.

Author's declaration

I declare that this thesis is the result of my own work unless otherwise stated. This dissertation has not been submitted for any other degree at the University of Glasgow or any other institute. Part of this thesis has been submitted for publication in the journal 'Viruses'.

Table of contents

Acknowledgement	2
Author's declaration	3
Table of contents.....	4
List of tables	8
List of figures	9
List of techniques I used in this study	11
Abbreviations	13
Abstract	16
1 Introduction.....	18
1.1 Retroviruses	18
1.1.1 Structure and classification of retroviruses	18
1.1.2 Replication cycle of retroviruses.....	20
1.1.3 Exogenous and endogenous retroviruses.....	22
1.2 Host resistance.....	25
1.2.1 The innate and adaptive immune systems	25
1.2.2 The intrinsic immune system	26
1.3 Gammaretroviruses as potential zoonotic agents.....	31
1.3.1 Human fossil viruses	31
1.3.2 Koala retrovirus: A recent example of trans-species infection.....	32
1.3.3 Porcine endogenous retroviruses: A potential zoonotic agent	32
1.3.4 Potentially widespread human exposure to feline leukaemia virus	33
1.3.5 XMRV controversy and its aftermath: XMLV found in human xenografts.....	34
1.4 Xenografting and cancer research	35
1.4.1 Infection of xenografts	35
1.4.2 Retroviral insertional mutagenesis	36
1.5 Aims of the study	38
1.5.1 To conduct a prospective study of the risks of acquiring XMLV infection in human cancer xenografts.	38
1.5.2 To investigate the susceptibility of human cells to FeLV and XMLV <i>in vitro</i> . 38	
1.5.3 To investigate the mechanisms of resistance of human cells to FeLV and XMLV.	39
1.5.4 To examine the significance of XMLV infection for human xenograft behaviour.....	39
2 Materials and methods	40
2.1 Materials	40

2.1.1	Cell culture.....	40
2.1.2	Chemically competent bacteria.....	44
2.1.3	Commercial kits.....	44
2.1.4	Buffers, solutions and reagents.....	45
2.1.5	Enzymes.....	46
2.1.6	Antibiotics.....	47
2.1.7	Antibodies.....	47
2.2	Methods.....	47
2.2.1	Infecting cells with virus.....	47
2.2.2	Confirmation of virus infection.....	49
2.2.3	Virus titration.....	49
2.2.4	Xenografting human cells into mice.....	50
2.2.5	Molecular biology.....	51
3	Infection of human xenografts with XMLV.....	70
3.1	Introduction.....	70
3.2	Materials and methods.....	71
3.3	Results.....	71
3.3.1	MCF7 cells xenografted into BALB/c mice become infected with XMLV	71
3.3.2	Primary childhood leukaemia cells passaged in NSG mice show no evidence of XMLV infection.....	77
3.3.3	THP-1 cells xenografted into NSG mice do not become infected with XMLV.....	78
3.3.4	The <i>Bxv1</i> provirus is present in BALB/c and C57BL mice but not in NSG mice.....	81
3.3.5	MCF7 cells do not get infected with XMLV when passaged in NSG mice but may acquire a non-replication competent defective virus.....	83
3.3.6	Raji cells xenografted into BALB/c mice formed regressing tumour nodules	88
3.4	Discussion.....	88
4	Susceptibility of human cells to XMLV infection.....	91
4.1	Introduction.....	91
4.2	Materials and methods.....	91
4.3	Results.....	91
4.3.1	XPR1 receptor expression.....	91
4.3.2	Single cell cloning of MCF7 XMLV cells indicates multiple XMLV insertions/integrations at different sites in different clones of MCF7 cells.	92
4.3.3	Titration of XMLV.....	94
4.3.4	Infection of a panel of cell lines with XMLV.....	96
4.3.5	Infection of THP-1 cells with XMLV.....	100
4.3.6	Infection of Raji cells with XMLV.....	101

4.3.7	Infection of human breast cancer cells with XMLV	102
4.3.8	Infection of CD34+ human cord cells with XMLV	103
4.3.9	Infection of human peripheral blood monocytic cells with XMLV ..	103
4.3.10	Specific infectivity of XMLV in human cells	104
4.4	Discussion	107
5	Susceptibility of human cells to FeLV	110
5.1	Introduction	110
5.2	Materials and methods	110
5.3	Results.....	111
5.3.1	PiT1 receptor expression.....	111
5.3.2	Infection of cell lines with FeLV B	111
5.3.3	Infection of THP-1 cells with FeLV B	112
5.3.4	Infection of Raji cells with FeLV B.....	113
5.3.5	Infection of human breast cancer cells with FeLV B	114
5.3.6	Infection of human PBMCs with FeLV B	114
5.3.7	Infection of CD34+ human cord cells with FeLV B	115
5.3.8	Infection of MCF7 cells with FeLV B and XMLV simultaneously	116
5.3.9	Specific infectivity of FeLV B in human cell lines	117
5.3.10	Specific infectivity of FeLV B in human PBMCs	120
5.4	Discussion	124
6	Mechanisms of resistance of human cells to FeLV	126
6.1	Introduction	126
6.2	Materials and methods	126
6.3	Results.....	127
6.3.1	FeLV B mutation analysis.....	127
6.3.2	Restriction factor expression analysis.....	132
6.3.3	The role of glycoGag in FeLV B.....	136
6.4	Discussion	140
7	Phenotypic effects of gammaretrovirus infection on human cells.....	144
7.1	Introduction	144
7.2	Materials and methods	144
7.3	Results.....	145
7.3.1	XMLV and FeLV B infected MCF7 cells show accelerated wound healing compared to uninfected MCF7 cells	145
7.3.2	THP-1 cells differentiate when exposed to XMLV supernatant	148
7.3.3	Raji cells infected with XMLV do not differentiate	154
7.4	Discussion	155
8	Effects of XMLV infection on human cell transcriptomes	157
8.1	Introduction	157

8.2	Materials and methods	157
8.3	Results.....	158
8.3.1	Changes in gene expression after XMLV infection	158
8.3.2	Validation of microarray by qRT-PCR	166
8.3.3	Comparison of change in miRNA expression.....	167
8.3.4	Comparison of FeLV B versus XMLV gene expression.....	169
8.4	Discussion	170
9	General discussion	175
	Appendices	181
	References.....	212

List of tables

Table 2.1 qRT-PCR assays for expression of restriction factors	62
Table 2.2 qRT-PCR assays for microarray validation	62
Table 4.1 XPR1 expression in cells.....	91
Table 5.1 PiT1 expression in different cells.....	111
Table 5.2 FeLV B titre from different cell lines using the QN10 assay	117
Table 5.3 FeLV B titre from PBMCs, Kyo1 and Reh supernatant.....	123
Table 6.1 Mutations in FeLV B <i>pol</i> region in different cell lines.....	128
Table 6.2 Preferred sequence context for deamination by APOBEC3 enzymes .	130
Table 6.3 PENHF and PENHFX QN10 titration	139
Table 6.4 Summary of restriction factor expression, PiT1 expression, mutations and susceptibility of FeLV B	141
Table 7.1 Analysis of wound assay	147
Table 8.1 Quality check of RNA samples.....	158
Table 8.2 Functional summary of entities with ≥ 1.5 fold change expression...	163
Table 8.3 Differentially expressed miRNAs	168

List of figures

Figure 1.1 Structure of FeLV	18
Figure 1.2 Replication cycle of retroviruses.....	21
Figure 1.3 Restriction of retroviruses	27
Figure 3.1 MCF7 BALB/c tumour explant.....	72
Figure 3.2 Flow cytometry of MCF7 explant cells	72
Figure 3.3 DERSE assay for gammaretrovirus detection	73
Figure 3.4 PCR for detecting XMLV in BALB/c explants.....	74
Figure 3.5 FACS sorting of MCF7 explant cells and PCR after FACS.....	75
Figure 3.6 PCR for <i>Emv1</i> in cells exposed to MCF7-BALB/c explant supernatant	76
Figure 3.7 PCR to detect XMLV in primary childhood leukaemia cells.....	78
Figure 3.8 PCR to detect XMLV in NSG explants	79
Figure 3.9 PCR for XMLV in NSG mouse blood	80
Figure 3.10 Analysis of <i>Bxv1</i> provirus.....	82
Figure 3.11 PCR for XMLV in NSG and BALB/c explants.....	85
Figure 3.12 PCR for exposure of MCF7 cells to BALB/c plasma	86
Figure 3.13 Phylogenetic trees for NSG defective virus	87
Figure 4.1 Probing XMLV insertions in XMLV infected MCF7 clones	92
Figure 4.2 Southern blot for XMLV-infected MCF7 single cell clones	93
Figure 4.3 DERSE assay for XMLV titration	95
Figure 4.4 PCR for XMLV titration.....	95
Figure 4.5 PCR for XMLV infection of panel of cell lines	96
Figure 4.6 DERSE assay for XMLV infected cells.....	97
Figure 4.7 Principles of the DERSE assay.....	98
Figure 4.8 PCR for XMLV infected panel of cells.....	99
Figure 4.9 PCR for XMLV infection of THP-1 cells	100
Figure 4.10 Southern blot for XMLV infection of THP-1 cells	101
Figure 4.11 PCR for XMLV infection of Raji cells.....	102
Figure 4.12 PCR for XMLV infection of MDA MB 231 cells.....	102
Figure 4.13 PCR for XMLV infection of CD34+ cells.....	103
Figure 4.14 PCR for XMLV infection of PBMCs	104
Figure 4.15 Titration of XMLV from different cell lines.....	105
Figure 4.16 Western blot of viral and cell protein lysates from XMLV infected cells	106
Figure 5.1 PCR for FeLV B infection of cell line panel	112
Figure 5.2 PCR for FeLV B infection of 293T cells	112
Figure 5.3 PCR for FeLV B infection of THP-1 cells.....	113
Figure 5.4 PCR for FeLV B infection of Raji cells	113
Figure 5.5 PCR for FeLV B infection of breast cancer cells	114
Figure 5.6 PCR for FeLV B infection of PBMCs.....	115
Figure 5.7 PCR for FeLV B infection of CD34+ cells	115
Figure 5.8 PCR for simultaneous FeLV B and XMLV infection of MCF7 cells	116
Figure 5.9 Western blot FeLV B virus proteins and specific infectivity.....	118
Figure 5.10 Western blot FeLV B infected cell proteins	119
Figure 5.11 PCR for FeLV B infection of PBMCs, Reh and Kyo1 cells.....	121
Figure 5.12 FeLV B copy number in PBMCs, Kyo1 and Reh at different times...	122
Figure 5.13 FeLV B virion proteins produced by infected cells	123
Figure 6.1 Graphical representation of hypermutation in the FeLV B	129
Figure 6.2 Expression of APOBEC3 mRNAs relative to permissive 293 cells.....	133
Figure 6.3 Expression of SAMHD1 mRNA in different cells.....	134
Figure 6.4 Expression of TRIM5 α mRNA in different cells	135

Figure 6.5 Expression of Tetherin mRNA in different cells	136
Figure 6.6 gPr80 ^{Gag} start codon sequence of PENHF and PENHFX transcripts ...	137
Figure 6.7 Transfection of 293T cells with PENHF and PENHFX	138
Figure 6.8 Infection of Kyo1 with PENHF and PENHFX	138
Figure 6.9 PCR for PENHF and PENHFX infection of PBMCs	140
Figure 7.1 Wound healing assay	146
Figure 7.2 Wound assay for freshly infected MCF7 cells	148
Figure 7.3 Altered morphology and cell number in XMLV treated THP-1 cells ..	149
Figure 7.4 PCR for CD14 expression	150
Figure 7.5 Flow cytometry for CD54 expression	151
Figure 7.6 PCR to detect <i>Mycoplasma</i>	152
Figure 7.7 THP-1 differentiation by XMLV free <i>Mycoplasma</i>	153
Figure 7.8 PCR for detecting source of <i>Mycoplasma</i>	154
Figure 8.1 Differential expression of transcripts	159
Figure 8.2 Differential expression of transcripts in terms of fold change	160
Figure 8.3 Differentially expressed genes with fold change ≥ 1.5	161
Figure 8.4 Heat map for signal intensity of top 50 individual gene entities	162
Figure 8.5 Host functions affected in XMLV infected Raji and MCF7 cells	164
Figure 8.6 Significant canonical pathways	165
Figure 8.7 Validation of microarray results by qRT-PCR	166
Figure 8.8 Validation of EGR1 gene	167
Figure 8.9 Differentially expressed miRNAs	168
Figure 8.10 Gene expression in XMLV vs FeLV B infected Raji cells	169

List of techniques I used in this study

- 1 Growth of cell lines and primary cells in tissue culture
- 2 Infection of cell lines and primary cells with viruses
- 3 Single cell cloning
- 4 Ficoll separation of viable cells
- 5 Serial dilution of virus supernatant and QN10 assay
- 6 DERSE assay reading by florescence microscopy
- 7 Processing cells for xenografting
- 8 Assisting during the process of oestrogen pellet implantation into mice
- 9 Assisting during the process of xenografting
- 10 Observing mice for tumours
- 11 Extracting tumour samples from euthanized mice
- 12 Processing and growing tumour explants in cell culture
- 13 DNA extraction from cell lines and mouse tissues
- 14 RNA extraction
- 15 cDNA synthesis
- 16 Designing primers for XMLV sequencing and detection, FeLV sequencing, NSG defective virus sequencing, endogenous *Bxv1* detection in mouse genome, *Emv1* detection, and XMLV probing
- 17 Standard PCR, gel electrophoresis and UV imaging
- 18 PCR product purification
- 19 Gel DNA extraction
- 20 Cloning virus sequences using chemically competent bacteria
- 21 Plasmid DNA extraction (both Miniprep and Maxiprep)
- 22 Rescuing, and complete sequencing of the XMLV genome
- 23 Application of CLC genomics to align sequences and interpret data
- 24 Online BLAST searching for related endogenous viruses
- 25 Use of online hypermutation analysis software to detect and plot hypermutations graphically
- 26 Real time PCR
- 27 Determining protein concentration in samples
- 28 Western blotting-all steps
- 29 Designing probes for southern blotting
- 30 Southern blotting-all steps
- 31 Wound healing assay

- 32 Use of Image J software for densitometry
- 33 Flow cytometry and FACS: All steps
- 34 Analysing flow cytometry and FACS data using CFlow Plus and FlowJo respectively
- 35 *Mycoplasma* detection and locating source of contamination
- 36 Use of IPA software to interpret microarray data

Abbreviations

AML	Acute monocytic leukaemia
APOBEC3 or A3	Apolipoprotein B mRNA-editing catalytic polypeptide 3
APC	Antigen presenting cells
ATM	Ataxia telangiectasia mutated signalling pathway
AURKA	Aurora kinase A
ALV	Avian leukosis virus
B-ALL	B cell acute lymphoblastic leukaemia
BH FDR	Benjamini and Hochberg false discovery rate
BLV	Bovine leukaemia virus
BLAST	Basic Local Alignment Search Tool
BrdU	Bromo deoxyuridine
<i>Bxv1</i>	B10 xenotropic virus 1
CA	Capsid
CKS2	CDC28 protein kinase regulatory subunit 2
CDC25C	Cell division cycle 25C
CCL4	Chemokine (C-C motif) ligand 4
CFS	Chronic fatigue syndrome
CML	Chronic myeloid leukaemia
cGAS	Cyclic GMP-AMP synthase
CCNB1	Cyclin B1
CCNB2	Cyclin B2
CDK1	Cyclin dependent kinase 1
CMV	Cytomegalovirus
dNTPs	Deoxynucleoside triphosphates
DERSE	Detectors of exogenous retroviral sequence elements
EBNA-1	EBV-encoded nuclear antigen-1
EBER	Epstein-Barr virus encoded RNAs
EGFR	Epidermal growth factor receptor
EGR1	Early growth response gene 1
EMLV	Ecotropic murine leukaemia virus
<i>Emv1</i>	Endogenous ecotropic murine leukaemia virus 1
ERV	Endogenous retroviruses
Env	Envelope
EBV	Epstein-Barr virus

ECL	Extra cellular loops
FACS	Fluorescence activated cell sorting
FANCD2	Fanconi anaemia complementation group D2
FeLV	Feline leukaemia virus
FC	Fold change
GaLV	Gibbon ape leukaemia virus
GPI	Glycophosphatidyl Inositol
glycoGag	Glycosylated Gag
GFP	Green fluorescent protein
Gag	Group specific antigen
GADD45A	Growth arrest and DNA-damage-inducible alpha
GADD45B	Growth arrest and DNA-damage-inducible beta
Th-1 cells	Helper T cell type 1
Th-2 cell	Helper T cell type 2
HERV	Human endogenous retroviruses
HIV-1	Human immunodeficiency virus-1
HMEC	Human mammary epithelial cells
HTLV	Human T cell leukaemia virus
hTHTR1	Human thiamine transporter 1
IPA	Ingenuity Pathway Analysis
IN	Integrase
ISG	Interferon stimulated gene
IL2	Interleukin 2
IL7R	Interleukin 7 receptor
ICAM1	Intracellular adhesion molecule 1
IAP	Intracisternal A particles
KoRV	Koala retrovirus
LTR	Long terminal repeat
LB medium	Luria Bertani medium
MA	Matrix
mRNA	Messenger RNA
miRNA	Micro RNA
MLV	Murine leukaemia virus
Mo MLV	Moloney murine leukaemia virus
MIP-1 β	Macrophage inflammatory protein-1 β
MOI	Multiplicity of infection
mA3	Murine APOBEC3

NSG	NOD/SCID/ γ_c^{null}
NC	Nucleocapsid
PBMC	Peripheral blood mononuclear cells
PMA	Phorbol 12-myristate 13-acetate
PCR	Polymerase chain reaction
PBS	Phosphate buffered saline
PiT1	Phosphate transporter 1
PiT2	Phosphate transporter 2
PLK1	Polo-like kinase 1
Pol	Polymerase
PMLV	Polytropic murine leukaemia virus
PERV	Porcine endogenous retroviruses
PR	Protease
qRT-PCR	Quantitative real time PCR
RIM	Retroviral insertional mutagenesis
RT	Reverse transcriptase
RSV	Rous sarcoma virus
SAMHD1	SAM domain and HD domain-containing protein 1
SIV	Simian immunodeficiency virus
SLC30A4	Solute carrier family 30 gene member 4
STING	Stimulator of interferon genes
SU	Surface protein of virus envelope
SV40	Simian virus 40
TGF alpha	Transforming growth factor receptor alpha
TLR	Toll like receptors
TM	Transmembrane protein of envelope
TRIM5 α	Tripartite motif-containing 5 α
TBST	Tris buffered saline tween
UDG	Uracil DNA glycosylase
Vif	Virus infectivity factor
XPR1	Xenotropic and polytropic retrovirus receptor 1
XMLV	Xenotropic murine leukaemia virus
XMRV	Xenotropic murine leukaemia virus-related virus
X-SCID	X-linked severe combined immunodeficiency
ZnT-4	Zinc transporter-4

Abstract

I have explored the infection of human cells by the gammaretroviruses XMLV (xenotropic murine leukaemia virus) and FeLV (feline leukaemia virus). For XMLV the main aim was to assess the risks and consequences of contamination of human-mouse xenografts. For FeLV, the aim was to explore the susceptibility of human cells *in vitro* to assess the risks and identify the barriers to zoonotic infection *in vivo*.

Xenografting of human cells to mice is used commonly in many disciplines of biomedical science. Infection of xenograft-derived cell lines has been reported as a common observation but it was unclear how many of these lines were infected due to *in vitro* cross-contamination rather than *de novo* infection *in vivo*. I conducted a prospective study and demonstrated that more than 40% xenografts passaged through BALB/c nude mice acquired XMLV. Xenografts passaged through NSG, another commonly used mouse strain for engraftment studies, did not yield replication-competent XMLV, although there was some evidence of activation of related replication-defective viruses. The source of XMLV in BALB/c mice appeared to be *Bxv1*, a locus encoding a replication competent virus which I showed was absent from NSG mice. I also showed that *de novo* isolated XMLV replicates to high copy number in MCF7 breast cancer and induces subtle changes in growth properties. Transcriptome analysis suggested that up regulation of EGR1 (early growth response gene 1) may be responsible for these growth effects. I also analysed susceptibility to XMLV infection in human cells and showed that while primary PBMCs are highly resistant, many cell lines can be infected. The Raji Burkitt's lymphoma cell line was found to be highly susceptible to XMLV and displayed a much larger transcriptional response compared to MCF7, with marked up regulation of a series of markers of innate immunity.

I examined the susceptibility of human cells to infection with FeLV B, the viral subtype which appears to be the most likely zoonotic agent. Cell lines of human origin were found to vary in susceptibility with no clear relationship to cell lineage. While some cell lines were completely susceptible for FeLV B, most showed limited virus replication and G to A hypermutation that correlated with the expression of APOBEC family members. Primary PBMCs and some leukaemia

cell lines showed profound resistance to FeLV B infection at an early stage of replication and accumulated proviral DNA with only a few mutations. The mediator of this early block has not yet been identified but appears likely to be important in preventing cross-species spread of gammaretroviruses to the human population.

1 Introduction

1.1 Retroviruses

Retroviruses are a large group of single stranded enveloped RNA viruses. The size of genomic retroviral RNA ranges between 7-12kb. The diameter of a retrovirus particle is approximately 80-100nm. All retroviruses replicate via a DNA intermediate which is then integrated into the host cell genome¹.

1.1.1 Structure and classification of retroviruses

Retroviruses can be classified into simple and complex retroviruses on the basis of the organisation of the viral genome. The genome of both simple and complex retroviruses carries basic genetic information comprising group specific antigen (*gag*), polymerase (*pol*), and envelope (*env*) regions. In addition to the basic genomic structure, the complex retroviruses also encode additional regulatory proteins by way of multiple splicing mechanisms². The structure of a simple gammaretrovirus e.g. feline leukaemia virus (FeLV) is shown in the Figure 1.1.

Figure 1.1 Structure of FeLV

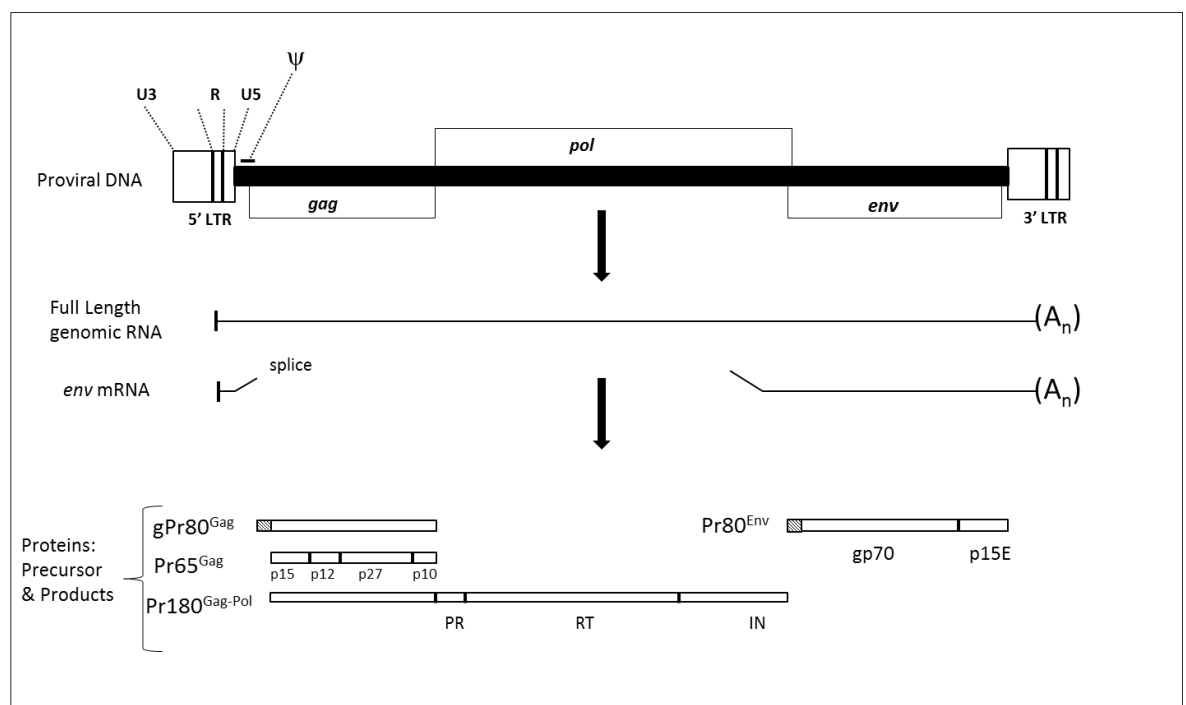


Figure 1.1 Structure of FeLV showing different segments along with the corresponding proteins encoded by these segments. See text for details.

As shown in Figure 1.1, gammaretroviruses like FeLV (and also murine leukaemia virus, MLV) are known to encode an alternate glycosylated form of the Gag polyprotein known as glycoGag or glycosylated Gag (gPr80^{Gag}) in addition to the major Gag polyprotein (Pr65^{Gag}) precursor of viral structural proteins^{3,4}. The MLV glycoGag is encoded by a CUG initiation codon^{4,5} upstream of the AUG initiation codon for Pr65^{Gag} whereas the glycoGag initiation codon for FeLV is AUG⁶. The gene product is glycosylated in the rough endoplasmic reticulum and later transported to the cell surface where it is cleaved into a 55kDa type II protein and a 40kDa protein⁷. The Gag polyprotein (Pr65^{Gag}) precursor of FeLV is further cleaved by protease enzymes in a step wise fashion to produce viral proteins that make up the matrix (MA, p15), capsid, (CA, p27) and virus nucleocapsid, (NC, p10)⁸. The Pr180^{Gag-Pol} precursor protein is formed when translation does not stop at the end of the *gag* gene and continues through the *pol* region. The fusion protein is then cleaved into a products of Gag precursor as well as protein products encoded by the *pol* region. The *pol* region is known to encode the enzymes protease (PR), reverse transcriptase (RT) and integrase (IN) enzymes⁸. The genomic RNA is spliced to generate *env* mRNA which encodes the viral proteins that make up the surface (gp70) and transmembrane (p15E) components of the viral envelope (Figure 1.1). In murine leukaemia virus (MLV), the capsid (CA) has been described as p30 rather than p27 on the basis of its apparent molecular size on SDS polyacrylamide gels⁹. ψ stands for the retroviral packaging sequences, which play an important role in packaging the retroviral RNA¹⁰. Retroviruses (Retroviridae) can be classified into the following seven groups (genera) according to the ICTV classification¹¹ given below:

1. Alpharetroviruses e.g. avian leukosis virus (ALV), Rous sarcoma virus (RSV).
2. Betaretroviruses e.g. mouse mammary tumour virus (MMTV).
3. Gammaretroviruses e.g. murine leukaemia virus (MLV), feline leukaemia virus (FeLV), gibbon ape leukaemia virus (GaLV).
4. Deltaretroviruses e.g. bovine leukaemia virus (BLV), human T cell leukaemia virus (HTLV).
5. Epsilonretroviruses e.g. walleye dermal sarcoma virus (WDSV).
6. Lentivirus e.g. human immunodeficiency virus-1 (HIV-1), simian immunodeficiency virus (SIV).
7. Spumaretroviruses e.g. simian foamy virus (SFV).

The genus gammaretrovirus includes mammalian, avian and reptilian viruses. The gammaretroviruses along with the alpharetroviruses, betaretroviruses and epsilonretroviruses are generally classed as simple retroviruses while the deltaretroviruses, lentiviruses and spumaretroviruses are complex retroviruses. Retroviruses were previously classified on the basis of their morphology under the electron microscope¹². From these studies the gammaretroviruses were previously designated type C retroviruses. Type C particles were observed to have a round central electron dense core that is formed during budding at the cell membrane. Other classes included intracellular type A particles characterised by an electron-lucent core, type B particles with a typically round eccentric electron-dense core and the type D particles showing a cylindrical electron dense core¹².

1.1.2 Replication cycle of retroviruses

1.1.2.1 Entry into the host cell

The first important step in the life cycle of retroviruses is entry into the host cell. To gain entry into the host cell, an interaction between glycoproteins present on the virus envelope and specific host cell receptors present on the host cell membrane is required (reviewed by Hunter *et al*¹³). This process initiates with the binding of a surface (SU) portion of the virus envelope to the cell surface receptor. The interaction drives a conformational change in the envelope region that leads to membrane fusion and finally entry of the virus into the cell^{2,13}. The replication cycle of a simple gammaretrovirus is summarised in the Figure 1.2.

Figure 1.2 Replication cycle of retroviruses

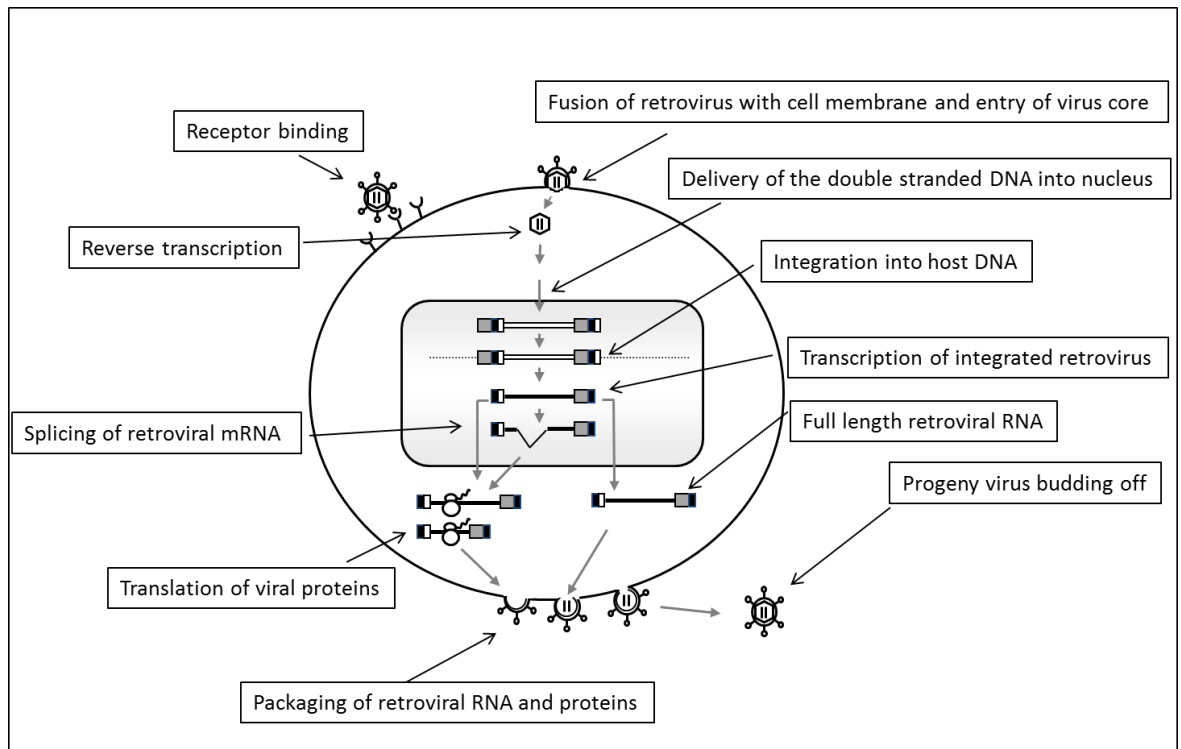


Figure 1.2 Different stages of a gammaretrovirus life cycle. Adapted from Retroviruses¹³. See text for details.

1.1.2.2 Reverse Transcription

The retrovirus enters the cell as a viral capsid core containing viral RNA and reverse transcriptase enzyme. Reverse transcription takes place while the virus particle is in the cytoplasm (Figure 1.2). The reverse transcriptase enzyme synthesizes the formation of double stranded DNA from the viral RNA template¹⁴. During the process of reverse transcription, the reverse transcriptase enzyme migrates twice from the 5' end to the 3' end of the viral RNA to duplicate the sequences present at the two ends, resulting in the formation of long terminal repeat sequences (LTR) at both ends of the proviral DNA¹⁴. The LTR is known to play a very important role in regulating viral gene expression and thus viral replication and in the process of insertional mutagenesis¹⁵.

1.1.2.3 Integration

The viral DNA formed moves from the cytoplasm to the nucleus where it is integrated into the host DNA with the help of viral integrase enzyme¹⁶. Integration is an important step in the life cycle of retroviruses¹⁶. It guards the virus DNA against degradation in the host cell, provides a stable environment for

viral DNA replication (retroviral DNA can't replicate autonomously) and allows transcription of the viral genome using cellular enzymes.

1.1.2.4 Transcription

Once integrated, the provirus can be expressed as an infectious virus or can remain dormant¹⁷. Transcription of the integrated virus takes place as a result of interaction between cellular factors and the viral LTR¹⁸.

1.1.2.5 Processing, packaging and budding

As a result of transcription, full length viral RNA transcripts are produced which undergo further processing by the cellular RNA processing system. The full length viral RNA also undergoes splicing resulting in the generation of smaller RNA transcripts (Figure 1.1)¹⁹. Both the full length and spliced viral RNA transcripts move into the cytoplasm (Figure 1.2). Gag and Pol proteins are translated from the full length viral transcripts by cellular ribosomes located in the cytoplasm. Env proteins are translated from the spliced virus transcripts (Figure 1.1& 1.2). The full length viral RNA also serves as retroviral genomic RNA. The full length viral RNA and the viral proteins are assembled at the periphery of the cell near the cell membrane where the virus particles finally bud off from the cell surface. After budding the virus particles undergo maturation by the cleavage action of the viral and cellular proteases on the viral proteins¹⁹.

1.1.3 Exogenous and endogenous retroviruses

The exogenous retroviruses described above are responsible for new infection of the host cells. However the exogenous retroviruses can become endogenous by infecting germ line cells and being vertically transmitted from parents to offspring. All vertebrates investigated including humans have been found to have endogenous retroviruses in their genome¹⁷.

1.1.3.1 Endogenous mouse retroviruses

About 37% of the mouse genome consists of retro elements (DNA which has been amplified and inserted into the genome via an RNA intermediate). One third of

these retro elements comprise endogenous retroviruses²⁰ including MLV²¹. About 60 copies of MLV are present in the mouse genome²². Endogenous retroviruses (ERV) are either actively expressed or remain silent. Most ERV are non-functional due to mutations and deletions²³ but recombination between ERV is very common²⁴.

1.1.3.1.1 Classification of endogenous murine leukaemia viruses

On the basis of host range of replication-competent representatives, the endogenous murine leukaemia viruses can be classified as

1. Xenotropic murine leukaemia virus (XMLV): Only infects non-mouse cells. There are about 1-20 XMLV copies per mouse strain. BALB/c mice have up to 12 XMLV while C57BL mice have up to 20 XMLV²⁴.
2. Ecotropic murine leukaemia virus (EMLV): Only infects mouse cells. There is a small number (up to six) of ecotropic proviruses in any mouse strain²⁴.
3. Polytopic murine leukaemia virus (PMLV): Infects both mouse cells and non-mouse cells²¹. There can be up to 40 copies of PMLV in lab mouse strains²⁵. PMLV proviruses are replication defective, but can recombine with EMLV to produce infectious virus²⁶.

1.1.3.1.2 Xenotropic murine leukaemia virus (XMLV)

XMLV is a gammaretrovirus and its genome consists of *gag*, *pol*, and *env* regions²⁰. XMLV was isolated for the first time from New Zealand Black (NZB) mice²⁷. Mouse strains differ in their capacity to produce infectious XMLV. XMLV is highly expressed in NZB and F/ST mice, moderately expressed in C57BL, C57L, BALB/c, DBA, AKR, NZW HRS and MA/My mice and rarely expressed in NFS, NIH Swiss, A, 129 and SWR mice²⁰. Strains like NZB and F/St spontaneously produce XMLV whilst other strains need activation by chemical induction, spleen cell stimulation by bacterial lipopolysaccharides (LPS) or by a graft versus host reaction²⁸. BALB/c splenocytes can be activated *in vitro* to express C type particles by treatment with bromo deoxyuridine (BrdU) and *in vivo* by a graft versus host reaction²⁹.

Four active XMLV proviruses have been mapped²⁰:

1. *Bxv1*: Present on chromosome 1 locus³⁰ and can be induced by chemical and LPS stimulation³⁰. *Bxv1* is present in around 1/3 of inbred mouse strains.
2. *Nzv1* and *Nzv2*: Present in NZB mice³¹.
3. *Mxv1*: Present in Ma/My mice in addition to *Bxv1*³².

Bxv1 has been identified in 17 strains. The source of *Bxv1* in the laboratory mouse has been traced back to the Japanese *Mus molossinus* house mouse²². Nude mice have a low rejection level to xenografting due to thymic aplasia and lack of T cell mediated immunity³³. T cells may not be completely absent in nude mice³⁴, and since *Bxv1* is induced by graft versus host reactions, infectious XMLV can be found in a tumour xenografted in immune deficient mice positive for *Bxv1*²⁰.

XMLV uses Xenotropic and polytropic retrovirus receptor 1 (XPR1) to enter cells. Like other gammaretrovirus receptors, XPR1 has multiple transmembrane domains (8 in this case), with four extra cellular loops (ECL)^{20,35}. There are 5 different forms of XPR1 in mice: XPR1^m, XPR1ⁿ, XPR1^c, XPR1^{Sxv}, XPR1^p²⁰. All of these with the exception of XPR1ⁿ permit XMLV infection with variable efficiency, XPR1^{Sxv} being the most efficient²⁰. Important receptor polymorphisms responsible for these differences have been mapped to lysine 500 on ECL3 and threonine 582 on ECL4 on the XPR1 receptors³⁶. Human XPR1 is located on chromosome 1³⁵ and is a homolog of mouse XPR1^{Sxv}. XPR1 is expressed in almost all human cell lines except RBCs³⁷ and human cell lines are generally susceptible to XMLV infection *in vitro* in common with many other mammalian species. Laboratory mice generally carry the XPR1ⁿ receptor and are not susceptible to XMLV²⁰, but their progenitor strains *Mus domesticus*, *Mus castaneus*, and *Mus musculus*³⁸ have been found to be susceptible to XMLV infection. Recently strains of laboratory mice have been found to be susceptible to XMLV infection²² owing to expression of XPR1^{Sxv}. It appears that ancestral mice were susceptible to XMLV infection, but selective pressure has led to loss of receptor entry function in most strains³⁹. Chickens, in contrast to other birds, are similarly refractory to XMLV. Mutations have been found in the chicken XPR1 receptor that render it

resistant to XMLV infection⁴⁰, leading to the suggestion that chicken may have acquired resistant XPR1 receptors due to counter-selection as chickens have been shown to catch and eat small rodents⁴⁰.

1.2 Host resistance

1.2.1 The innate and adaptive immune systems

The innate immune system acts in a less specific manner to combat invading viruses and may respond within hours of infection. The innate immune system encompasses sentinel cells e.g. macrophages, natural killer cells, dendritic cells and soluble factors produced by infected cells such as interferon⁴¹. The toll like receptors (TLR) play a major role in these processes⁴². The TLR known for sensing different viruses or their replication intermediates are TLR2, TLR3, TLR4, TLR7, TLR8 and TLR9^{42,43}. Binding of a ligand to TLR activates an intracellular signalling cascade resulting in the production of different cytokines including type 1 interferon and also activation of dendritic cells⁴². Interferon signalling stimulates the expression of interferon-responsive genes including restriction factors that confer antiviral activity⁴⁴. Retroviruses have been generally been regarded as invisible to the innate immune system, failing to induce interferon, but recent studies suggest that retroviruses can induce innate immune responses via the cGAS-cGAMP-STING (stimulator of interferon genes) pathway through activation of cyclic GMP-AMP synthase (cGAS) by newly synthesized proviral DNA^{45,46}.

Macrophages and dendritic cells are phagocytes⁴⁷. After phagocytosis and degradation of virus or virus-infected cells, they migrate to the lymph nodes where they present the antigen to the helper T cells of the adaptive immune system and are therefore known as antigen presenting cells (APC)⁴⁸.

The adaptive immune system comprises T cells and the B cells. T cells are further subdivided into helper and cytotoxic T cells. Adaptive immunity is highly dependent on the information shared by the innate system about the viral infection via the APCs. The APCs activate the helper T cells and cause them to differentiate into either helper T cell type 1 (Th-1) or helper T cell type 2 (Th-2). Th-1 cells are formed by the IL12 produced by the activated macrophages

and dendritic cells⁴⁹ while the Th-2 cells are formed by IL4 from the activated T cells⁵⁰. Th-1 cells secrete IL2 and IFN- γ that favour the activation of cytotoxic T cells⁵¹. IFN- γ is also involved in macrophage activation and stimulation of B cells to produce complement fixing and opsonising IgG antibodies⁵². The Th-2 cells on the other hand produces IL4 and IL13 that lead to production of IgG neutralising antibody and IgE antibody by the B cells⁵². The adaptive immune system also has the ability to develop immune memory as a result of viral infection. Immune memory provides more effective protection against repeated infection by the same virus^{53,54}. Thus both the innate and adaptive immune systems behave in a responsive manner and require time to respond to retroviral infection⁵⁵. This may be advantageous to the invading retrovirus as it can give the retrovirus sufficient time to integrate and evade recognition.

1.2.2 The intrinsic immune system

Eukaryotes have developed an intrinsic immune system in addition to the innate and adaptive immune systems to counteract retroviral infections⁵⁵. Most of the current knowledge about these phenomena stems from studies on HIV and primate lentiviruses⁴¹. The intrinsic system consists of constitutively expressed proteins serving as antiretroviral restriction factors. These proteins are expressed at constant level and their antiretroviral activity is independent of any retrovirus related signalling. This system exists in a primed state to combat invading retroviruses⁵⁵. However, a retroviral-generated signal can also up-regulate expression of these restriction factors after activation of the host innate system⁴³. Here the demarcation between the intrinsic and innate systems breaks down. The intrinsic system restriction factors are constantly expressed in cells as components of the intrinsic system primed to restrict retrovirus infection as a first line of anti-retroviral defence, but are also stimulated by interferon as part of the innate immune response thus reinforcing their antiretroviral capabilities⁵⁶. The most significant intrinsic immune proteins that have been described so far include APOBEC3, TRIM5 α , SAMHD1 and Tetherin. Their mechanisms of action are illustrated in Figure 1.3.

Figure 1.3 Restriction of retroviruses

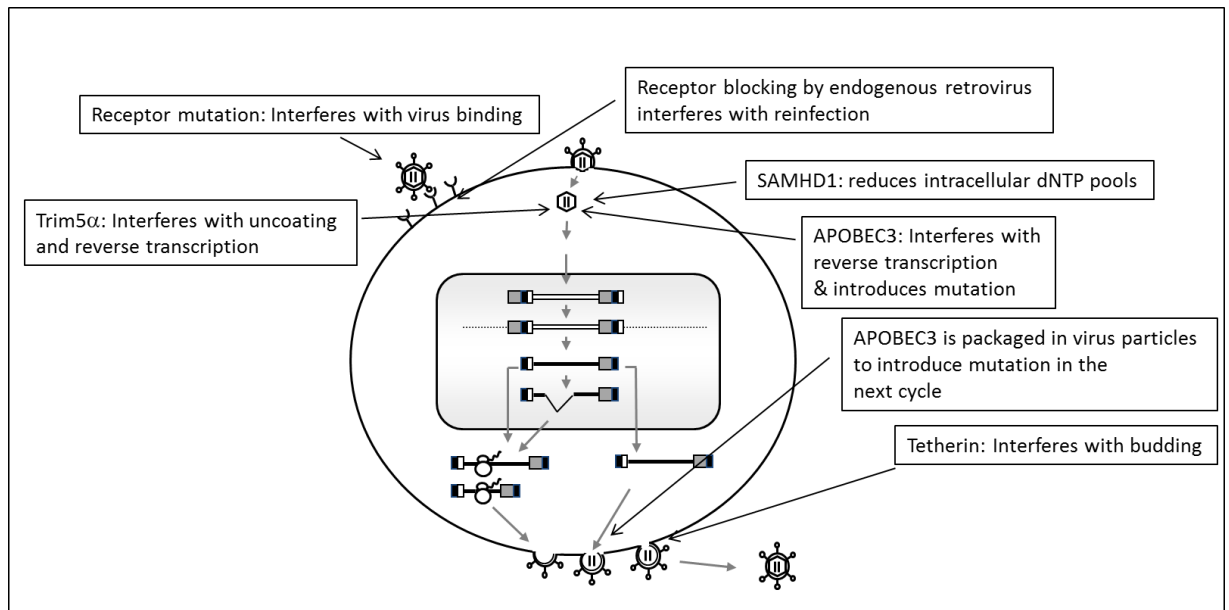


Figure 1.3 Different mechanisms used by host cells to restrict retroviruses have been shown. See text for details.

The intrinsic immune system is very efficient due to the fact that it is always ready to face the retrovirus infection. It is also extremely specific for retroviruses and plays an important role in preventing or weakening a retrovirus infection. Due to constant expression levels of restriction factors, the intrinsic immune system is able to resist initial retroviral challenge but the system can become saturated if very high retroviral titres are present. Thus the intrinsic immune system is primarily important as a first line defence to counteract retrovirus infection⁵⁷. The important intrinsic factors (Figure 1.3) are discussed below.

1.2.2.1 APOBEC3 enzymes

Apolipoprotein B mRNA-editing catalytic polypeptide 3 (APOBEC3 or A3) comprises a family of cytidine deaminase enzymes. While recognised as mediators of intrinsic resistance, the APOBEC3 genes are also interferon stimulated genes (ISGs)^{58,59}. They are constitutively expressed in a cell-type specific manner^{60,61}. While mice have a single gene, the human genome has seven members of the APOBEC3 family *viz* APOBEC3A, APOBEC3B, APOBEC3C, APOBEC3D, APOBEC3F, APOBEC3G and APOBEC3H⁶².

1.2.2.1.1 Mechanism of APOBEC3 action

APOBEC3 can interact with the retroviral RNA and become packaged along with the retroviral particles. When these virus particles infect new cells, the APOBEC3 enters the cells along with the viral core⁶³. The newly delivered APOBEC3 enzyme is capable of deaminating cytidine residues to form uracil in the minus DNA strand that is synthesized as a result of reverse transcription. This results in G to A hypermutations in the plus DNA strand^{55,64}. APOBEC3 can also edit viral RNA thus giving rise C to T mutation in the plus DNA strand⁶⁵. Depending on the number and location of the mutations, APOBEC3 activity can prove lethal for the virus. In general the APOBEC3 family results in G to A hypermutations in the plus DNA strand, but different members of the family have different preferences for dinucleotide/trinucleotides⁶⁶. The APOBEC3G enzyme is unique in preferring GG sites^{67,68}. A mutation occurring at a TGG site can result in a stop codon, which will often be fatal for viral replication. APOBEC3C can attack both GG and GA sites but it shows preference for the latter⁶⁹. APOBEC3F, APOBEC3B, APOBEC3D, and APOBEC3H enzymes prefer GA sites^{55,68,70,71} which are less likely to induce a non-functional protein but hypermutation can still have fatal consequences for the virus. Excessive uracil residues in the minus DNA strand can also make the virus susceptible to uracil DNA glycosylase (UDG) mediated degradation⁷². APOBEC3 is also known to interfere with the reverse transcription of retroviral RNA^{73,74} and the integration of reverse transcripts⁷⁵. Thus APOBEC3 is also capable of affecting retroviral infectivity by a cytidine-deaminase independent mechanism⁷⁶⁻⁷⁸.

Gammaretroviruses like XMRV and MLV have been shown to be susceptible to human APOBEC3G mediated restriction⁷⁹. XMRV has been reported to be resistant to APOBEC3F, APOBEC3B and APOBEC3C⁸⁰, however the role of APOBEC3F is more controversial as others have claimed XMRV to be susceptible to both APOBEC3G and APOBEC3F mediated restriction⁸¹. PERV, another gammaretrovirus, has also been reported to be significantly restricted by APOBEC3G by a cytidine deaminase independent mechanism⁸². Murine APOBEC3 (mA3) expressed by mammary epithelial cells is known to play an important role in reducing the infectivity of milk borne MMTV transmitted to offspring⁸³. The potential use of APOBEC3 over-expression to prevent or treat retroviral infection

has been widely discussed⁸², but may not be completely safe as over expression of APOBEC3 has been reported to lead to the development of cancer^{84,85}.

1.2.2.1.2 Virus infectivity factor (Vif): A retroviral mechanism to counteract APOBEC3

HIV-1 encodes a regulatory protein, Vif protein which antagonises APOBEC3 activity. Vif protein reduces intracellular APOBEC3 levels by ubiquitin mediated degradation^{86,87}. It has been shown that APOBEC3C, APOBEC3D, APOBEC3F, and APOBEC3G are all sensitive to Vif mediated degradation⁷¹ while APOBEC3A and APOBEC3B are resistant, however APOBEC3B has been reported to inhibit both Vif negative and Vif positive HIV-1⁸⁸. Others have reported that APOBEC3A, APOBEC3B and APOBEC3C are somewhat inefficient at restricting Vif negative HIV-1 while APOBEC3G, APOBEC3F, and to some extent APOBEC3D are more effective^{69,71}.

1.2.2.1.3 Glycosylated Gag

MLV does not express a homologue of HIV-Vif but is nevertheless inefficiently restricted by mouse mA3^{89,90}. It has been reported that glycoGag plays a role in assisting MLV to counteract mouse mA3 mediated resistance both *in vivo* and *in vitro*⁹¹. XMRV does not encode glycoGag but introduction of MLV glycoGag to XMRV increases the infectivity of XMRV independently of human APOBEC3 expression⁹². The exact mechanism of glycosylated Gag function is not clear though it has been found that glycoGag favours virus budding or release from cells⁹³.

1.2.2.2 TRIM5 α

Tripartite motif-containing 5 α (TRIM5 α) is another important antiretroviral restriction factor⁹⁴. TRIM5 α has 3 protein domains at the N terminal *viz* RING, B-BOX and the coiled coil domains⁹⁵. The C terminal of TRIM5 α has a SPRY/B30.2 domain and is responsible for identifying and binding to the incoming virus capsid containing the retroviral RNA and enzymes⁹⁶. Retroviruses whose capsids are not recognised can escape TRIM5 α mediated inhibition. The RING domain has ubiquitin ligase activity and is considered to play a role in TRIM5 α mediated

restriction⁹⁷. The coiled coil domain helps TRIM5 α to form dimers and the B-Box can aid in the formation of multimers. It has been suggested that the formation of multimers improves the ability of TRIM5 α to recognise incoming viral capsid^{98,99}.

1.2.2.3 Tetherin

Tetherin is a type II transmembrane protein that plays a role as an antiretroviral restriction factor¹⁰⁰. It expresses a glycosylphosphatidylinositol (GPI) lipid anchor at the C terminus and a transmembrane domain at the N-terminus¹⁰¹. Each Tetherin monomer has three extracellular cysteines. Disulphide bonds between these extracellular cysteines enables Tetherin to exist as a dimer¹⁰². One end of Tetherin may get embedded in virus particles at the time of budding. The other end of the protein, which is still embedded in the cell membrane, prevents the newly formed virus particle moving away from the cell surface. Thus Tetherin causes virus retention on the cell surface by a tethering mechanism¹⁰³. HIV-1 uses its Vpu protein to counteract Tetherin mediated restriction¹⁰⁴. Vpu is a type I transmembrane protein that can directly bind to Tetherin via interaction between their transmembrane domains^{105,106} and can down regulate Tetherin from the cell surface by causing its internalisation and lysosome mediated degradation^{107,108}. Vpu can also displace Tetherin from virus assembly sites on the cell membrane thus affecting Tetherin's ability to inhibit virus release without changing the total cell surface Tetherin levels¹⁰⁵.

1.2.2.4 SAMHD1

SAM domain and HD domain-containing protein 1 (SAMHD1) is another ISG and an important restriction factor for HIV¹⁰⁹. SAMHD1 is known to reduce intracellular deoxynucleoside triphosphates (dNTPs), thus interfering with the synthesis of viral DNA by reverse transcriptase¹¹⁰. SAMHD1 has been found to restrict HIV-1 infection in dendritic cells and macrophages¹¹¹. However SAMHD1 mediated restriction was not found to affect HIV-2 infection. This is because HIV-2 expresses Vpx protein (not encoded by HIV-1) that reduces SAMHD1 activity by proteasomal degradation^{111,112}.

1.2.2.5 Receptor status and Interference

Lack of susceptibility to retrovirus infection can be due to the absence of cell surface receptors required for infection or a mutation in the receptors conferring resistance. Cells can also resist reinfection by the same retrovirus due to interference. Following retroviral infection the cell produces envelope proteins that bind and block the receptors rendering the cells resistant to re-infection by the same virus (virus A) but not to viruses that can use alternative receptors (virus B). Similarly, cells infected with virus B are resistant to virus B but not to virus A. This is known as reciprocal interference. Non reciprocal interference can arise when viruses can use more than one receptor¹¹³. Interference can also take place due to expression of endogenous retroviral envelope gene sequences in the host cell genome. The Fv4 gene for example is a defective *env* present endogenously in some mouse strains¹¹⁴, and its expression is akin to receptor interference making cells resistant to infection by Friend murine leukaemia virus¹¹⁵. Newly acquired proviruses that are restricted by interference can recombine with different endogenous envelope sequences to form new viruses that enter cells using different envelope glycoproteins thereby enabling re-infection. The mink cell focus-forming (MCF) viruses, for example arise through recombination of exogenous murine leukaemia viruses with endogenous elements and are capable of re-infection using different receptors¹¹⁶. Finally a variation or mutation in the retroviral receptors can also affect the ability of retrovirus to infect the cell. One example of this is XPR1 receptor variation and its effect on XMLV infection which has been described earlier.

1.3 Gammaretroviruses as potential zoonotic agents

1.3.1 Human fossil viruses

Human endogenous retroviruses (HERV) make up approximately 8% of the human genome¹¹⁷. They integrated into human DNA millions of years ago and have been transmitted vertically throughout human generations¹¹⁸. The current human race is considered to represent the descendants of survivors of pandemics caused by exogenous counter-parts of HERV¹¹⁸. HERV have been broadly classified on the basis of their sequence resemblance to other retroviruses. Class I HERVs are

closely related to gammaretroviruses and are considered to be among the oldest HERVs. Examples of class I HERVs include HERV W and HERV H¹¹⁹. The class II HERVs are related to beta retroviruses while the class III HERVs are related to spumaretroviruses¹¹⁹. HERVs have undergone lethal mutations throughout the ages making them incapable of producing infectious virus. Recently the presence of HERV sequences has been associated with a number of diseases including cancer and autoimmune disease¹²⁰.

1.3.2 Koala retrovirus: A recent example of trans-species infection

Endogenization of most retroviruses appears to be ancient, dating from millions of years ago, but recent information from studies of the koala provides a contemporary example. Koala retrovirus (KoRV) is an endogenous gammaretrovirus found in koalas¹²¹. KoRV uses the PiT1 receptor to enter cells and shows up to 78% sequence similarity to gibbon ape leukaemia virus (GaLV), an exogenous gammaretrovirus of gibbon apes¹²¹. Southeast Asian mice are considered a likely source of origin for GaLV¹²². The infection and endogenization of koalas with KoRV may have occurred as little as two centuries ago¹²³. Current estimates based on 5' and 3' LTR divergence are not very accurate, however an initial infection could have taken place up to 49,900 years ago¹²⁴. Since gibbon apes and koalas live in different continents, a rodent vector has been proposed to be responsible for trans-species transmission from Asia to northern Australia¹²⁵. In support of this hypothesis the prevalence of KoRV is high in koalas in northern Australia whereas the prevalence is low in south Australian koalas¹²⁶. KoRV has been related to a high incidence of leukaemia and lymphomas in koalas^{121,125}.

1.3.3 Porcine endogenous retroviruses: A potential zoonotic agent

Porcine endogenous retroviruses (PERV) are endogenous retroviruses present in the porcine germ line and are transmitted vertically to offspring. PERV was detected in early studies on the basis of type C particles observed in porcine cells^{127,128}, and was later on definitively characterised as a gammaretrovirus family with three subtypes PERV A, PERV B and PERV C¹²⁹.

In order to cope with the high demand of human organs for transplantation, the use of porcine xenografts has been actively considered. The presence of PERV in the genome of porcine cells, however poses a potential risk of PERV infection for the recipient and also for a new pandemic^{130,131} and is a real concern¹³². Work to address this hazard has shown that PERV is produced by porcine islet xenografts in mice¹³³ and that PERV A and PERV B are capable of infecting human cells *in vitro*^{131,134}. PERV A uses HuPAR-1 and HuPAR-2 receptors¹³⁵. The receptor(s) for PERV B have not been characterised. To date there exists no evidence for human infection with PERV *in vivo*^{136,137} but the possibility of acquiring PERV by the recipient cannot be excluded.

1.3.4 Potentially widespread human exposure to feline leukaemia virus

Feline leukaemia virus (FeLV) is a naturally occurring retrovirus of household cats that can cause a variety of diseases in its host. FeLV is a simple retrovirus consisting of LTR, *gag*, *pol* and *env* regions¹³⁸. Genetic recombination takes place when FeLV replicates *in vivo* and FeLV is a common cause of lymphoma in cats. Like MLV, FeLV can cause malignancy by insertional mutagenesis¹³⁸. Members of the FeLV family usually co-exist in the natural host. Three subgroups of FeLV i.e. FeLV A, B and C have been widely studied. They use different receptors to enter host cells. FeLV A is generally considered to be an ecotropic virus. It uses the thiamine transporter THTR1 to enter feline cells but has a very low affinity for the human thiamine transporter hTHTR1¹³⁹. It is virtually always present in cats viraemic for FeLV. FeLV A envelope pseudotypes have been reported to infect non feline cells thus showing the virus is not ecotropic in the true sense¹⁴⁰. FeLV B often co-exists with FeLV A in infected cats and arises as a result of recombination between FeLV A and endogenous FeLV-related sequences¹⁴¹. FeLV B utilizes the phosphate transporters PiT1 or PiT2 to enter cells¹⁴². FeLV B can infect human cells *in vitro* and these cells can produce infectious virus¹⁴⁰. FeLV C arises from FeLV A as a result of mutations in a single variable region of the envelope gene¹⁴³. FeLV C utilizes the heme transporters FLVCR1 or FLVCR2¹⁴⁴. FeLV C strains cause rapidly fatal aplastic anaemia¹⁴⁵. Some FeLV strains can utilize both THTR1 receptors as well as FLVCR1/FLVCR2 to enter into the host cells¹⁴⁶. In this study FeLV B was focussed on as the more likely zoonotic agent as it is present in up to 50% FeLV isolates¹⁴⁷ and can

replicate without cytopathic effect in human cells *in vitro*. In the domestic environment, human exposure to FeLV occurs through shedding of virus in the saliva of infected cats. While FeLV C strains can also infect non-feline cells, they are rare in nature (~1% of isolates) and may induce cytopathic effects due to blockade of haem transport¹⁴⁰. FeLV is a significant cause of leukaemia and lymphomas in its natural host¹⁴⁸. There is no evidence of FeLV infection of humans *in vivo*¹⁴⁹. With an FeLV infection rate of up to 3% in domestic cats¹⁵⁰, the mechanism(s) by which humans resist FeLV infection are of obvious interest.

1.3.5 XMRV controversy and its aftermath: XMLV found in human xenografts

1.3.5.1 XMRV Controversy

Xenotropic murine leukaemia virus-related virus (XMRV) was initially reported as a new cross-species infection of the human population but instead appears to be an artefact of xenotransplantation and *in vitro* reagent contamination. The virus appears to have been formed as a result of a recombination event between two defective endogenous murine leukaemia viruses, pre XMRV1 and pre XMRV2¹⁵¹. XMRV has 93% sequence similarity to XMLV (*Bxv1*)²⁰. Both XMRV and XMLV use the XPR1 receptor to enter cells¹⁵². When certain prostate cancer lines were found to contain XMRV^{153,154}, there was a concern that there could be a viral aetiology to some prostate cancers. An apparent correlation was noted when RNase L mutant prostate cancer was described to be associated with XMRV¹⁵⁵. XMRV was also claimed to be isolated from chronic fatigue syndrome (CFS) patients resulting in the experimental use of antiretroviral treatment for CFS¹⁵⁶. XMRV was also claimed to be related to a number of other diseases¹⁵⁷. However these results could not be reproduced¹⁵⁸. The presence of polytropic murine leukaemia virus (PMLV) in CFS patients occurred as a result of contamination of mouse DNA in human samples¹⁵⁹. PMLV refers to endogenous murine leukaemia virus, which can infect both mouse cells and non-mouse cells²¹. Using a very sensitive PCR to detect mouse mitochondrial cytochrome oxidase and Intracisternal A particles (IAP) most samples previously positive for XMRV were also found to be positive for mouse DNA¹⁶⁰. Moreover many commercial kits used in XMRV related studies have subsequently been found to be contaminated with mouse DNA¹⁶¹. Simmons *et al*¹⁶² carried out a double blind study and confirmed that most of the previous

XMRV related results were due to contamination issues. The human prostate cancer cell line 22Rv1 is now considered to be the source of XMRV¹⁶³. 22Rv1 was developed by repeated passaging through nude mice for 7 years. This cell line served as prostate cancer model and has been distributed worldwide¹⁵¹.

1.4 Xenografting and cancer research

Xenografting of human cancer cells in the laboratory mouse is a well-established procedure for the isolation and characterisation of cells that drive tumour development³³. The leukemic stem cell theory, which led John Dick and co-workers to establish the cancer stem cell hypothesis mainly depends on the mouse as a surrogate host and a detection system for cells capable of reconstituting primary tumours¹⁶⁴. The development of immune deficient mice with reduced ability to reject xenografts¹⁶⁵ has further increased the use of mice as hosts for cancer cell line development and xenografting.

1.4.1 Infection of xenografts

1.4.1.1 Historical observations

Infection of xenografts with retroviruses is not a new observation. For example human rhabdomyosarcoma cells passaged through the cat were found to be infected with type C virus as early as 1972¹⁶⁶. This type C virus known as RD114, was characterised as an endogenous feline virus¹⁶⁷. Animal vaccines prepared using feline cells have recently been found to be contaminated with infectious RD114 gammaretrovirus^{168,169} therefore presenting a potential threat for trans-species spread of infection.

Type C particles infecting rhabdomyosarcoma cells passaged through mice were also reported in 1973 by Todaro *et al*¹⁷⁰. A study in 1979 observed that a substantial number (up to 35%) of human urogenital tumours xenografted into nude mice became infected by type C particles expressing MLV antigens¹⁷¹. Type C particles were also found in 1 out of 20 human tumours passaged through mice. The positive tumour was an oat cell carcinoma and the induction of C type particles was attributed by the authors to (unknown) factors produced by these carcinoma cells¹⁷².

1.4.1.2 Horizontal spread of XMLV infection

XMLV infected cells have the potential to horizontally infect other cell lines used in the same tissue culture laboratory¹⁷³. Spread of XMLV from small cell lung carcinoma (SCLC) N417 cells to non-xenografts has been reported¹⁷⁴. In a screen for XMLV, Hue *et al*¹⁷⁵ reported 9 out of 411 cancer cell lines to be positive for the virus. Another study¹⁷⁶ identified 3 XMLV positive cell lines out of 58 commonly used for cancer drug research. Of these the prostate cancer cell lines LAPC-4 and VCaP were positive for XMLV (*Bxv1*) and a non-small cell lung carcinoma (NSCLC) cell line, EK VX was infected with DG75 XMLV. Unidentified XMLV has also been found in a number of non xenografted melanoma cell lines Sk Mel28, Sk Mel25, Mel Juso and MML-1¹⁷⁷. Other non xenografted cell lines infected with XMLV include A2780 (ovarian cancer cell line), BHY (Squamous cell carcinoma), COCM1 (colon cancer), Daudi (Burkitt's lymphoma cell line), IMR-5 (Neuroblastoma), MUTZ-1 Myeloid leukaemia¹⁷⁵ and Jurkat J6¹⁷⁸. In addition Zhang *et al*¹⁷³ found that XMLV can spread horizontally from xenografted cells to other cell lines maintained in the same lab facility. They found that 13 out of 78 cells lines (17%) treated in the same tissue culture laboratory in which xenografts were used were positive for XMLV. In contrast all 50 cultures treated in a xenograft free laboratory were free from XMLV contamination. Thus contamination of different cell lines with XMLV has been studied retrospectively and *in vitro* spread cannot be excluded. There is no recent prospective study however, showing the likelihood of acquiring XMLV *in vivo* and this may be a reason why contamination of xenografts by XMLV has been overlooked as a potential confounding factor by most scientists using xenograft models^{179,180}.

1.4.2 Retroviral insertional mutagenesis

Retroviral integration is also very important for oncogenesis¹⁸¹. Retroviruses exert their oncogenic action by disrupting host gene expression or coding sequences¹⁸². Targets for retroviral insertional mutagenesis (RIM) include proto-oncogenes, tumour suppressor genes and oncogenic miRNAs¹⁵. Where and how the provirus integrates can determine the mechanism by which it can alter host gene function¹⁵. Different retroviruses prefer different integration sites. For example HIV-1 preferentially inserts within the active genes¹⁸³ whereas MLV integration is biased towards transcriptional start sites. Avian sarcoma leukosis

virus, in contrast shows a weak preference for active genes but no preference for transcription start sites¹⁸⁴. The integration preference of MLV effectively may increase the likelihood of effects on adjacent genes. For example X-linked severe combined immunodeficiency (X-SCID) is a genetic disorder where lack of γ c gene in children results in immune deficiency¹⁸⁵. X-SCID is treated by bone marrow transplant¹⁸⁶, an attempt to treat X-SCID by MLV vector based gene therapy was initially successful but later resulted in the development of leukaemia due to insertional mutagenesis^{187,188}. RIM can result in a selective advantage to the cells and subsequent clonal outgrowth. Clonal tumours share the same viral insertion sites whereas polyclonal tumours have multiple insertions at different sites. The insertion sites which are common in polyclonal tumours may mediate the initiation and progression of the tumour, while subsequent insertions may further aid tumour growth and selection¹¹⁶. For efficient oncogenesis, a retrovirus cannot be strongly cytopathic and must be capable of overcoming the barriers to super-infection created by the resident virus¹⁵.

1.4.2.1 Change in cellular behaviour secondary to XMRV infection

XMRV has been studied to a greater extent as compared to XMLV for its effects on cellular behaviour due to its initially reported association with human diseases. Since XMRV shares 93% sequence similarity with *Bxv1* XMLV (described earlier) and both use XPR1 for cell entry, the effects of both viruses on cell behaviour will also be discussed here.

LNCaP, PC3 and 22Rv1 are prostate cancer cell lines used as models for prostate cancer research. 22Rv1 is now believed to have acquired XMRV infection as a result of repeated passaging in mice and is known to produce high titres of infectious XMRV¹⁵¹. 22Rv1 with higher XMRV expression is invasive *in vitro*. Suppression of XMRV expression not only results in reduced invasiveness *in vitro* but also results in reduced angiogenesis and increased necrosis of primary tissue xenografts. It appears that the properties of 22Rv1 xenografts with respect to migration, invasion and angiogenesis are to some extent dependent on continued XMRV expression¹⁸⁹.

1.4.2.2 Changes in cellular behaviour following XMLV infection

The XMLV Env protein has been reported to affect tumourigenic properties in LNCaP cells. Infection of the LNCaP prostate cancer cell line with XMLV resulted in release of a factor that reduces vascular smooth muscle differentiation making the tumour more haemorrhagic¹⁹⁰. The medium from XMLV infected LNCaP cells was also reported to down regulate expression of markers associated with the differentiation of vascular smooth muscle cells *in vitro*, smooth muscle cells treated with conditioned medium showed an increase in migration across a membrane *in vitro*¹⁹⁰. Conditioned medium from XMLV infected LNCaP cells was also reported to induce an increase in tube formation in human umbilical endothelial cells in Matrigel *in vitro*¹⁹⁰.

1.4.2.3 Changes in cellular behaviour due to other retroviruses

Several murine leukaemia viruses have cytopathic or cytotoxic effects on animal cells¹⁹¹. Some retroviruses such as avian haemangioma retrovirus, mouse mammary tumour virus, spleen focus forming virus and the Jaagsiekte sheep retrovirus exert oncogenic transformation via their envelope proteins¹⁹²⁻¹⁹⁵. The MLV envelope protein, in contrast induces spongiform degeneration of nervous tissue¹⁹⁶ and the glycoprotein precursor, apoptosis in mink cells¹⁹⁷.

1.5 Aims of the study

1.5.1 To conduct a prospective study of the risks of acquiring XMLV infection in human cancer xenografts.

Although human cancer xenografts have been reported to acquire infection with murine retroviruses, the extent of this risk to routine experiments was unknown and the factors affecting the likelihood of infection (cell lines, mouse strain) were poorly understood.

1.5.2 To investigate the susceptibility of human cells to FeLV and XMLV *in vitro*.

While human cell express receptors that facilitate entry of murine and feline gammaretroviruses, a systematic study of the susceptibility of primary cells

and established cell lines of different tissue origin has not previously been reported.

1.5.3 To investigate the mechanisms of resistance of human cells to FeLV and XMLV.

While some of the known retroviral restriction factors have been reported to affect murine retroviruses replicating in human cells, no information was available for feline leukaemia viruses although human exposure in the domestic environment is more likely with these agents. In particular, the susceptibility of FeLV to human APOBEC cytidine deaminases was not previously explored. These factors are likely to be relevant to the risks of cross-species infection with FeLV.

1.5.4 To examine the significance of XMLV infection for human xenograft behaviour.

If infection of human cancer xenografts with XMLV occurs at any significant frequency, the effects of infection on cell behaviour must be considered. Apart from the obvious risk of insertional mutagenesis, little was known about other chronic infection on human cell behaviour, the effects of XMLV infection in two susceptible human cancer cell lines was therefore explored at the transcriptome level by gene expression microarray analysis.

2 Materials and methods

2.1 Materials

2.1.1 Cell culture

2.1.1.1 Cell lines and media

2.1.1.1.1 MCF7 cells

A human mammary adenocarcinoma cell line derived from the pleural effusion of a 69 year old Caucasian female who underwent a mastectomy¹⁹⁸. MCF7 cells are epithelial cells in morphology and express oestrogen receptors¹⁹⁹. During experiments, two sources of MCF7 cells were used, one was gifted by Karen Blyth (Beatson Laboratories, Glasgow) and the other by Anne Terry (Molecular Oncology Laboratory, University of Glasgow). Media requirements: MEM (10370047 Gibco) containing 10% FCS (HyClone, Perbio), 100µg/ml Penicillin/Streptomycin (15140 Gibco), 2mM Glutamine (25030 Gibco), 0.01mg/ml Insulin (I9278 Sigma, 10mg/ml) and 1mM Sodium pyruvate (11360 Gibco).

2.1.1.1.2 DERSE (Detectors of exogenous retroviral sequence elements) cells

DERSE cells are indicator cells. They were developed at the National Cancer Institute by transfection of pBabe.iGFP-puro into LNCaP cells. The pBabe.iGFP-puro is an MLV vector. It encodes puromycin resistance and a cytomegalovirus (CMV) promoter driven Green Fluorescent Protein (GFP) reporter gene which is interrupted by an intron. After infection and mobilization by a gammaretrovirus, the intron interrupted GFP gene is expressed in the second round of infection. The cells were a gift from Dr Kyeong Eun Lee and Vineet Kewal Ramani. Media requirements: RPMI 1640 (21875 Gibco) supplemented with 10% FCS (HyClone, Perbio), 100ug/ml Penicillin/Streptomycin (15140 Gibco), 2mM Glutamine (25030 Gibco), Puromycin (P9620 Sigma) selection at 1µg/ml medium.

2.1.1.1.3 CEM cells

Human T lymphoblastoid cell line derived from the peripheral buffy coat of a 4-year-old Caucasian female with acute lymphoblastic leukaemia²⁰⁰. CEM cells are

T lymphoblasts in morphology. Media requirements: RPMI 1640 (21875 Gibco) supplemented with 10% FCS (HyClone, Perbio), 100µg/ml Penicillin/Streptomycin (15140 Gibco), 2mM Glutamine (25030 Gibco).

2.1.1.1.4 CEMSS cells

A subline derived from CEM cells²⁰¹ which does not express APOBEC3G and is therefore susceptible to Vif-negative HIV-1⁸⁶. CEMSS cells were a kind gift from Michael Malim. Media requirements: RPMI 1640 (21875 Gibco) supplemented with 10% FCS (HyClone, Perbio), 100µg/ml Penicillin/Streptomycin (15140 Gibco), 2mM Glutamine (25030 Gibco).

2.1.1.1.5 Kyo1 cells

Philadelphia chromosome t(9;22) positive human leukaemia cells established from the peripheral blood of a 22-year-old Japanese man with chronic myeloid leukaemia (CML) in myeloid blast crisis in 1981²⁰². Kyo1 cells are undifferentiated myeloid cells and can differentiate into erythroid and monocytic lineages²⁰². Media requirements: RPMI 1640 (21875 Gibco) supplemented with 10% FCS (HyClone, Perbio), 100µg/ml Penicillin/Streptomycin (15140 Gibco), 2mM Glutamine (25030 Gibco).

2.1.1.1.6 K562 cells

Human leukaemia cell line (Philadelphia chromosome t(9;22) positive) derived from pleural effusion of a 53 year-old woman chronic myeloid leukaemia (CML) in blast crisis²⁰³. They are multipotent cells and can differentiate into erythroid, monocytic and granulocytic lineages^{203,204}. Media requirements: RPMI 1640 (21875 Gibco) supplemented with 10% FCS (HyClone, Perbio), 100µg/ml Penicillin /Streptomycin (15140 Gibco), 2mM Glutamine (25030 Gibco).

2.1.1.1.7 U937 cells

Human histiocytic lymphoblastoid cell line derived from pleural fluid from a 37 year-old man with generalised diffuse histiocytic lymphoma²⁰⁵. U937 are monocytes in morphology. Media requirements: RPMI 1640 (21875 Gibco) supplemented with 10% FCS (HyClone, Perbio), 100µg/ml Penicillin/Streptomycin (15140 Gibco), 2mM Glutamine (25030 Gibco).

2.1.1.1.8 Jurkat cells

Human acute T cell leukaemia cell line E61 clone²⁰⁶. Jurkat cells are T lymphoblasts in morphology. Media requirements: RPMI 1640 (21875 Gibco) supplemented with 10% FCS (HyClone, Perbio), 100µg/ml Penicillin/Streptomycin (15140 Gibco), 2mM Glutamine (25030 Gibco).

2.1.1.1.9 Reh cells

Reh cell line is derived from acute lymphoblastic leukaemia (non-T; non-B)²⁰⁷. Reh cells are lymphoblast cells in morphology, and may represent pre-B lymphoblasts²⁰⁸. Media requirements: RPMI 1640 (21875) supplemented with 10% FCS (HyClone, Perbio), 0.05mM 2-mercaptoethanol (Sigma M7522), 100µg/ml Penicillin/Streptomycin (15140 Gibco), 2mM Glutamine (25030 Gibco).

2.1.1.1.10 THP-1 cells

A human leukemic cell line derived from the blood of a boy with acute monocytic leukaemia (AML-5)²⁰⁹. THP-1 cells are monocytes in morphology. THP-1 can be differentiated into macrophages using Phorbol 12-myristate 13-acetate (PMA), Retinoic acid, or 1-25 dihydroxy vitamin D₃²¹⁰⁻²¹². THP-1 cells were gifted by Anne Terry (Molecular Oncology Laboratory, University of Glasgow). Media requirements: RPMI 1640 (21875) supplemented with 10% FCS (HyClone, Perbio), 0.05mM 2-mercaptoethanol (Sigma M7522), 100µg/ml Penicillin/Streptomycin (15140 Gibco), 2mM Glutamine (25030 Gibco).

2.1.1.1.11 293 cells

293 cells are human embryonic kidney cells transformed by Adenovirus²¹³. The 293 cells are epithelial cells in morphology. 293T cells were derived from 293 cells and express the simian virus 40 (SV40) large T antigen. They are resistant to neomycin. Both 293 and 293T are used interchangeably. Media requirements: DMEM (31966 Gibco) supplemented with 10% FCS (HyClone, Perbio), 100µg/ml Penicillin/Streptomycin (15140 Gibco), 2mM Glutamine (25030 Gibco).

2.1.1.1.12 MDA MB 231 cells

Human breast adenocarcinoma cell line derived from the pleural effusion of a 51 year old Caucasian female²¹⁴. MDA MB 231 cells are epithelial cells in morphology. They express epidermal growth factor receptor (EGFR) and transforming growth factor receptor alpha (TGF alpha)²¹⁵. Media requirements:

DMEM (31966 Gibco) supplemented with 10% FCS (HyClone, Perbio), 100µg/ml Penicillin/Streptomycin (15140 Gibco), 2mM Glutamine (25030 Gibco).

2.1.1.1.13 QN10 cells

S+L- feline embryonic fibroblast cells obtained from Oswald Jarrett, University of Glasgow. They are used to titre FeLV. Media requirements: DMEM (42430 Gibco) supplemented with 10% FCS (HyClone, Perbio), and 1mM Sodium pyruvate (11360 Gibco) 100µg/ml Penicillin/Streptomycin (15140 Gibco), 2mM Glutamine (25030 Gibco).

2.1.1.1.14 AH927 cells

AH927 cells are a feline embryonic fibroblast cell line. Media requirements: DMEM (31885 Gibco) supplemented with 10% FCS (HyClone, Perbio), 100µg/ml Penicillin/Streptomycin (15140 Gibco), 2mM Glutamine (25030 Gibco).

2.1.1.1.15 Raji cells

B lymphocyte cell line derived from Burkitt's lymphoma. Raji cells were gifted by Karen McAulay (LRF virus centre, University of Glasgow). Media requirements: RPMI 1640 (21875 Gibco) supplemented with 10% FCS (HyClone, Perbio), 100µg/ml Penicillin/Streptomycin (15140 Gibco), 2mM Glutamine (25030 Gibco).

2.1.1.2 Primary cells and media

2.1.1.2.1 CD34+ human cord stem cells

Human CD34+ cord blood cells are hematopoietic stem cells. They are primary undifferentiated cells having the ability to differentiate into different hematopoietic lineages²¹⁶. Human cord blood CD34+ cells were gifted by Anna Kilbey (University of Glasgow). Media requirements: Stem Span medium (Stem cell technologies) supplemented with FGF-1 10ng/ml (Miltenyi), SCF 20ng/ml (Miltenyi), TPO 10ng/ml (Miltenyi), IGF BP2 100ng/ml (Miltenyi), ANGPTL5 500ng/ml (Miltenyi), Heparin 10µg/ml (Sigma), 100µg/ml Penicillin/Streptomycin (15140 Gibco), 2mM Glutamine (25030 Gibco).

2.1.1.2.2 Peripheral blood mononuclear cells (PBMCs)

PBMCs comprise mononucleated cells e.g. lymphocytes (i.e. both T and B lymphocytes and Natural killer cells), monocytes and dendritic cells. The PBMCs were obtained in two batches; the first from Cambridge Bioscience and the

second from the University of Glasgow Transfusion service. The cells were spun at 100g for 10 minutes. The cells were then plated at a density of 1×10^6 cells/ml in RPMI (21875 Gibco) supplemented with 10% FCS (HyClone, Perbio), 100µg/ml Penicillin/Streptomycin (15140 Gibco), 2mM Glutamine (25030 Gibco), 5µg/ml PHA (Sigma) and 200units/ml human IL2 (Peprotech) for 3 days at 37°C and 5%CO₂. On Day 3, the cells were washed in RPMI and were further grown in RPMI supplemented with 200 units/ml IL2 or were frozen in 10% DMSO with 90% FCS (HyClone, Perbio).

2.1.1.2.3 Primary human childhood leukaemia cancer cells

Primary human childhood leukaemia cancer cells were donated by Pamela Kearns (University of Birmingham). They were grown in RPMI (21875 Gibco) supplemented with 10% FCS, IL3 (MACS 130-093-908), 100ng/ml, IL7 (MACS 130-093-937) 100ng/ml, IL10 (MACS 130-093-947) 100ng/ml and FLT3L 100ng/ml (Peprotech).

2.1.1.3 Viruses

Xenotropic murine leukaemia virus (XMLV) rescued from BALB/c mice.

FeLV molecular Clone (pFGB).

FeLV B wild-type (PENHF) and gycoGag mutant (PENHFX).

2.1.2 Chemically competent bacteria

E. coli One-shot TOP10: (Invitrogen). Genotype: F⁻ *mcrA* Δ (*mrr-hsdRMS-mcrBC*) Φ80 *lacZ*ΔM15 Δ*lacX74 deoR recA1 araD139* Δ(*ara-leu*)7697 *galU galK rpsL* (Str^R) *endA1 nupG*.

2.1.3 Commercial kits

2x Power SYBR green RT PCR kit (4368702, Applied Biosciences)

2x Reddy mix PCR master mix (AB 0575, Thermo)

DNeasy blood and tissue kit (69506, Qiagen)

ECL western blotting detection reagents (Amersham Biosciences)

EndoFree plasmid maxi kit (12362, Qiagen)

Lipofectamine transfection kit (Invitrogen) stored at 4°C

Pfu Ultra II Hotstart PCR master mix (600850, Agilent technologies)

QIAprep Spin Miniprep kit (27104, Qiagen)
QIAquick gel extraction kit (28704, Qiagen)
QIAquick PCR purification kit (28704, Qiagen)
QuantiTect reverse transcription kit (205310, Qiagen)
Quick ligation kit (M2200S, New England Biolabs)
Reverse transcriptase kit (Qiagen)
RNeasy mini kit (74104, Qiagen)
Topo TA cloning kit (K4575-J10, Invitrogen)

2.1.4 Buffers, solutions and reagents

10x TBST (Tris buffered saline tween) buffer solution: 0.1M Tris base, 1.5M NaCl, 0.5% Tween-20, pH 8.0.

1M Tris HCl: 121g Tris base, 800ml dH₂O. Adjust pH with concentrated HCl and made up to 1L.

20x NuPAGE MOPS SDS running buffer: Available commercially. Make 1x solution for use.

20x SSC buffer: 3M NaCl in 0.3M sodium citrate (pH 7.0).

50x TAE (Tris-acetate-EDTA) buffer solution: 2 M Tris base, 50mM Na₂EDTA, 1M glacial acetic acid.

Ammonium persulphate: 10% (w/v) stock solution in dH₂O, freshly made.

DNA loading buffer: 30% glycerol, 0.25% (w/v) bromophenol blue, 0.25% (w/v) xylene cyanol, in dH₂O. Stored at room temperature and used at a 1:5 dilution.

Ethidium bromide: Working solution 3mg/ml. Stored at room temperature in the dark.

NuPAGE blot transfer buffer: For one gel, 20ml of 20x NuPAGE transfer buffer, 40ml methanol and 0.4ml NuPAGE antioxidant was added to a final volume of 400ml dH₂O. To prepare transfer buffer for two gels transferred simultaneously, add 20ml of 20x NuPAGE transfer buffer, 80ml methanol and 0.4ml NuPAGE antioxidant in a final volume of 400ml in dH₂O.

NuPAGE top tank buffer: Add 500µl of NuPAGE antioxidant to 200ml of 1x NuPAGE MOPS SDS buffer.

NuPAGE reducing agent (Life Technologies).

Phosphate buffered saline (PBS): 140mM NaCl, 2.7mM KCl, 10mM Na₂HPO₄, 1.8mM KH₂PO₄ (pH 7.3).

Protein loading buffer: I added 5µl NuPAGE LDS sample buffer (4x, Life Technologies) and 2µl NuPAGE reducing agent (10x) to samples in a 20µl final volume. I then heated the samples at 70°C for 10 minutes before loading.

Stripping solution: 20ml 2M glycine pH 2.5, 20ml 10% SDS to 160ml dH₂O.

Taqman lysis buffer (TLB): Tris HCl pH 8 (20mM), IGEPAL (0.9%), Tween 20 (0.9%), dH₂O.

TE buffer: 10mM Tris-HCl, 1mM Na₂EDTA pH 8.0

Whole cell lysis buffer: Hepes pH7 (20mM), EDTA (5mM), EGTA (10mM), NaF (5mM), DTT (1mM), KCL (0.4M), Triton-X-100 (0.4%), Glycerol (10%), dH₂O, Okadaic acid 0.1µg/ml (Merck), Pepstatin A 5µg/ml (Sigma), Leupeptin 5µg/ml (Sigma), PMSF Phenyl methane sulfonyl fluoride 50µg/ml (Sigma), Benzamidin 1mM (Sigma), Aprotinin 5µg/ml (Sigma).

Biorad protein dye reagent: for protein estimation (Bio Rad, USA).

Matrigel: for preparation of cells for xenografting (354230 Becton Dickinson, Europe)

Rapid-hyb buffer: for use with radiolabelled probes (GE Healthcare Amersham)

RNaseZap: RNase decontamination solution (AM9780, Life technologies).

Trypsin-EDTA (Invitrogen) 0.5% 1x liquid, stored at -20°C.

Ultra pure X-Gal (Invitrogen) stored as solid at -20°C.

LB based agar medium powder (fas-s, InvivoGen).

LB (Luria Bertani) medium: 20g of LB powder (Sigma) was added and mixed with 1 litre of water until a uniform solution was formed. 200ml was aliquoted into glass bottles and autoclaved at 121°C for 15 minutes and stored at 4°C. 200µl (100mg/ml) ampicillin was added to 200ml before use.

SOC media: 2% tryptone, 0.5% yeast extract, 10mM NaCl, 2.5mM KCl, 10mM MgCl₂, 10mM MgSO₄, and 20mM glucose (Invitrogen, UK).

Water soluble oestrogen: (E4389-100MG Sigma).

2.1.5 Enzymes

Antarctic phosphatase enzyme (M0289S, NEB)

BamHI restriction enzyme (R3136S, NEB)

EcoRI restriction enzyme (Invitrogen)

EcoRV restriction enzyme (Promega)

2.1.6 Antibiotics

Puromycin (Sigma), stored as 5mg/ml solution at -20°C.

Ampicillin (Sigma) 100mg/ml stored at -20°C.

2.1.7 Antibodies

Mouse anti-human HLA-ABC antibody (BD 560965/FITC).

APC mouse anti-human CD54 antibody (559771, BD Biosciences).

Mouse monoclonal antibody VPG19.1 against FeLV p27^{Gag} and also Pr65^{Gag} precursor protein. VPG19.1 was gifted by Brian Willett, University of Glasgow.

Goat anti-mouse IgG antibody with HRP conjugated to it (P0260, DAKO UK Ltd).

Rat IgG monoclonal antibody R187 against p30^{Gag} capsid (CA) polypeptide of MLV and also Pr65^{Gag} precursor protein²¹⁷. R187 was gifted by Sam Wilson, University of Glasgow.

Anti-rat IgG antibody with HRP conjugated to it (A9037-1ML, Sigma).

APC mouse IgG1 antibody (555751, BD Biosciences) used as an isotype control.

2.2 Methods

2.2.1 Infecting cells with virus

2.2.1.1 Infecting cancer cell lines with virus

The source of FeLV B for infection was supernatant from FeLV B infected AH927 cells (unless specified). The source of XMLV (*Bxv1*/BALB/c origin) was supernatant from MCF7 cells infected with XMLV (unless specified). Wild-type and glycoGag mutant FeLV B Plasmids (PENHF and PENHFX) were used to transfect 293T cells (described later). These 293T cells transfected with PENHF and PENHFX FeLV B were the source of normal and glycoGag mutant FeLV B for glycoGag experiments. Viral infections were carried out by growing the virus producing cells (MCF7 or 293T or AH927 cells) at 2×10^5 /ml medium in a T25 flask and taking off the supernatant after 48 hours of culture and using filtered (0.45µm) supernatant to infect fresh cells. Fresh medium was added after 2 hours of infection and cells were grown for at least 14 days (unless specified) before extracting DNA. Pellets were made and stored in -80°C freezer.

2.2.1.2 Infecting human CD 34+ cells

To infect human CD34+ cord blood stem cells, 4 wells in a 24 well plate were coated with retronectin and left at 4°C overnight. On the next day the retronectin was completely drained off using a pipette tip. Then 0.9ml of fresh filtered (0.45µm filter) virus containing supernatant was added to each well. The plate was then spun for 60 minutes at 4°C at speed of 2000g in an Eppendorf centrifuge. The viral supernatant was removed and 0.5ml of fresh viral supernatant was added to each well and spun again at 2000g for 60 minutes at 4°C. CD34+ cells suspended in 0.5ml cell span medium with 2x cytokines were added to each well supplemented with 8µg/ml polybrene and incubated at 37°C for 7 hours. After 7 hours, the medium was removed (cells adherent to retronectin) and replenished with 0.5ml fresh cell span medium with 1x cytokines (as described earlier) and incubated overnight at 37°C with 5% CO₂. On the next day, 0.5ml fresh filtered (0.45µm) viral supernatant with 1x cytokines was added and left for 6 hours at 37°C. Medium was transferred into a 15ml Falcon tube. The wells were rinsed with PBS and added to Falcon tubes. 0.5ml of dissociation buffer was added to each well and left for 2-3 minutes, then added to Falcon tubes. The wells were then rinsed twice with 1ml fresh cell span medium and transferred to Falcon tubes. The volume in each Falcon tube was then made up to 9ml and spun at 1000 rpm with no brakes for 5 minutes. The cells were resuspended in 0.5ml cell span with cytokines. The cells were incubated for 40 hours, then harvested and pellets made for DNA extraction with a DNeasy blood and tissue kit (Qiagen) according to the manufacturer's instructions. Standard PCR was carried out using appropriate primers and thermal cycling conditions given in the Appendix 1.

2.2.1.3 Infecting PBMCs

To infect PHA treated PBMCs, 1x10⁶ cells were suspended in filtered (0.45µm) virus supernatant (FeLV B molecular clone, XMLV, PENHF and PENHFX FeLV B) and incubated for 6 hours at 37°C and 5% CO₂. The PBMCs were then washed in RPMI and grown in RPMI with 200 units/ml human IL2 for 2 weeks at 37°C and 5% CO₂. 2ml cell supernatant was harvested at Days 3, 7, 10 and 14 and immediately frozen in dry ice and stored at -80°C. Cell supernatant at Day 14 was titrated on QN10 cells as described later. Cell supernatant was also used to

infect MCF7 cells. XMLV supernatant was titrated on MCF7 cells as described later. The PBMCs were harvested at Day 14 and cells pellets made for DNA and RNA extraction using appropriate kits as described later. Standard PCR was carried out using appropriate primers and thermal cycling conditions given in Appendix 1.

2.2.2 Confirmation of virus infection

2.2.2.1 DERSE assay

3×10^4 cells/ml were seeded in 6 well plates (2ml per well). After 72 hours, supernatant was removed from the DERSE cells and replaced with 100 μ l virus supernatant (virus dilutions for FeLV B and XMLV) and 300 μ l fresh medium. 0.5ml of medium was added after one hour. The whole medium was replaced the following day with fresh medium (2ml). GFP expression was monitored every 3-4 days for a total period of 3 weeks using fluorescence microscope.

2.2.2.2 Standard PCR

Standard PCR was carried out using Reddy mix (AB 0575 Thermo) according to manufacturer's instructions. A G-Storm Thermal Cycler was used for cycling. Agarose gel (16500-500 Invitrogen) electrophoresis carried out with ethidium bromide used to stain the gel. Different sets of primers used to detect and confirm viral infection along with the thermal cycling conditions are given in Appendix 1.

2.2.3 Virus titration

2.2.3.1 QN10 assay

QN10 cells S+L- feline embryonic fibroblast cells were used as an assay to titrate FeLV. FeLV-producing cells were plated at a density of 2×10^5 /ml in a T25 flask (Corning). QN10 cells were counted and plated at 2×10^5 /plate in 4ml medium in gridded plates. These were incubated at 37°C overnight. The next day serial dilutions of cell free viral supernatant were prepared in medium supplemented with 4 μ g/ml polybrene. Medium was removed from the plates and replaced with 1ml of virus dilutions. Plates were returned to the incubator and shaken every 15

minutes for 2 hours. After 2 hours virus supernatant was removed and cells were fed with 4ml fresh medium. Foci were counted on Day 7-10 to calculate the virus titre.

2.2.3.2 Serial dilutions/infection of susceptible cells and PCR

For viruses which could not be titrated on QN10 cells, serial dilution and infection of susceptible cells was used as an alternative option. The viral supernatant was filtered using a 0.45µm filter and then serially diluted in suitable medium. The dilutions were then used to infect a susceptible cell line (MCF7 or 293T). DNA extraction was carried out using a Qiagen DNeasy blood and tissue kit as described earlier. Standard PCR using the primers for virus detection were used (given in Appendix 1).

2.2.4 Xenografting human cells into mice

Female BALB/c mice and nude mice were obtained from Charles River. In one experiment they were fed on oral oestrogen (E4389-100MG Sigma, 1µg/ml) treated drinking water for at least a week before inoculations were performed. MCF7 cells (5×10^6 cells) suspended in 50µl Matrigel (354230/BD) were inoculated into the BALB/c nude mice. Both subcutaneous and intramammary xenografting was carried out. In another experiment, slow release oestrogen pellet (SE-121 Innovative research of America) was implanted subcutaneously into BALB/c and NSG mice one day prior to MCF7 intramammary xenografting. The NSG mice were also obtained from Charles River UK Ltd (Margate), and bred locally in the Veterinary Research Facility, University of Glasgow.

THP-1 cells (10^6 cells) suspended in 100µl PBS were inoculated IV via the tail vein into NSG mice (24 hours after 1Gy radiation) and into BALB/c nude mice.

Raji cells (10^6 cells) suspended in 100µl PBS were xenografted subcutaneously into BALB/c mice. All animal experimentation was carried out with appropriate ethical approval and a Home Office licence.

2.2.4.1 Processing post-xenografted cells

Cells derived from tumour masses in the liver and mouse blood cells following xenotransplantation were harvested. These cells, which contained a mixture of human (THP-1) cells and contaminating mouse cells, were grown in RPMI 1640 supplemented with 0.05mM 2-mercaptoethanol (Sigma M7522). Once they started growing, cell pellets were made for DNA and checked by PCR (G-Storm). Meanwhile, filtered supernatant from THP-1 primary tumour cells was used to infect 293T cells. These cells were checked for the presence of XMLV using primers for *env*¹⁷³.

MCF7 primary tumour cells were grown in MEM medium for 4 weeks. Once they started growing, flow cytometry (BD Accuri C6) and FACS (BD FACSAria) were carried out using mouse anti-human HLA-ABC antibodies (560965/FITC) to detect the percentage of human cells in the explant cells and to sort the human MCF7 cells from the mouse cells. Filtered supernatant from the post xenografted MCF7 cells was used to infect fresh MCF7 cells. These cells were checked for the presence of XMLV using primers for XMRV *gag* and XMLV *env*¹⁷³. Spleen DNA from BALB/c nude mice was used as a positive control. Filtered blood plasma was used to infect MCF7 cells which were later checked for XMLV infection by PCR. Blood was also grown in MEM medium to let any MCF7 cells grow out in culture. Post xenografted primary human childhood leukaemia cancer cells were donated by Pamela Kearns (University of Birmingham). These were grown in tissue culture (as described above) and supernatant was used to infect 293T cells. DNA was made from the infected 293T cells and checked for XMLV.

2.2.5 Molecular biology

2.2.5.1 DNA and RNA extraction from cells

DNA extraction was carried out using a DNeasy kit (69506 Qiagen). All DNA extraction work was carried out at the bench in the Molecular Oncology main laboratory. The surfaces were cleaned before and after DNA extraction and special care (e.g. changing gloves and using filtered pipette tips) were taken to avoid cross contamination between samples.

DNA extraction was carried out according to manufacturer's instructions. Cells (up to 10^6) were suspended in 200 μ l PBS. 20 μ l proteinase K (0.15mg/ml) was then added, followed by the addition of 4 μ l RNase. The cell suspension was

vortexed and left for 2 minutes at room temperature. 200µl of lysis buffer (AL) supplied in the kit was then added and the cell lysate vortexed and incubated at 56°C for 10 minutes. Then 200µl of 100% ethanol was added and the whole mixture vortexed. The mixture was then pipetted into a DNeasy mini spin column (supplied with the kit) and centrifuged for 1 minute at 8000 rpm. The flow through was discarded. The column was then washed using buffer AW1 and then buffer AW2. Finally DNA was eluted using buffer AE into a clean Eppendorf tube. Quantification was carried out using a Nanodrop spectrophotometer (Thermo Scientific). The DNA was used for PCR and stored at 4°C.

To carry out PCR directly from cells, Taqman Lysis buffer (TLB) was used. Cells were pelleted by spinning at 6000 rpm for 2 minutes. The supernatant was removed and the cell pellet stored at -20°C or lysis carried out immediately in TLB buffer. For lysis, the cell pellet was suspended in 10µl TLB with proteinase K (10mg/ml). The suspension was incubated for 1 hour at 55°C and heated at 95°C for 10 minutes to inactivate proteinase K. The cell lysate was used directly as a template for standard PCR reaction at 2µl/reaction.

RNA extraction was carried out using an RNeasy mini kit (74104 Qiagen). All the surfaces and pipettes were wiped with RNaseZap, an RNase decontamination solution (Life Technologies, AM9780). RNase free pipette tips and Eppendorfs were used throughout.

RNA was extracted according to the manufacturer's instructions. A cell pellet (maximum of 10^7 cells) was lysed using 350-600µl of lysis buffer (RLT) supplied with the kit. One volume of 70% ethanol was added to the lysate and vortexed. The lysate was then transferred into RNeasy mini spin column and spun at 8000 rpm for 15 seconds. This was followed by serial washes with buffer RW1 and buffer RPE, provided with the kit. Finally the RNA was eluted in RNase free water. Quantification was carried out using a Nanodrop spectrophotometer (Thermo Scientific) and Agilent 2100 Bioanalyzer. The RNA was stored at -20°C. cDNA was made from 1µg RNA using a Quantitect RT kit (205311, Qiagen).

2.2.5.2 DNA extraction from animal tissue (spin column protocol)

A DNeasy kit (69506 Qiagen) was used to extract DNA from animal tissues, including mouse tail tissue according to manufacturer's instructions as follows: 25mg tissue (10mg spleen) was cut into small pieces, ground down in liquid nitrogen and placed in a 1.5ml micro centrifuge tube. 180µl buffer ATL and 20µl

proteinase K were added and mixed thoroughly by vortexing, then incubated at 56°C until the tissue was completely lysed, vortexing occasionally during the incubation period to disperse the sample. Lysis usually took place within 1-3 hours. If the lysate appeared gelatinous then either the incubation period was extended or the amount of proteinase K was increased to 40µl, ensuring the sample was completely submerged in buffer containing proteinase K. RNase A (100mg/ml) was added, vortexed and incubated at room temperature for 2 minutes (liver and kidney have high levels of RNA while rodent tails have low levels). 200µl buffer AL was added to the sample and mixed thoroughly by vortexing, then 200µl ethanol (100%) was added and mixed again to produce a white precipitate. Extracted DNA was pipetted into a DNeasy mini spin column, placed in a 2ml collection tube and centrifuged at 8000 rpm for 1 minute. The mini spin column was placed in a new 2ml collection tube and 500µl buffer AW1 was added (provided in the kit) and spun for 1 minute at 8000 rpm. The mini spin column was placed in a new 2ml collection tube, 500µl buffer AW2 added and centrifuged at 14000 rpm to dry the DNeasy membrane. The mini spin column was placed in clean 1.5ml microcentrifuge tube and 200µl buffer AE pipetted directly onto the DNeasy membrane. The sample was incubated at room temperature for 1 minute and then spun for 1 minute at 8000 rpm. This procedure was repeated to increase yield. The DNA was quantified using a Nanodrop spectrophotometer (Thermo Scientific) and stored at 4°C.

2.2.5.3 cDNA synthesis

cDNA synthesis was carried out using a Qiagen reverse transcriptase kit (205311, Qiagen) according to manufacturer's instructions. The template RNA was thawed on ice. gDNA wipe-out buffer, Quantiscript reverse transcriptase enzyme and Quantiscript RT buffer (provided with the kit), RT primer mix and RNase free water were thawed at room temperature, centrifuged and stored on ice. Each DNA elimination reaction was prepared by adding 7 x gDNA wipe-out buffer, 1µg RNA, and water to make a total volume of 14µl and incubated for 2 minutes at 42°C. To prepare the reverse transcription mix, 1µl Quantiscript reverse transcriptase enzyme was added to 4µl Quantiscript RT buffer, 1µl RT primer, and all of the DNA elimination reaction (14µl) and incubated at 42°C for 15 minutes. The Quantiscript reverse transcriptase enzyme was inactivated by incubating at 95°C. The cDNA was stored at -20°C after adding the 20µl reaction

to 380µl PCR grade water (DEPC) and aliquoted 100µl into 0.5ml tubes at a concentration of 2.5ng/µl cDNA.

2.2.5.4 Southern blotting

Day 1

20µg of DNA was digested with 100 units of appropriate restriction enzyme in suitable buffer. The final volume was always less than 300µl. The samples were mixed gently so as not to damage the DNA and were incubated at 37°C overnight.

Day 2

The digests were vortexed and incubated again for 2 hours at 37°C. DNA was then precipitated by adding a half volume of 7.5M NH₄OAC and two volumes of ethanol e.g. to a 300µl digest, 150µl NH₄OAC and 900µl ethanol were added. The precipitate next was vortexed to mix. The digests were left for 20 minutes to precipitate and then the tubes were spun for 10 minutes at 13000 rpm in a microcentrifuge. The supernatant was then removed and the DNA pellet was air dried. The pellet was then resuspended overnight in 35µl TE buffer at 37°C.

Day 3

Resuspended digests were mixed and kept at 37°C. A 200ml 0.8% agarose TAE gel was then prepared and the gel was then poured into a cast with an appropriate comb. After the gel set, it was placed in the buffer tank in 1x TAE buffer. Loading dye was added to the samples to a final 1x concentration and a short vortexing followed by spinning was carried out. One or two lanes of markers (2µg λ HindIII and 500cpm/minute labelled λ HindIII markers, water and loading dye) were prepared. The samples were then loaded on the gel with markers in the outer lanes. An overnight electrophoresis was carried out at 22V.

Day 4

The gel was allowed to run until the bromophenol dye reached 2/3rd of the gel's length. The gel was then stained with ethidium bromide and visualised under a

UV transilluminator. DNA appeared as a continuous smear with no defined bands. The gel area above the wells, outside the markers and the bottom of the gel was cut and discarded. One of the corners of the gel was marked for orientation purposes. The gel dimensions were also measured. The gel was then placed in denaturation buffer for 30 minutes. The gel was next transferred into neutralisation buffer for 30 minutes. Meanwhile, two pieces of Whatman blotting paper were cut according to the gel size. One piece of Hybond N hybridisation membrane was also cut of the same size. One corner of the membrane was labelled with a pen for orientation purposes. A platform was prepared in a Pyrex dish containing 20x SSC buffer. The gel was placed facing down on 3 sheets of Whatman blotting paper wet with 20x SSC. Then Hybond N membrane was placed on top of the gel and all air bubbles were removed. Two pieces of Whatman blotting paper wet with 20x SSC buffer were placed on top of the gel and all air bubbles were removed. The area around the gel was covered and paper towels were placed at the top to draw 20x SSC via the gel and the membrane. A paperweight was placed on the top and the blot was left overnight.

Day 5

The capillary suction setup for the blot was dismantled the next day. The Hybond N membrane was then placed facing up on a dry piece of Whatman blotting paper. The DNA on the membrane was bonded by putting the membrane in Stratalinker set to work at optimal crosslink. The membrane was then stored in a dry place or was used for hybridisation using a suitable probe.

Probing the blot

The hybridisation oven was pre-warmed to 65°C and 10-15ml aliquot of Rapid-hyb buffer was heated. The Hybond N membrane was then made wet with 2x SSC buffer and placed in a hybridisation bottle. The excessive 2x SSC was poured away and replaced with warm Rapid-hyb buffer. It was then allowed to rotate slowly in the hybridisation oven at a rotation speed of 5-6 for 20 minutes. The probes were labelled in a supervised radiation room. DNA probe was labelled with ³²P-dCTP according to the manufacturer's protocol. The labelled probe fragment was purified by passing it through a NICK Column as described in the

protocol. The labelled probes were heated at 95-100°C for 5 minutes and then chilled rapidly on ice. 2×10^5 - 1×10^6 cpm/ml of probe was added to filter in the bottle avoiding direct contact with the filter. These were then mixed in the oven at a speed of 5-6 for 1-2 hours at 65°C. The probe was poured off down a suitable radiation sink. The membrane was then rinsed with 2x SSC and poured off without letting the membrane dry at any point. The pre-warmed wash buffer 0.1x SSC & 0.5% SDS was filled to 1/3rd the length of bottle. The bottle was then allowed to rotate in the oven at full speed for 20 minutes. The membrane was removed using 2x SSC and rinsed in 2x SSC. Keeping the membrane damp, it was transferred to a fold of transparent plastic. The plastic was sealed with heat after removing any liquid. The membrane was applied to a film and placed it in a cassette overnight. The corner of the film was cut to match that of the blot to allow orientation.

2.2.5.5 Western blotting

Lysate preparation

The cell pellet was first thawed on ice and then resuspended in 100µl lysis buffer per 10^6 cells. The lysates were then rotated for 10 minutes at 4°C. After this, the lysates were spun for 30 minutes at a speed of 13000 rpm at 4°C in a centrifuge. The supernatant was then removed into precooled 1.5µl tubes and the protein concentration was then determined. The lysates were stored at -80°C.

Protein estimation

To prepare a standard protein curve, a range of increasing BSA protein concentrations was prepared in water. Biorad protein dye reagent was diluted 1:5 in dH₂O and filtered through 1mm Whatman paper. Standard BSA protein solution (20µl) was then mixed with 1000µl of dye reagent in a plastic cuvette and read at OD 595nm against a water-blank in a plastic cuvette. The graph was plotted with OD 595nm on the Y-axis and protein concentration on the X-axis. To estimate the protein concentration of the lysates, 2µl of lysate and 18µl of dH₂O were added to a plastic cuvette along with 1000µl of protein dye reagent and was read as above. The protein concentration of samples were read directly

from the graph and multiplied by 10 (dilution factor) to get the actual protein concentration.

Preparing and running protein gels

800ml of 1x NuPAGE MOPS SDS running buffer was made from 20x stock. To make top tank buffer, 500µl of NuPAGE antioxidant was added to 200ml of 1x NuPAGE MOPS SDS buffer. 5µl NuPAGE LDS sample buffer (4x) and 2µl NuPAGE reducing agent (10x) were added to samples in a 20µl final volume. The samples were then heated at 70°C for 10 minutes.

At the same time, the gel pouch was cut open and packaging buffer was poured away. The gel was rinsed with ionised water. The tape at the bottom of gel cassette was peeled off. The comb from the gel was then gently removed in a single movement. The wells were then rinsed with 1x running buffer and then filled with top tank buffer removing any bubbles present. The buffer core was placed in the tank with electrodes on opposite sides. The unlocked tension wedge in the tanks was put behind the buffer core. The gel cassettes were then put in the tank on either sides of the buffer core with wells facing each other. In case of running one gel, buffer dam was used and was placed opposite to the gel. The gel was locked by pulling the lever on tension wedge. The top tank buffer was then poured in between the two gels and was checked for any leakage. Next the samples were loaded into the wells. Then 600ml 1x running buffer was poured into lower tank through the gap in the tension wedge. The lid on the tank then placed in its position. The gel was run at 200V for 50 minutes or until the dye front reached the bottom of the gel.

Protein transfer

400ml of 1x NuPAGE transfer buffer was prepared according to manufacturer's instructions. The Hybond ECL and 2 pieces of Whatman blotting paper were cut into 8.7cm x 7.7cm size for each gel. Blotting pads and Hybond ECL were soaked in 1x transfer buffer. The gel cassettes were removed from the buffer tank. The plates were split apart using a gel knife. The wells were then removed from the gel. A soaked Whatman blotting paper was placed on the gel and any bubbles removed. The gel was removed from the cassette and a soaked Hybond ECL was

placed on gel and the soaked Whatman blotting paper on top of it. All bubbles were removed. The gel sandwich was then put in a Blot Module in between pre-soaked blotting pads. The blotting module was then placed in a buffer tank and the tension wedge was locked. The transfer buffer was then poured into Blot Module to cover the gel-membrane sandwich. The outer chamber was filled with 650ml deionised water. The process of transfer was carried out at 30V for one hour.

Protein detection

The blot was blocked overnight in 5% milk in TBST buffer at 4°C and then washed for 10 minutes thrice with 1x TBST. After washing, the blot was incubated with primary antibody diluted in 5% milk in TBST. The blot was then washed for 10 minutes thrice with 1x TBST. The blot was then incubated with secondary antibody diluted in 5% milk in TBST. The blot was then washed again for 10 minutes thrice with 1x TBST. ECL detection solution (Thermo Scientific) was used according to manufacturer's instructions to detect proteins on the blot. The blots were evenly coated with the ECL solution and incubated for 4 minutes. The blot was then wrapped in Saran wrap and exposed to 18 × 24 cm Hyperfilm ECL (28-9068-36, Amersham) for 2 minutes. The film was then developed and assessed for intensity of the band. Longer exposures were carried out if needed.

2.2.5.6 XMLV and FeLV B proof reading PCR for sequencing

DNA made from MCF7 cells infected with XMLV was used as template for sequencing XMLV. Forward and reverse primers were designed based on N417 XMLV accession number HQ246218 and are given in Appendix 1. DNA made from cell lines and primary cells infected with FeLV B was used as template for sequencing FeLV B *pol* region. The primers used to amplify FELV B *pol* region are given in Appendix 1.

Pfu Ultra II Hotstart PCR master mix (600850, Agilent technologies) was used according to manufacturer's instructions to amplify the DNA. The thermal cycling conditions are given in the Appendix 1. A Reddy mix PCR step to add A-overhangs to the amplified PCR product followed this. To add A-overhangs, 5µl of Pfu PCR reaction, 7.5µl of distilled water, and 12.5µl Reddy Mix were added

together and this was heated for 10 minutes at 72°C. After this, the product was purified using QIAquick PCR purification kit (Qiagen, 28704).

2.2.5.7 PCR product purification

PCR product purification was carried out using a QIAquick PCR purification kit (Qiagen, 28704). PCR product purification was carried out according to the manufacturer's instructions. 5 volumes of buffer PB were added to 1 volume of PCR reaction mix. The mixture was then transferred to a QIAquick column and washed with buffer PE. Finally the DNA was eluted in buffer EB (10mM Tris.Cl, pH 8.5) or water. It could then be used for cloning purposes.

2.2.5.8 Preparation of agar plates

One sachet of LB based agar medium powder (fas-s, InvivoGen) was put into a conical flask and 200ml of water was added to it. It was then heated in microwave for 3 minutes. After cooling to room temperature, 200µl (100mg/ml) ampicillin was added and left for a few minutes to get rid of bubbles. It was then poured gently into 10cm² petri dishes. The petri dishes were kept slightly open for some time to let the agar set. Dishes were stored for up to two weeks at 4°C before use. Before use 40µl of 40mg/ml X-Gal in DMF (dimethylformamide) was added and spread with a spreader.

2.2.5.9 Transformation and cloning

Transformation was carried out using One Shot Top-10 chemically competent *E. coli* (C4040-10, Invitrogen). The PCR product to be cloned was ligated using a TA Topo cloning kit (k4575-j10, Invitrogen). 1µl of salt solution was added to 4µl of purified PCR product with A-overhangs (A-overhangs were added to PCR product by carrying out an extra Reddy Mix PCR step at 72°C for 12 minutes) and incubating it at room temperature for 5 minutes. 2µl of this was added to chemically competent *E. coli* without pipetting and then it was incubated for 10 minutes on ice. The *E. coli* cells were heat shocked at 42°C for 30 seconds without shaking and then immediately transferred to ice. 250µl of SOC solution was then added to the tube containing *E. coli* and the tube was shaken horizontally at 200 rpm at 37°C for 1 hour. 10 and 50µl of the transformation mix was then transferred onto pre-warmed X-Gal coated agar plates (20µl of SOC was

used to spread the 10µl transformation mix) and incubated at 37°C overnight. The next day, the plates were examined for any white colonies (blue colonies were discarded).

All the white colonies in the petri dish were marked and a number was assigned to each of them. A master plate was made from a fresh X-Gal coated agar plate. Slots for the number of white colonies that were going to be selected were made on the master plate. Each white colony was touched with a plastic loop and transferred to a slot on the master plate. Then the loop was dipped into LB medium in a bijou (2ml LB medium per Bijou). The same process was repeated with all white colonies. The master plate was kept inverted in an incubator at 37°C overnight. The Bijou was kept in a shaker at 37°C 200 rpm overnight. On the next day plasmid extraction was carried out.

2.2.5.10 **Plasmid extraction (Miniprep)**

For small scale plasmid extraction, a QIAprep Spin Miniprep kit (Qiagen, 27104) was used. Plasmid extraction was carried out according to manufacturer's instructions. The bacteria grown overnight were pelleted by centrifugation at 8000 rpm for 3 minutes at room temperature. The bacterial pellet was then resuspended in buffer P1 and transferred to a microcentrifuge tube. Buffer P2 was then added and mixed by inverting 4-6 times. Buffer N3 was then added and mixed thoroughly by inverting 4-6 times. Buffer P1, P2 and N3 were provided with the kit. The lysate was centrifuged for 10 minutes and the supernatant carefully removed. The supernatant was then applied to a QIAprep spin column and washed with buffer PB and buffer PE. The plasmid DNA was then eluted in buffer EB or water. Quantification was carried out using Nanodrop. The plasmids were then digested with EcoRI enzyme (15202013, Invitrogen) and run on an agarose gel. The gel was then imaged using a UV transilluminator. The appropriate plasmids were then sent to Source Bioscience for sequencing. Sequence data was analysed using CLC Genomics 5 software.

2.2.5.11 **Plasmid extraction (Maxiprep)**

For endotoxin-free large-scale plasmid extraction, an EndoFree plasmid Maxi kit (Qiagen, 12362) was used. Plasmid extraction was carried out according to

manufacturer's instructions. The overnight LB culture was centrifuged at 6000g for 15 minutes at 4°C. The pellet was then resuspended in 10ml buffer P1. 10ml buffer P2 was then added and the mixture incubated at room temperature for 5 minutes. 10ml of chilled buffer P3 was then added and the whole lysate was transferred into the barrel of a QIAfilter Cartridge and incubated for 10 minutes. The lysate was then filtered through the QIAfilter Cartridge using a plunger. 2.5ml of buffer ER was then added to the filtrate and incubated on ice for 30 minutes. The filtered lysate was then applied on a Qiagen-tip 500 and allowed to empty by gravity flow. The Qiagen-tip 500 was equilibrated with 10ml buffer QBT prior to adding the lysate. Qiagen-tip 500 was then washed twice with buffer QC. The DNA was then eluted with buffer QN in an endotoxin free tube. The DNA was then precipitated by adding 10.5ml isopropanol and centrifuged at 15000g for 30 minutes at 4°C. The supernatant was then decanted carefully. The DNA pellet was then washed with 5ml of endotoxin free 70% ethanol and centrifuged at 15000g for 10 minutes. The supernatant was then decanted and the pellet air dried for 5-10 minutes. The DNA was then dissolved in 200µl of buffer TE. The quantification was carried out using a Nanodrop. The plasmid could then be used for transfection.

2.2.5.12 **Restriction factor expression analysis**

Expression analysis of different restriction factors was carried out by qRT-PCR (described ahead). Expression of the following restriction factors was carried out: APOBEC3A, APOBEC3B, APOBEC3C, APOBEC3D, APOBEC3F, APOBEC3G, Tetherin, TRIM5 α , and SAMHD1. Restriction factor expression analysis was carried out for the following cell lines and primary cells: 293, CEM, CEMSS, THP-1, PBMC, Reh, Raji and Kyo1 cells. The primers assays used for qRT-PCR were ordered from Qiagen and are shown in Table 2.1.

Table 2.1 qRT-PCR assays for expression of restriction factors

Primer assay	Catalogue no.
APOBEC3A	QT00042763
APOBEC3B	QT00040733
APOBEC3C	QT00058198
APOBEC3D	QT00044639
APOBEC3F	QT00045262
APOBEC 3G	QT00070770
SAMHD1	QT00084322
BST2 (TETHERIN)	QT00019663
TRIM5 α	QT01028125

Table 2.1 showing the qRT-PCR assays used to determine the expression of different restriction factors.

2.2.5.13 Validation of microarray data

The validation was carried out by qRT-PCR as described ahead. The primers assays used for qRT-PCR validation were ordered from Qiagen and are shown in Table 2.2.

Table 2.2 qRT-PCR assays for microarray validation

Primer assay	Catalogue no.
CCL4	QT01008070
EGR1	QT00218505
TSPAN2	QT00046480
PCOLCE2	QT00003479
IL7R	QT00053634
SLC30A4	QT00031255
IFI44	QT00014399
CCNB1	QT00006615

Table 2.2 showing the qRT-PCR assays used to validate the microarray data.

2.2.5.14 XPR1 expression analysis

XPR1 expression analysis was carried out for the following cell lines and primary cells: CEM, CEMSS, Kyo1, Jurkat, Reh, K562, 293, PBMC, MCF7, THP-1, and mouse cells (negative control). Human XPR1 QuantiTect primer assay (QT01882741, Qiagen) was used for this analysis was carried out by qRT-PCR as described below.

2.2.5.15 **Real Time PCR**

Real time PCR was carried out using SYBR Green (1112324, Applied Biosciences) on a 7500 ABI RT PCR system. Anne Terry assisted in some Real Time PCR experiments. All primers were ordered from the Qiagen. Each primer was diluted in DEPC water to make a 6 μ M 10x master stock. The forward and the reverse primers were then mixed in 1:1 to make a 5x primer mix. To get a final 0.6 μ M (1x) concentration, 5 μ l of this primer mix was used per 25 μ l of reaction. 100ng cDNA was used for each reaction. Human genomic DNA (4ng/ μ l) was used as a “no amplification control”. Water was used as a “no template control”. Human HPRT primers were used as endogenous control primers. A plate map was used to plan sample position on the plate. Each sample was plated in triplicate. Standard cycling conditions were used with an additional dissociation stage. Results were analysed on 7500 system software.

2.2.5.16 **Gel electrophoresis and UV imaging**

PCR products and digested DNA were analysed by running on agarose gel by electrophoresis. A 1% agarose gel was made by adding ultrapure agarose powder (16500-500, Invitrogen) in 1x TAE buffer. This was then heated until the agarose melted completely. Then 10 μ l ethidium bromide (10mg/ml) was added. It was then poured into appropriate sized casts with comb. Once the gel was set, it was then placed in tanks containing 1x TAE buffer. Samples were mixed with 10x loading dye. An appropriate size ladder (100bp or 1kb) was also loaded beside the samples on the gel. Gel electrophoresis was carried out for an hour at 110V/75mA. The gel was then visualised using a UV transilluminator (Syngene Bio imaging, Cambridge) and a digital image was recorded. If needed, the DNA bands were excised and extracted.

2.2.5.17 **Gel extraction**

Gel extraction was carried out using a QIAquick gel extraction kit (Qiagen, 28704). Gel extraction was carried out according to manufacturer's instructions. After cutting the selected bands on an agarose gel with a clean sharp scalpel under UV light, the slice was weighed and then 3 volumes of buffer QG was added. It was then incubated at 50°C for 10 minutes or until the gel became completely dissolved with constant vortexing after 2-3 minutes. Then 1 volume

isopropanol was added and mixed. The whole mixture was then transferred to a QIAquick column and washed with buffer QG and buffer PE according to manufacturer's instructions. Finally the DNA was eluted in water or buffer EB (provided with the kit).

2.2.5.18 **Designing the XMLV probe for southern blotting**

A probe was designed to carry out southern blot of XMLV infected cells. The primers used for the probe along with the thermal cycling conditions are given in the Appendix 1. The PCR product was purified using PCR purification kit according to manufacturer's instructions as described earlier. The cleaned PCR product was run on a 1% agarose gel and visualised under a UV transilluminator to confirm the appropriate size of the probe. The probe was stored at -20°C.

2.2.5.19 **GlycoGag sequencing**

Primers were designed on the basis of the FeLV B *gag* sequence and are given in Appendix 1. Plasmids for wild-type (PENHF) and glycoGag mutant FeLV B (PENHFX) were sent to Source BioScience for sequencing.

2.2.5.20 ***Mycoplasma* detection**

Primers used to detect *Mycoplasma* by PCR are given in Appendix 1. The *Mycoplasma* status was also confirmed by a commercial kit, Venor-Gen (Minerva Biolabs).

2.2.5.21 **XMLV *env* cloning**

2.2.5.21.1 Designing primers

Primers were designed with and without restriction sites to amplify XMLV *env*. The primers are given in the Appendix 1.

2.2.5.21.2 XMLV *env* amplification by nested PCR

Pfu Ultra II Hotstart PCR master mix (Agilent technologies, 600850) was used according to manufacturer's instructions to amplify XMLV *env* from XMLV infected MCF7 cell DNA. In the first round of nested PCR, the primers without restriction enzyme site (F4 and R1) were used. The thermal cycling conditions

are given in the Appendix 1. 1µl PCR product from the first round was used in the 2nd round of nested PCR. The primers used in the 2nd round were F4-BamHI and R1-Sall. The same cycling conditions were used for the 2nd round as well. After adding A-overhangs to the PCR product from the 2nd round, PCR purification using a QIAquick PCR purification kit, ligation using a TA Topo cloning kit and transformation of One Shot *E. coli* was carried out as described earlier. Plasmid extraction was also carried out using a QIAprep Spin Miniprep kit (Qiagen, 27104) as described earlier.

2.2.5.21.3 Digestion of plasmids

The plasmid DNA was digested using BamHI restriction enzyme (NEB, R3136S). 5µg of plasmid DNA was incubated with 1µl of BamHI enzyme and 2µl of 10x Cutsmart buffer for 1 hour at 37°C. In a similar fashion, 5µg pBabe vector was also digested with 1µl of BamHI enzyme.

2.2.5.21.4 Phosphatase treatment

The digested pBabe vector (5µg) was treated with 1µl of Antarctic phosphatase enzyme (M0289S, NEB) to prevent spontaneous re-ligation of cut ends. Incubation was carried out at 37°C for 15 minutes. To inactivate the enzyme, it was then heated for 5 minutes at 65°C.

2.2.5.21.5 Ligation of XMLV *env* and pBabe vector

PCR purified and BamHI digested XMLV *env* (50ng) insert was ligated with phosphatase treated pBabe vector (64ng) using a T4 DNA ligase enzyme (NEB, M2200S) kit according to manufacturer's instructions. The incubation was carried out for 5 minutes at room temperature. The ligation mix was then used directly for transforming One Shot chemically competent *E. coli* as described earlier. The plasmid extraction was carried out using a QIAprep Spin Miniprep kit (Qiagen, 27104) as described earlier. The plasmid was digested with EcoRI and run on agarose gel to check the size of insert. To determine the orientation of the insert, plasmid was sent to Source BioScience for sequencing.

2.2.5.21.6 Transfection of 293T cells

293T cells were transfected using a Lipofectamine Transfection Reagent kit (Invitrogen, 18324-012). First of all, 6µg DNA plasmid (to be transfected) was diluted in 300µl serum free medium. Then the PLUS reagent (provided in the kit)

was vortexed and 48 μ l of it was added to the diluted DNA. This DNA mixture was vortexed and then incubated at room temperature for 15 minutes. 12 μ l Lipofectamine reagent (provided in kit) was diluted in 300 μ l serum free medium and then vortexed. The pre-complexed DNA mixture and the diluted lipofectamine were combined and vortexed and then incubated at room temperature for 15 minutes. Then 2.4ml serum free medium was added per transfection mix and the entire contents transferred to a 60mm dish of cells (media removed). The cells were incubated for 3 hours after which 3ml fresh media containing 2x FCS was added to it. On the Day 3 (72 hours later) the cells were split in 1:10. The cells were kept growing for at least 14 days. DNA was then extracted to be checked by PCR for successful transfection.

2.2.5.22 **Specific infectivity XMLV and FeLV B**

CEM, CEMSS, Kyo1, THP-1, Reh and 293T cells were infected with XMLV multiple times to saturate the cells. The supernatant was used to prepare the virus pellet and also to titrate onto 293T cells. Cell pellets were prepared for protein, DNA and RNA analysis.

CEM, CEMSS, Kyo1, THP-1, Reh, AH927 cells were infected with FeLV B multiple times to saturate the cells. The supernatant was used to prepare the virus pellet and also to titrate on QN10 cells. Cell pellets for protein, DNA and RNA analysis were prepared.

Kyo1 cells were infected with PENHF and PENHFX (wild-type and glycoGag mutant FeLV B respectively) multiple times to saturate the cells. The supernatant was used to obtain the virus pellet and also to titrate on QN10 cells. Cell pellets were prepared for protein, DNA and RNA analysis.

2.2.5.23 **Wound assay**

MCF7 cells (both infected and non-infected) were seeded (at 1x10⁶ cells/well) in a 6 well plate and were grown to confluence. A wound was made with a pipette tip, washed with PBS and fresh medium added. The cells were grown for another three days and serial images were taken at regular intervals using Leica camera and software. The wound size was measured using Image J and a graph was plotted using Microsoft Excel.

2.2.5.24 **Ficoll separation of viable cells**

The cells were spun and resuspended in 5ml of medium. The cells were layered very slowly and gently, on to 5ml Ficoll (Sigma) so that the two layers were separated with an interface. The mixture was then spun for 10 minutes at 3000rpm (brakes at 5). The viable cells formed a white granular layer at the interface of the medium and Ficoll layers. The viable cells were carefully removed with a pipette while holding the tube with the interface at eye level. The viable cells were washed twice with 10ml of medium by spinning at 1000 rpm for 5 minute to remove Ficoll. The cell pellet consisting of viable cells was obtained. The cells were resuspended in fresh medium, were counted and then plated.

2.2.5.25 **Flow cytometry and fluorescence activated cell sorting (FACS)**

Flow cytometry and FACS were carried out using BD Accuri C6 flow cytometer and BD FACSAria cell sorter respectively. Adherent cells were harvested using trypsin and it was ensured that cells were separated from each other by pipetting them up and down several times. This was followed by three washes (three cycles of spinning and re-suspension in 0.1% BSA +PBS). BSA was prepared on the same day and was chilled by keeping in the fridge for at least an hour before use. 1×10^7 cells/ml were suspended using PBS+0.1% BSA and $50 \mu\text{l}$ (5×10^5 cells) and was put into flow cytometry/ FACS tubes (Falcon 12mm x 75mm tubes). $1 \mu\text{l}$ Fc block antibody was added per tube in order to prevent non-specific binding. Cells were incubated with this antibody for 10-15 minutes in the fridge in the dark. The specific antibody (e.g. anti HLA-antibody) was then added to the samples without any washes and incubated in the dark in the fridge for 30 minutes. The cells were washed twice using 0.1% BSA +PBS. Finally they were resuspended in 0.5ml 0.1%BSA+PBS and strained using a $70 \mu\text{m}$ strainer (BD $70 \mu\text{m}$ Strain) into a fresh tube on ice. The rack was then wrapped in foil and placed in the fridge to do flow cytometry in 3 hours. Non-antibody control sample and an isotype antibody control samples were also prepared. In case of FACS, collection tubes (15ml Falcon with 5ml medium) were prepared and kept on ice. Approx. 2.5×10^5 cells were collected (takes 15min) into the collection tube. Sorted cells were grown in T25 flask in 5ml warm medium and kept at 37°C and 5% CO_2 in a tissue culture incubator.

2.2.5.26 **Single cell cloning of MCF7 XMLV cells**

MCF7 single cell cloning was carried out by serial dilutions (Corning). MCF7 XMLV single cell suspension (1×10^5 cells/ml) was prepared. First the dispensing tray was filled with 12ml of conditioned medium (50% fresh medium and 50% conditioned medium from uninfected MCF7 cells) and then using an 8-channel pipette, 100 μ l of medium was added to all the wells in 96 well plate except A1 which is left empty. 200 μ l of cell suspension was added to well A1. Using a single channel pipette, 100 μ l was transferred from the first well to the second well (B1) and 1:2 dilutions were repeated down the entire column discarding 100 μ l from the last well (H1). Using an 8-channel pipette 100 μ l of fresh medium was transferred to each well in column 1. Then 100 μ l from wells in the first column was transferred to the second and this was repeated for each column, discarding 100 μ l from each well in the last column (A12-H12). The final volume of each well was made up to 200 μ l by adding fresh medium. The cells were incubated at 37°C in 5% CO₂. Wells with single cells were marked the next day and grown for 10 days. Medium was replaced with conditioned medium after every 3-4 days. Cells were transferred to a 24 well plate after 10 days then subsequently to a 12 well plate and were further expanded as required. DNA was extracted and southern blotting carried out. The pattern of XMLV insertion was observed and compared with the MCF7 XMLV from BALB/c mice.

2.2.5.27 **Affymetrix RNA expression Array**

MCF7 cells and Raji cells were grown in two sets of three T25 flasks at 2×10^5 cells/ml. One set was infected with XMLV supernatant filtered with a 0.45 μ m filter. Both sets were kept under the same conditions for 15 days after infection. DNA was made using a Qiagen DNeasy kit and the XMLV infection was confirmed by PCR. RNA was prepared using a Qiagen RNeasy kit according to manufacturer's protocol. The concentration was measured by Nanodrop and Bioanalyzer. The RNA samples were analysed by Atlas Biolabs (Germany). Affymetrix Expression Profiling was carried out using GeneChip Human Gene 2.0 ST Array.

2.2.5.28 Analysis of data

Primer designing and alignment & analysis of sequence data was carried out using CLC Genomics Workbench 5 software. The National Centre for Biotechnology Information (NCBI) online Basic Local Alignment Search Tool (<http://blast.ncbi.nlm.nih.gov/>) was used to search the *de novo* rescued viral sequences for similarity. Phylogenetic trees were generated by the neighbour-joining method with bootstrap analysis at 100 replicates using CLC Genomics Workbench 5 software. The Los Alamos National Laboratory online tool for hypermutation analysis²¹⁸ was used to analyse hypermutations. The data for flow cytometry and FACS were analysed using CFlow Plus and FlowJo software respectively. Microsoft Excel was used to perform basic statistical data analysis. Image J was used to analyse wound size in wound assay and for western blot densitometry. Ingenuity Pathway Analysis online (IPA) was used to analyse gene expression data. 7500 ABI software was used to analyse RT PCR data.

3 Infection of human xenografts with XMLV

3.1 Introduction

The use of human-mouse xenografts is an important research tool in many fields of biological research²¹⁹⁻²²¹. While infection of human xenografts with murine retroviruses is a long-standing observation^{170,171}, earlier experiments did not clearly demonstrate the risk of acquiring infection or the potential impact of these viruses as confounding factors. The recent emergence of XMRV as an apparent aetiological agent of several human diseases^{153,154,156,222-224} followed by discrediting of these claims with evidence that XMRV was a laboratory contaminant¹⁵⁸, led to a renewed interest in the role of murine retroviruses as xenograft contaminants. A recent study reported that up to 23% of human cancer cell lines that have undergone xenografting in mice were found to be infected with XMLV but at the same time 17% of non-xenograft derived cell lines in the same laboratory facility were also infected. As cells maintained in a xenograft-free laboratory facility were found to be uniformly free of XMLV, *in vitro* cross-contamination appeared to be the major source²⁰³. I therefore decided to carry out a prospective study of XMLV generation using two different mouse strains commonly used for xenograft study models.

The aim of the studies described in this chapter was to prospectively test whether xenografting human cancer cells into mice can lead to the infection of cancer cells by endogenous murine leukaemia viruses. A secondary aim was to test whether infection of xenografted cells is dependent on the type of cancer cells or the strain of mice used for xenografting. A further aim was to rescue and characterise any endogenous retrovirus that has infected cancer cell xenografts.

3.2 Materials and methods

Materials and methods have been discussed in detail in Chapter 2.

3.3 Results

3.3.1 MCF7 cells xenografted into BALB/c mice become infected with XMLV

To initiate my study on the risks of xenograft infection with endogenous murine retroviruses, I chose the MCF7 human breast cancer cell line which the host laboratory had previously shown was highly susceptible to infection with another gammaretrovirus, feline leukaemia virus (FeLV B). The chosen recipient strain was BALB/c as cells from this strain were shown in early studies to activate viruses with high efficiency in response to mitogen stimulation²²⁵. Eight BALB/c nude mice were used for xenografting. The inoculations were carried out on my behalf and in my presence by Susan Mason (Beatson Laboratories). In the literature both intramammary and subcutaneous sites have been used for MCF7 xenografting^{180,226}. In my experiment MCF7 cells (5×10^6) were inoculated into the intramammary region in six out of the eight BALB/c mice, while the remaining two BALB/c mice received subcutaneous inoculations. In order to test whether oestrogen had any impact on xenografting, mice receiving subcutaneous inoculations were kept on oral oestrogen dissolved in drinking water, while the mice receiving intramammary inoculations did not receive oestrogen. Only one mouse (out of 8) developed a tumour. The tumour developed in one of the two mice that received inoculation in the subcutaneous region (kept on oral oestrogen). None of the mice that received the intramammary inoculations (kept on non-oestrogen diet) developed any tumour. The mouse with the tumour was culled on the 74th day. The size of tumour was 0.6cm at that time as shown in Figure 3.1.

Figure 3.1 MCF7 BALB/c tumour explant



Figure 3.1 MCF7 tumour explant from a BALB/c mouse showing its size.

The tumour explant cells were dissociated by finely dissecting with a scalpel blade. The cell suspension was washed with fresh MEM medium and grown *in vitro* in tissue culture incubator at 37°C. Cells were passaged every 5 days. Flow cytometry with mouse anti-human HLA-ABC antibodies (BD 560965/FITC) was carried out (as described in Chapter 2) after the 5th passage. The results are shown in the Figure 3.2.

Figure 3.2 Flow cytometry of MCF7 explant cells

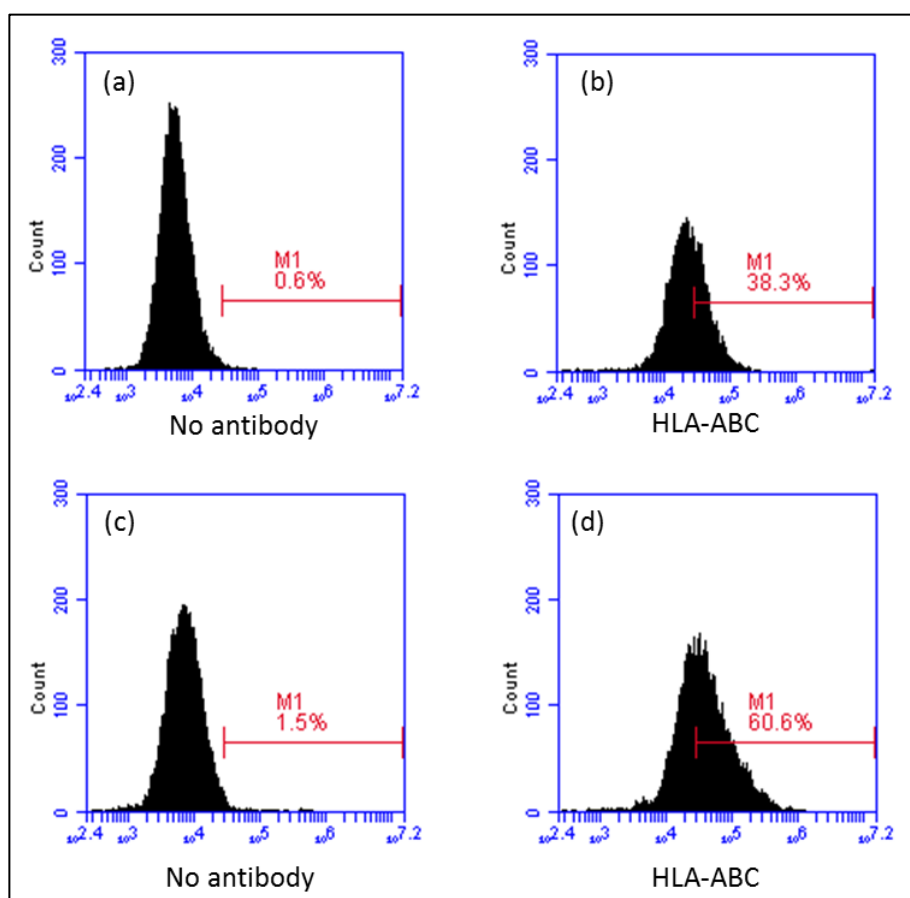


Figure 3.2 Flow cytometry of MCF7 explant cells using mouse anti-human HLA-ABC antibodies to determine the percentage of cells of human origin. (a) MCF7 cells with no antibody. (b) MCF7 cells with HLA-ABC anti-human antibody. (c) MCF7 explant cells with no antibody. (d) MCF7 explant cells with HLA-ABC anti-human antibody. Flow cytometry analysis was carried out using CFlow Plus software.

Figure 3.2 shows that the flow cytometry results confirmed that more than 50% of the explanted cells were of human origin. The next step was to see whether or not the explant cultures produced replication competent viruses. The DERSE assay was used for this purpose. The DERSE assay is of general use for the detection of replication competent gammaretroviruses. DERSE cells contain a vector in which GFP expression is interrupted by an intron. If the vector is spliced and packaged by an incoming retrovirus it may be transferred to a bystander cell where it will express intact GFP. If DERSE cells are exposed to replication competent gammaretrovirus, the cells would produce foci of green fluorescence under the fluorescence microscope. In this experiment DERSE assay was performed using filtered (0.45µm) supernatant taken from the explant cells. On the 5th day, GFP-positive green cells were seen under the fluorescence microscope as shown in Figure 3.3b indicating that the explant cells were releasing a replication competent gammaretrovirus.

Figure 3.3 DERSE assay for gammaretrovirus detection

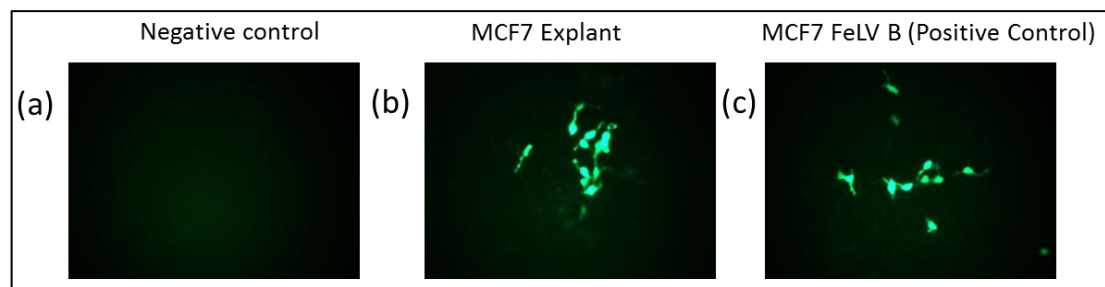


Figure 3.3 (a) DERSE cells exposed to filtered supernatant from uninfected MCF7 cells were used as a negative control. (b) DERSE cells infected with MCF7 explant supernatant. (c) DERSE cells infected with MCF7 FeLV B supernatant used as positive control.

The DERSE assay was carried out in triplicate and repeated on three separate occasions. The DERSE assay revealed that MCF7 primary tumour explant cells were releasing a replication competent gammaretrovirus. As the MCF7 primary tumour cells were contaminated with mouse cells, and there are many endogenous mouse retrovirus sequences in the mouse genome, the virus could not be directly identified from the explant cells by PCR. The virus released from the explant cells needed to be isolated first by passage to uninfected human cells before further characterisation. Fresh MCF7 cells (1×10^6 cells) were infected with filtered MCF7 primary tumour explant supernatant (10th passage). The infected MCF7 cells were grown for 14 days and DNA was extracted. The

likely identity of this virus as XMLV was demonstrated by PCR with specific primers as shown in the Figure 3.4.

Figure 3.4 PCR for detecting XMLV in BALB/c explants

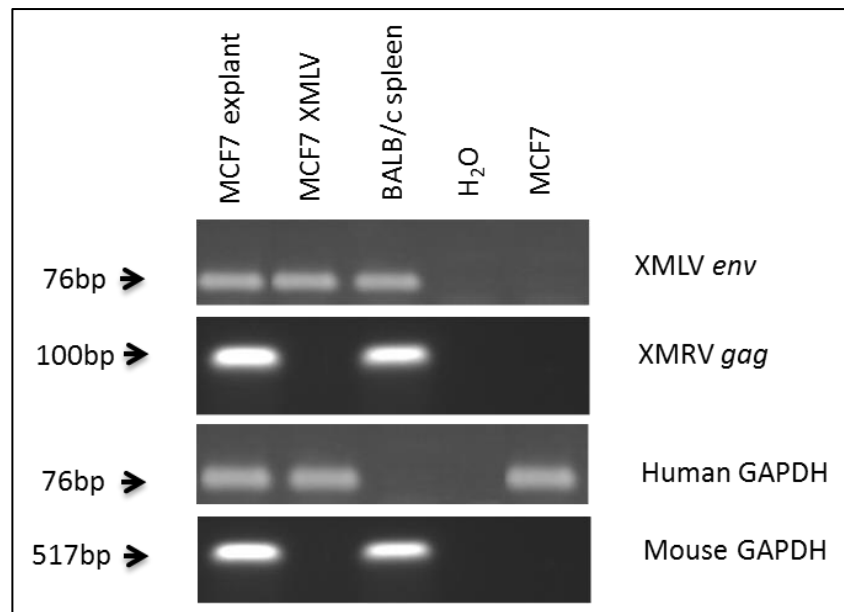


Figure 3.4 PCR using envelope primers specific for XMLV and *gag* primers specific for XMRV. Human GAPDH primers and mouse GAPDH primers were used as internal control for human and mouse DNA respectively. Non-infected MCF7 cells were used as a negative control.

In Figure 3.4, MCF7 explanted cells were positive when tested with XMLV primers. The MCF7 cells exposed to explant supernatant were also positive for XMLV *env* primers showing that explanted tumour cells were producing an infectious XMLV-like virus. Mouse tissues were also positive for both XMRV and XMLV-related sequences as demonstrated by a positive signal in BALB/c spleen mouse DNA because these viral sequences are present in the mouse germline. The MCF7 explant contained mouse tissue, which explains the positive signal with XMRV *gag* and mouse GAPDH primers, but infectious XMRV was not present in the explanted cells.

This experiment showed that naive MCF7 cells have been infected with an infectious virus related to XMLV that is released from MCF7 explant cells.

The Figure 3.2 showed that the MCF7 explant cells contained a good proportion of mouse cells in addition to the human MCF7 cells. In order to see if the MCF7 cells in the explant cells were infected with XMLV, fluorescence activated cell sorting (FACS) was carried out as described in Chapter 2 using anti-human HLA-

ABC antibody (BD 560965/FITC) as shown in Figure 3.5(a-c) and cells were grown for two weeks after FACS. DNA from the post FACS MCF7 cells was analysed by PCR for the presence of XMLV infection and the presence of mouse cells (Figure 3.5d).

Figure 3.5 FACS sorting of MCF7 explant cells and PCR after FACS

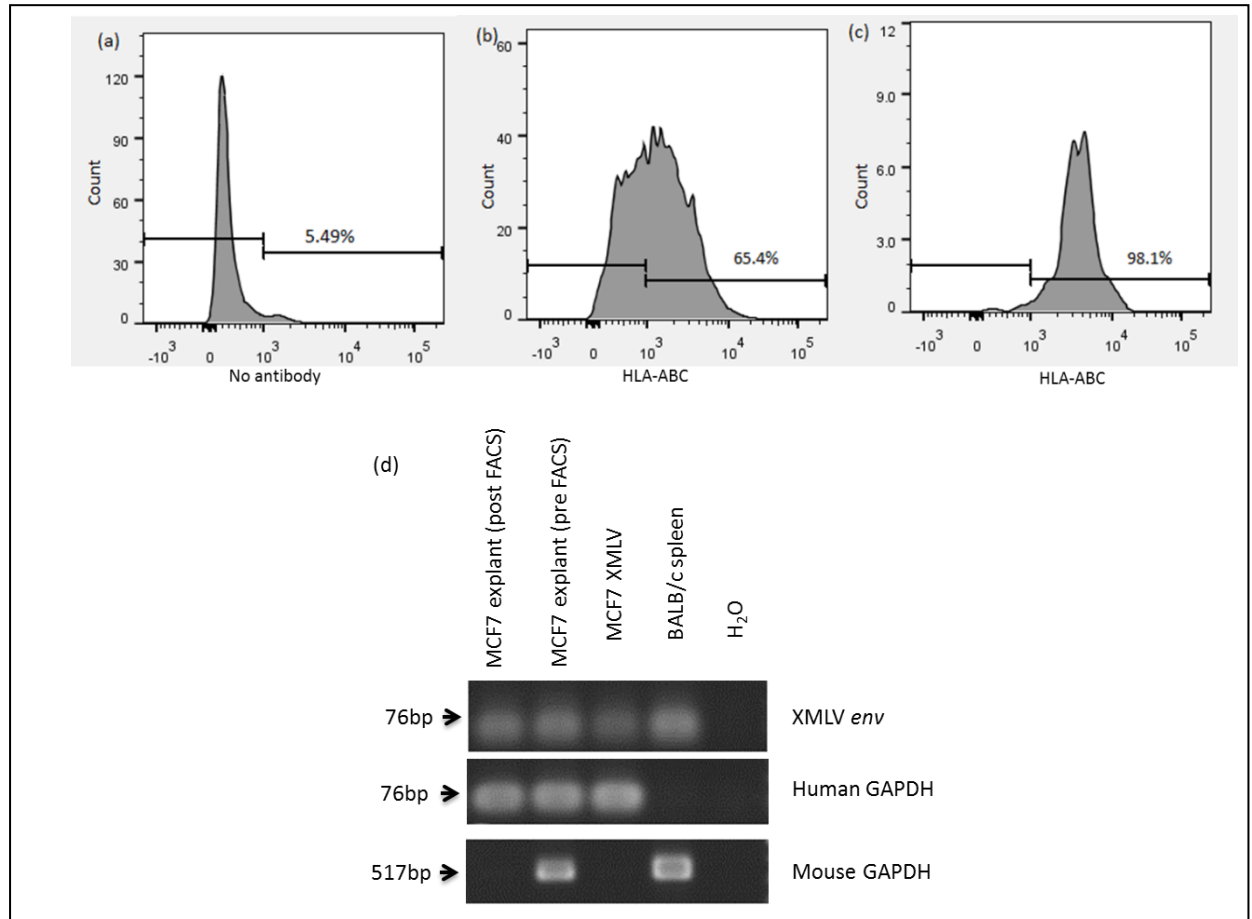


Figure 3.5 FACS carried out on MCF7 explant cells using mouse anti-human HLA-ABC antibodies to sort human cells. (a) MCF7 explant cells without antibody (b) MCF7 explant cells with HLA-ABC antibody (c) FACS redone on the sample collected in Figure 3.5b using HLA-ABC anti-human antibody to make sure the collected cells were of human origin. (d) PCR carried out on MCF7 explant cells after FACS using *env* primers specific for XMLV. Human GAPDH primers and mouse GAPDH primers were used as internal control for human and mouse DNA respectively. FACS analysis was carried out using FlowJo software.

Figure 3.5 shows that MCF7 explant cells lost the mouse cells after FACS, but still retained the XMLV signal, showing that they were infected with XMLV.

My host laboratory had not previously grown or worked with endogenous murine retroviruses and the next step was to identify and characterise the XMLV-like virus rescued from the MCF7 explant cells. For this purpose primers were designed on the basis of N417 (accession number HQ246218) viral genome

sequence information. Using these primers, segments of the virus were amplified, cloned and fully sequenced. The newly recovered virus was found to be 99.96% identical to the *Bxv1* proviral locus, confirming its identity as XMLV. There were 3 base differences in the MCF7 explant compared to *Bxv1*. Two were G to A mutations and one was an A to G mutation. The first G to A mutation was at position 1781 (*gag*), the second was at 5731 in the *pol* region. The third mutation which was an A to G mutation was at position 5825 in the *env* region. The alignment of *Bxv1* (accession no.AC115959.17) and BALB/c XMLV rescued from MCF7 explants is given in Appendix 2.

BALB/c mice are known to carry locus for an inducible endogenous ecotropic murine leukaemia virus *Emv1* on chromosome 5²²⁷. To rule out the possibility of *Bxv1Emv1*-pseudotype MLV virus²²⁸, MCF7 cells exposed to supernatant from the MCF7-BALB/c explants were also checked by PCR for the presence of *Emv1* as shown in the Figure 3.6.

Figure 3.6 PCR for *Emv1* in cells exposed to MCF7-BALB/c explant supernatant

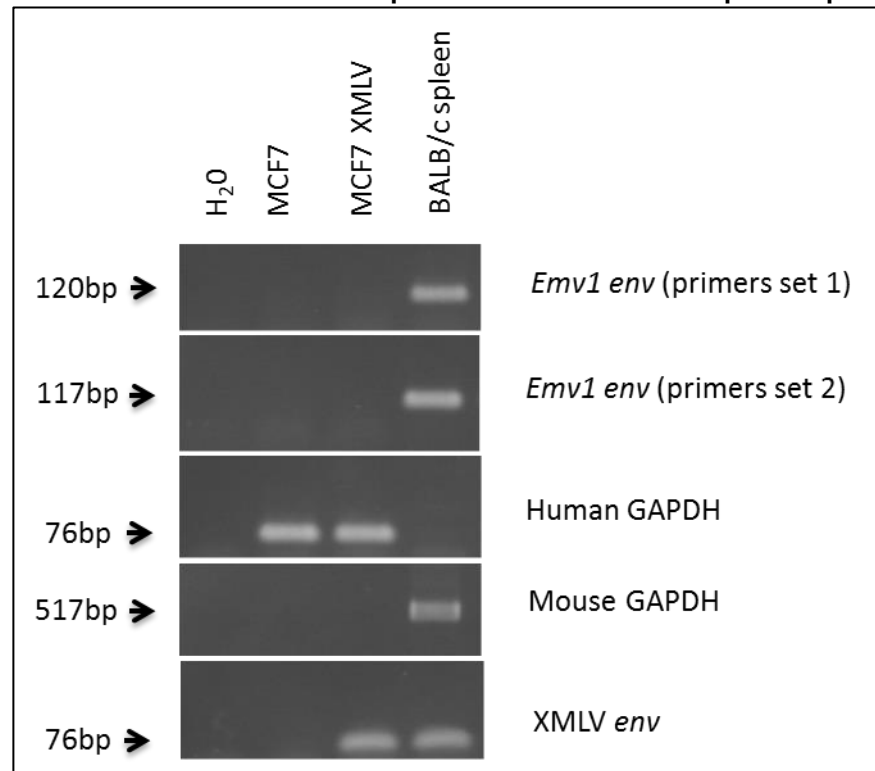


Figure 3.6 PCR using two sets of primers specific for *Emv1 env*. Human and mouse GAPDH primers were used as internal control to detect human and mouse DNA. XMLV *env* primers were used to detect XMLV infection. MCF7 XMLV represents MCF7 cells exposed to MCF7-BALB/c explant supernatant.

The MCF7 cells exposed to MCF7 BALB/c explant supernatant were free of *Emv1* virus, thus showing that the MCF7 explants were releasing only XMLV and not any *Bxv1Emv1* pseudotype MLV virus.

3.3.2 Primary childhood leukaemia cells passaged in NSG mice show no evidence of XMLV infection.

The results above demonstrated that xenotransplanted cells can be infected with XMLV when passaged in BALB/c nude mice. NSG mice are now widely regarded as the strain of choice for the xenotransplantation and passage of leukemic cells due to their strong immune deficit and lack of rejection^{165,229,230}. To investigate whether human cells passaged through NSG mice become infected with XMLV, I examined primary childhood B cell acute lymphoblastic leukaemia (B-ALL) cells that were previously passaged extensively in NSG mice. The primary cell explants named B-ALL HB spleen and B-ALL CL spleens were grown *in vitro* for 10 days. Filtered (0.45µm) supernatant from the primary B-ALL was used to perform DERSE assay and also to infect 293T cells (Both MCF7 and 293T cells are susceptible to XMLV as shown in Chapter 4). No evidence of infection was detected by DERSE assay. The DERSE assay was carried out in triplicate. PCR of 293T cells exposed to primary cells supernatant using primers specific for XMLV is shown in Figure 3.7.

Figure 3.7 PCR to detect XMLV in primary childhood leukaemia cells

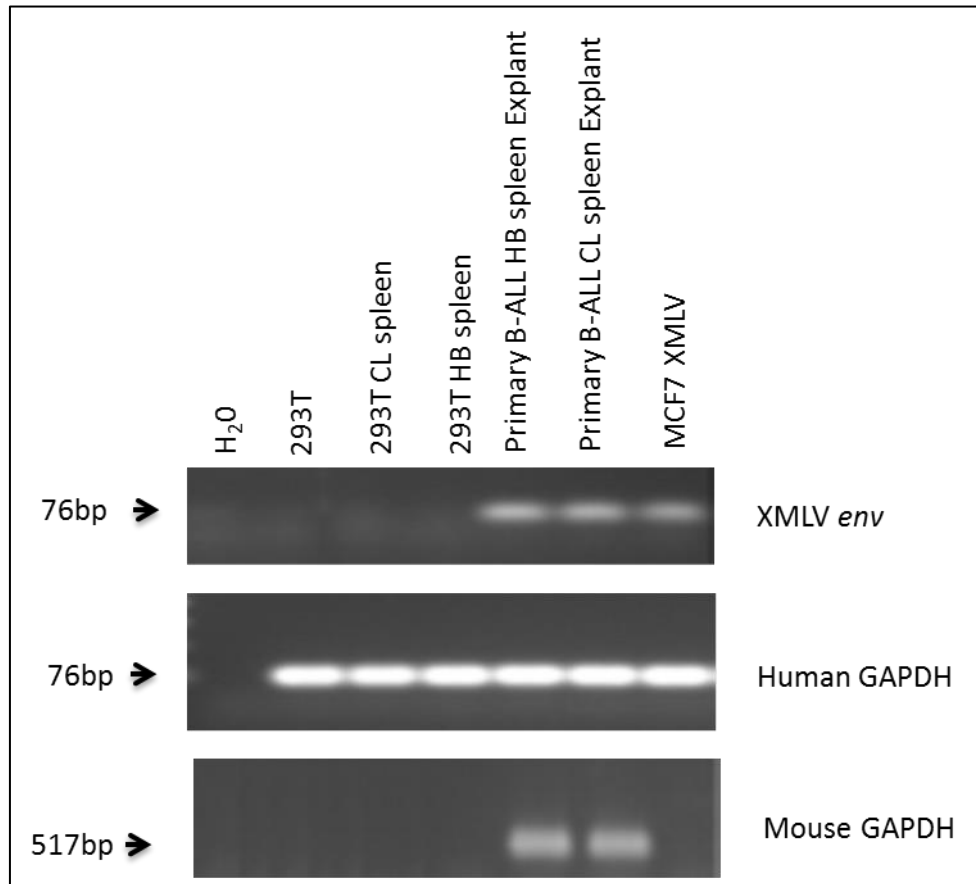


Figure 3.7 PCR using envelope primers specific for XMLV. Human GAPDH primers and mouse GAPDH primers were used as internal control for human and mouse DNA respectively. Uninfected 293T cells were used as a negative control for XMLV and mouse DNA. MCF7 XMLV was used as a positive control for XMLV.

Figure 3.7 shows that both (HB spleen and CL spleen) explanted samples of primary B-ALL cells were positive for XMLV sequences. However, 293T cells exposed to the supernatant of these primary explants were negative for XMLV suggesting that the primary B-ALL explants were not producing infectious XMLV. As the primary explants were also positive for mouse GAPDH (indicating mouse tissue contamination) it was considered most likely that the positive XMLV signal was due to the presence of XMLV sequences in the mouse germline.

3.3.3 THP-1 cells xenografted into NSG mice do not become infected with XMLV

While I was unable to detect infectious XMLV in primary B-ALL xenograft samples, I had the opportunity to test whether THP-1 cells, an acute monocytic leukaemia cell line, would acquire XMLV infection when xenografted into NSG

mice. This experiment represented the control arm of another study in which the effect of FeLV infection on xenograft behaviour was being tested. THP-1 cells were inoculated into NSG mice. Four mice were used for this experiment. All of the mice i.e. NSG6, NSG8, NSG9, NSG10 developed lumps in the liver region and were culled humanely at 71, 44, 47 and 50 days respectively. Tumour tissue was identified post mortem and liver nodules removed. One liver nodule from each mouse was finely chopped and plated *in vitro* in RPMI in tissue culture incubator. THP-1 explant cells began to grow out within 2-3 days in tissue culture. Filtered (0.45µm) supernatant of THP-1 explants (at passage 5 and 10) was used to perform the DERSE assay and passage 10 supernatant was used to infect 293T cells. No evidence of infection was detected by DERSE assay. PCR of 293T cells exposed to THP-1 explants supernatant using primers specific for XMLV is shown in Figure 3.8.

Figure 3.8 PCR to detect XMLV in NSG explants

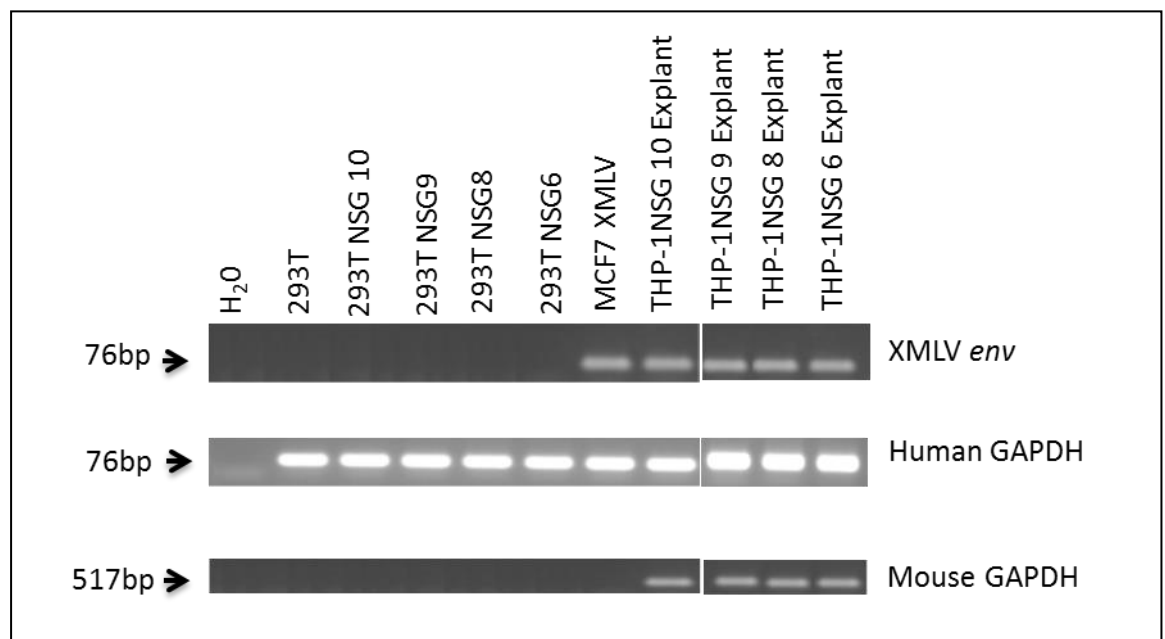


Figure 3.8 PCR using envelope primers specific for XMLV. Human GAPDH primers and mouse GAPDH primers were used as internal control for human and mouse DNA respectively. The uninfected 293T cells were used as negative control for XMLV and mouse DNA. MCF7 XMLV was used as positive control for XMLV.

Figure 3.8 shows that all explanted samples of THP-1 cells (NSG6, 8, 9 & 10) are positive for XMLV sequences. But the 293T cells exposed to the supernatant of these THP-1 explants (293T NSG6, 8, 9 & 10) were negative for XMLV thus the THP-1 explants were not producing any infectious XMLV. All the THP-1 explants

were also positive for mouse GAPDH (indicating mouse tissue contamination), thus the positive XMLV signal appears to be due to the presence of murine DNA.

THP-1 explant cells were also established from NSG6 and NSG10 mice blood. NSG mouse blood was washed in RPMI medium twice to remove any plasma and the blood cells were cultured in RPMI and incubated in a tissue culture incubator. THP-1 explant cells took 4 passages (20 days) to start appearing among the blood cells. These THP-1 blood explants were grown in tissue culture until the 10th passage. At the 10th passage, filtered (0.45µm) supernatant from THP-1 NSG6 and NSG10 blood explants was used to perform the DERSE assay and also used to infect 293T cells. No evidence of infection was detected by the DERSE assay. Standard PCR of 293T cells exposed to THP-1 blood explant supernatant using primers specific for XMLV is shown in Figure 3.9.

Figure 3.9 PCR for XMLV in NSG mouse blood

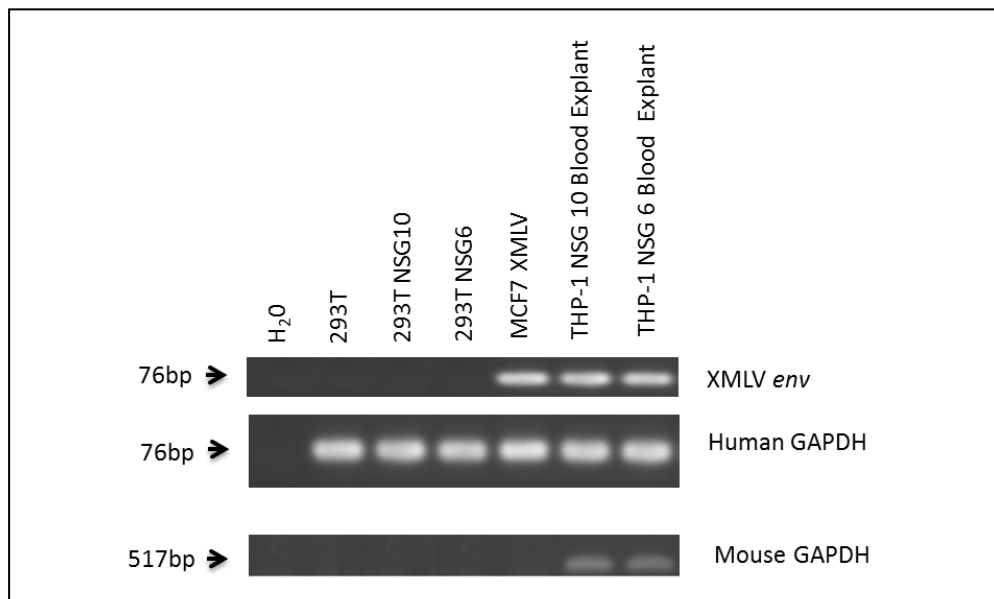


Figure 3.9 PCR using envelope primers specific for XMLV. Human GAPDH primers and mouse GAPDH primers were used as internal control for human and mouse DNA respectively. Uninfected 293T cells were used as negative control for XMLV and mouse DNA. MCF7 XMLV was used as positive control for XMLV.

Figure 3.9 shows that both blood explant samples of THP-1 cells (NSG6, 10) were positive for XMLV sequences. But the 293T cells exposed to the supernatant of these THP-1 explants (293T NSG6, 10) were negative for XMLV thus the THP-1 blood explants did not produce any infectious XMLV. All the THP-1 explants were also positive for mouse GAPDH (indicating mouse tissue contamination), thus the

positive XMLV signal was likely due to the presence of XMLV sequences in the mouse germline.

The next step was to test whether THP-1 cells xenografted into BALB/c nude mice would acquire any XMLV. For this purpose, THP-1 cells were inoculated via tail vein into BALB/c mice. Four mice were used for this experiment. The mice were observed for 16 weeks post-inoculation. None of the mice developed detectable tumours. So this experiment was inconclusive.

3.3.4 The *Bxv1* provirus is present in BALB/c and C57BL mice but not in NSG mice

The results discussed above demonstrate that neither primary B-ALL nor THP-1 cells acquired infectious XMLV following passage in NSG mice. It was conceivable that these cells are not susceptible to XMLV infection or that the NSG mice do not release any infectious virus when used for xenografting. An obvious question was whether *Bxv1* locus, the probable major source of XMLV in BALB/c mice^{30,172}, is present in NSG mice or not. This question could not be answered without experimental test because NSG mice have a breeding history that includes the *Bxv1* positive C57BL strain²³¹. To answer this question I generated primers which could specifically detect the *Bxv1* locus but not other XMLV sequences present in the mouse genome. Primers based on the *Mus musculus* chromosome 1 (accession no. AC115959) were used to amplify the junction between *Bxv1* provirus and the adjacent mouse genome (Figure 3.10b). The use of junctional primers to specifically identify *Bxv1* has been previously validated by others²².

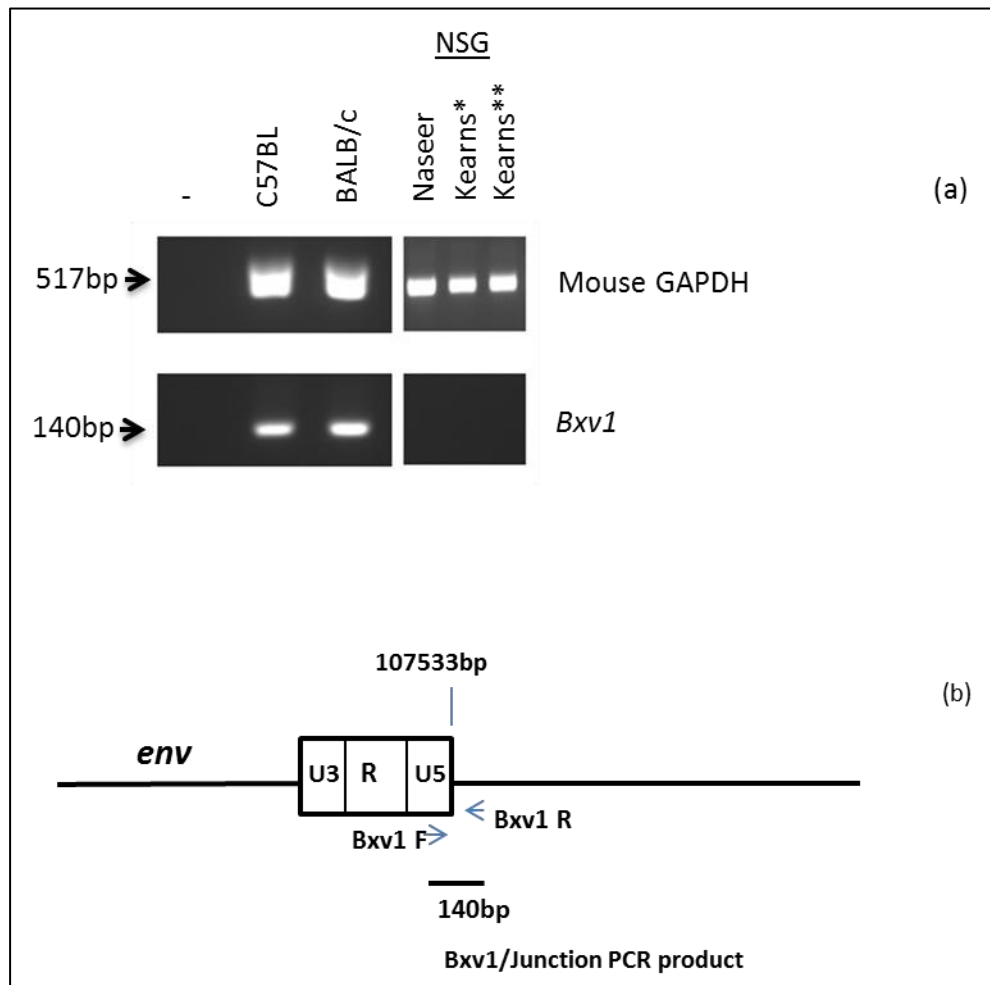
Figure 3.10 Analysis of *Bxv1* provirus

Figure 3.10 (a) PCR using *Bxv1* primers specific for the *Bxv1* locus in the mouse genome. Mouse GAPDH primers were used as internal control for mouse DNA. *Pamela Kearns B-ALL HB spleen primary xenograft sample, ** Pamela Kearns B-ALL CL spleen primary xenograft sample. Naseer stands for NSG samples that I obtained from NSG mice (b) *Bxv1* provirus in *Mus musculus* chromosome1 showing the location of the junctional *Bxv1* primer binding.

Figure 3.10a shows that the C57BL and BALB/c mouse DNA samples were both positive for *Bxv1* junctional primers demonstrating that the *Bxv1* locus is present in both of these strains. The NSG samples I obtained and those received from Pamela Kearns were negative for *Bxv1* junctional primers thus showing that the *Bxv1* locus was not present in NSG mice. NSG mice presumably lost the *Bxv1* locus during repeated inbreeding with NOD/Shi-scid mice. These results show that the *Bxv1* locus is present in BALB/c and C57BL mice and may be responsible for the acquisition of XMLV by xenografted cells. The absence of the *Bxv1* locus in NSG mice may explain why XMLV was not detected in leukemic cells passaged through these mice. It is theoretically possible that other loci could produce infectious MLV but no replicating virus was detected in these experiments.

3.3.5 MCF7 cells do not get infected with XMLV when passaged in NSG mice but may acquire a non-replication competent defective virus

In order to confirm my previous result and to explore the importance of the mouse strain in acquisition of XMLV infection, MCF7 cells were xenografted into four BALB/c and four NSG mice at intramammary sites. Though both the subcutaneous and intramammary site were used for xenografting in the earlier experiment involving BALB/c mice, tumour development was only seen in the mouse receiving a subcutaneous xenograft that also received oral oestrogen. In light of the importance of oestrogen for MCF7 xenograft development²³², I elected to use subcutaneous oestrogen pellets for all mice receiving xenografts. The intramammary site was used for MCF7 cell-xenografting as this site has been used successfully in many studies in combination with the use of oestrogen pellets^{180,233}. Oestrogen pellets were inserted subcutaneously 1 day before xenografting.

In this round of experiments all mice developed tumours in a very short time. All tumours were observed as isolated masses in the mammary region and were monitored for size. Mice were culled when the tumour mass reached 0.8-1 cm in size, which occurred from 10 to 25 days after xenografting. Each tumour tissue was separately extracted, finely diced to produce a single cell suspension and grown in MEM medium *in vitro* at 37°C and 5% CO₂ in a tissue culture incubator. These MCF7 explants were established and grown in tissue culture until the 10th passage. At the 10th passage filtered (0.45µm) supernatant from MCF7 explants was used to infect fresh MCF7 cells.

While XMLV *env* primers can detect XMLV by PCR with reasonable efficiency, the PCR product obtained using XMLV *env* was very small (70bp) and migrated on gels close to primer dimers. I therefore tested further primers to ensure sensitive and specific detection of MLV-related sequences in MCF7 cells exposed to the NSG explants. I was able to detect BALB/c XMLV (and also a defective virus from the NSG explants, described below) using both the XMLV *env* primers and XMLV-LTR primers and also with another set of primers (Fn3, Rn3) given in Appendix 1. As compared with XMLV *env*, the band was very clear with XMLV-LTR

primers (due to larger PCR product size) and easily distinguishable from primer dimers; for this reason I used LTR primers in this and subsequent experiments for detecting XMLV (*Bxv1*). PCR of MCF7 cells exposed to MCF7 explant (BALB/c and NSG) supernatant using XMLV-LTR primers is shown in Figure 3.11.

Figure 3.11a shows that MCF7 cells infected with BALB/c-4 supernatant were positive with the XMLV LTR primers, while the MCF7 cells exposed to supernatants from the BALB/c-1, 2 and 3 were negative for XMLV. All the MCF7 cells exposed to BALB/c supernatants were negative for mouse DNA showing that positive XMLV signal for MCF7 cells exposed to BALB/c-4 supernatant was likely due to being infected with XMLV and not mouse DNA contamination. The Figure 3.11b shows that when the supernatant from MCF7 cells previously exposed to BALB/c-4 explant supernatant were used to infect fresh MCF7 cells, the cells became infected with XMLV. This showed that the virus from the BALB/c-4 mice was replication competent. The virus from the BALB/c mice was sequenced and it was found to be virtually identical to the XMLV proviral locus *Bxv1*.

Figure 3.11 PCR for XMLV in NSG and BALB/c explants

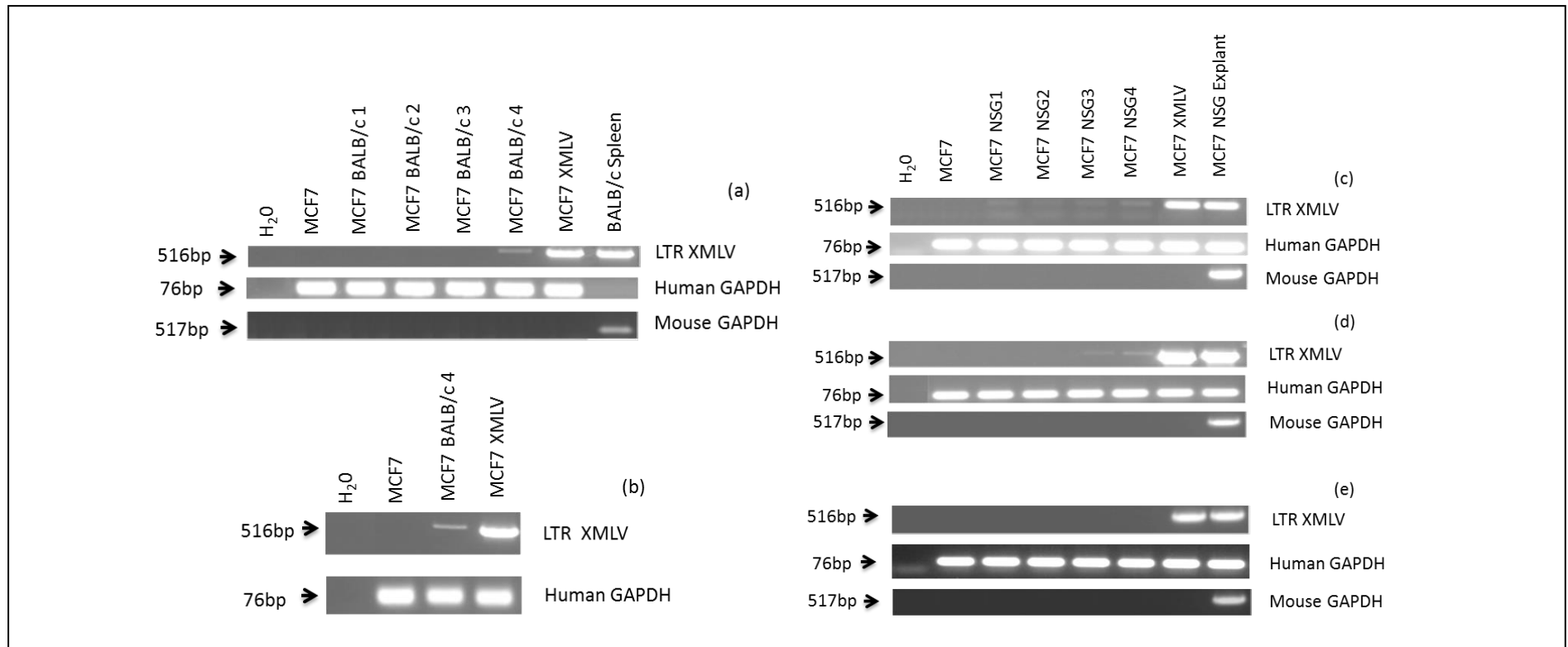


Figure 3.11 PCR using LTR primers specific for XMLV. Human GAPDH primers and mouse GAPDH primers were used as internal control for human and mouse DNA respectively. (a) PCR of MCF7 cells exposed to MCF7 BALB/c explant (1-4) supernatant. (b) Secondary infection of MCF7 cells with supernatant from MCF7 cells previously exposed to BALB/c-4 explant supernatant, indicating that the virus was replication competent. (c) PCR of MCF7 cells exposed to MCF7 NSG explant (1-4) supernatant (passage 10). (d) PCR of MCF7 cells exposed to MCF7 NSG explant (1-4) supernatant (passage 12). (e) Secondary infection of MCF7 cells with supernatant from MCF7 previously exposed to passage 10 NSG explant supernatant indicating the virus was not capable of a further round of spread and did not appear to be replication competent. In all the experiments involving MCF7 cells exposed to supernatant from explants (both NSG and BALB/c), uninfected MCF7 cells were used as a negative control, MCF7 XMLV was used as positive control for XMLV.

I also cultured blood cells *in vitro* from the BALB/c mice in this experiment (Figure 3.11a & b). The blood cells were washed in MEM medium and then grown in MEM in a tissue culture incubator. Fresh uninfected MCF7 cells were also exposed to plasma from these mice and the cells were grown for two weeks in a tissue culture incubator. No human cells were found in blood cells cultured from the BALB/c mice showing that MCF7 were not metastasised in the blood. PCR to detect XMLV in MCF7 cells exposed to BALB/c plasma is shown in the Figure 3.12.

Figure 3.12 PCR for exposure of MCF7 cells to BALB/c plasma

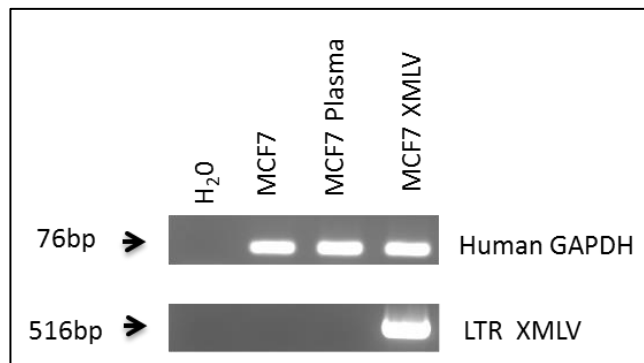


Figure 3.12 PCR using LTR primers specific for XMLV. Human GAPDH primers were used as an internal control. Uninfected MCF7 cells were used as a negative control. MCF7 cells infected with XMLV were used as a positive control.

Figure 3.12 shows that no infection was seen by PCR in MCF7 cells exposed to mouse plasma suggest that free XMLV was not present in these mice.

In Figure 3.11c a positive signal was seen with XMLV-LTR primers when supernatant from each of the four NSG mice explants was used to infect fresh MCF7 cells. The experiment was repeated by infecting fresh MCF7 cells with supernatant from NSG explants (12th passage) and this time only two explants had a positive signal (Figure 3.11d) showing that the capacity for infection was lost in 2 NSG explants. On later passage the infectivity was completely lost in all the four NSG explants (15th passage -not shown). Supernatants from MCF7 cells previously exposed to passage 10 NSG explants (Figure 3.11c) were also used to infect fresh MCF7 cells but the viral sequences could not be transmitted to the fresh MCF7 cells as shown in the Figure 3.11e. This suggests that the virus that initially came from the NSG explants may have been a non-replicating defective virus that was transiently induced. It is possible that the defective virus may have been released from the mouse cells present among the NSG explant cells

and that as the non-established mouse cells died off in culture, virus release was lost. The MCF7 cells, which were positive with the defective virus, were free of mouse cells confirming that they became infected with the defective virus but were unable to produce infectious particles.

The defective virus was sequenced, revealing homology to murine endogenous PMLV like MLV sequences on mouse chromosome 13, but it was clearly distinct from *Bxv1* XMLV as shown in the Figure 3.13.

Figure 3.13 Phylogenetic trees for NSG defective virus

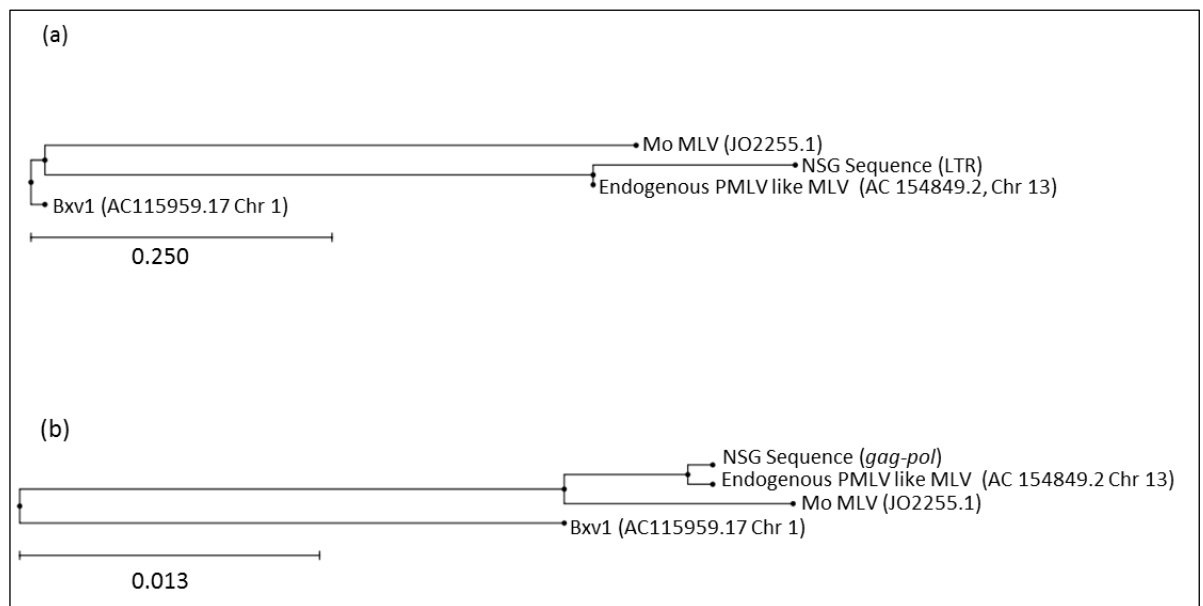


Figure 3.13 Phylogenetic trees for (a) LTR and (b) *gag-pol* sequences from the defective virus in the MCF7 tumour explants derived from NSG mice. The accession numbers are shown in brackets for Mo MLV, endogenous PMLV like MLV (chromosome 13) and *Bxv1* (chromosome 1). Trees were generated by the neighbour-joining method with bootstrapping at 100 replicates using CLC Genomics Workbench 5 software.

The NSG-derived defective virus sequences showed close resemblance to endogenous PMLV like MLV, (derived from chromosome 13, C57BL/6J BAC library) from which it differed only by a few G to A transitions. This suggested cytidine deamination during replication as a possible cause of this divergence²³⁴. The alignment of NSG-derived defective virus sequences, endogenous PMLV like MLV, *Bxv1* and Mo MLV sequences is shown in the Appendix 3 and 4.

3.3.6 Raji cells xenografted into BALB/c mice formed regressing tumour nodules

As described above, I was able to induce and rescue XMLV by xenografting MCF7 cells into BALB/c mice. When THP-1 cells were used for xenografting in BALB/c mice, no tumour tissue developed. Next I wanted to see if it was possible to induce and rescue XMLV using another susceptible cell line. For this purpose I used the Raji cell line, a Burkitt's lymphoma cell line, as *in vitro* experiments had confirmed that these cells were highly susceptible to XMLV infection (described in Chapter 4). Raji cells were inoculated subcutaneously into eight BALB/c nude mice. The Raji cells formed tumour nodules initially in all the mice. However, these nodules rapidly regressed and no viable explants could be recovered from this experiment.

3.4 Discussion

In this chapter I have demonstrated that MCF7 explant cells obtained from BALB/c mice acquired XMLV, although whether infection of human cells was initiated *in vivo* or after explant was not addressed directly. I have also confirmed that both BALB/c and the C57BL mice have a provirus at the *Bxv1* locus on chromosome 1. This endogenous proviral locus has been identified in 17 strains of mice²², representing a third of all inbred strains and can be induced by graft versus host reaction¹⁷². The results presented here suggest that the use of mice carrying a provirus at the *Bxv1* locus is likely to present a significant risk for acquisition of XMLV infection of cancer cell grafts. In these experiments, two MCF7 BALB/c xenografts infected with XMLV out of a total of 5 samples (one in each experiment, i.e. 40% overall) became infected. The same experiment was later repeated by Anne Terry in our group with my assistance. Using 12 BALB/c mice, our results confirmed that >40% of MCF7 explants from the BALB/c mice acquired XMLV. Various factors are likely to affect the risk of XMLV infection of xenografts, including the duration of *in vivo* passage. Strain-specific differences in immune function may also influence the likelihood of XMLV induction. It is even possible that mouse cells may be induced to produce XMLV when co-cultured *in vitro* with human cells. However, XMLV would not be expected to reinfect and replicate in the mouse cells due to the polymorphic XPR1 receptor which does not support viral entry in this strain³⁶. The extent to which XMLV

infection was present in the xenograft cells *in vivo* is unknown but could be analysed in future by analysis of explants cells e.g. by immunofluorescence for viral gene products.

XMLV infection of xenografts is likely to pass unnoticed unless samples are specifically screened for XMLV, and at present many researchers using xenograft approaches appear to be unaware of the potential for contamination. For example Warrington *et al*¹⁸⁰ recently used an MCF7-BALB/c xenograft model to demonstrate the effects of dietary selenium on the growth of MCF7 intramammary tumours. They made no reference to the XMLV status of their MCF7 xenografts and were presumably unaware of confounding effects that XMLV might have had on their results. Similarly Huuse *et al*¹⁷⁹ used the MCF7-BALB/c xenograft model to explore the effects of docetaxel, an anti-cancer drug, on MCF7 xenografts, once again ignoring XMLV as a possible confounding factor. Thus the use of xenografting for reconstituting primary tumours and cell line development¹⁶⁴ or for other experimental purposes demands that XMLV status should be established especially when *Bxv1* positive mice have been used. XMLV infection could potentially alter the characteristics of the cell line under investigation e.g. by insertional mutagenesis or could also act as a source of contamination for other cell lines or samples used in the laboratory¹⁷³. The example of XMRV also highlights the danger of false associations of retroviral infection with human diseases¹⁵⁸. Despite the demise of XMRV as a human pathogen, XMLV is formally classed as a potential biohazard for workers in tissue culture or those handling these xenografts in the animal house.

While my studies indicate that NSG mice lack a provirus at the *Bxv1* locus on chromosome 1, there are about 1-20 XMLV copies per mouse strain²⁰ suggesting that other loci might contribute to the generation of viruses capable of infecting xenografts. Moreover, loci known to generate fully replicative XMLV are present in other strains of mice. For example the *Nzv1* and *Nzv2* variants of XMLV are present in NZB mice. The Ma/My strain of mice has *Mxv1* XMLV in addition to *Bxv1*. The NSG mouse strain does not have a locus known to release a fully replicative XMLV, but it does have many defective XMLVs. An apparently defective replication-incompetent virus was observed to be released from the NSG cancer cell explants when screened at the 10th passage. This defective virus signal was sequentially lost on subsequent passages. Only 2 out of 4 NSG explants

displayed detectable viral sequence at the 12th passage while at passage 15, no sequence was detected in the explant cultures. It is possible that the defective virus was being released by mouse cells present along with the explant cells and that the gradual loss of these non-immortalised cells with passage explains the disappearance of infectivity. The sequence alignment of the defective virus showed that it was not *Bxv1* rather it showed sequence similarity to an endogenous polytropic like MLV (PMLV). Recently it has been shown that endogenous ecotropic murine leukaemia virus (EMLV) can become activated and replicate in NSG mice²³⁵. The source of this EMLV has been described as the endogenous proviral locus *Emv30*. Replicating EMLV has been shown to be capable of generating murine myeloid leukaemia by insertional mutagenesis in NSG xenograft recipients. Since EMLV can recombine with other endogenous retroviral sequences and result in the generation of PMLV, the possibility of direct infection of human xenografts with a recombinant variant from NSG mice cannot be excluded. Since the defective virus sequences resembled an endogenous PMLV- like MLV, the possibility of pseudotype formation must be considered. The potential for generation of human-tropic viruses from NSG mice may therefore compromise additional published results.

Raji cells xenografted into BALB/c mice initially formed nodules but these regressed rapidly before explant samples could be obtained. The basis for this regression is not known. Raji cells have been previously shown by others to form subcutaneous tumours in other mouse strains^{236,237}. As the Raji cells I used in this study are highly susceptible to XMLV infection, it is conceivable that the cells became infected with XMLV during the process of xenografting, and that this might have an influence on xenograft behaviour in the BALB/c nude mice which are athymic but retain some aspects of immune function including natural killer cell activity³⁴. The effects of XMLV infection on the Raji cell transcriptome would be potentially interesting in this respect and are considered later in this thesis (Chapter 8).

4 Susceptibility of human cells to XMLV infection

4.1 Introduction

While MCF7 cells are readily infected with XMLV, the extent of sensitivity of other human cancer cell lines was not clear, although some studies of host range had been conducted for XMRV²³⁸.

The main aim of the experiments described in this chapter was to investigate which human cell lines are susceptible to XMLV. To assess whether cells might be resistant at the level of entry receptor expression, I also decided to determine the expression of XPR1 receptor in different cells.

4.2 Materials and methods

Materials and methods have been discussed in detail in Chapter 2.

4.3 Results

4.3.1 XPR1 receptor expression

The expression of XPR1 in different cell lines and primary cells was checked by qRT-PCR as described in Chapter 2 and is shown in Table 4.1.

Table 4.1 XPR1 expression in cells

Cells	Human XPR1 expression
CEM	1.7
CEMSS	1.3
Kyo1	2
Jurkat	1.7
Reh	1.6
K562	4.1
293	1
PBMC	1.6
MCF7	1.4
THP-1	1.6
Mouse	0

Table 4.1 Expression of XPR1 in different cells relative to 293 cells. Mouse cells were used as a negative control.

Table 4.1 shows that XPR1 mRNA was found to be expressed in all human cells tested, this suggested that difference in the receptor expression was not a major determinant of their differential susceptibility to XMLV infection.

4.3.2 Single cell cloning of MCF7 XMLV cells indicates multiple XMLV insertions/integrations at different sites in different clones of MCF7 cells

As discussed in Chapter 3 MCF7 cells can grow as xenografts in mice and explanted tissue can be used as a source of infectious virus for subsequent infection of fresh MCF7 cells *in vitro*. To investigate the susceptibility of MCF7 cells to XMLV further and potential implications for insertional mutagenesis of xenografts I examined the number of proviral copies that had integrated in individual infected cells. For this purpose, MCF7 cells were infected with XMLV and grown as single cell clones as described in Chapter 2 so that viral copy number per cell could be estimated. Twelve sublines, derived from single cell clones, were developed and southern blotting was carried out on these lines to look at the number and pattern of proviral insertions.

To explore the integration pattern of XMLV in the MCF7 genome, a probe was designed as shown in Figure 4.1. The probe was designed so that I could detect a constant internal fragment and variable flanking fragments when used with a single restriction enzyme, in this case EcoRV.

Figure 4.1 Probing XMLV insertions in XMLV infected MCF7 clones

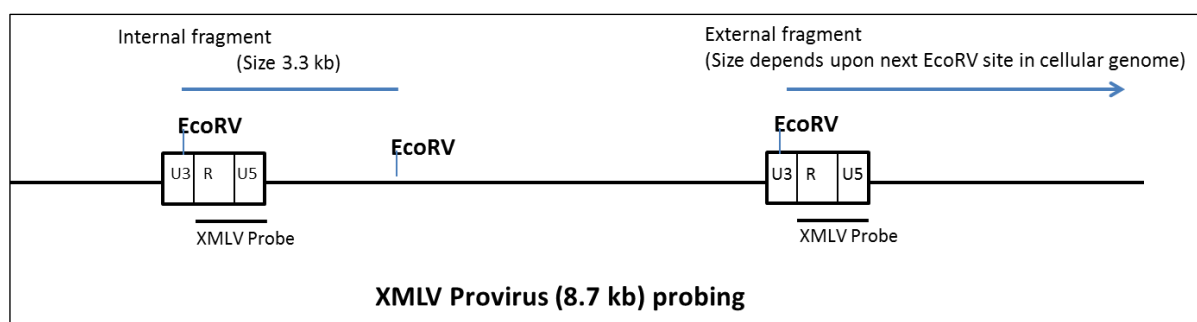


Figure 4.1 The XMLV probe (380 bp) can bind to both LTR regions of the inserted XMLV provirus. After EcoRV restriction-enzyme digestion of XMLV infected MCF7 DNA, constant-sized internal (3.3kb) and variable-sized junction fragments were generated. The size of junction fragment was dependent on the gap between the EcoRV restriction enzyme site in the LTR of inserted XMLV provirus and the nearest EcoRV restriction enzyme site located in the adjacent MCF7 genome.

The blot was probed using the probe described above. The southern blot is shown in the Figure 4.2.

Figure 4.2 Southern blot for XMLV-infected MCF7 single cell clones

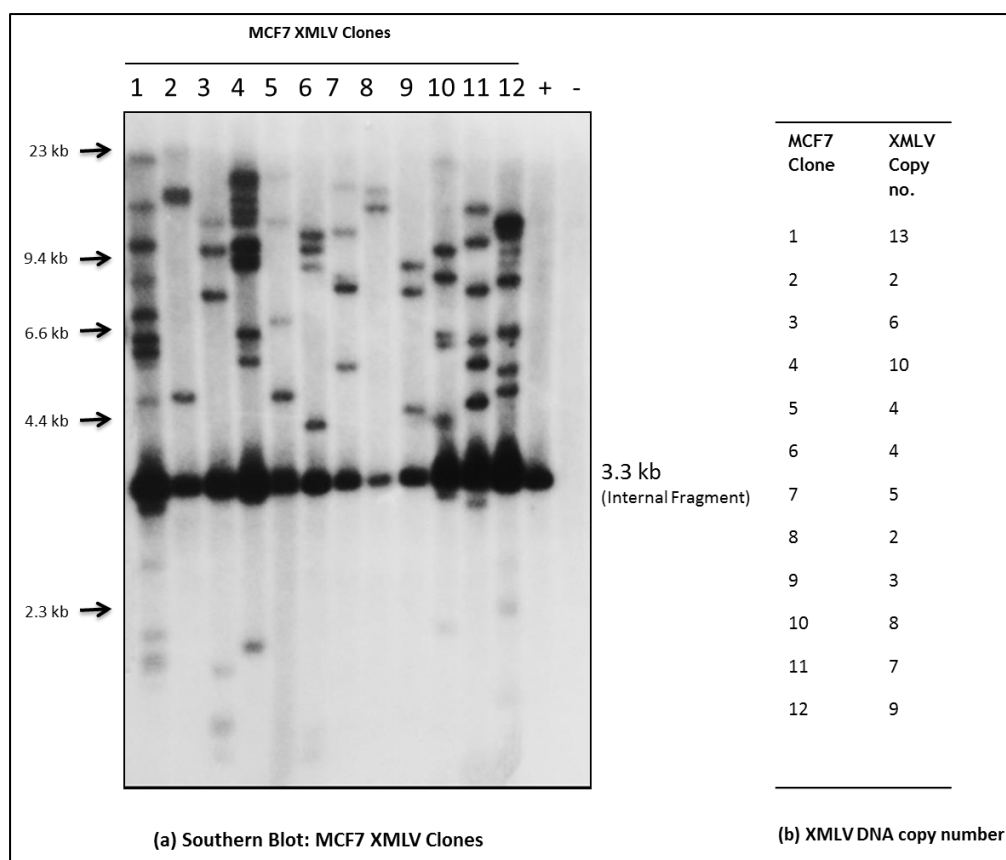


Figure 4.2 (a) Southern blot MCF7 XMLV clones 1-12. MCF7 XMLV cells from which the clones were derived were used as positive control (+). Non-infected MCF7 cells were used as negative (-) control. (b) XMLV DNA estimated copy number in MCF7 XMLV clones.

As shown in Figure 4.2a all twelve MCF7 sublines showed the presence of the XMLV internal fragment band of 3.3kb demonstrating that all clones were successfully infected. This band was absent from uninfected MCF7 cells indicating that it was specific to the recently acquired XMLV proviral DNA. The positive control showed the internal band and a smear rather than the presence of identifiable individual flanking bands. The different cell lines showed some variation with regard to both the intensity of the internal fragment and the number of obvious flanking bands suggesting that viral copy number varied between the different clones (Figure 4.2b), with an estimated 3-13 copy per cell (an average of 6 copy per cell). In principle, viral receptor interference should prevent reinfection of already infected cells but the copy number variation observed here would suggest that this blockade was not complete. In addition, the observation that even within a clone the flanking bands showed different

intensities indicates a degree of oligoclonality with regard to insertion sites and the likelihood that some integrations are present only in a subset of cells. The possibility that continued reintegration of XMLV could be occurring in these clonal sublines is supported by previous observations by Laurent *et al*²³⁹ who showed that XMRV proviral copy number per cell could accumulate over time in LNCaP prostate cancer cells. These authors demonstrated that low viral gene expression could result in inefficient interference thus permitting ongoing infection. The likelihood of retroviral DNA inserting adjacent to a cellular proto-oncogene or within a tumour suppressor gene in a single cell is extremely low but in a natural infection the frequency of such events increases as the virus spreads through a large and susceptible population²⁴⁰. The low level continued infection observed in the MCF7 cells could increase the risk of altered cell properties due to insertional mutagenesis, especially if each newly infected cell can be re-infected after an initial hit of integration. MLVs operate as insertional mutagens in their natural host and induce leukaemias and lymphomas in which multiple integration events and activation of cooperating oncogenes has been widely documented^{241,242}. Thus the possibility that XMLV infection of xenografts and xenograft derived cell lines could result in dysregulation of genes involved in controlling cell behaviour with resultant clonal outgrowth should be considered.

4.3.3 Titration of XMLV

The next step was to determine the titre of XMLV produced from XMLV infected MCF7 cells. For this purpose serial 1/10 dilutions of filtered XMLV supernatant were prepared and were used to infect 1×10^6 fresh MCF7 cells. The supernatant from these MCF7 cells on Day 14 were used to perform DERSE assay as shown in the Figure 4.3.

Figure 4.3 DERSE assay for XMLV titration

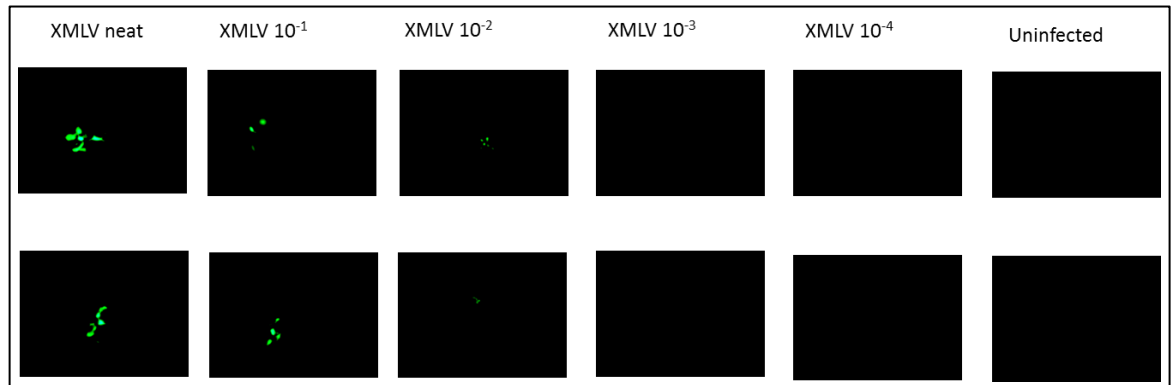


Figure 4.3 DERSE assay for XMLV titration. The GFP positive green cells indicate a positive DERSE test.

Figure 4.3 shows that the GFP activity could be seen in neat and 1/10 dilutions but was only weakly detected in the DERSE cells exposed to supernatant from 1/100 XMLV dilution. PCR was also performed using the DNA extracted from the day 14 samples using primers specific for XMLV as shown in Figure 4.4.

Figure 4.4 PCR for XMLV titration

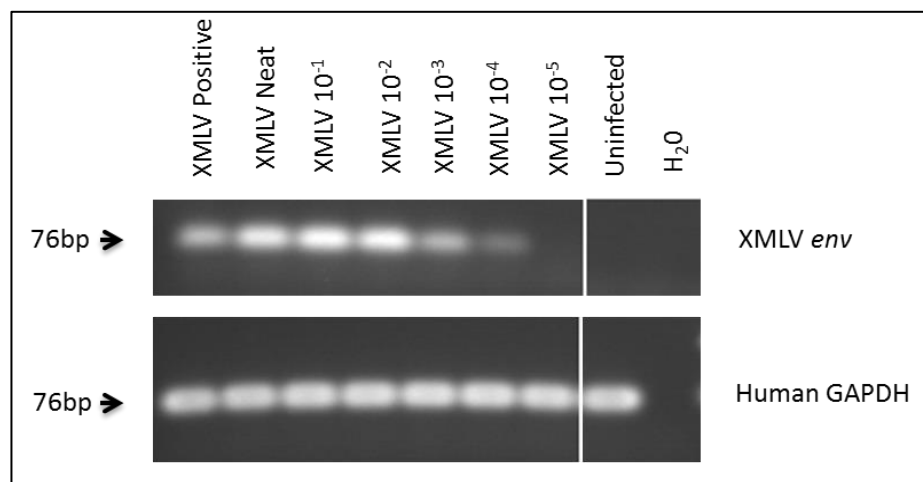


Figure 4.4 PCR for XMLV titration using *env* primers specific for XMLV and human GAPDH primers as an internal control. MCF7 cells infected with XMLV were used as positive control.

Figure 4.4 shows that on the Day 14, XMLV infection was detected in MCF7 cells infected with 10^{-4} diluted XMLV. Thus PCR was the more sensitive method to analyse XMLV titre. The titration of XMLV by PCR method was repeated three times and each time the results were found to be the same. The supernatant from the MCF7 cells infected with XMLV (titre= 10^4 virus particles/ml) was used as a stock solution for subsequent infections unless stated otherwise.

4.3.4 Infection of a panel of cell lines with XMLV

A panel of cell lines including Kyo1, K562, U937, Reh, Jurkat, MCF7 and CEM were infected with XMLV at a multiplicity of infection (MOI) of 0.02 (5×10^5 suspension cells infected with 1 ml of XMLV supernatant and 1×10^6 adherent MCF7 cells infected with 2 ml of supernatant). The cells were grown for 2 weeks before DNA extraction. XMLV infection was confirmed by PCR using primers specific for XMLV as shown in Figure 4.5.

Figure 4.5 PCR for XMLV infection of panel of cell lines

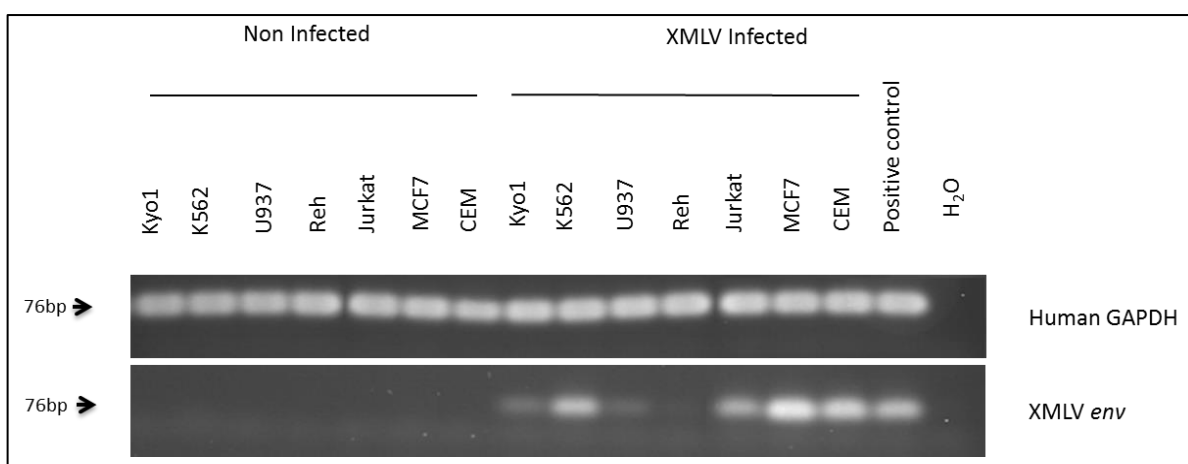


Figure 4.5 PCR using *env* primers specific for XMLV and human GAPDH as an internal control. MCF7 cells infected with XMLV were used as a positive control.

Figure 4.5 shows that by PCR the order of susceptibility of the cell lines was MCF7>CEM>K562>Jurkat>Kyo1>U937>Reh. The uninfected cells were negative for XMLV confirming that the cells were not previously contaminated. The supernatants from these infected cells were used to perform the DERSE assay. The result is shown in Figure 4.6.

Figure 4.6 DERSE assay for XMLV infected cells

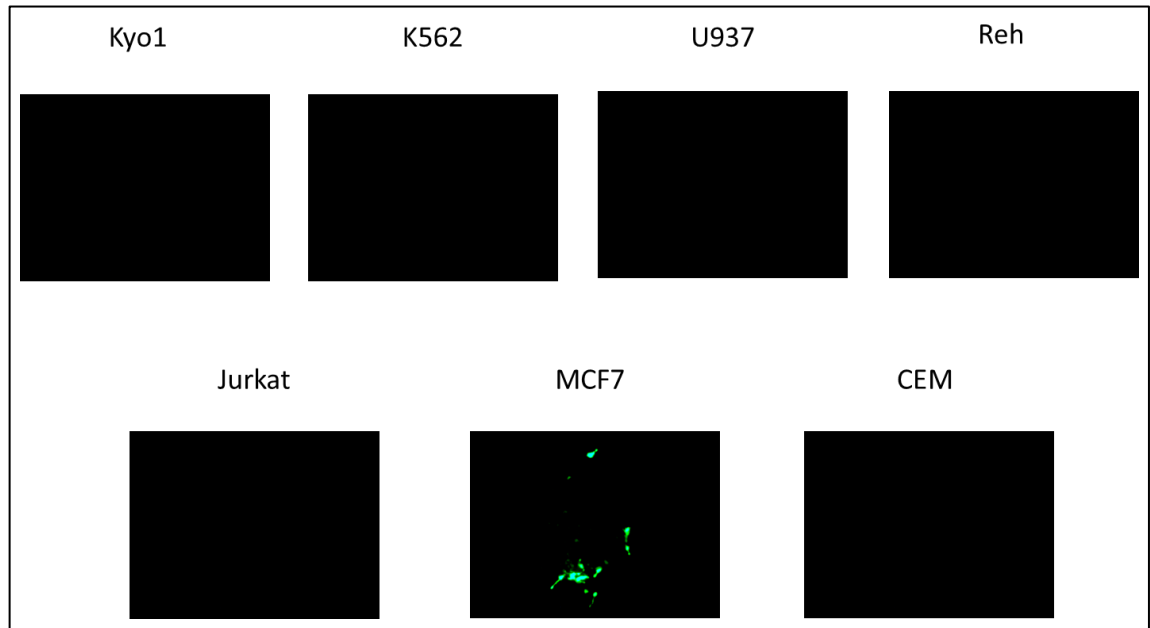


Figure 4.6 DERSE assay for different cell lines infected with XMLV for 14 days. The GFP positive green cells indicate a positive DERSE test.

Figure 4.6 shows that GFP positive green cells were seen only in MCF7 cells. No GFP activity was observed in the assays performed for other cell lines, showing that either the titre of infectious virus released by other cell lines is low or that any virus released from these cells is defective and not capable of producing a positive result using the DERSE assay. It may also mean that the DERSE assay is relatively insensitive to low titre virus and unsuitable for end-point titration. The principles of the DERSE assay system are shown in Figure 4.7 and a rationale for its failure to detect low titre virus is considered below. The DERSE assay was carried out in triplicate for each cell line.

Figure 4.7 Principles of the DERSE assay

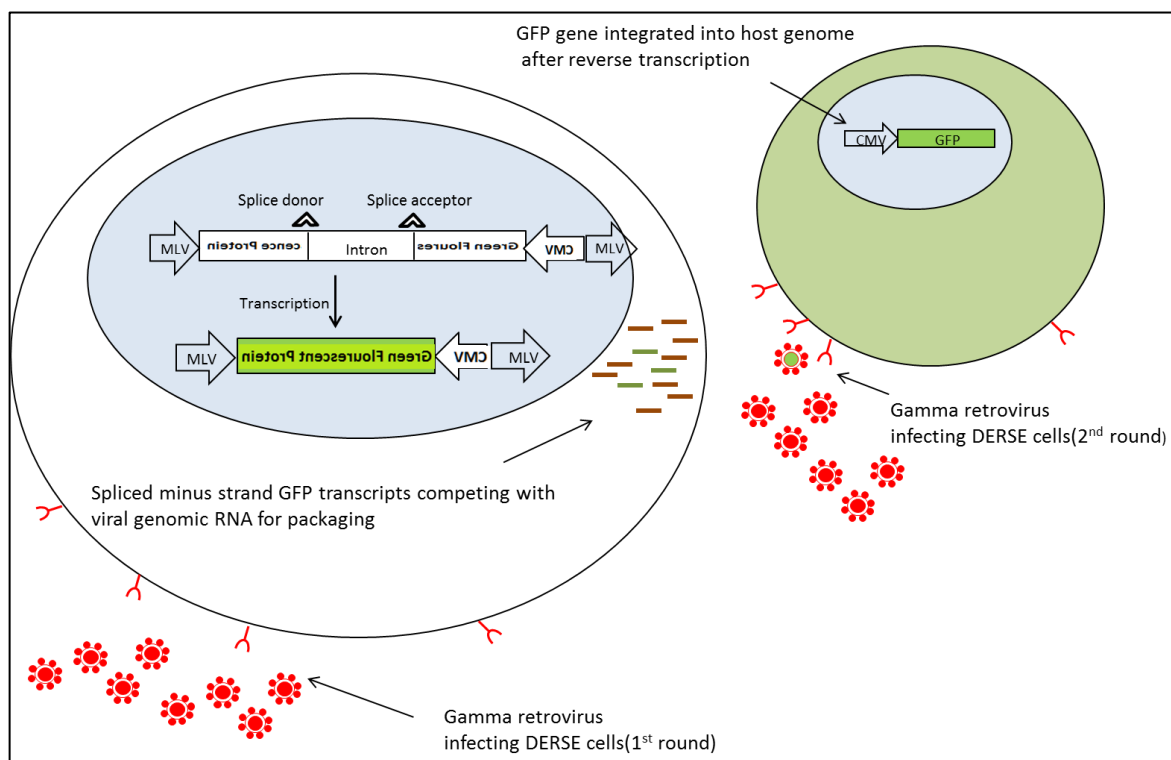


Figure 4.7 Shows the principles of the DERSE assay system. The figure is partially adapted from Aloia *et al*²⁴³. The DERSE cells are LNCaP cells transfected with a pBabe MLV vector carrying an intron interrupted GFP sequence. The orientation of GFP sequence is reverse as compared to the vector with the intron oriented in the forward direction. The CMV promoter drives transcription of the minus strand GFP sequence which can be spliced to remove the intron but retain the viral RNA packaging signal. When a replication competent gammaretrovirus infects DERSE cells, the minus-strand GFP sequence can be packaged and delivered to a neighbouring DERSE cell. When this spliced vector infects a new cell, the integrated vector can express the intact GFP sequence from the CMV promoter.

High titre incoming virus will infect the DERSE cells at high multiplicity, increasing the chance of generating particles carrying the spliced GFP vector and carrying it to a neighbouring cell. Low multiplicity infection may generate a sub-threshold level of infectious particles with a low probability of vector-containing particles (Figure 4.7). This effect may be magnified if the vector is packaged less efficiently than the RNA of the incoming virus. If my hypothesis is correct, it may be possible to activate the system with a high titre of a second gammaretrovirus that uses a different receptor even after saturation of the DERSE cells following low titre spread of XMLV. It would have been interesting to explore this question further if time has permitted.

A further experiment was carried out with a panel of cells including 293T, CEM, CEMSS, Kyo1 and Reh exposed to XMLV at MOI=0.2 (5×10^5 suspension cells infected with 1 ml of XMLV supernatant and 1×10^6 adherent MCF7 cells infected

with 2 ml of supernatant) using supernatant from the MCF7 cells infected with XMLV. CEMSS is a subline of CEM that differs in its very low expression of APOBEC3G, a restriction factor known to play an important role in restricting HIV and MLV²⁴⁴. The cells were re-infected with filtered XMLV supernatant from the MCF7 cells on Day 3 and Day 7 to ensure saturation of XMLV infection. In the experiment I tested the effects of saturating infection with three separate exposures to XMLV. The cells were grown for 2 weeks and DNA was extracted from the 14 day samples. XMLV infection was confirmed by PCR using primers specific for XMLV as shown in Figure 4.8.

Figure 4.8 PCR for XMLV infected panel of cells

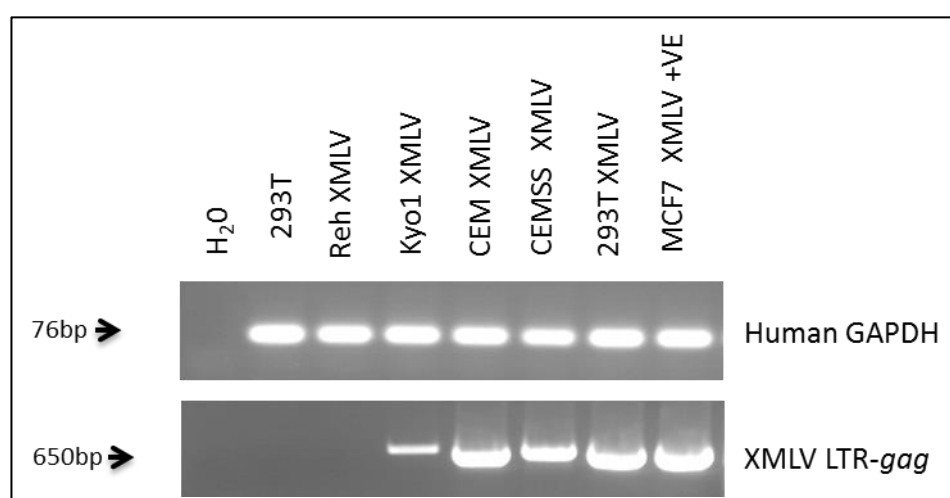


Figure 4.8 PCR using LTR-*gag* primers specific for XMLV and human GAPDH primers as control. Uninfected 293T cells were used as negative control. MCF7 cells infected with XMLV were used as a positive control for XMLV.

Figure 4.8 shows that 293T cells, CEM cells and CEMSS cells are susceptible to XMLV. The Kyo1 cells again appeared to be only partially susceptible to XMLV even after multiple rounds of infection though the infection was much increased when compared to single round of infection. The Reh cells appear to be highly resistant to XMLV infection even after multiple rounds of infection. This experiment was carried out once with the cells infected in a panel, however they were individually infected with XMLV in multiple other experiments. To compare the specific infectivity of XMLV in these different cell lines, this experiment was further analysed as described later in this chapter.

4.3.5 Infection of THP-1 cells with XMLV

As THP-1 cells were being used by my colleagues in xenograft-experiments in NSG mice (Chapter 3) this provided an opportunity to test whether THP-1 cells become infected with XMLV *in vivo*. To test *in vitro* susceptibility I infected THP-1 and MCF7 cells at MOI=0.2 (5×10^5 THP-1 cells infected with 1 ml of XMLV supernatant and 1×10^6 adherent MCF7 cells infected with 2 ml of supernatant). Cells were grown for 2 weeks before DNA extraction. XMLV infection was tested by PCR using primers specific for XMLV as shown in Figure 4.9.

Figure 4.9 PCR for XMLV infection of THP-1 cells

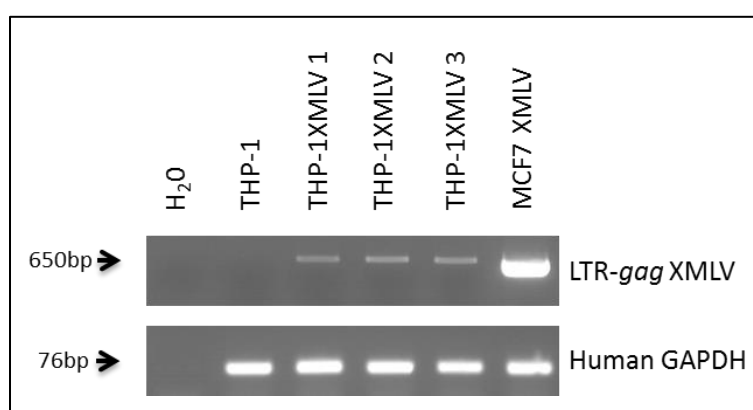


Figure 4.9 PCR using LTR-*gag* primers specific for XMLV and human GAPDH primers as control. Uninfected THP-1 cells were used as negative control. MCF7 cells infected with XMLV used as positive control for XMLV.

Figure 4.9 shows THP-1 cells infected with XMLV in triplicate. We can see that the LTR-*gag* band for the MCF7 cells, (positive control for XMLV) was very strong compared with the THP-1 cells. Thus THP-1 cells were considered to be only weakly susceptible to XMLV infection. A southern blot analysis of these THP-1 cells infected with XMLV was carried out with Nancy Mackay's help as shown in Figure 4.10.

Figure 4.10 Southern blot for XMLV infection of THP-1 cells

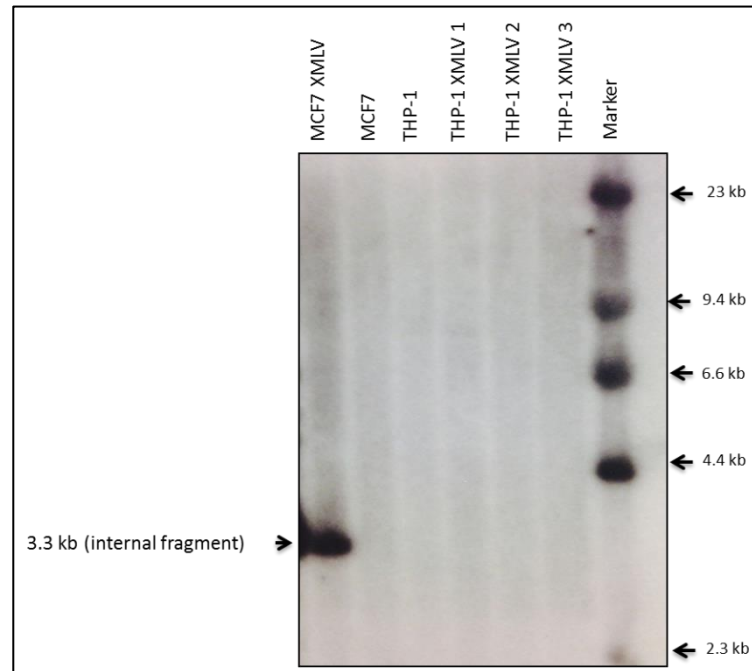


Figure 4.10 Southern blot using probe specific to detect XMLV LTR region. The probe was described in detail in earlier in this chapter. EcoRV enzyme was used to digest DNA for southern blotting. The probe can detect internal fragment of 3.3kb and external fragments of variable size depending on the location of XMLV insertion in the host genome and the nearby EcoRV restriction site.

Figure 4.10 shows that THP-1 cells infected with XMLV showed no detectable internal fragment on southern blotting. The relevant band can be seen clearly in MCF7 cells infected with XMLV (positive control). Note that this analysis would be expected to detect the internal fragment from unintegrated as well as integrated XMLV. Together with the weak PCR detection of XMLV in infected THP-1 cells in Figure 4.9, these results indicate that very few of the THP-1 cells are infected with XMLV. Furthermore, PCR is more sensitive than southern blot for the detection of low levels of proviral DNA.

4.3.6 Infection of Raji cells with XMLV

I also infected Raji cells with XMLV at MOI=0.2 (5×10^5 cells infected with 1 ml of XMLV supernatant). The XMLV infection was confirmed by PCR using primers specific for XMLV as shown in Figure 4.11.

Figure 4.11 PCR for XMLV infection of Raji cells

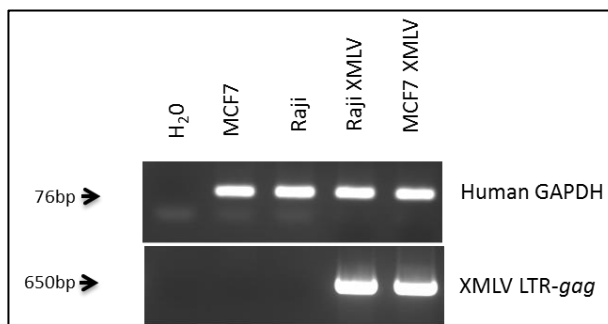


Figure 4.11 PCR carried out using LTR-*gag* primers specific for XMLV and human GAPDH primers as an internal control. Uninfected MCF7 cells were used as a negative control. MCF7 cells infected with XMLV were used as a positive control.

Figure 4.11 shows that Raji cells are susceptible to infection with XMLV. The PCR band intensities for Raji cells infected with XMLV and the MCF7 cells infected with XMLV were comparable. This experiment was further analysed and is discussed in Chapter 7.

4.3.7 Infection of human breast cancer cells with XMLV

I also attempted to infect human breast cancer cell lines MDA MB 231 cells, and MCF7 cells (control) with XMLV at MOI=0.2 (1×10^6 cells infected with 2 ml of supernatant). XMLV infection was confirmed by PCR using primers specific for XMLV as shown in Figure 4.12.

Figure 4.12 PCR for XMLV infection of MDA MB 231 cells

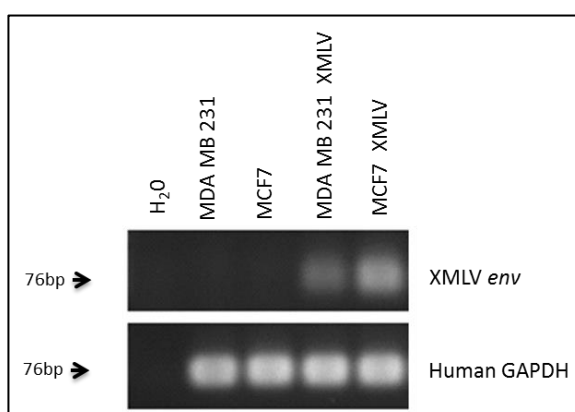


Figure 4.12 PCR analysis with *env* primers specific for XMLV and human GAPDH primers as an internal control. MCF7 cells infected with XMLV were used as a positive control.

Figure 4.12 shows that MDA MB 231 cells are susceptible to XMLV infection. Susceptibility to XMLV infection appeared to be lower for MDA MB 231 than for the highly susceptible MCF7 cells. This experiment was carried out twice.

4.3.8 Infection of CD34+ human cord cells with XMLV

In order to test the susceptibility of primary human cells to XMLV infection, CD34+ cord blood cells were also exposed to XMLV at MOI= 0.1 (1.6×10^5 cells infected with 2ml supernatant) as described in Chapter 2. CEMSS were used as control cells. PCR was carried out using appropriate primers for XMLV as shown in Figure 4.13.

Figure 4.13 PCR for XMLV infection of CD34+ cells

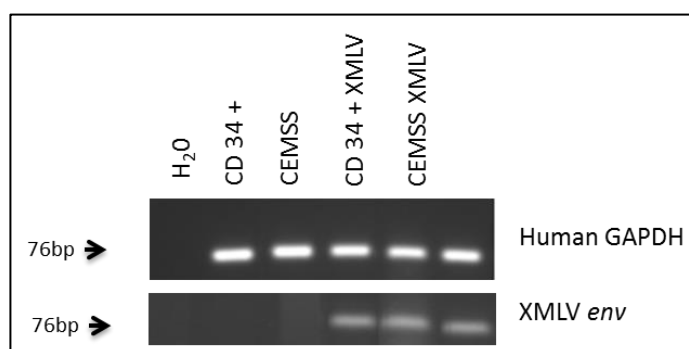


Figure 4.13 PCR carried out using *env* primers specific for XMLV and human GAPDH primers as an internal control. MCF7 cells infected with XMLV were used as positive control.

The Figure 4.13 shows that human cord blood CD34+ cells can be infected with XMLV. CEMSS cells used as a control were also infected with XMLV (Figure 4.13).

4.3.9 Infection of human peripheral blood monocyctic cells with XMLV

PHA treated PBMCs were infected with XMLV at MOI=0.01 (10^6 cells exposed to 1 ml of supernatant). PCR was carried out using appropriate primers for XMLV as show in Figure 4.14.

Figure 4.14 PCR for XMLV infection of PBMCs

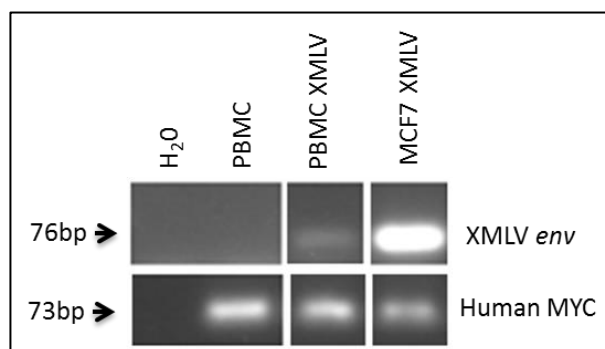


Figure 4.14 PCR carried out using *env* primers specific for XMLV and human MYC primers as an internal control. MCF7 cells infected with XMLV were used as positive control.

Figure 4.14 shows that PBMCs can get infected with XMLV. However the susceptibility of PBMCs to XMLV appears to be low. This is indicated by the weak band from PBMCs infected with XMLV as compared to the MCF7 cells infected with XMLV (positive control).

4.3.10 Specific infectivity of XMLV in human cells

The panel of cell lines 293T, CEM, CEMSS, Kyo1 and Reh infected with XMLV (Figure 4.8) were also assessed for the specific infectivity of XMLV released by these cells. These experiments paralleled ongoing experiments with FeLV which were pursued in greater depth and are described in Chapter 5. It was noted that some human leukaemia cell lines released abundant FeLV particles with reduced infectivity, indicating a late restriction to replication to FeLV and possibly also XMLV infection.

Serial 1/10 dilutions of filtered supernatant from these infected cells were used to infect 293T cells as described in Chapter 2. The XMLV titre was determined by PCR using primers specific for XMLV as shown in Figure 4.15.

Figure 4.15 Titration of XMLV from different cell lines

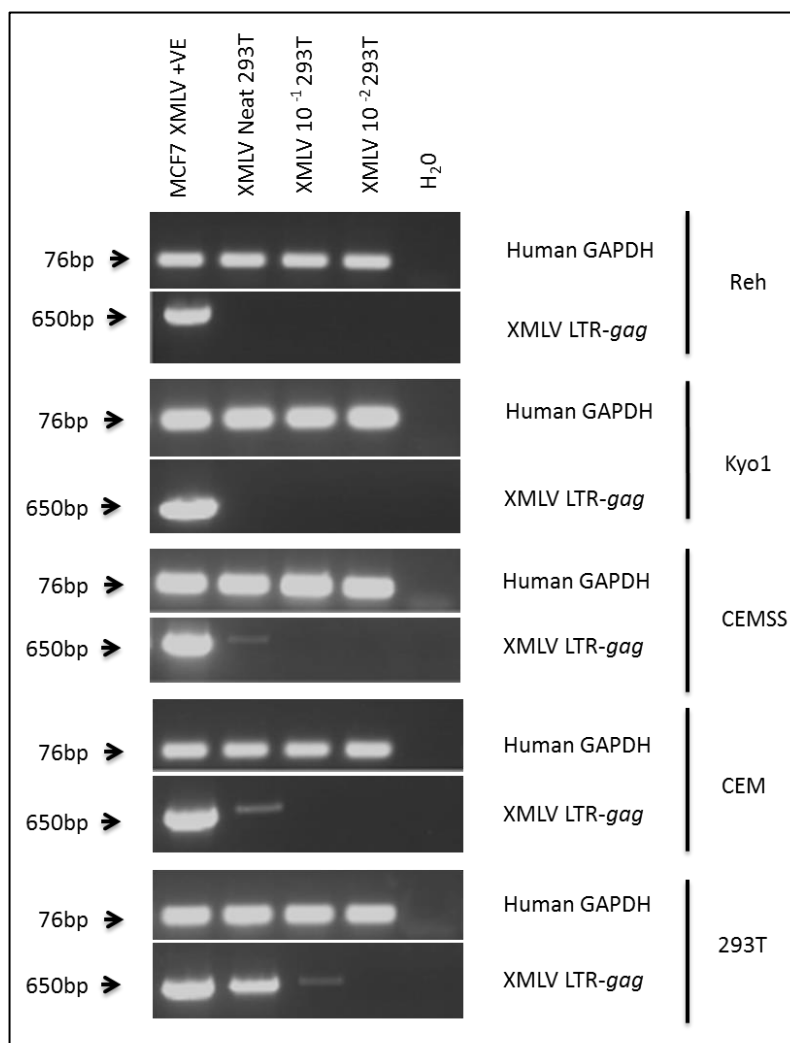


Figure 4.15 Titration of XMLV from different cell lines by PCR using XMLV LTR-gag primers specific for XMLV and human GAPDH primers as an internal control. MCF7 cells infected with XMLV were used as positive control.

No XMLV infection was observed in 293T cells infected with neat supernatant from the Reh and Kyo1 cells (Figure 4.15). XMLV infection can be detected in 293T cells infected with neat supernatant from CEM cells as well as CEMSS cells. Bands can be seen in the 293T cells infected with neat and 1/10 dilution of XMLV supernatant from the saturated 293T cells. This analysis indicates that the titre of XMLV released by 293T cells is ~10 infectious units per ml, while the titre of virus released from CEM and CEMSS is ~1U/ml. No infectious virus was detected in supernatant from the Kyo1 or Reh cells.

Next I compared the total level of virus released by different cell lines infected with XMLV with the infectivity of the released XMLV. I also analysed the virus protein content within the infected cells. For this purpose, the supernatants

from day 14 XMLV infected cells were used to prepare clarified lysates after viral pelleting by ultracentrifugation (at 25000 rpm). Cell protein lysates were also prepared from cells harvested on Day 14 and western blots were performed as shown in Figure 4.16.

Figure 4.16 Western blot of viral and cell protein lysates from XMLV infected cells

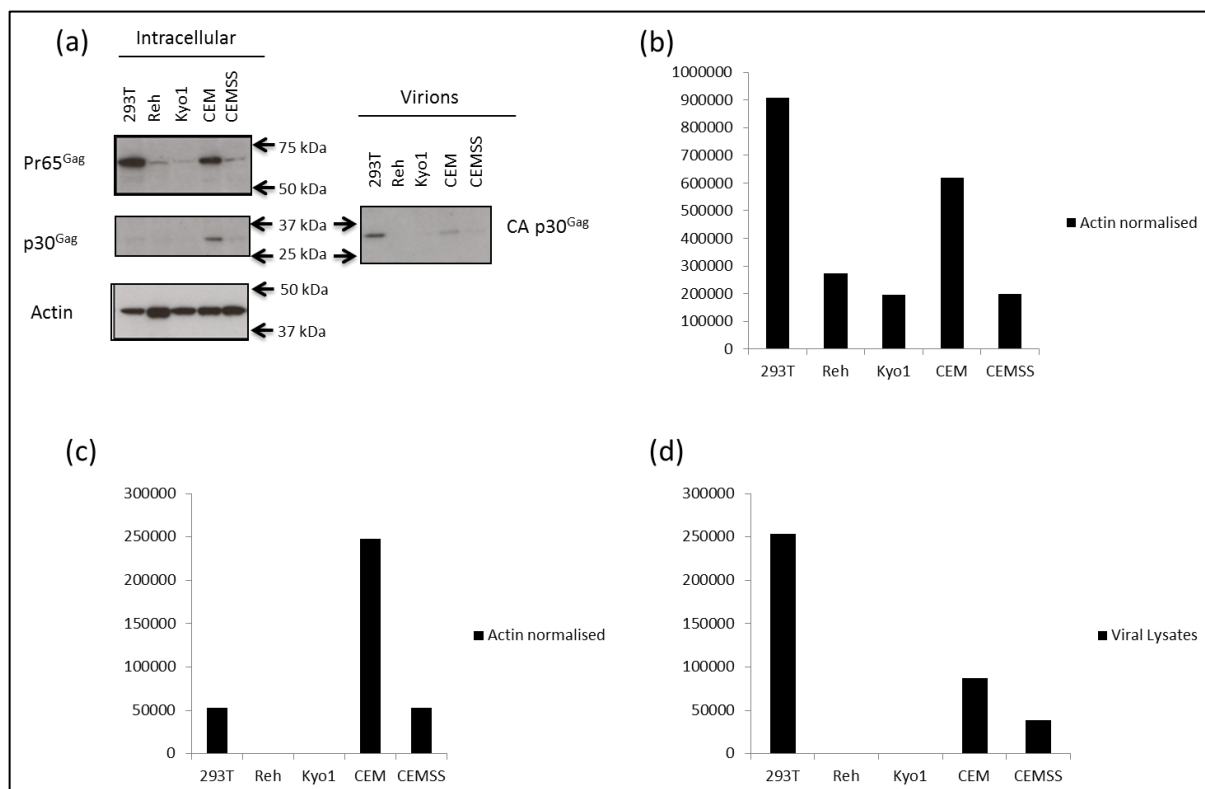


Figure 4.16 (a) Western blot of cellular and viral proteins from the XMLV infected cell lines using anti p30^{Gag} antibody. (b) Densitometry of XMLV intracellular Pr65^{Gag} western blot. (c) Densitometry of XMLV intracellular p30^{Gag} western blot. (d) Densitometry of XMLV virion CA p30^{Gag} western blot. Densitometry of cellular proteins was determined after normalising for the actin loading control. Background has been subtracted from all the densitometry values.

The level of XMLV precursor Pr65^{Gag} intracellular protein was greatest in the 293T cells, followed by CEM cells, Reh cells, CEMSS cells and Kyo1 cells respectively. The levels of cell-associated processed p30^{Gag} were highest for CEM, followed by 293T cells, CEMSS cells while it was undetectably low in Reh cells and Kyo1 cells. In the western blot analysis of viral particle-related protein, the highest p30^{Gag} XMLV capsid (CA) protein level was found in 293T cells followed by CEM cells, and CEMSS cells while it was detectably low in Reh cells and Kyo1 cells. A comparison of the western blot data with titration data showed a reasonable correlation for all the cell lines.

Human PBMCs were also exposed to XMLV. The presence of XMLV DNA in exposed PBMCs was confirmed by PCR as shown in Figure 4.14. The supernatant on Day 14 was used to infect 293T cells. No infectious XMLV was detected.

4.4 Discussion

In this chapter, I have demonstrated that XMLV can infect MCF7 cells and accumulate high copy numbers of integrated proviruses per cell. The ability of XMLV to insert at multiple sites in individual cell clones means that there is an increased chance of inserting adjacent to important oncogenes or within tumour suppressor genes and therefore a risk of affecting cell behaviour by insertional mutagenesis¹⁸¹. The pool of MCF7 XMLV cells from which the clones were derived was presumed to be polyclonal with respect to XMLV insertions. The clones were selected randomly from the pool without intentionally applying any selective pressure. However, the low density culture environment may have increased selection pressures, possibly enhancing the likelihood of a competitive advantage in cells sustaining insertions at specific loci. Such pressures could also arise when culturing the cells in the presence of cytotoxic drugs or repeat xenografting.

Different retroviral subfamilies and genera display different integration preferences and this has implications both for the lifecycle of virus and the host. For example, HIV-1 displays a preference for integration within active genes/transcription units¹⁸³, whilst MLV tends to insert near transcription start sites²⁴⁵. XMRV, which shares 93% sequence similarity with XMLV²⁰, and uses the same receptor i.e. XPR1¹⁵², also shows a strong preference for transcription start sites¹⁸². By analogy with other MLVs it is therefore possible that XMLV can play a role in gene activation resulting in a potential selective advantage to infected cells. In my experiments, the position of insertions or their proximity to important cellular genes was not investigated. Similarly, differences in the growth characteristics of the different clones were not explored. Future studies could include monitoring the clonal expansion and investigating the insertion sites conferring defined advantages in adverse or challenging conditions. Such experiments might formally demonstrate that XMLV can act as an efficient mutagen in human cells.

I have demonstrated that XPR1 mRNA was expressed in all the human cells investigated, and the difference in receptor expression was unlikely to be a major determinant of their differential susceptibility. This could be confirmed in future experiments by the use of pseudotype vectors expressing the XMLV envelope protein.

Different cell lines did not appear to be equally susceptible to XMLV infection. MCF7 cells, 293T cells, Raji cells K562 cells, CEM cells and CEMSS cells were found to be significantly susceptible. I demonstrated that MCF7 was the most susceptible cell line, releasing the highest titre of XMLV. 293T cell line was found to be the next in terms of susceptibility to XMLV infection and infectious XMLV titre released. CEM and CEMSS produced a similar virus titre. THP-1 cells, Kyo1 cells, U937 cells, Jurkat cells and MDA MB 231 cells were found to be partially susceptible. The infection was clearly detectable in Kyo1 cells by PCR but they did not release any infectious XMLV. Reh and PBMCs were found to be the least susceptible. The infection could easily be detected by PCR in PBMCs but not in Reh cells. Neither of these cell lines released detectable infectious XMLV. This shows that there is some restriction to replication in the Kyo1 cells, PBMCs and Reh affecting susceptibility to XMLV infection in case of Reh and PBMCs, and the infectiousness of the released virus (if any) in all three cell lines.

I was also able to infect CD34+ primary human cord cells. Cancer cells undergo various genetic abnormalities during the process of cancer development. This could result in the differential behaviour of the cell lines. For example both MCF7 and MDA MB 231 cells are epithelial cell and are derived from breast adenocarcinoma pleural effusions^{198,214}. MCF7 was highly susceptible to XMLV infection while the MDA MB 231 was relatively less susceptible. K562 appeared to be more susceptible as compared to Kyo1 cells though both of them are undifferentiated myeloid cells derived from CML patients^{202,203}. THP-1 and U937 both are undifferentiated monocytes^{205,209} and both appeared to show low susceptibility to XMLV infection. Jurkat cells are T lymphoblast²⁰⁶ while Reh are pre-B lymphoblast^{207,208}, Jurkat cells seem to be better susceptible to XMLV as compared to the Reh. Possible reasons for the differences in susceptibility are explored further in subsequent chapters. The susceptibility of these cell lines for another simple gammaretrovirus e.g. FeLV would be worth studying as this will

provide us with useful information on general features affecting gammaretroviral susceptibility of human cells.

5 Susceptibility of human cells to FeLV

5.1 Introduction

In the previous chapter, different cell lines and primary cells were investigated for susceptibility to XMLV infection. This was carried out to discover which cell lines and primary cells are at risk of acquiring XMLV during the process of xenografting or by horizontal transfer in laboratory facilities where xenografts are used. An important question arising from these experiments is whether the susceptibility of different cell lines to XMLV represents a general resistance to gammaretroviral infection. As my colleagues in the host laboratory were studying feline leukaemia viruses with the aim of using these agents as cancer gene discovery tools in human cells, I was able to make use of the groundwork and the viruses that they had selected for study. The possibility that FeLV may cause zoonotic infection and the factors affecting resistance of human cells to these gammaretroviruses becomes the second major theme for my thesis studies. In earlier studies my colleagues identified FeLV B strains as the most likely zoonotic agents on the basis of their presence in many field isolates and their ability to infect human cells without obvious cytopathic effect.

The main aim of the studies described in this chapter was to test which human cell lines are susceptible to FeLV B. As cells displayed differential susceptibility I also decided to examine the level at which resistance was operating by testing the ability of cell lines to support early entry and reverse transcription and to compare the specific infectivity of virions released after saturating infection of several human cell lines.

5.2 Materials and methods

Materials and methods have been discussed in Chapter 2.

5.3 Results

5.3.1 PiT1 receptor expression

The expression of PiT1 receptor mRNA (Anne Terry's unpublished results) is shown in the Table 5.1. PiT1 is expressed in all cells and shows no correlation with the susceptibility of various cell-types to FeLV B infection.

Table 5.1 PiT1 expression in different cells

Cells	PiT1 expression
293	1
Kyo1	1.8
THP-1	1.4
CEM	1.6
CEMSS	1.5
Reh	3.5
PBMC	1
MCF7	1.1

Table 5.1 The expression of PiT1 in different cell lines and PBMCs relative to 293 cells (Anne Terry's unpublished results).

5.3.2 Infection of cell lines with FeLV B

Supernatant from the AH927 cells infected with FeLV B (titre= 5×10^5 particles/ml) was used to infect all cells with FeLV B unless otherwise stated. A panel of cell lines including CEM, CEMSS, Reh, MCF7 and Kyo1 were infected with FeLV B at MOI=1 (5×10^5 suspension cells infected with 1 ml of FeLV B supernatant and 1×10^6 adherent MCF7 cells infected with 2 ml of supernatant). The cells were grown for 2 weeks and DNA was extracted from the Day 14 samples. FeLV B infection was confirmed by PCR using primers specific for FeLV B as shown in Figure 5.1.

Figure 5.1 PCR for FeLV B infection of cell line panel

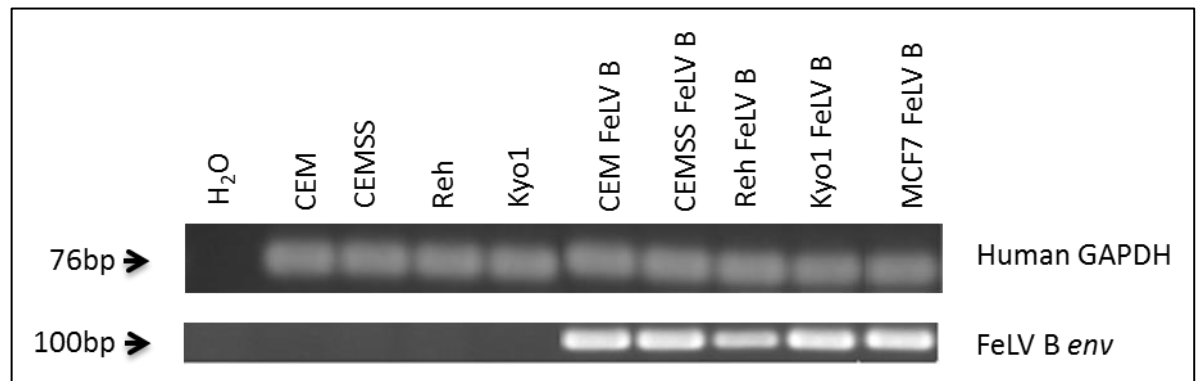


Figure 5.1 PCR using *env* primers specific for FeLV B. Human GAPDH primers were used as an internal control.

Figure 5.1 shows that CEM, CEMSS, MCF7 and Kyo1 cells are susceptible and get infected with FeLV B. The Reh cells were also detectably infected although the level of proviral DNA was low as compared to other cell lines. This experiment was carried out twice.

293T cells were also infected with FeLV B at MOI=1. The FeLV B infection was confirmed by PCR using primers specific for FeLV B as shown in Figure 5.2.

Figure 5.2 PCR for FeLV B infection of 293T cells

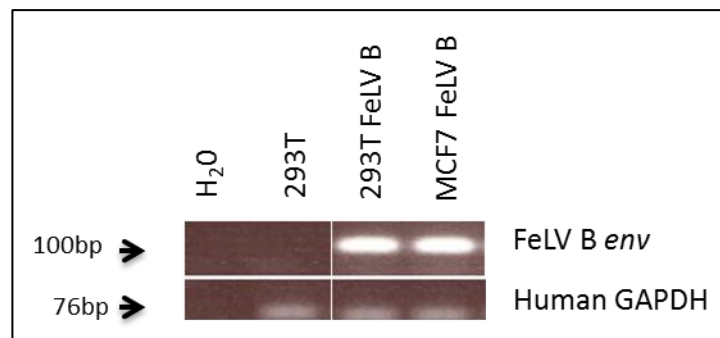


Figure 5.2 PCR using *env* primers specific for FeLV B and human GAPDH primers as an internal control. As the previous experiment demonstrated that MCF7 cells were capable of being infected, DNA from MCF7 cells infected with FeLV B was used as a positive control in this experiment. Uninfected 293T cells were used as a negative control.

The Figure 5.2 shows that 293T cells are susceptible to FeLV B infection.

5.3.3 Infection of THP-1 cells with FeLV B

THP-1 cells were also infected with FeLV B at MOI=1 (5×10^5 THP-1 cells infected with 1 ml of FeLV B supernatant). MCF7 cells were used as control. FeLV B

infection was confirmed by PCR using primers specific for FeLV B as shown in Figure 5.3.

Figure 5.3 PCR for FeLV B infection of THP-1 cells

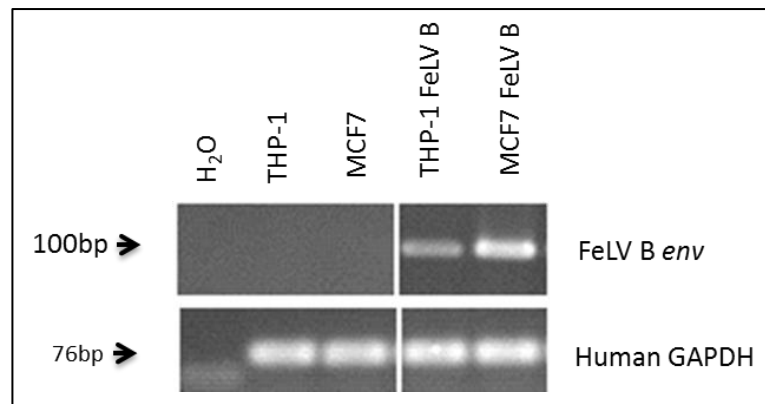


Figure 5.3 PCR using *env* primers specific for FeLV B and human GAPDH primers as an internal control. Uninfected MCF7 and THP-1 cells were used as a negative control.

Figure 5.3 shows that THP-1 cells are not as susceptible to FeLV B infection as the MCF7 cells.

5.3.4 Infection of Raji cells with FeLV B

Raji cells were also infected with FeLV B at MOI = 1 (5×10^5 Raji cells infected with 1 ml of FeLV B supernatant). The FeLV B infection was confirmed by PCR using primers specific for FeLV B as shown in Figure 5.4.

Figure 5.4 PCR for FeLV B infection of Raji cells

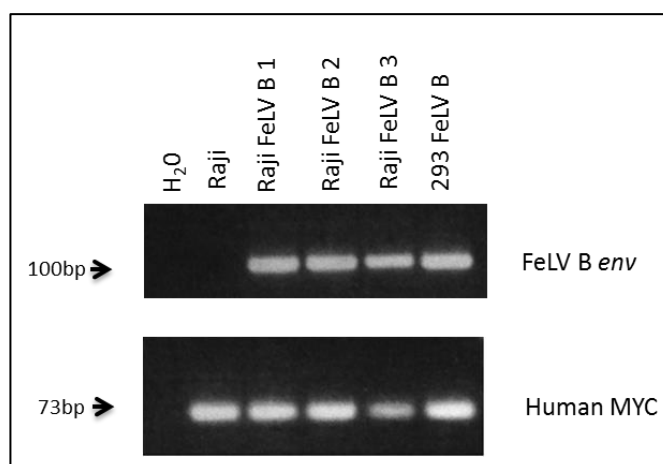


Figure 5.4 PCR using *env* primers specific for FeLV B and human MYC primers as an internal control. FeLV B infected 293 cell-DNA was used as positive control.

Figure 5.4 shows that Raji cells (in triplicate) are highly susceptible to FeLV B infection.

5.3.5 Infection of human breast cancer cells with FeLV B

An invasive breast cancer cell line, MDA MB 231 was next infected with FeLV B at MOI=1 (1×10^6 MDA MB 231 cells infected with 2 ml of FeLV B supernatant). This experiment was repeated three times. The FeLV B infection was confirmed by PCR using primers specific for FeLV B infection as shown in Figure 5.5.

Figure 5.5 PCR for FeLV B infection of breast cancer cells

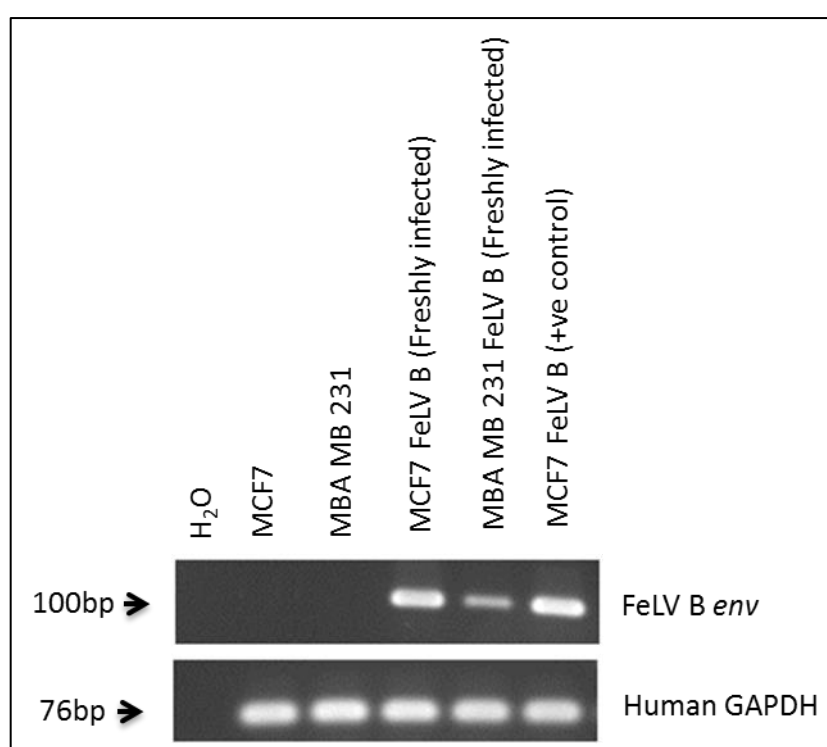


Figure 5.5 PCR using *env* primers specific for FeLV B and human GAPDH primers as an internal control. FeLV B infected MCF7 cell DNA was used as a positive control.

Figure 5.5 shows MDA MB 231 cells are also susceptible to FeLV B infection but at lower level than MCF7 cells.

5.3.6 Infection of human PBMCs with FeLV B

PHA treated human peripheral blood mononuclear cells (PBMCs) were infected with FeLV B at MOI=0.5 (1×10^6 PBMCs infected with 1 ml of FeLV B supernatant). This experiment was repeated three times. PCR carried out using DNA extracted

on 14th day of FeLV B infection (Figure 5.6) shows that PBMCs can get infected with FeLV B.

Figure 5.6 PCR for FeLV B infection of PBMCs

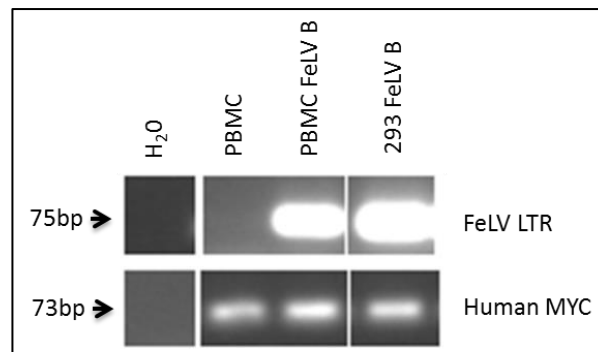


Figure 5.6 PCR using *env* primers specific for FeLV B and human MYC primers as an internal control. FeLV B infected 293 cell-DNA was used as a positive control.

5.3.7 Infection of CD34+ human cord cells with FeLV B

Human CD34+ cells were also infected with FeLV B at MOI=1. This infection was carried out by Anne Terry. PCR was carried out on the DNA extracted from the infected and uninfected CD 34+ cells showed that CD34+ cells can get infected with FeLV B as shown in Figure 5.7.

Figure 5.7 PCR for FeLV B infection of CD34+ cells

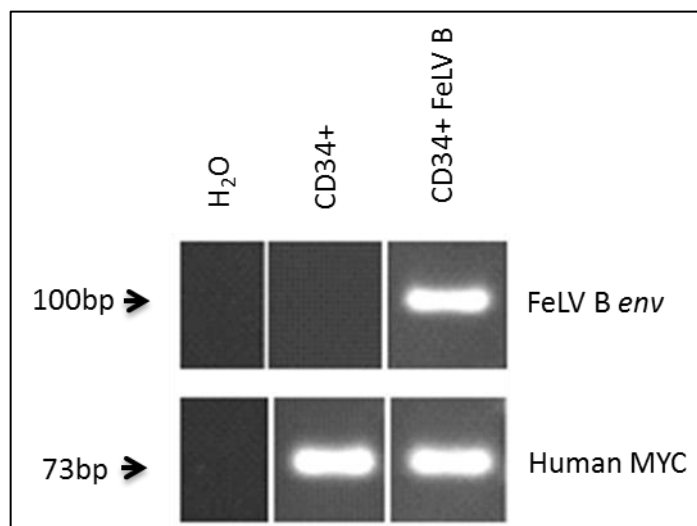


Figure 5.7 PCR using *env* primers specific for FeLV B and human MYC primers as an internal control. Water was used as a “non-DNA” control.

5.3.8 Infection of MCF7 cells with FeLV B and XMLV simultaneously

FeLV B and XMLV both use different cell surface receptors for infection. XPR1, the receptor used by XMLV, is a phosphate exporter³⁷, while PiT1, the receptor used by FeLV B, is a phosphate transporter²⁴⁶ and it is responsible for uptake of phosphate into the cells from the surroundings. I was interested to see if dual infection could be tolerated in the same cell line. For this purpose, MCF7 cells were infected simultaneously with filtered XMLV and FeLV supernatants. The FeLV B and XMLV infection was confirmed by PCR using primers specific for FeLV B and XMLV respectively as shown in Figure 5.8.

Figure 5.8 PCR for simultaneous FeLV B and XMLV infection of MCF7 cells

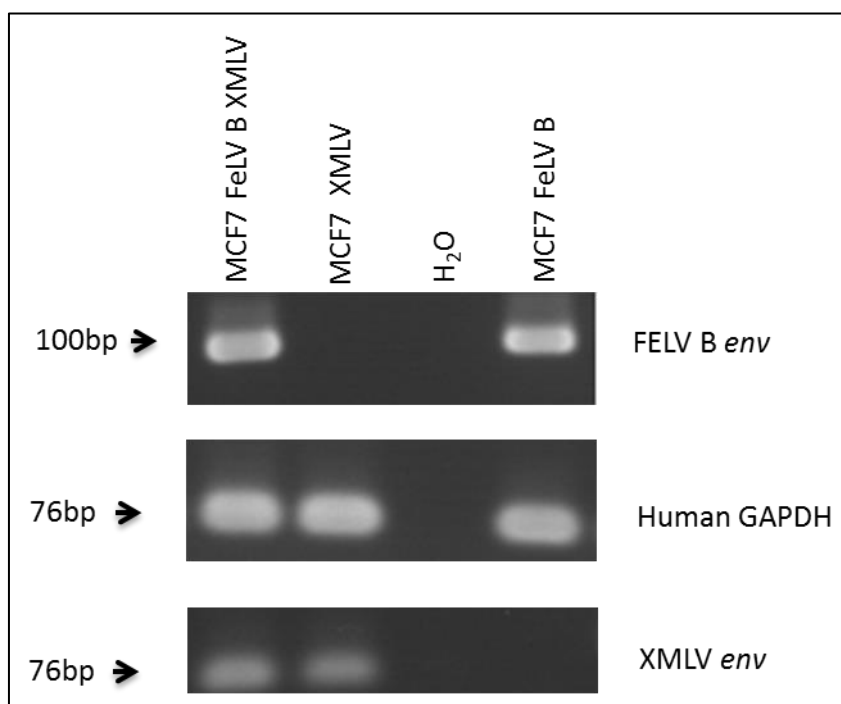


Figure 5.8 PCR using *env* primers specific for FeLV B and XMLV and human GAPDH primers as an internal control. MCF7 cells infected with FeLV B alone and MCF7 cells infected with XMLV alone were used as positive control for the respective primers.

In Figure 5.8, we can see that MCF7 cells exposed simultaneously to XMLV and FeLV B get infected with both viruses. This shows that the two viruses FeLV B and XMLV can coexist in the same cells without obvious cytopathic effect. This experiment was carried out once.

5.3.9 Specific infectivity of FeLV B in human cell lines

I have already shown that different cell lines vary in their susceptibility to FeLV B infection. I next wished to determine whether cell lines showed any differences in virus processing and release and whether these variations affected the quality and/or quantity of released virus. In order to find the specific infectivity of FeLV B in different cell lines, CEM, CEMSS, Reh, Kyo1, THP-1 and AH927 cells were infected with FeLV B. The cells were re-infected with FeLV B on the Day 3 to ensure saturation and grown for 2 weeks before harvesting. The cell lines were cultured until Day 14 to ensure replication. The FeLV B specific infectivity experiment was carried out twice. The supernatant from the cell lines on the Day 14 was titrated and added to QN10 cells. The results of the titration experiments are shown in Table 5.2.

Table 5.2 FeLV B titre from different cell lines using the QN10 assay

Cell line	Titre
CEM	4.43×10^4
CEMSS	6.26×10^4
Kyo1	3.6×10^3
Reh	3.87×10^2
THP-1	5.4×10^3
AH927	3.67×10^5

Table 5.2 Titration on QN10 cells shows the yield of infectious virus units capable of forming foci.

Table 5.2 shows that the greatest titre of infectious FeLV B was obtained from the feline AH927 cells. Among the human cell lines, the production of infectious particles was comparable between the CEM and CEMSS cell lines. THP-1 and Kyo1 both showed a moderate production of infectious particles while the Reh showed the least production of infectious particles. The next step was to quantify the total virus particle-related protein released by each cell line.

To determine the total virus particle-related protein released in the supernatant by each cell line, the Day 14 supernatant from FeLV B infected cells was used to prepare viral lysate and western blotting was carried out on the virus lysate as shown in Figure 5.9.

Figure 5.9 Western blot FeLV B virus proteins and specific infectivity

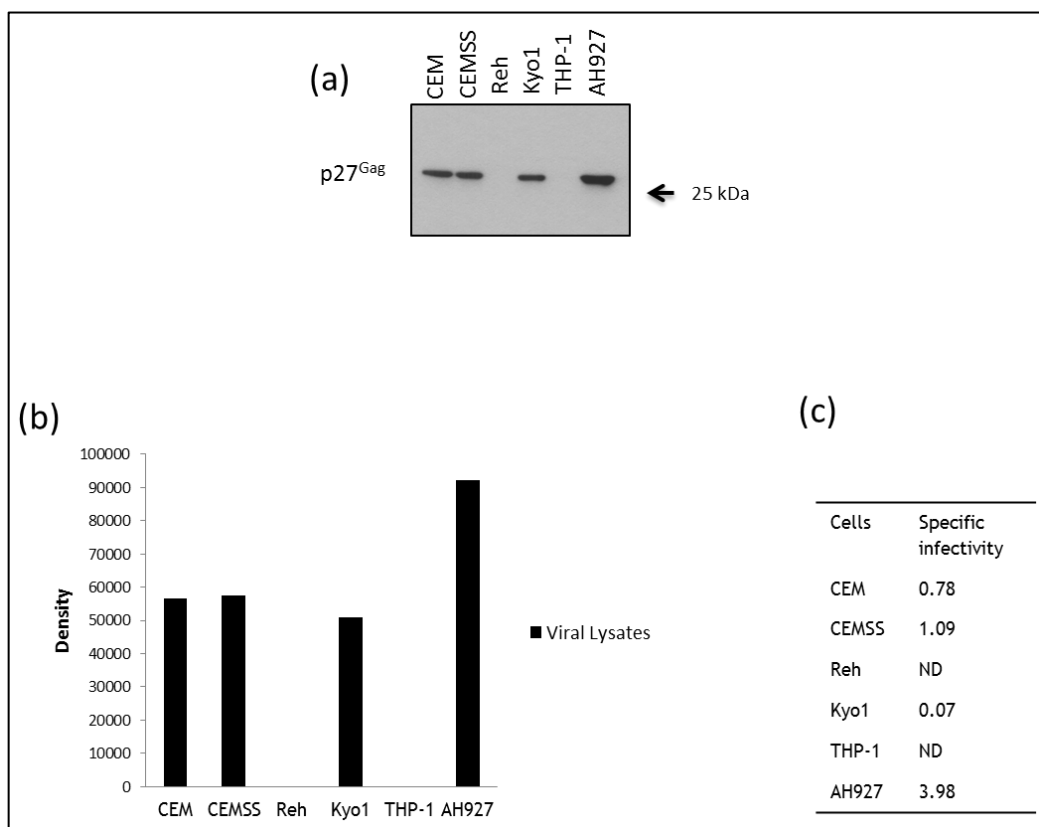


Figure 5.9 (a) Western blot for virion proteins using anti p27^{Gag} antibody. (b) Densitometry of virion CA p27^{Gag} western blot. (c) Specific infectivity of FeLV B calculated by dividing FeLV B titre (Table 5.2) by the virion particle-related protein values (Figure 5.9b). ND refers to calculations not done due to undetectable virion particle-related proteins in the western blot.

Figure 5.9 shows that the greatest quantity of FeLV B protein was produced by the AH927, followed by CEM and CEMSS cells. A large quantity of virion protein was shed by Kyo1 cells. Virion capsid protein was below detectable levels for Reh and THP-1 cells in this western blot analysis. This shows that the titre of infectious FeLV B particles produced by AH927, CEM and CEMSS correlates to some extent with the total quantity of virus released in the supernatant. On the other hand Kyo1 cells shed a significant quantity of virus particle-related protein but subsequent infectivity appeared to be low indicating that the virus particles released by Kyo1 cells were of reduced infectivity. The next step was to examine the intracellular levels of virus-specific protein being processed within different cell lines.

To examine virus protein processing within each infected cell line, the Day 14 FeLV B infected cell-pellet from each cell line was used to prepare cellular protein extracts and western blotting was carried out with Anne Terry's help. As

described in Chapter 1, The FeLV B Gag precursor protein (Pr65^{Gag}) is cleaved by protease enzymes to produce viral proteins that make up the matrix (MA, p15), capsid, (CA, p27) and virus nucleocapsid, (NC, p10)⁸. The quantity of Pr65^{Gag} and cell-associated p27 capsid protein, for each cell line was analysed here. The results are shown in the Figure 5.10.

Figure 5.10 Western blot FeLV B infected cell proteins

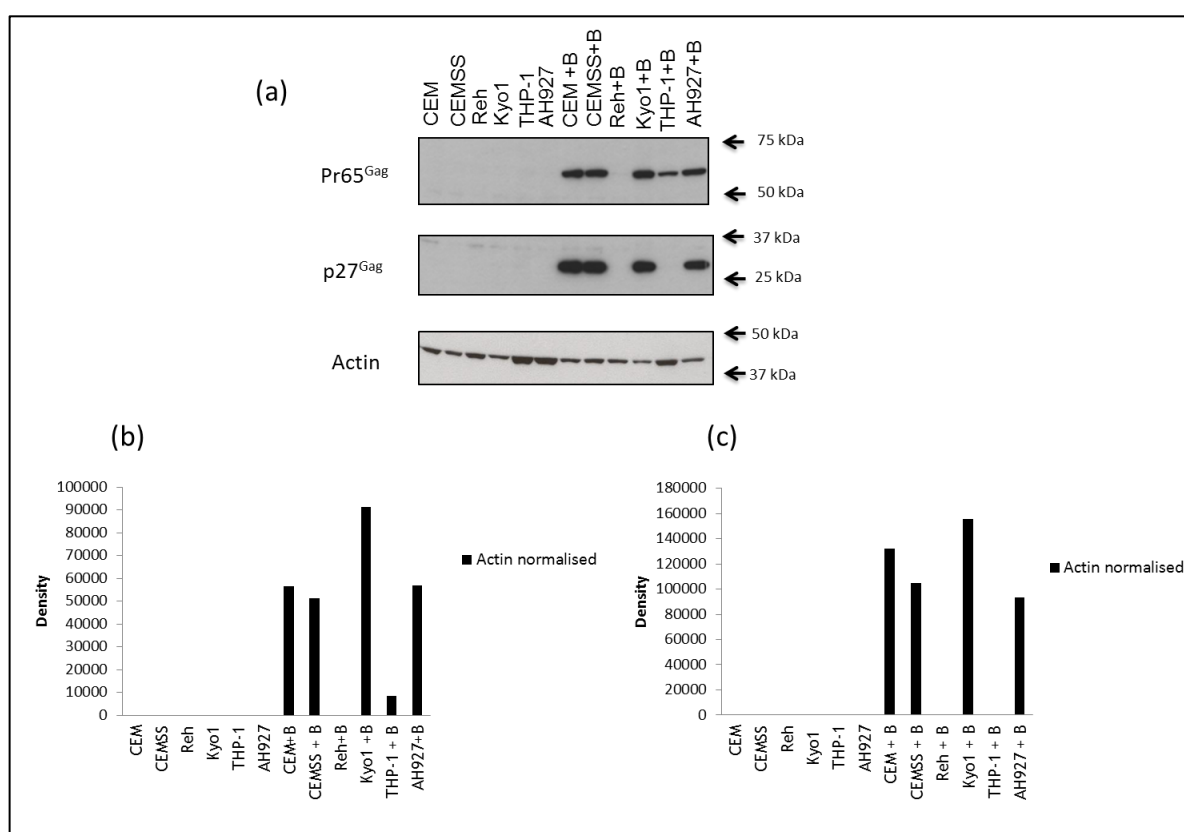


Figure 5.10 (a) Western blot of cellular proteins from the FeLV B infected cell lines using anti p27^{Gag} antibody. (b) Densitometry of FeLV B intracellular Pr65^{Gag} western blot. (c) Densitometry of FeLV B intracellular p27^{Gag} western blot. The densitometry of the cellular proteins was determined after normalising for the actin loading control.

Figure 5.10 shows that unprocessed FeLV B Pr65^{Gag} was seen in greatest quantity in Kyo1 cells, followed by AH927, CEM, and then CEMSS. Lower quantities of unprocessed FeLV B Pr65^{Gag} were seen in THP-1 and undetectably low levels in Reh cells. The level of p27^{Gag} followed a similar pattern with the exception of THP-1, where no processed p27^{Gag} could be seen. This suggested a block to processing of Pr65^{Gag} in these cells. In the case of Kyo1 cells, the relatively low infectivity of virions compared to those produced by AH927 feline fibroblasts was not simply due to lower production and processing of Gag gene products. The ratio of cell associated p27^{Gag} to Pr65^{Gag} was also higher for CEM and CEMSS as

compared to that in the AH927. The possible explanation for this could be that the particles are released easily in AH927 cells while there may be a restriction to release from Kyo1, CEM and CEMSS resulting in higher levels of processed virion proteins in these cells. The Reh cell line was consistent in having undetectably low levels of intracellular and released virion proteins, and a low titre of released virus. It was concluded that there is a block to FeLV B replication in Reh cells affecting earlier stages of the growth cycle.

5.3.10 Specific infectivity of FeLV B in human PBMCs

The above experiments show how the specific infectivity of FeLV B differed in established human cell lines. As these cell lines may have acquired defects in the course of transformation and establishment, I also wanted to test the susceptibility of primary human blood cells as this might be more informative with regard to resistance to zoonotic spread. For this purpose, PBMCs were infected with FeLV B in two different experiments. In the first experiment the CEM cell line was used as a control. Both CEM and PBMCs were infected with supernatant from FeLV B infected AH927 cells at MOI=0.08 (6×10^6 cells infected with 1 ml of FeLV B supernatant). Cells were harvested on Day 14, and were used to prepare pellets for DNA, RNA and protein extraction. FeLV B infection of PBMCs was confirmed by PCR and is shown in Figure 5.6. Day 14 supernatant from PBMCs was used for titration on QN10 cells and also for preparing cell free virus pellets. No infectious FeLV titre was detected in infected PBMC supernatant. The total virus particle-related protein released by PBMCs was also investigated by western blot analysis of the cell free viral pellet obtained from the supernatant as described later (Figure 5.13).

In a second experiment, I examined proviral DNA levels soon after exposure of cells to FeLV B to confirm that the PCR product detected in PBMCs was due to newly synthesised proviral DNA rather than contaminating DNA in the infecting virus stock. Reh and Kyo1 cells were used as controls for PBMCs infection. PBMCs, Reh and Kyo1 cells were infected with filtered ($0.45 \mu\text{m}$) supernatant from AH927 cells infected with FeLV B at MOI=0.08 (6×10^6 cells infected with 1 ml of FeLV B supernatant). Samples were obtained at 30 minutes, 6 hours and 72 hours after FeLV B infection and used to prepare DNA. PCR was carried out to follow FeLV B infection and is shown in Figure 5.11.

Figure 5.11 PCR for FeLV B infection of PBMCs, Reh and Kyo1 cells

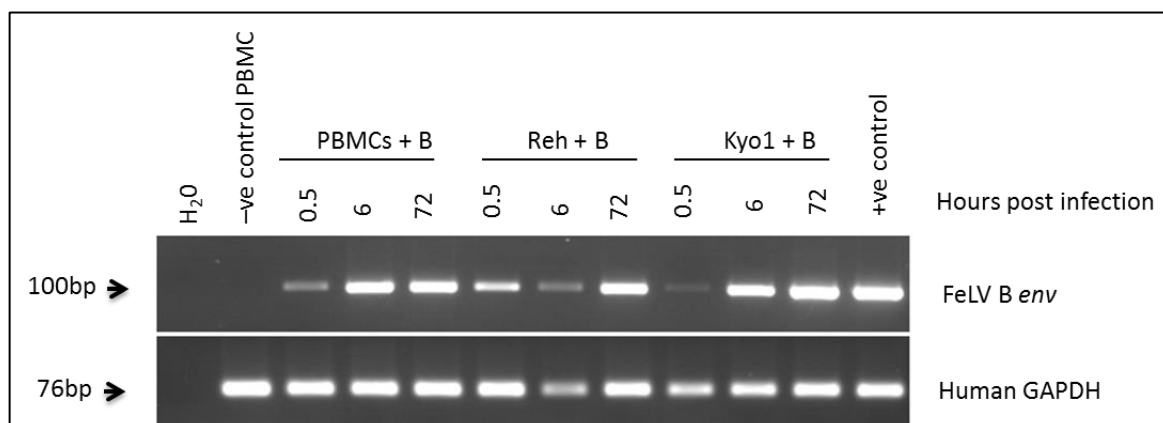


Figure 5.11 PCR carried out using *env* primers specific for FeLV B and human GAPDH primers used as an internal control. The infection of FeLV B in PBMCs, Reh and Kyo1 cells was checked at 30 minutes, 6 hours and 72 hours. DNA of 293T cells infected with FeLV B was used as a positive control.

This analysis showed that, with the possible exception of Reh, there was very little proviral DNA detectable in newly infected cells (30 minutes after exposure) and that levels increased in all cases by 6-72 hours. This suggested that the virus was successfully entering PBMCs and Reh cells at levels comparable to the more permissive Kyo1 cells. Since this analysis was carried out by standard semiquantitative PCR, the next step was to measure viral DNA more accurately by Real Time PCR. The results are shown in Figure 5.12.

Figure 5.12 FeLV B copy number in PBMCs, Kyo1 and Reh at different times

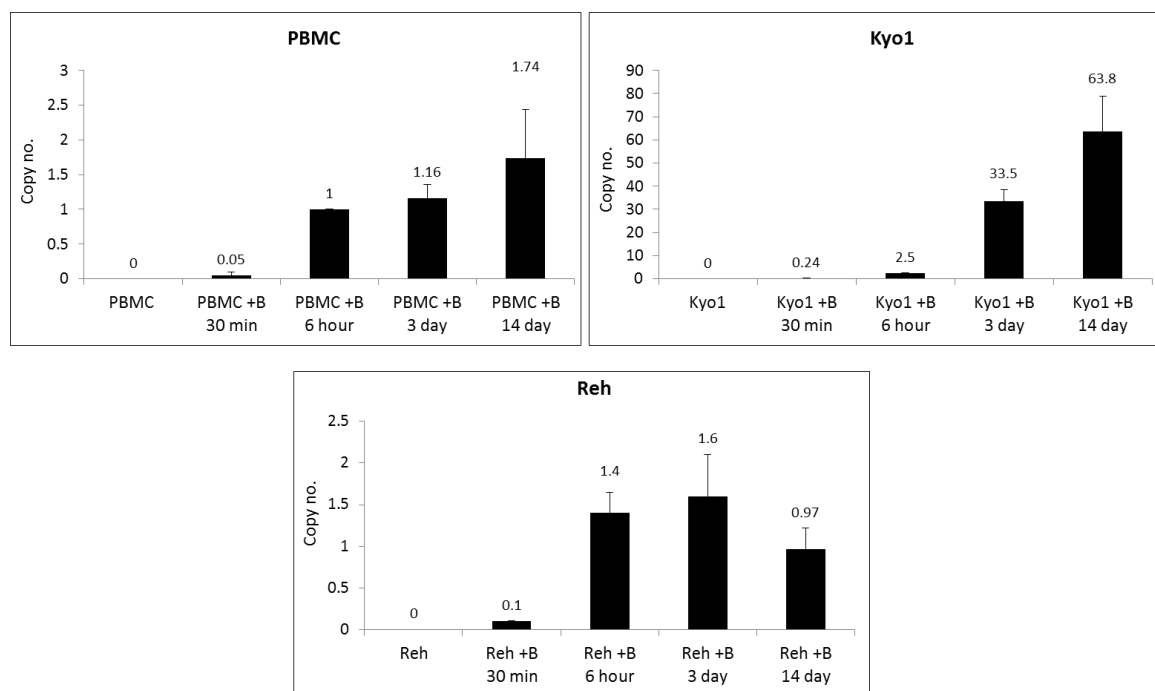


Figure 5.12 FeLV B copy number in PBMCs, Kyo1 and Reh cells at different time points determined by real time PCR using FeLV B *env* primers. All the values were normalised against the PBMC 6-hour FeLV B copy number. Error bars represent standard deviation.

As can be seen, these analyses confirmed the very low levels of proviral DNA detectable at the 30 minute time point, and the 10-20-fold amplification by 6 hours. However, there was a marked difference in the Kyo1 cells, where levels of proviral DNA continued to amplify to 3 days and 14 days after infection, while levels reached a plateau in the PBMCs and Reh cells. In order to further confirm this observation, titration experiments were carried out to calculate the number of infectious particles released by Reh, Kyo1 and PBMCs.

Day 14 supernatant from PBMCs, Reh and Kyo1 cells was titrated on QN10 cells. The titre is given in Table 5.3.

Table 5.3 FeLV B titre from PBMCs, Kyo1 and Reh supernatant

Cell line	Titre
PBMC	0
Reh	2
Kyo1	47
AH927	3.3×10^5

Table 5.3 Titration on QN10 cells shows the yield of infectious virus units capable of forming foci.

As shown in Table 5.3, no infectious FeLV B was detected in day 14 supernatants of the PBMCs, while a very low titre was noted from the Reh cells. The titre from Kyo1 was 47, consistent with the relatively low infectivity of virions released from these cells. AH927 was used as a positive control for the titration experiments. The titre of FeLV B released from AH927 cells was 3.3×10^5 . I also investigated the levels of virion-related protein released by PBMCs in both experiments along with the Reh and Kyo1 cells in the second experiment.

To investigate virion-related proteins released in the two experiments involving PBMCs, cell free virus pellet was obtained from Day 14 supernatant from the infected PBMCs, Reh and Kyo1 cells (2nd experiment) and PBMCs and CEM cells (1st experiment). Virion protein lysates were prepared and analysed by western blotting for the presence of FeLV B as shown in the Figure 5.13.

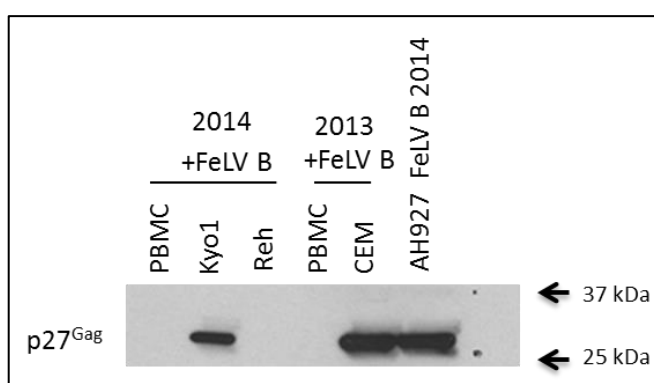
Figure 5.13 FeLV B virion proteins produced by infected cells**Figure 5.13 Western blot for virion proteins using anti p27^{Gag} antibody. FeLV B infected AH927 cell supernatant was used as a positive control for FeLV B viral protein.**

Figure 5.13 shows that supernatant from the PBMCs did not release any detectable FeLV proteins. Levels of protein released by Reh cells were also below detection by western blot, despite the presence of low levels of infectious

virus. In conclusion, the early stages of FeLV replication occur with similar efficiency in Kyo1, Reh and PBMCs, but only Kyo1 cells support production of viral protein and significant levels of virus particle production.

5.4 Discussion

In this chapter, I have demonstrated that different human cell lines and primary cells are susceptible to FeLV B infection but to a variable extent. I have identified three broad phenotypes: highly susceptible (293T, MCF7), partially susceptible (CEM, CEMSS, Kyo1, THP-1) and highly resistant (PBMC, Reh). These findings confirm and extend previous reports of human cells susceptibility to FeLV B infection *in vitro*¹⁴⁰.

FeLV B uses PiT1 or PiT2 phosphate transport receptors to enter human cells¹⁴². A complete absence of PiT1 and PiT2 receptors may make the cells resistant to FeLV B infection. The expression of PiT1 receptor mRNA (Anne Terry's unpublished results) showed no correlation with the susceptibility of various cell-types to FeLV B infection. This is also supported by the fact that gammaretroviruses like GaLV and amphotropic MLV using PiT1 and PiT2 respectively do not show a correlation between level of receptor mRNA expression and degree of susceptibility of human cells to infection by these viruses²⁴⁷, suggesting that other mechanisms may be involved in resistance.

As observed for XMLV, the lineage and origin of the cell lines showed little or no correlation with the susceptibility to FeLV B infection. For example the two breast epithelial cancer cell lines e.g. MCF7 and MDA MB 231 showed a marked difference in susceptibility. THP-1 cells (undifferentiated monocyte cell line) showed a unique block at the level of Gag precursor processing, although it is conceivable that the lower levels of Pr65^{Gag} produced in these cells was below the threshold required to initiate budding and activation of the viral protease as has been suggested for some retroviruses²⁴⁸. PBMCs were found to be resistant to XMLV infection but perhaps more susceptible to entry of FeLV B. CD34+ human cord cells showed more or less similar susceptibilities to both XMLV and FeLV B.

I have also demonstrated that in different cell lines the barrier to virus replication was not present at the same stage of replication. These experiments

also indicated that the virus released from different cell lines not only varied in quantity but also in infectivity. AH927 produced the greatest levels of total virus particle-related proteins and the highest titre of infectious virus released into culture supernatant and was used as the primary source of FeLV B and the standard for comparison in the specific infectivity experiments. The relatively low levels of unprocessed and processed intracellular FeLV proteins in AH927 cells indicate efficient virus processing and release. Several human leukaemia cell lines, (Kyo1, CEM and CEMSS) showed high levels of unprocessed and processed intracellular viral proteins but slightly lower levels of released virion particle-related protein and significantly lower infectious virus titres. These results suggest that virus particle release is somewhat delayed in the human leukaemia cell lines compared to the highly productive feline fibroblasts. However, the four to fifty-fold reduction in specific infectivity of the released virus particles appeared to be a more significant finding as a potential barrier to cross-species infection. The Reh cells on the other hand did not show any detectable intracellular or virus particle-related protein by western blot. The titre of infectious virus released by Reh cells was also very low. It appeared that the block to Reh infection might be at an early stage of infection after reverse transcription but before proviral integration or transcription.

PBMCs were found to be the least susceptible although, as in Reh cells, the early steps of proviral DNA synthesis appeared to proceed normally. Provirus persisted in PBMC cultures but PBMCs did not produce any detectable level of virus particle-related protein released into the supernatant or infectious virus titre. These observations were confirmed and extended by quantitative DNA PCR analyses that showed a clear difference between cells in which FeLV B infection was blocked at an early stage (PBMC, Reh) and those in which productive infection occurred (Kyo1).

6 Mechanisms of resistance of human cells to FeLV

6.1 Introduction

In the previous chapters, different cell lines and primary cells were investigated for susceptibility to XMLV and FeLV infection. It has also been demonstrated that human cell lines varied in terms of their susceptibility to FeLV B, and that the FeLV B was able to infect PBMCs but was not capable of replicating successfully. I wished to explore the mechanism for this resistance in PBMCs and the less susceptible cell lines further for potential relevant resistance to zoonotic infection of FeLV, which is still not well understood.

The main aim of the studies described in this chapter was to explore the barriers to replication of FeLV B, in human cells. Towards this aim, I sequenced FeLV B propagated in human cells to screen for mutations indicative of APOBEC3 activity which has been reported to restrict gammaretrovirus infectivity by mechanisms including G to A hypermutation of the viral genome²³⁴. I also examined the level of mRNA expression of APOBEC3 genes and other established retroviral restriction factors in different cell lines to see if the mutations and differential susceptibility correlated with restriction factor gene expression. I also explored the role of the glycoGag precursor protein, which is known to play an important role in virus release, infectivity and spread⁹³ and has been reported to counteract APOBEC3 activity in MLV⁹¹. FeLV also encodes a glycoGag precursor³ but this had not been examined for its effects on FeLV replication and APOBEC resistance in human cells.

6.2 Materials and methods

Materials and methods have been discussed in Chapter 2.

6.3 Results

6.3.1 FeLV B mutation analysis

To get a better understanding of differences in susceptibility of human cells to gammaretrovirus replication, I decided to look for G to A hypermutation in the *pol* region of FeLV B in cells infected with FeLV B. For this purpose primers capable of amplifying the *pol* region of FeLV B were used (given in Appendix 1). The cell lines checked for hypermutation included FeLV B infected 293 cells, THP-1 cells, Kyo1 cells, CEM cells, CEMSS cells, Reh cells and PBMCs. The details of the hypermutation analysis are summarised in the Table 6.1.

While no mutations were detected in the highly susceptible 293 cells (Table 6.1), all the leukaemia cell lines displayed evidence of G->A mutations at rates ranging from 0.4 to 6.2 per kilobase of FeLV genome sequenced. A small number of other mutations were also seen. Notably, the CEMSS cell lines, which is permissive for Vif defective HIV due to its low expression of APOBEC3G⁸⁶, displayed a higher mutation rate than the parental CEM cell line. Despite the early block and low virus output from Reh cells, it was possible to obtain sequence that indicated virus replication with G->A mutations at similar levels to the more permissive cell lines.

Table 6.1 Mutations in FeLV B *pol* region in different cell lines

Cell line	Total nucleotides sequenced	No. of clones sequenced	G to A mutation	G to A mutation rate (mutation/kb)	Non G to A mutation
293	3600	3	0	0	0
THP-1	6000	5	37	6.17	1
Kyo1	10800	9	43	3.98	1
CEM	7200	6	3	0.42	1
CEMSS	9600	8	8	0.83	1
Reh	1200	1	3	2.5	1

THP-1		From				Kyo1		From				CEM		From				
		G	A	T	C			G	A	T	C			G	A	T	C	
TO	G					TO	G	1				TO	G					
	A	37					A	43						A	3			
	T		1				T							T				1
	C						C							C				
Others		Addition mutations: 4				Others		Addition mutations: 2				Others						

CEMSS		From				Reh		From			
		G	A	T	C			G	A	T	C
TO	G		1			TO	G				
	A	8					A	3			
	T						T				
	C						C			1	
Others						Others		Addition mutations: 4			

Table 6.1 Showing mutations in FeLV B *pol* region in different cell lines infected with FeLV B (above) and showing the nature of non G to A mutations (below).

As the human APOBEC3 enzymes have been shown to have subtle differences in mutational target sequence preference, I wished to see how the mutations in FeLV compared and determine whether any prediction could be made about the family member responsible for the mutations. An online tool for hypermutation analysis²¹⁸ was used to display the mutations in graphical form with a colour code according to the dinucleotide at the target site as shown in Figure 6.1.

Figure 6.1 Graphical representation of hypermutation in the FeLV B

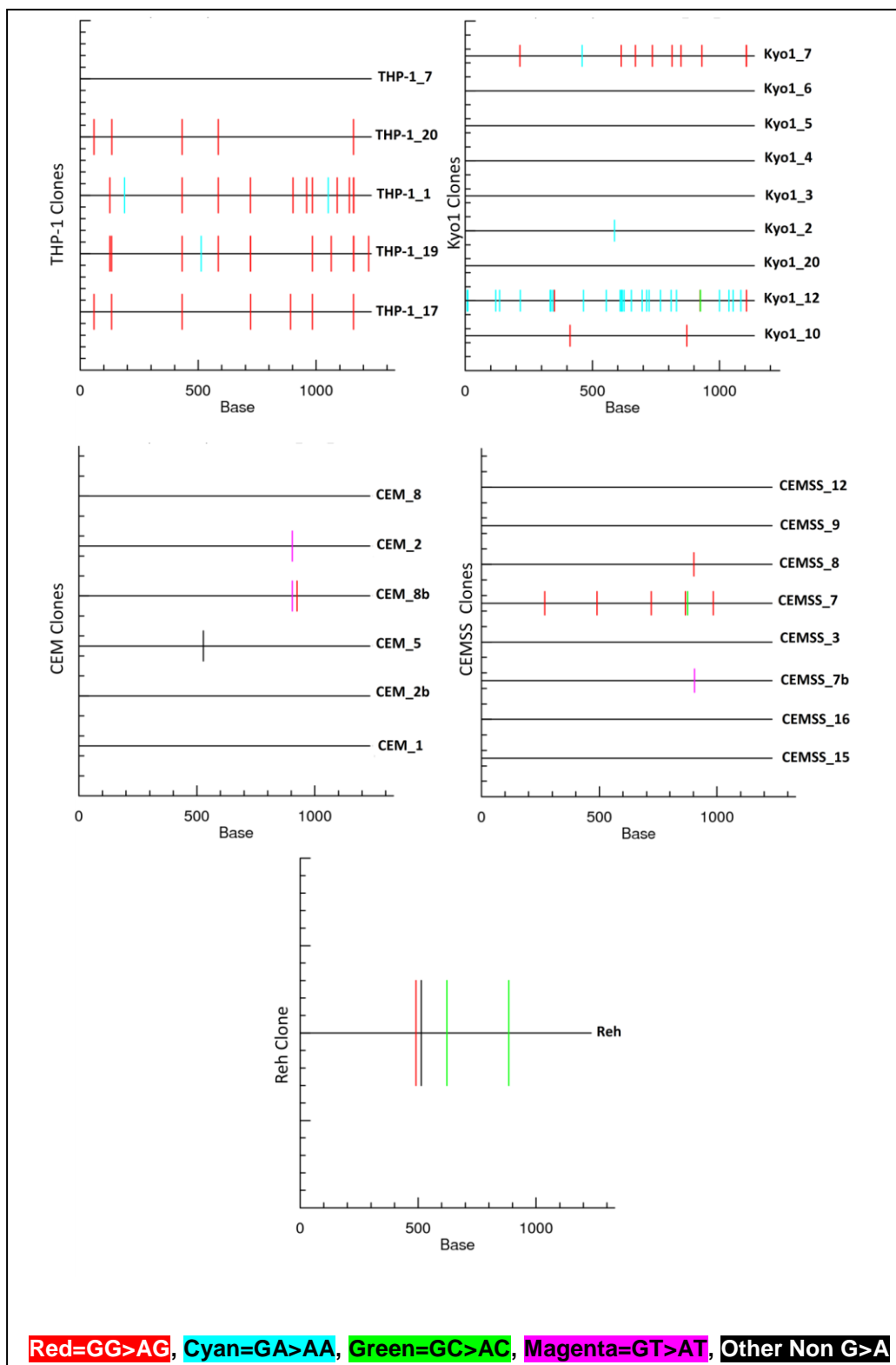


Figure 6.1 shows graphical representation of hypermutation in FeLV B *pol* region. In THP-1 cell line, out of 37 G to A mutations, 34 were GG to AG (red lines) and only 3 were GA to AA (cyan lines). In Kyo1 cells, out of 43 G to A mutations, only 14 were GG to AG (red lines), while 28 were GA to AA (cyan lines) and one was GC to AC mutation (green line). In CEM cells, out of 3 G to A mutations, 1 was GG to AG (red line) and 2 were GT to AT (magenta lines). In the CEMSS cells, out of 8 G to A mutations, 6 were GG to AG (red lines), 1 was GC to AC (green line), and 1 was GT to AT mutation (magenta line). In the Reh cell line, out of 3 G to A mutations, only one was GG to AG (red line), while the remaining 2 were GC to AC (green lines) mutations.

GG to AG mutation is the most likely effect of APOBEC3G or, with a lesser preference, APOBEC3C activity⁶⁹. GA to AA could also arise as a result of APOBEC3G (though less frequently as compared to GG to AG) but is the preferential change induced by APOBEC3F, APOBEC3B or APOBEC3C activity. While these overlapping dinucleotide preferences don't allow definitive identification of the enzymes responsible, the predominance of GG to GA changes in THP-1 was suggestive of APOBEC3G activity, while Kyo1 cells showed a more complex pattern that was unlikely to be created by APOBEC3G alone. Surprisingly, G->A changes were also most frequent in CEMSS cells, despite their anticipated low levels of APOBEC3G mRNA.

In order to have a deeper look into the preference sequence for deamination and the APOBEC3 enzymes responsible for it, analysis of the nucleotides upstream and downstream of the deaminated nucleotide was carried out as shown in the Table 6.2.

Table 6.2 Preferred sequence context for deamination by APOBEC3 enzymes

THP-1	-2	-1	0	1	2	Kyo1	-2	-1	0	1	2
G	0	0	0	2	5	G	8	2	0	3	4
A	7	0	0	19	13	A	8	0	0	9	16
T	7	4	1	8	12	T	10	28	1	18	16
C	24	34	37	9	8	C	18	14	43	14	8
n=38	C	C	C	A	A	n=44	C	T	C	T	A/T
CEM	-2	-1	0	1	2	CEMSS	-2	-1	0	1	2
G	1	0	1	1	0	G	0	1	0	1	2
A	1	2	0	0	1	A	2	1	0	1	0
T	2	1	0	1	1	T	4	0	1	4	6
C	0	1	3	2	2	C	3	7	8	3	1
n=4	T	A	C	C	C	n=9	T	C	C	T	T
Reh	-2	-1	0	1	2						
G	0	2	0	1	1						
A	1	0	1	0	1						
T	1	0	0	2	1						
C	2	2	3	1	1						
n=4	C	G/C	C	T	G/A/T/C						

Table 6.2 Preferred sequence context for deamination by APOBEC3 enzymes of the different cell lines. Position zero "0" indicates deaminated nucleotide on the virus negative strand. -1, -2 and +1, +2 indicate adjacent nucleotides upstream and downstream of the deaminated (zero position) nucleotide respectively. "n" denotes the total number of nucleotide mutations analysed. Letters at the bottom of each table show the preferred sequence context for deamination by the respective cell line's APOBEC3 machinery.

In most cases, the preferred site for deamination is dC (deoxycytidine) in the minus virus DNA strand resulting in G to A hypermutation in the plus virus DNA strand. The preferred sequence context for deamination of nucleotides in the

pol region of FeLV B in the THP-1 cells was CCC. In Kyo1 cells, CTC appeared to be preferred sequence for deamination. In CEM cells, TAC appeared to be the preferred sequence for deamination while in CEMSS cells TCC was the preferred sequence for deamination. Reh cells showed an equal preference for deamination for CCC and CGC (The underlined nucleotide indicates the deaminated nucleotide, the ones written before it are -1 and -2 respectively). APOBEC3G is known to show a preference for CCC nucleotide sequence^{66,70} while APOBEC3F shows a preference for CTC⁷⁰ and APOBEC3B prefers GTC or CTC⁷⁰. This indicates that THP-1 show an APOBEC3G hypermutation signature while Kyo1 cells show an APOBEC3F preference.

PBMCs infected with FeLV B were also checked for mutations. Amplification of the *pol* fragment from Day 3 infected PBMCs generated 2 clones but repeated efforts were required to generate these clones. The 2 clones were free of mutations. No clones could be amplified or sequenced from Day 14 infected PBMC cells. The basis of this difficulty in cloning PCR products from the FeLV infected PBMCs has not been established.

6.3.2 Restriction factor expression analysis

The next step was to compare the mRNA expression of different restriction factors in the panel of cell lines. The expression was investigated by qRT-PCR as described in Chapter 2. All expression analyses were normalised and compared against a baseline of the permissive 293 cell line. The expression of different restriction factors is described below.

6.3.2.1 APOBEC3 expression

The expression of different APOBEC3 gene mRNAs in a panel of cells is shown in Figure 6.2.

Expression levels of APOBEC3A, 3D, 3F and 3G were markedly higher in PBMCs than in the other cell lines in line with a published analysis of these genes across multiple tissues and cell lines⁶¹, the most extreme differences were noted for APOBEC3A and APOBEC3G which displayed 170-200-fold increased expression over the 293 cell baseline (Figure 6.2). My results also recapitulated observations on the CEMSS subline, showing reduced levels of all APOBEC family members compared to the CEM parental line apart from 3C and 3F. APOBEC3B expression was highest in THP-1 cells, close to 20-fold higher than baseline, while APOBEC3C was highest in PBMCs and Kyo1 cells (Figure 6.2).

Taking these data together, it is not easy to correlate expression levels with hypermutation activity or the early blocks to FeLV infection seen in PBMCs and Reh cells. However, the levels of 3G and 3B show some inverse association with specific infectivity of virus released from several lines (CEM>Kyo, THP-1) and it is notable that both of these enzymes have been reported to be encapsidated.

Figure 6.2 Expression of APOBEC3 mRNAs relative to permissive 293 cells

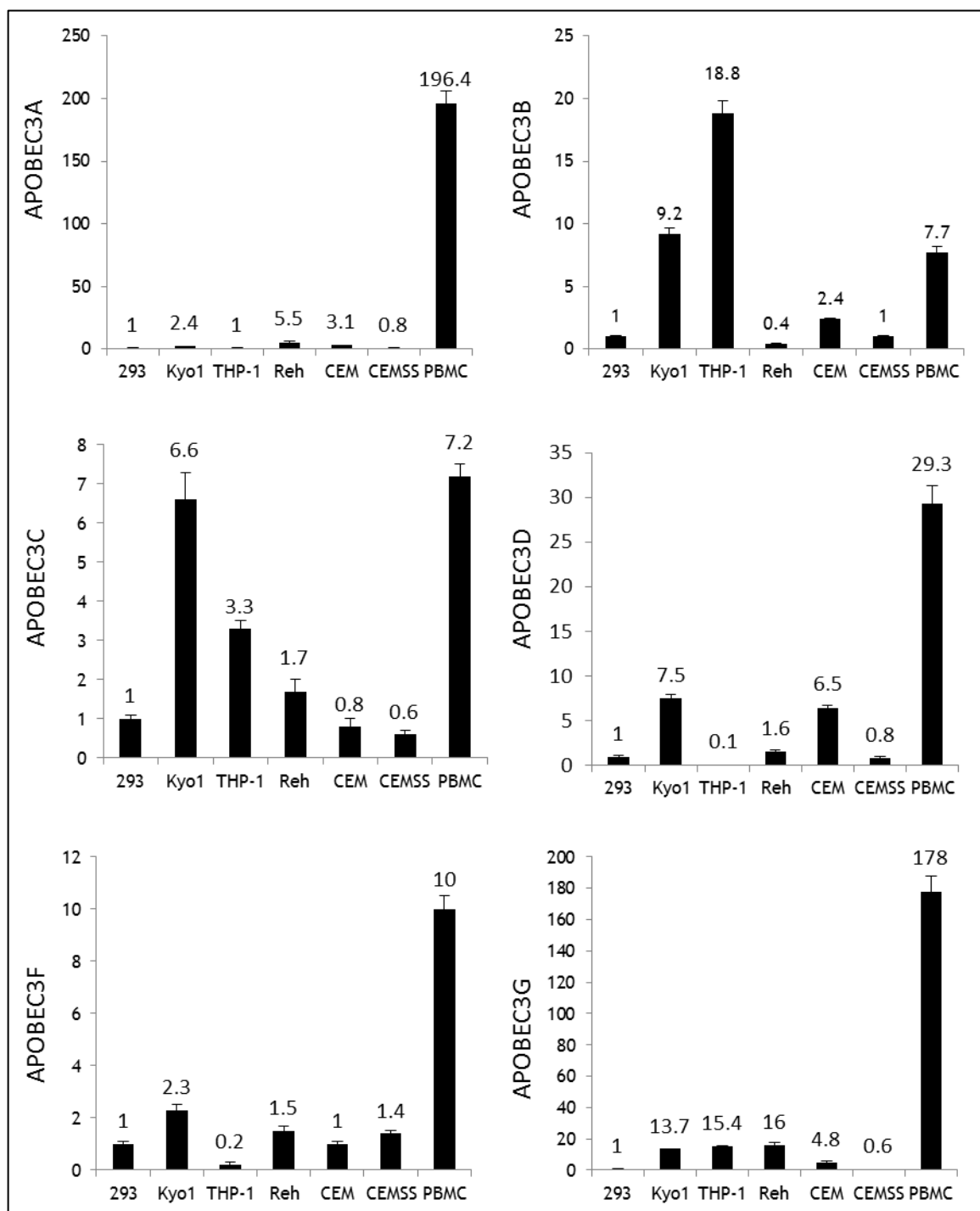


Figure 6.2 Expression of different APOBEC3 restriction enzyme mRNAs in different cells by qRT-PCR. All expression analyses were normalised and compared against 293 cell line. Error bars represent standard deviation.

While APOBEC3G appears to be the best candidate for the predominant mutational activity against FeLV B, the activity detected in CEMSS cells despite low expression levels of all family members suggests that mRNA levels alone cannot account for the differences in activity and the lack of mutations seen in permissive 293 cells. The possibility that APOBEC activity underlies the early

block to infection in PBMCs despite the low level of mutations might also be suggested by the extremely high levels of APOBEC3A and APOBEC3G, and it is notable that Reh are the next highest expressers of both genes. The relatively strong mutational activity in Kyo1 cells is also correlated with higher APOBEC3G expression compared to baseline, although the strong expression of several other family members (APOBEC3B, APOBEC3C and APOBEC3D) precludes any firm conclusion (Figure 6.2).

6.3.2.2 SAMHD1 expression

I examined the expression of other candidate restriction factors including SAMHD1 as shown in Figure 6.3. SAMHD1 was highly expressed in the THP-1 monocytic leukaemia cell lines, and was also higher in PBMCs compared to baseline. Very low expression was observed in CEM and CEMSS cells. The SAMHD1 gene did not appear to be a likely candidate for the early block in Reh cells.

Figure 6.3 Expression of SAMHD1 mRNA in different cells

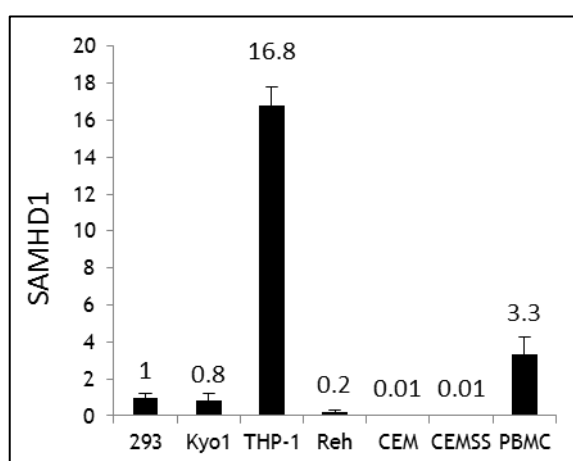


Figure 6.3 Expression of SAMHD1 in different cells by qRT-PCR. The expression was normalised and compared against 293 cell line. Error bars represent standard deviation.

THP-1 cells show a defect in processing intracellular virion protein which cannot be attributed to SAMDH1 expression on the basis of its reported mode and site of action. The expression of SAMHD1 was checked thrice for each sample in triplicate.

6.3.2.3 TRIM5 α

The expression of TRIM5 α in different cells is shown in Figure 6.4. Although TRIM5 α has not been shown to restrict gammaretroviruses, I found that its expression was markedly higher than the 293 cell baseline in all case. Expression was observed to be highest in Reh followed by Kyo1 cells.

Figure 6.4 Expression of TRIM5 α mRNA in different cells

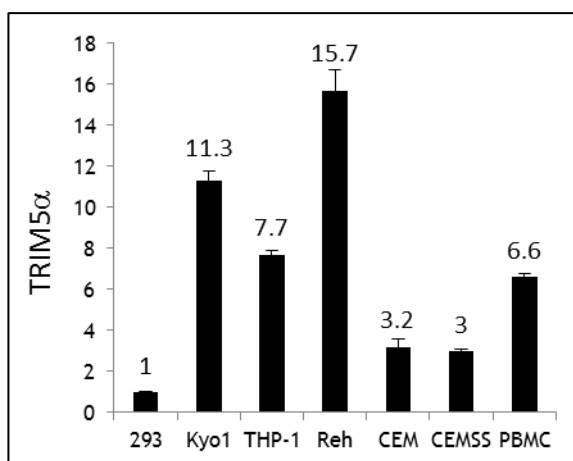


Figure 6.4 Expression TRIM5 α in different cells by qRT-PCR. The expression was normalised and compared against 293 cell line. Error bars represent standard deviation.

The lowest expression in leukaemia cell lines was in CEM which had comparable levels to the CEMSS subline. The level of expression was also comparable in PBMCs and THP-1 cells though it was slightly lower in PBMCs. As TRIM5 α typically acts at before reverse transcription⁹⁶ it appears unlikely as a candidate for the early block to replication in Reh and PBMCs. Also, Kyo1 cells which do not display the early block expressed quite high levels of TRIM5 α . The expression of TRIM5 α was checked thrice for each cell line in triplicate.

6.3.2.4 Tetherin

The expression of Tetherin in different cells is shown in Figure 6.5. The expression of Tetherin was high in THP-1, CEM and PBMCs.

Figure 6.5 Expression of Tetherin mRNA in different cells

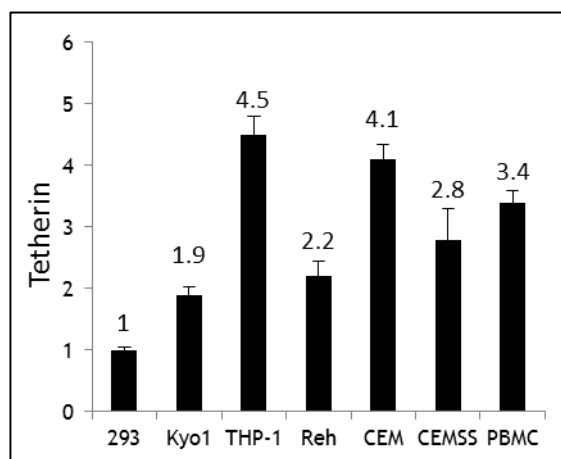


Figure 6.5 Expression Tetherin in different cells by qRT-PCR. The expression was normalised and compared against 293 cell line. Error bars represent standard deviation.

The expression of Tetherin was higher in CEMSS as compared to Kyo1 and Reh cell lines. This showed that Tetherin expression did not correlate with FeLV B titre or virion-related protein released by the infected cells in general. Tetherin expression was checked twice for each cell line in triplicate.

6.3.3 The role of glycoGag in FeLV B

As described in Chapter 1, simple gammaretroviruses like MLV and FeLV also encode an alternative type of Gag known as glycosylated Gag in addition to the normal Gag protein. Glycosylated Gag in MLV assists in viral budding and has also been reported to counter APOBEC3-mediated restriction^{91,93}. I wanted to investigate whether glycoGag is able to affect FeLV B specific infectivity. I received two relevant plasmids PENHF and PENHFX from Anne Terry. PENHF is a clone of wild-type FeLV B capable of producing glycosylated Gag, while the PENHFX has a mutation in the glycoGag start codon region, and is unable to synthesise glycoGag. The first important step was to confirm the difference between PENHF and PENHFX FeLV B plasmids in terms of the glycoGag start codon region. I designed primers (FeLV B *gag*, given in Appendix 1) to sequence the *gag* region from the PENHF and PENHFX FeLV B plasmids. The sequence of PENHF and PENHFX in the glycoGag start codon region is shown in the Figure 6.6.

Figure 6.6 gPr80^{Gag} start codon sequence of PENHF and PENHFX transcripts

PENHF										
Proviral DNA	CTG	ATG	TCT	CGA	GCC	TCT	AGT	GGG	ACA	GCC
Proviral mRNA	CUG	AUG	UCU	CGA	GCC	UCU	AGU	GGG	ACA	GCC
Polypeptide	Leu	Met	Ser	Arg	Ala	Ser	Ser	Gly	Thr	Ala

PENHFX										
Proviral DNA	CTG	ATG	TCT	CGA	<u>TCG</u>	AGC	CTC	TAG	TGG	GAC
Proviral mRNA	CUG	AUG	UCU	CGA	<u>UCG</u>	AGC	CUC	UAG	UGG	GAC
Polypeptide	Leu	Met	Ser	Arg	Ser	Ser	Leu	-	Trp	Asp

Figure 6.6 Sequences of PENHF and PENHFX in the glycoGag start codon region upstream of the normal Pr65^{Gag} start codon showing the presence of AUG start codon in both sequences and the presence of UAG stop codon only in PENHFX due to addition of 4 nucleotides in PENHFX which results in a frame shift mutation after the start codon region, resulting in termination of glycoGag translation in PENHFX. The normal Gag precursor could however be translated in PENHFX as its initiation site is unaffected.

Figure 6.6 shows that PENHFX is a glycoGag mutant form of FeLV B. I wanted to see if a partially susceptible cell line like Kyo1 would replicate the wild-type (PENHF) and the glycoGag mutant FeLV B (PENHFX) in a different or similar manner. For this purpose I first transfected 293T cells with FeLV B (PENHF) and the glycoGag mutant FeLV B (PENHFX) plasmids using the Lipofectamine transfection reagent (Invitrogen) according to manufacturer's protocol as described in Chapter 2. DNA was extracted from the transfected 293T cells on Day 14 and PCR carried out using primers specific for FeLV B as shown in the Figure 6.7.

Figure 6.7 Transfection of 293T cells with PENHF and PENHFX

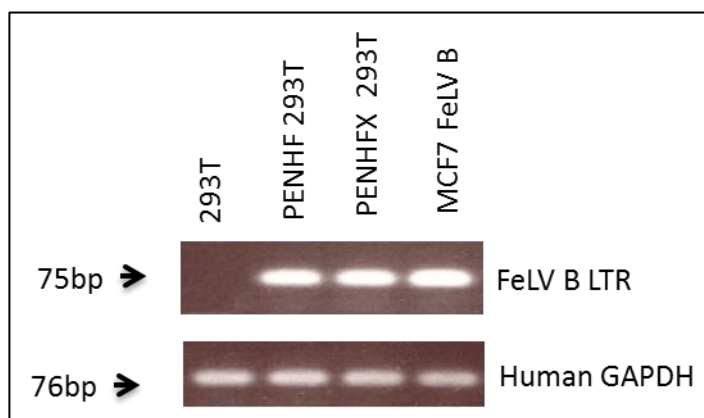


Figure 6.7 PCR carried out using LTR primers specific for FeLV B and human GAPDH primers used as an internal control. DNA of MCF7 cells infected with FeLV B was used as a positive control.

Figure 6.7 shows that the 293T cells were successfully transfected with PENHF (wild-type FeLV B) and PENHFX (glycoGag mutant FeLV B) plasmids. The next step was to infect Kyo1 cells using the supernatant from the PENHF and PENHFX transfected 293T cells. For this purpose 5×10^5 Kyo1 cells were infected with filtered ($0.45 \mu\text{m}$) supernatant from the PENHF and PENHFX transfected 293T cells. The cells were saturated by a repeated infection on the Day 3, again using the supernatant from the PENHF and PENHFX transfected 293T cells. On Day 14 of infection, cell pellets were made and DNA was extracted. The DNA was used for PCR to confirm infection of Kyo1 cells using specific primers as shown in Figure 6.8.

Figure 6.8 Infection of Kyo1 with PENHF and PENHFX

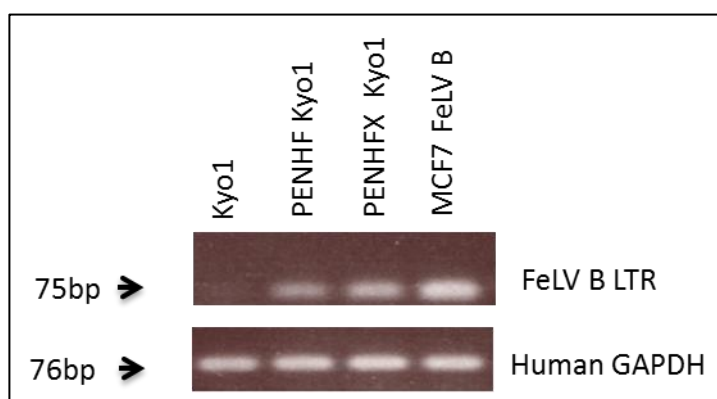


Figure 6.8 PCR carried out using LTR primers specific for FeLV B and human GAPDH primers used as an internal control. DNA of MCF7 cells infected with FeLV B was used as a positive control.

Figure 6.8 shows that Kyo1 cells were infected with PENHF and PENHFX. The supernatants from Day 14 PENHF and PENHFX infected Kyo1 cells were used to perform a QN10 titration assay. The results of the QN10 titration assay are shown in the Table 6.3.

Table 6.3 PENHF and PENHFX QN10 titration

Cells	Titre
Kyo1 PENHF	1.52×10^2
Kyo1 PENHFX	1.5×10^2
AH927 FeLV B	4.2×10^5

Table 6.3 Titration on QN10 cells shows the yield of infectious virus units capable of forming foci from the different infected cell lines.

The Table 6.3 shows that the titre released from the Kyo1 cells was equivalent for glycoGag mutant (PENHFX) and wild-type (PENHF) FeLV B. Supernatant from AH927 cells infected with FeLV B was used as positive control for titration. This analysis suggests that both the wild-type and glycoGag mutant FeLV B have similar specific infectivities when grown in the partially susceptible cell line Kyo1.

The next step was to see if the glycoGag mutant was impaired in human PBMCs. PBMCs were infected with filtered ($0.45\mu\text{m}$) supernatant from the PENHF and PENHFX transfected 293T cells. Cells were harvested on Day 14, and were used to prepare pellets for DNA. Confirmation of FeLV B infection of PBMCs was carried out by PCR and is shown in the Figure 6.9.

Figure 6.9 PCR for PENHF and PENHFX infection of PBMCs

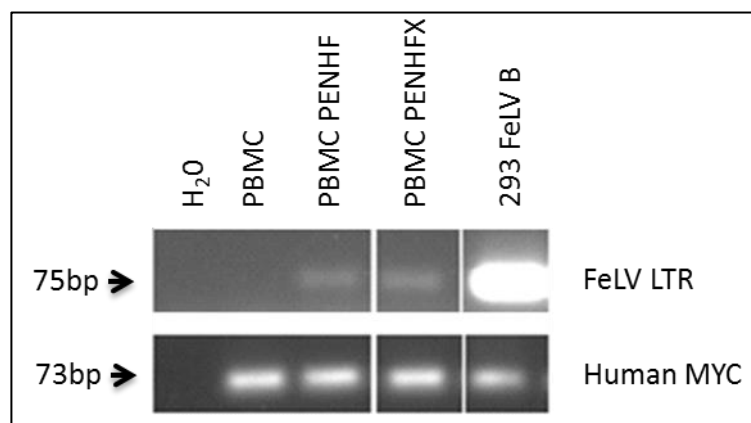


Figure 6.9 PCR carried out using LTR primers specific for FeLV B and human MYC primers used as an internal control. DNA from 293 cells infected with FeLV B was used as a positive control.

Figure 6.9 shows that PBMCs can become infected with both PENHF and the PENHFX. Day 14 supernatant from PBMCs was used for titration on QN10 cells. No titre was obtained from PENHF or PENHFX infected PBMC supernatant indicating that PBMCs do not release any infectious virus from either the wild-type or glycoGag mutant infected cells.

6.4 Discussion

In this chapter, I demonstrated the expression of restriction factors in different cells and the mutations induced in FeLV B after infecting these cells. This was carried out to seek mechanistic insight into the difference in susceptibility and processing of virus by these cells and the production of infectious particles and is summarised in the Table 6.4.

No evidence of hypermutation in FeLV B was observed in the highly susceptible 293 cell line which is also susceptible to rapidly spreading infection with FeLV, presumably due to the negligible levels of restriction factor activity in this cell line. All other cell lines examined showed evidence of APOBEC3-induced mutations and reduced specific infectivity of virions, although the identity of the APOBEC3 genes responsible for FeLV mutations could not be fully elucidated from the spectrum observed. The THP-1 cell line showed a predominance of GG target sites suggestive of APOBEC3G activity, while Kyo1 cells showed a predominance of GA targets, suggestive of A3F or other family members.

Table 6.4 Summary of restriction factor expression, PiT1 expression, mutations and susceptibility of FeLV B

Cells	A3A	A3B	A3C	A3D	A3F	A3G	SAMHD1	TRIM5 α	Tetherin	PiT1	Total mutation/ bp sequenced	G to A mutation (%)	FeLV B entry	FeLV B titre	FeLV B Intra cellular Pr65 ^{Gag}	FeLV B Intracellular p27 ^{Gag}	FeLV B Virion p27 ^{Gag}
293	1	1	1	1	1	1	1	1	1	1	0/3600	0	+	ND	ND	ND	ND
Kyo1	2.4	9.2	6.6	7.5	2.3	13.7	0.8	11.3	1.9	1.8	44/10800	97.7	+	++	++	++	++
THP-1	1	18.8	3.3	0.1	0.2	15.4	16.8	7.7	4.5	1.4	38/6000	97.4	+	+	+	0	0
Reh	5.5	0.4	1.7	1.6	1.5	16	0.2	15.7	2.2	3.5	4/1200	75	+	+	0	0	0
CEM	3.1	2.4	0.8	6.5	1	4.8	0.01	3.2	4.1	1.6	4/7200	75	+	+++	++	++	++
CEMSS	0.8	1	0.6	0.8	1.4	0.6	0.01	3	2.8	1.5	9/9600	89	+	+++	++	++	++
PBMC	196.4	7.7	7.2	29.3	10	178	3.3	6.6	3.4	1	3/13200	100	+	0	ND	ND	0

Table 6.4 Summary of restriction factor expression in a panel of cells compared with FeLV B susceptibility, processing, infectious virus titre, PiT1 receptor expression and mutations in FeLV B *pol* region. The restriction factor expression and PiT1 expression have been compared to corresponding expressions in 293 cells.

While most studies on restriction factor activity for the APOBEC3 genes have focused on HIV as a target, extrapolation to FeLV is not straightforward as HIV encodes a potent counter-measure by expression of the Vif accessory protein that can degrade some APOBEC3 family members⁷¹. It has been reported that Moloney murine leukaemia virus is specifically susceptible to A3B and A3G due to the ability of these proteins to become encapsidated via binding to MLV Gag²⁴⁹. However, this report is not consistent with recent evidence that APOBEC3 encapsidation occurs quite non-specifically via broadly specific RNA binding²⁵⁰.

THP-1 cells also expressed high levels of SAMHD1. SAMHD1 is known to inhibit HIV-1 infection in non-dividing macrophages and dendritic cells, primarily by depleting nucleotide pools¹¹¹ and its high expression in THP-1 cells is not surprising. The fact that THP-1 are dividing suggests that SAMHD1 restriction will not be operative in these cells. TRIM5 α is another restriction factor known to inhibit HIV infection²⁵¹ and is known to be operative against some murine leukaemia virus strains (N-tropic, but not B-tropic)²⁵². It is expressed more highly in Reh cells but as this factor appears to act at a stage prior to reverse transcription it seems unlikely as a candidate for the block after proviral DNA synthesis that I observed. The occurrence of G to A mutations in CEMSS cells despite low levels of APOBEC3 gene expression is hard to account for and merits further study. It is possible that the levels of mRNA expression are not fully representative of protein levels or functional activity.

I did not check the restriction factor protein levels in different cells and also whether all cell lines were expressing same restriction factor proteins or their variants or mutant forms were not confirmed. The variant or mutant forms of these restriction factor proteins could have a great impact on the antiviral properties of these restriction factors. It is also likely that host resistance does not depend on any single restriction factor activity and may be due to an interplay between different restriction factors, and the combined effect resulted in the observed differences in the specific infectivity of the virus released.

It has been shown that XMRV used to infect macaques showed an initial rise in plasma levels, which later on disappeared from the plasma after 4 weeks,

though XMRV DNA was still detectable in PBMCs up to 119 days after infection²⁵³ suggesting a limited gammaretrovirus replication *in vivo*. XMRV was efficiently restricted by the host restriction factors, with APOBEC3 playing a significant role, shown by the increasing G to A mutation, thus highlighting one of the mechanisms why gammaretrovirus do not infect humans despite high levels of human exposure to these agents²⁵³. The expression of APOBEC3A, APOBEC3D and APOBEC3G was very high in PBMCs which may conceivably be responsible for the undetectably low infectious titre and virion particle release. I was able to clone and sequence only 2 templates of FeLV from the PBMCs in spite of repeated efforts. These efforts were repeated later by Nancy Mackay who used an alternative PCR protocol (unpublished results) and obtained 9 clones which showed only 3 G to A mutations despite the high level of APOBEC3 expression in PBMCs. It seems likely that this reflects the lack of replication and the inability of APOBEC to mutate incoming viral DNA. APOBEC3 is also known to inhibit retrovirus infection by mechanisms other than G to A mutations e.g. by interfering with reverse transcription or integration of the retroviral DNA into the cell^{76,77}. Therefore a cytidine deaminase independent mechanism can be a possible explanation in this case which needs to be investigated further.

Tetherin is known for restricting HIV particle release¹⁰⁰ but no correlation was observed between expression of Tetherin and virion particle-related protein released into the supernatant.

I also found no difference in the infectious titre of wild-type and glycoGag mutant FeLV B released from infected Kyo1 cells. The glycoGag protein has been described to play a role in MLV budding or release from cells⁹³. MLV glycoGag has also been described to counteract mouse APOBEC3 activity⁹¹. Repairing the defective glycoGag of XMRV has also been shown to increase its infectivity⁹². I confirmed the presence of mutation in the glycoGag start codon region in the FeLV B mutant (PENHFX) plasmid as compared to the wild-type FeLV B which could result in a stop codon in the glycoGag transcript but found no difference in its ability to replicate or evade APOBEC activity in Kyo1 cells or human PBMCs.

7 Phenotypic effects of gammaretrovirus infection on human cells

7.1 Introduction

In the previous chapters, it has been shown that many human cell lines are susceptible to XMLV infection. Therefore the cell lines developed by xenografting or used in xenograft experiments or kept in the same laboratory may get infected with XMLV¹⁷³. The presence of XMLV contamination may affect human cell biology and thus act as a confounding factor for experimental results.

The main aim of studies described in this chapter was to investigate whether gammaretroviral infection/contamination of samples (especially XMLV) could affect the behaviour of cells.

7.2 Materials and methods

Materials and methods have been discussed in detail in Chapter 2.

7.3 Results

7.3.1 XMLV and FeLV B infected MCF7 cells show accelerated wound healing compared to uninfected MCF7 cells

As shown in Chapter 4 that XMLV can successfully infect MCF7 cells and integrate at multiple sites in the MCF7 genome. As retroviruses can exert their oncogenic action by disrupting host gene expression or coding sequences¹⁵, ongoing integration of XMLV provirus could affect the behaviour of the cell line by activating/deactivating adjacent genes. In addition to the risk of insertional mutagenesis there are other mechanisms by which XMLV may conceivably affect cell behaviour, including effects mediated by ligation of entry receptors and expression of viral proteins that may affect cell function. The aim of these experiments was to investigate whether gammaretrovirus infection of MCF7 cells could affect their migratory properties, determined by their ability to migrate across an artificially created wound in a confluent layer of cells. Wound assays were carried out on MCF7 cells that had been infected with either XMLV or FeLV B for at least 14 days, as described in Chapter 2. The experiments were repeated three times and in each experiment 5-6 wounds were made. From these, wounds with comparable size and shape were selected resulting in the measurement of three wounds per sample in experiments 1 and 2, and five wounds per sample in experiment 3. Wound healing was monitored using Image J software and serial images recorded at regular intervals. The results are shown in Figure 7.1 and demonstrate that viral infection, with either FeLV or XMLV, modestly influenced the rate of wound healing as discussed below.

Figure 7.1 Wound healing assay

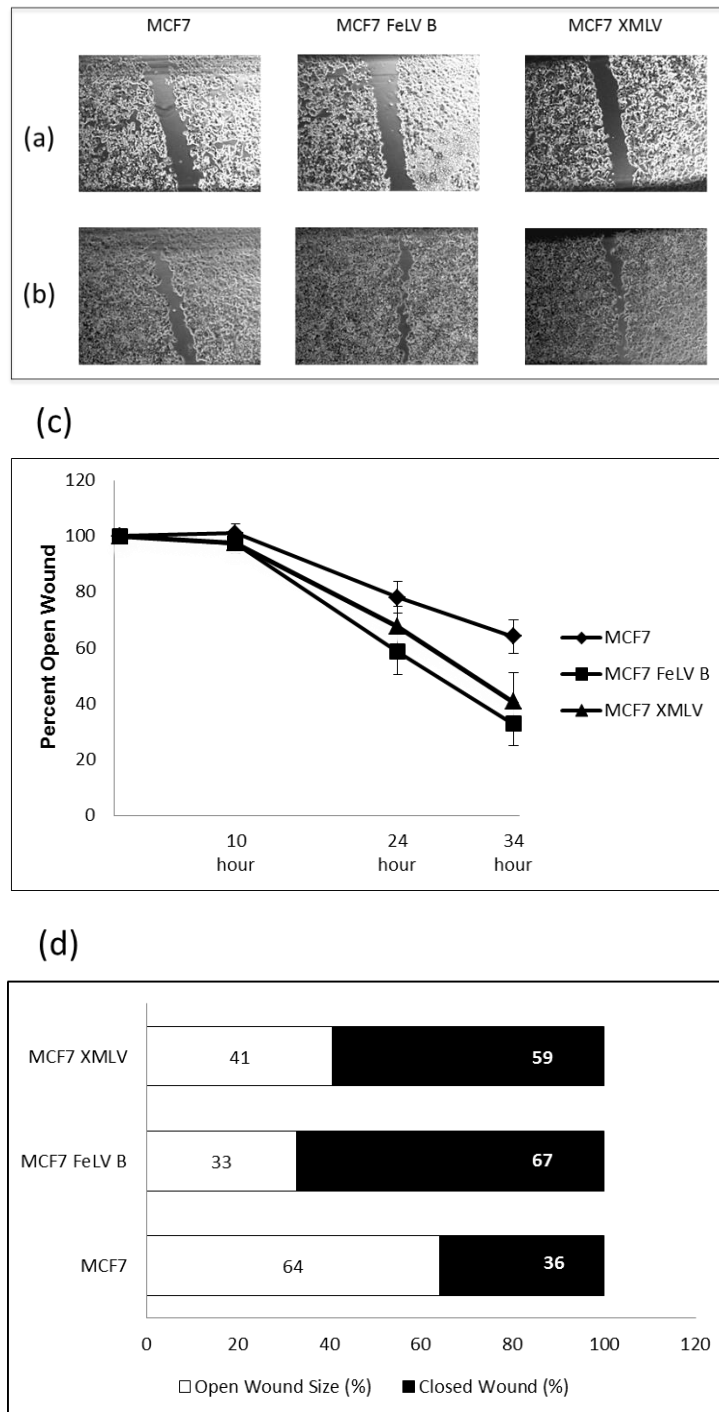


Figure 7.1 Wound healing assay. (a) Images of wounds at time zero. (b) Images of partially healed wounds at 34 hours. (c) Percentage of open wound at different time intervals. Error bars represent standard deviation. (d) Percentage of open and closed wound after 34 hours.

Figure 7.1 (a & b) shows that at 34 hours the wound size in XMLV and FeLV B infected MCF7 cells is reduced compared to uninfected controls. At this time point the wound had closed by 67% ($\pm 7.7\%$) and 59% ($\pm 10.3\%$) in MCF7 FeLV B and MCF7 XMLV infected cells respectively. By contrast the wound had only closed by 36% ($\pm 6\%$) in uninfected MCF7 cells (Figure 7.1d). T-test was applied to the data

obtained for the three different experiments separately at the 34-hour time point. These results are shown in Table 7.1.

Table 7.1 Analysis of wound assay

		T-test (p value)
1st Experiment (3 wound per sample)	MCF7/MCF7B	0.009*
	MCF7/MCF7X	0.02*
	MCF7B/MCF7X	0.72
2nd Experiment (3 wound per sample)	MCF7/MCF7B	0.001*
	MCF7/MCF7X	0.007*
	MCF7B/MCF7X	0.121
3rd Experiment (5 wound per sample)	MCF7/MCF7B	0.001*
	MCF7/MCF7X	0.011*
	MCF7B/MCF7X	0.485

Table 7.1 Statistical analysis of wound assay using Student T-test. MCF7B and MCF7X denote MCF7 cells infected with FeLV B and XMLV respectively. *p value <0.05 has been taken as significant.

The foregoing results demonstrate that in all three experiments wound healing was significantly accelerated in FeLV B and XMLV cells compared to control cells. Although statistically significant, the difference between infected and control cells was relatively modest. The results suggest that both viruses can alter wound healing while there was no significant difference between FeLV B and XMLV infected cells. These data should be considered preliminary due to relatively small sample size and the conclusions drawn would benefit from further repeat experiments.

As the cells were chronically infected with XMLV or FeLV B there is a possibility that the effects on wound healing were due to evolution of the infected cell lines, perhaps due to insertional effects. To explore this further these experiments were repeated in cells freshly infected with FeLV B as shown in Figure 7.2.

Figure 7.2 Wound assay for freshly infected MCF7 cells

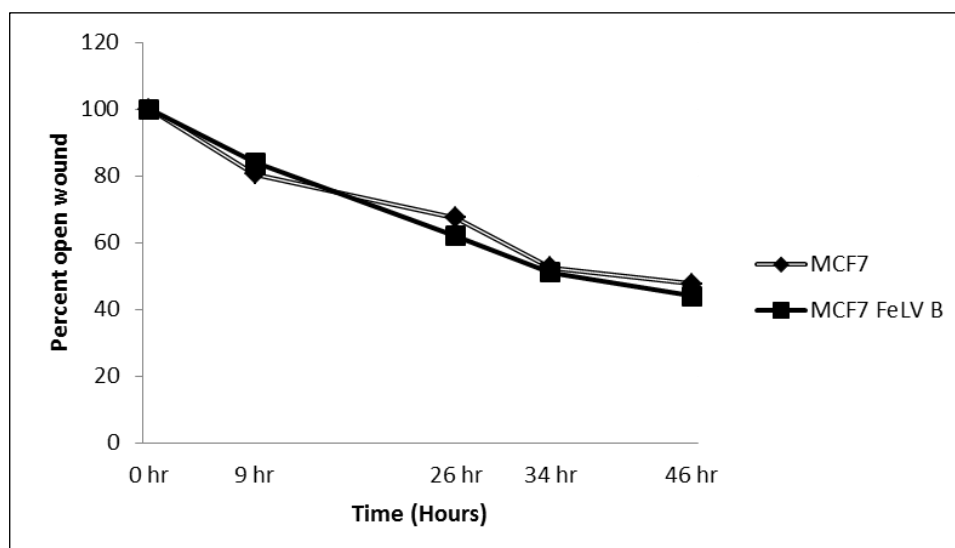


Figure 7.2 Wound healing in fresh FeLV B infected MCF7 cells and the uninfected MCF7 cells.

In contrast to the results observed in cells that had been infected for greater than 14 days before carrying out the wound healing assays, no difference was seen in the rate of wound closure between MCF7 cells freshly infected with FeLV B and uninfected cells. This experiment was only carried out once with five wounds per sample but, the discordant result suggests that longer term infection may be required to alter cell behaviour, perhaps driven by clonal expansion following insertional mutagenesis.

7.3.2 THP-1 cells differentiate when exposed to XMLV supernatant

In the above experiments, it has been shown that gammaretrovirus infection can alter the behaviour of infected MCF7 cells, although the effect is modest. To investigate whether infection had a discernible effect in other susceptible cells I infected THP-1 cells with XMLV as described in Chapter 2 and as shown in Figure 7.3.

Figure 7.3 Altered morphology and cell number in XMLV treated THP-1 cells

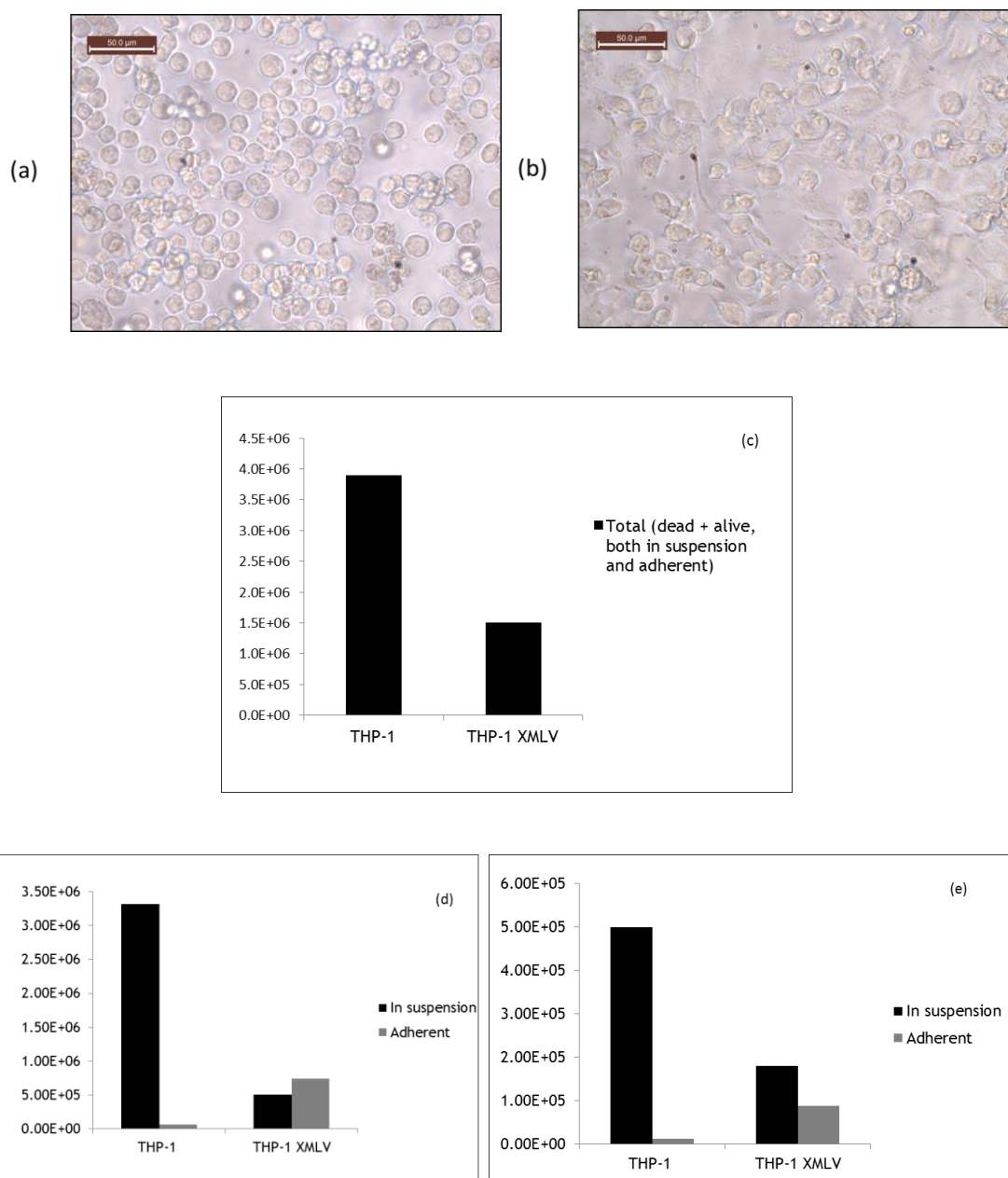


Figure 7.3 (a) & (b) THP-1 cells before and 48 hours after XMLV infection respectively. (c) Total number of THP-1 cells 96 hours after infection with XMLV. (d) Number of live cells 96 hours after infection. (e) Number of dead cells 96 hours after infection.

Supernatant treated cells showed rapid morphological changes not observed in control cells. The phenotype is shown in Figure 7.3 (a & b) and was characterised by an obvious change in cell number, cell appearance and an increased tendency to adhere to the surface of the tissue culture plate. In addition Figure 7.3 (a & b) also shows that the THP-1 cells became spindle shaped after exposure to XMLV-infected cell supernatant. The cells also appeared to be enlarged and were adherent to the flask. To investigate whether

the growth of THP-1 cells was affected, the cells were counted 96 hours after XMLV infection at which point cells exposed to viral supernatant showed a greater than two-fold reduction in total cell number (1.5×10^6) compared to non-infected cells (3.9×10^6) (Figure 7.3c). Among the uninfected THP-1 cells the majority of cells (3.3×10^6) were alive and in suspension with only a small number of live adherent cells (6.3×10^4), moreover a relatively small proportion of cells were dead (5.1×10^5) as shown in Figure 7.3 (d & e). In contrast, the majority of live XMLV infected cells were adherent (7.3×10^5 were adherent, 5×10^5 in suspension) as shown in Figure 7.3d. Among XMLV infected THP-1 cells, the total number of dead cells was 2.7×10^5 as shown in Figure 7.3e. Thus XMLV infection of THP-1 cells seemed to have a dual effect; it reduced their viability and changed their properties making them more prone to adhere to the surface of the plate. This experiment was repeated three times in triplicate.

The next step was to see whether the THP-1 cells exposed to the XMLV supernatant were differentiated or not. For this purpose the expression of CD14, a surface marker upregulated during macrophage differentiation, was assayed by PCR. THP-1 cells were exposed to supernatant from XMLV infected MCF7 cells and grown for 48 hours before RNA was harvested using the RNeasy kit (Qiagen) as described in Chapter 2. This experiment was performed in duplicate. The primer design as well as the thermal cycling conditions were as described by Park *et al*²⁵⁴ and the results are shown in Figure 7.4.

Figure 7.4 PCR for CD14 expression

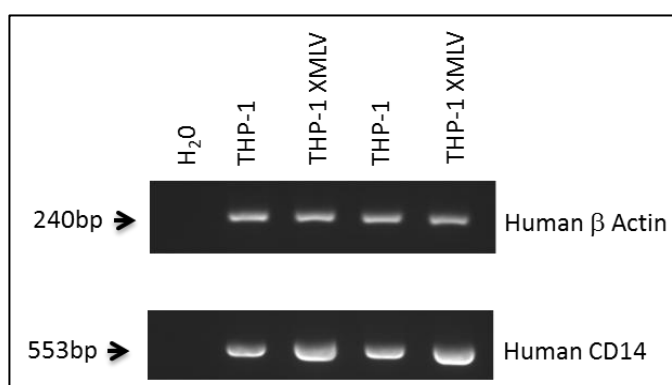


Figure 7.4 CD14 expression in THP-1 cells infected with XMLV using CD14 specific primers. Human β Actin primers were used as an internal control.

Figure 7.4 shows that both samples of THP-1 cells exposed to XMLV expressed slightly more CD14 compared to uninfected THP-1 control cells. This result suggested that the infected THP-1 cells were undergoing differentiation.

To further demonstrate differentiation in XMLV infected THP-1 cells, flow cytometry was carried out using anti-human CD54 antibodies. CD54, also known as intracellular adhesion molecule 1 (ICAM1), is another surface marker for macrophages. CD54 expression is known to be higher in natural and PMA stimulated macrophages compared to monocytes²⁵⁵. The THP-1 cells were exposed to supernatant from XMLV infected MCF7 cells and were grown for 2 days before analysing CD54 cell surface expression by flow cytometry using APC mouse anti-human CD54 (559771, BD Biosciences) antibody shown in the Figure 7.5.

Figure 7.5 Flow cytometry for CD54 expression

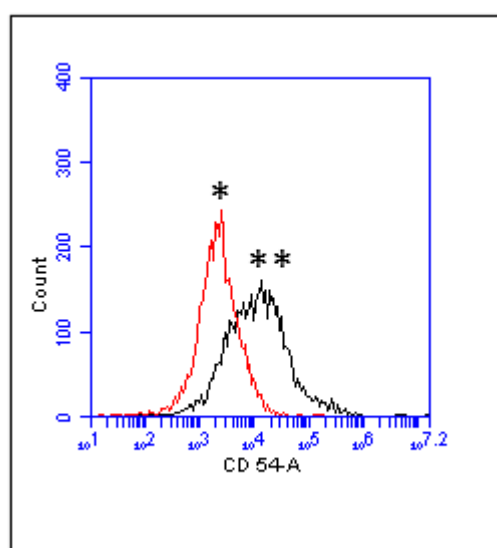


Figure 7.5 Flow cytometry using anti-human CD54 antibody in uninfected THP-1* and XMLV infected THP-1 cells.**

Figure 7.5 shows that THP-1 cells infected with XMLV show higher levels of CD54 expression compared to the uninfected THP-1 cells. This shows that the THP-1 cells exposed to supernatant from the XMLV infected MCF7 cells showed changes consistent with increased differentiation towards a macrophage phenotype.

These results suggested that XMLV could induce the THP-1 cells to differentiate but other factors present in supernatant of XMLV infected THP-1 cells could be responsible for this phenotypic change. To ensure the effects were XMLV

mediated I assayed the XMLV infected MCF7 cells, and 293T cells, for *Mycoplasma* contamination using PCR, by designing and ordering primers used by Zakharova *et al*²⁵⁶. The results of the PCR are shown in the Figure 7.6.

Figure 7.6 PCR to detect *Mycoplasma*

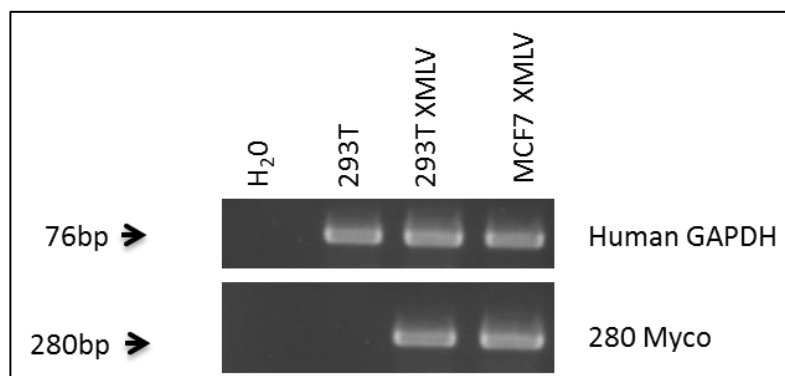


Figure 7.6 PCR carried out using *Mycoplasma* specific primers and human GAPDH primers as an internal control.

XMLV infected MCF7 cells and XMLV infected 293T cells were positive for *Mycoplasma* using 280 Myco primers (Figure 7.6). The uninfected 293T cells were negative. A positive control for *Mycoplasma* was not available at this point but these results were later confirmed by my colleague Nancy Mackay using a commercial *Mycoplasma* detection kit (Venor-Gen, Minerva Biolabs).

The next step was to see the effect of XMLV-free *Mycoplasma*, *Mycoplasma*-free XMLV, and both XMLV and *Mycoplasma*-free MCF7 supernatant on THP-1 cells. In performing this experiment I was fortunate in having two sources of MCF7 cells, the original potentially contaminated cells and a clean source thought to be *Mycoplasma* free. THP-1 cells were exposed to *Mycoplasma*-contaminated but XMLV-negative MCF7 cell supernatant, *Mycoplasma*-negative MCF7 cell supernatant and supernatant from XMLV infected *Mycoplasma*-negative MCF7 cells. All supernatant were filtered using 0.45µm filter. Fresh medium was added after 2 hours. Both suspension and adherent cells were counted after 24 hours using a haemocytometer. These experiments were carried out in triplicate and the results are summarised in Figure 7.7.

Figure 7.7 THP-1 differentiation by XMLV free *Mycoplasma*

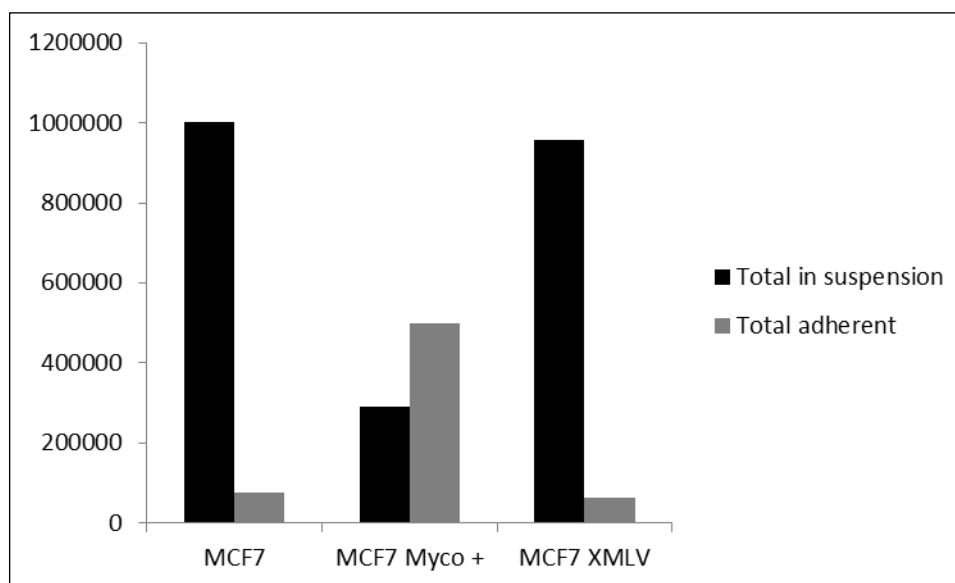


Figure 7.7 Comparison of the effects of XMLV and *Mycoplasma* (separately) containing MCF7 cell supernatant on THP-1 cells. Uninfected MCF7 cell supernatant was used as negative control.

Figure 7.7 shows that THP-1 cells exposed to *Mycoplasma* free MCF7 cell supernatant and *Mycoplasma*-free XMLV infected MCF7 cell supernatant had a similar number of suspension cells. In the case of *Mycoplasma* free MCF7 cell supernatant, 1×10^6 THP-1 cells ($\pm 5.3 \times 10^4$) were found to be in suspension, but only 7.5×10^4 ($\pm 1.5 \times 10^4$) were found to be adherent. In the case of THP-1 cells exposed to XMLV infected (*Mycoplasma* free) MCF7 cell supernatant, 9.6×10^5 cells ($\pm 8.1 \times 10^4$) were found to be in suspension while only 6.5×10^4 ($\pm 8.6 \times 10^3$) cells were found to be adherent. By contrast THP-1 cells exposed to the *Mycoplasma* contaminated XMLV-free MCF7 cell supernatant showed a change in their morphology and a greater proportion of the THP-1 cells ($5 \times 10^5 \pm 5.3 \times 10^4$) were found to be adherent to the flask while only 2.9×10^5 cells ($\pm 8.8 \times 10^4$) were in suspension. This shows that XMLV infected MCF7 cells and uninfected MCF7 cell-supernatant had very little effect on the THP-1 cells, but the *Mycoplasma* contaminated MCF7 cell supernatant induced significant changes in the THP-1 cultures. Thus the changes observed earlier were most possibly due to *Mycoplasma*. The CD14 and CD54 differentiation experiments were not repeated for XMLV free *Mycoplasma* infected THP-1 cells, because of the concern of potentially spreading the contamination to other colleagues using the same laboratory facility.

After detecting *Mycoplasma* in my samples, it was very important to detect the source of *Mycoplasma*. For this purpose, PCR was carried out for *Mycoplasma* using original MCF7 cell DNA, from cells that were received from Beatson and used for xenografting, the MCF7 primary tumour explants from these cells, and also MCF7 gifted by Anne Terry (University of Glasgow) were used. The PCR results are shown in the Figure 7.8.

Figure 7.8 PCR for detecting source of *Mycoplasma*

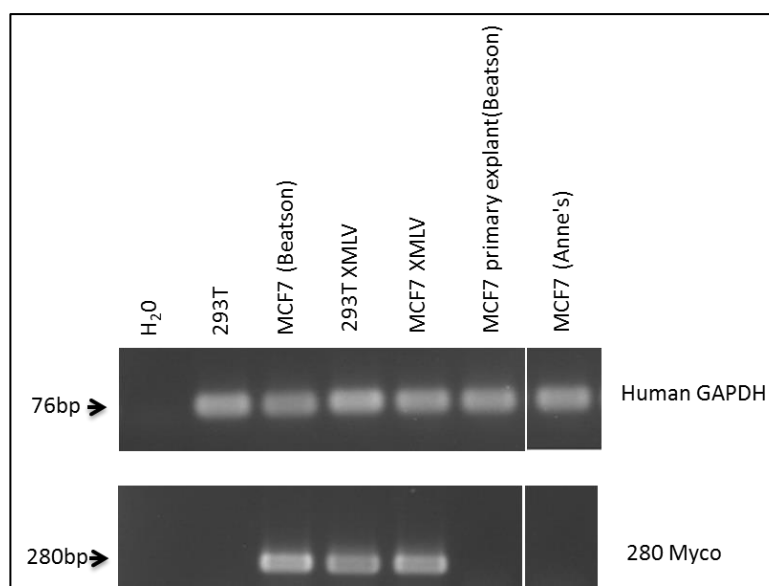


Figure 7.8 PCR carried out using *Mycoplasma* specific primers and human GAPDH primers as an internal control.

These results confirm MCF7 cells received from Beatson (Figure 7.8) were contaminated with *Mycoplasma*. These were the cells used for xenografting experiments, however MCF7 cells recovered from explants showed no evidence of *Mycoplasma* infection. This observation suggests that passage through the mouse had cleared the cells of *Mycoplasma* infection.

7.3.3 Raji cells infected with XMLV do not differentiate

An interesting observation was made by Sturzel *et al*²⁵⁷. They claimed that Raji cells (Burkitt's lymphoma cell line) undergo syncytium formation when infected with XMRV. As described earlier, XMRV shares 93% sequence similarity with XMLV and also uses the same receptor XPR1 to enter cells, therefore I decided to check the effects of XMLV infection on Raji cells. Any change in behaviour would mean significant implications for the study of lymphoma cells when used for

xenografting. For this experiment, Raji cells were infected with filtered supernatant from MCF7 cells infected with XMLV as described in Chapter 2. Despite evidence of infection no discernible change was observed in the morphology of XMLV infected Raji cells, nor was there any evidence of syncytium formation. This experiment was repeated three times. The supernatant used to infect Raji cells was free of *Mycoplasma* contamination. The effects of *Mycoplasma* on Raji cell behaviour were not determined.

7.4 Discussion

In this chapter I have demonstrated that gammaretrovirus particularly XMLV, could affect the behaviour of cancer cells. The wound-healing assay was carried out to see if there are any effects of XMLV and FeLV B infection on the properties or behaviour of MCF7 cells. It was found that the gammaretroviral (XMLV and FeLV B) infected MCF7 cells showed a slightly increased rate of wound healing compared to the uninfected MCF7 cells. The starting size of the wound was very important for wound healing. It was found that narrow wounds healed rapidly as compared to wide wounds of the same sample of cells. To overcome this confounding factor, only wounds of comparable starting sizes were selected for analysis. It was also found that when very recently infected MCF7 cells were used for the wound-healing assay, no difference was seen between the rate of wound healing in the infected and uninfected MCF7 cells. Only the MCF7 cells chronically infected with XMLV and FeLV B showed a difference in wound healing. The mechanism by which infected MCF7 cells healed more quickly compared to uninfected MCF7 cells is not known but the possibility of insertional mutagenesis and clonal expansion cannot be ruled out. There have been similar claims that XMRV infection can increase the *in vitro* migration rate of LNCaP prostate cancer cells^{189,258}. Whether the effects in the case of XMLV are due to the direct action of viral proteins or the consequences of insertional activation of key cellular genes is unknown as yet. Whatever the exact explanation is, XMLV/FeLV B affects the migratory properties of cells, although in the context of these experiments, the effect is a relatively minor one. These results demonstrate that XMLV infection of xenografts or through horizontal contamination of other samples in the laboratory may potentially alter the results of the experiments under consideration. These results emphasise the need for investigators to be more widely aware of these potential confounding

factors. Other gammaretroviruses with the capacity to infect human cells may also present a risk, e.g. GaLV has been reported as an *in vitro* contaminant, highlighting the need for precautions and thorough testing of cell lines for adventitious infection¹⁷⁸.

I have also demonstrated that infection of THP-1 cells, a monocytic leukaemia cell line with *Mycoplasma* resulted in a change of phenotype, inducing adhesion, reduced viability and differentiation along the macrophage lineage. These effects of *Mycoplasma* infection on THP-1 cells and human monocytes have already been described by others^{259,260}. These results were a potent reminder that other factors need to be eliminated when investigating the effects of XMLV carried within the supernatant derived from primary virus producing cells. The effects of *Mycoplasma* on Raji cells were never determined. I was not able to demonstrate syncytia formation in Raji cells when infected with XMLV. This was contrary to the findings of Sturzel *et al*²⁵⁷ who reported that Raji cells displayed syncytia formation following XMRV infection.

Experiments originally conducted with *Mycoplasma* contaminated XMLV were subsequently repeated with *Mycoplasma* free XMLV. The results for all the experiments were the same as before, specifically accelerated wound healing was not related to *Mycoplasma* infection. Another interesting fact was noticed that *Mycoplasma* infection could be cleared by passaging contaminated cells through mice. This result has also been previously reported by Carroll & Kennedy²⁶¹.

Thus it is very important not only to screen for gammaretrovirus contamination in cells grown in laboratories working with viruses; cells should be screened for *Mycoplasma* and other intracellular contaminants as well. Since both gammaretroviruses as well as *Mycoplasma* contamination can affect the cell behaviour and thus the overall results of the experiment, it may be worthwhile considering specifically reporting that cells used in certain types of experiments are free of gammaretrovirus and *Mycoplasma*.

8 Effects of XMLV infection on human cell transcriptomes

8.1 Introduction

In the previous chapters, I have shown that a number of human cell lines are susceptible to XMLV infection. I have also shown that XMLV (and FeLV B) can affect the behaviour of human cells. I have also shown that XMLV susceptible cell lines MCF7 and Raji cells behaved differently when used for xenografting. MCF7 cells formed tumour nodules and the MCF7-BALB/c tumour explants released infectious XMLV. Raji cells, on the other hand, when used for xenografting into BALB/c mice initially formed lumps, which later regressed (Chapter 3). Thus it was interesting to determine whether XMLV infection of human cells could result in a significant change in the cell transcriptome that might explain changes in cell behaviour.

The main aim of the studies described in this chapter was to investigate whether persistent XMLV infection affects the expression pattern of human cellular genes and whether the altered expression pattern could be correlated with any known host genetic pathway or function. It was also of interest to see whether or not the change in expression pattern was cell type or gammaretrovirus specific. Two XMLV susceptible cell lines: MCF7 and Raji cells were selected for this purpose.

8.2 Materials and methods

Materials and methods have been discussed in Chapter 2.

8.3 Results

8.3.1 Changes in gene expression after XMLV infection

RNA was extracted from MCF7 and Raji cells infected with XMLV as described in Chapter 2. The quality and the quantity of this RNA was determined using a Nanodrop spectrophotometer (Thermo Scientific) and was confirmed with Anne Terry's help using Agilent 2100 Bioanalyzer and is given in Table 8.1.

Table 8.1 Quality check of RNA samples

Sample	Conc. (ng/ μ l)	OD 260/280	OD 260/230
MCF7 1	739	2.05	2.19
MCF7 2	820	2.06	1.38
MCF7 3	730	2.04	2.11
MCF7 XMLV 1	640	2.08	1.62
MCF7 XMLV 2	840	2.06	1.70
MCF7 XMLV 3	690	2.06	2.10
Raji 1	270	2.07	2.12
Raji 2	430	2.10	2.16
Raji 3	200	2.04	2.13
Raji XMLV 1	310	2.08	1.88
Raji XMLV 2	830	2.05	2.23
Raji XMLV 3	670	2.07	2.21

Table 8.1 Quantity and quality of RNA samples determined by Nanodrop. All the RNA samples satisfied the desired quality requirements (OD_{260/280} > 1.5; OD_{260/230} >1.0).

Approximately 500ng of RNA for each sample was submitted for Affymetrix human Gene 2.0 ST expression analysis. All the steps needed for the microarray including cDNA synthesis and amplification, cDNA purification, fragmentation and labelling, hybridization, washing and scanning of appropriate Affymetrix Gene Chip and primary data analysis including normalization and calculation of p value for each transcript across infected and uninfected triplicate samples and calculation of fold change (FC) was performed by the Atlas Biolabs. I confirmed fold changes by recalculation and investigated a total number of 48,416 transcripts/entities to detect differentially expressed genes. A summary of transcripts with a differential expression at various levels of significance is shown in the Figure 8.1.

Figure 8.1 Differential expression of transcripts

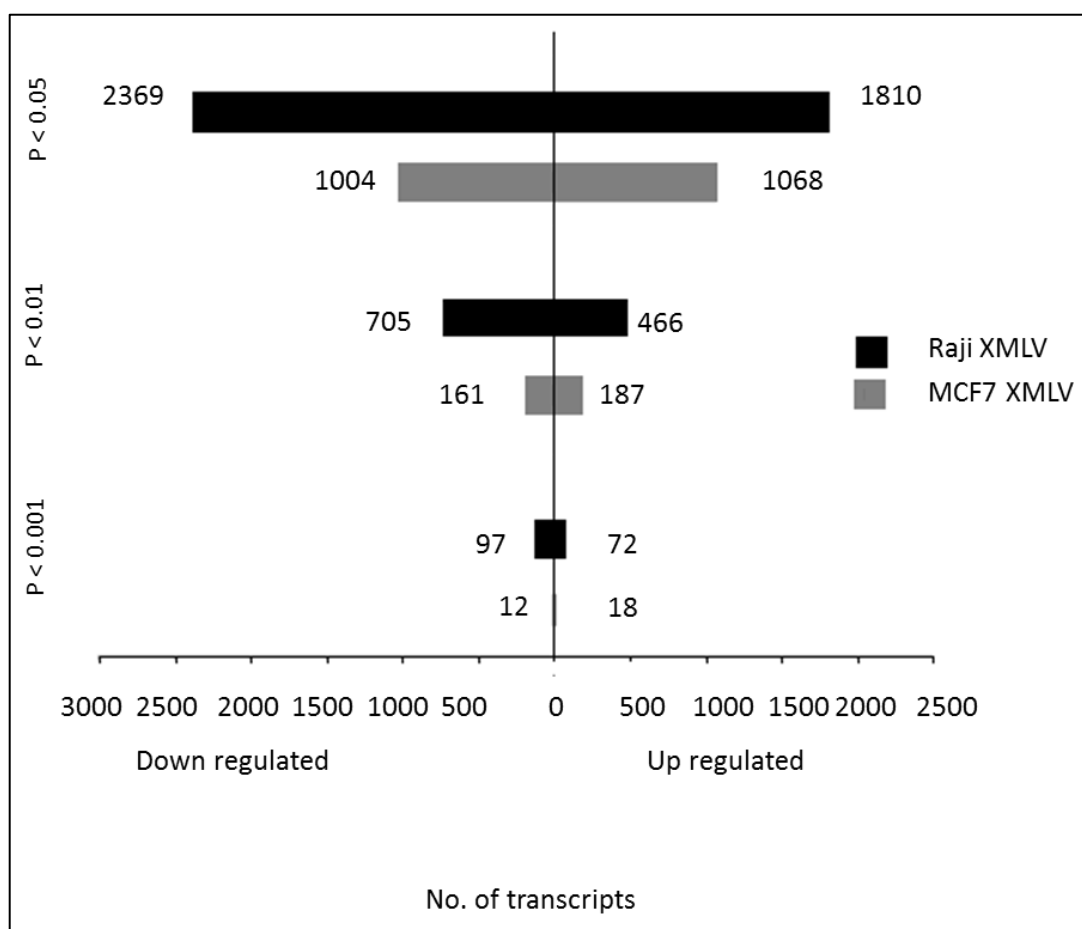


Figure 8.1 Number of up regulated and down regulated transcripts for XMLV infected MCF7 and Raji cells at different levels of significance.

Figure 8.1 shows that in the Raji cells infected with XMLV, many more biological entities have shown a change in the expression levels when these are sorted by p value. A similar difference was noted when the probe sets were sorted by fold change (Figure 8.2).

Figure 8.2 Differential expression of transcripts in terms of fold change

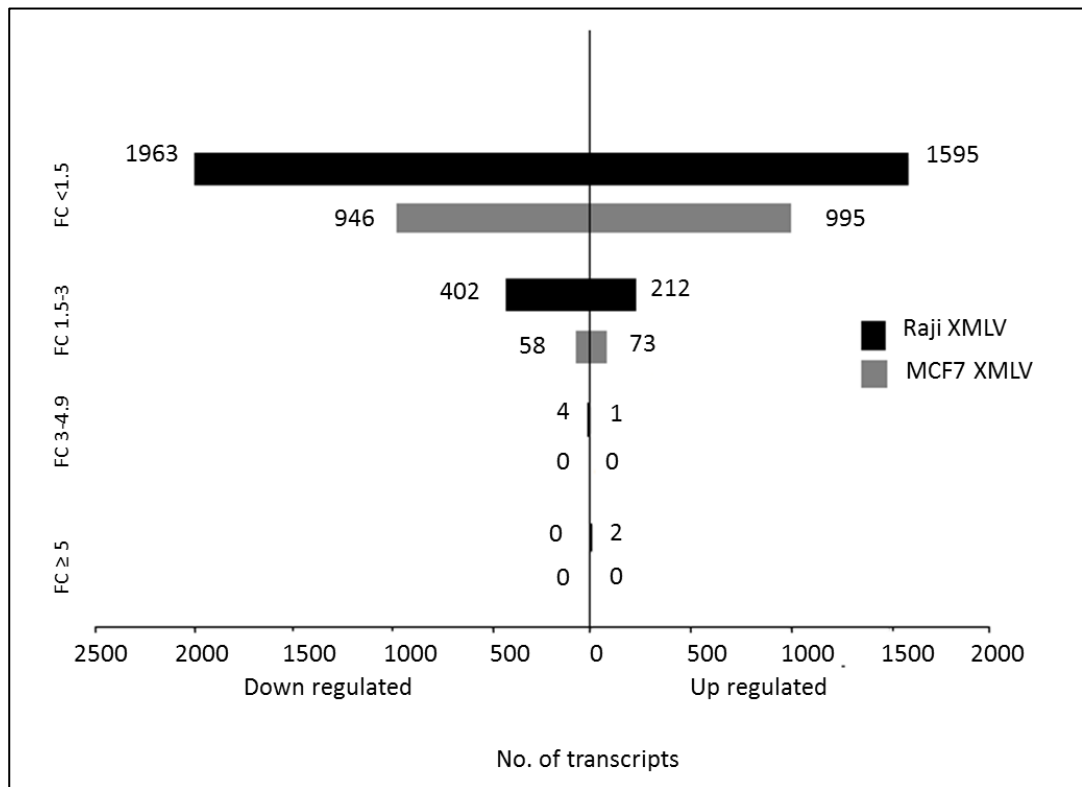


Figure 8.2 Number of up regulated and down regulated transcripts for XMLV infected MCF7 and Raji cells at different levels of fold change.

It is generally recommended to use multiple testing corrections for large data sets to exclude false positives. The Benjamini and Hochberg False Discovery Rate (BH FDR) which is known to be high in terms of stringency, was applied using the formula “FDR = p value x (n/rank of the entity), significant if < 0.05”²⁶². Where “n” is the total number of entities and “rank of an entity” is its serial number when entities are arranged in ascending order of their p values. Applying this stringent test left only 99 probe sets with a FDR of <0.05 in the Raji set and none from the MCF7 array. However, while this very stringent statistical test is robust for elimination of false positives, it can lead to exclusion of genuine differences²⁶³. I noticed that many of the highly significant changes by FDR represented very small fold changes while some genes with larger fold changes fell just short of the stringent cut-off. Also, some of these genes and transcripts just under the threshold were represented by more than one probe set or by orthologues with similar changes in expression level, indicating the likelihood that the stringent FDR cut-off was eliminating real differences. I therefore decided to analyse the dataset using a compromise threshold of standard p value <0.05 and fold change ≥ 1.5 . These provisional datasets were subjected to

further analysis and validation of selected genes that appeared likely to be biologically significant.

The entities from both the XMLV infected MCF7 and Raji cells that have shown a fold change (FC) ≥ 1.5 in expression level were analysed by Ingenuity Pathway Analysis (IPA) software. The total number of genes selected for analysis is summarised in Figure 8.3.

Figure 8.3 Differentially expressed genes with fold change ≥ 1.5

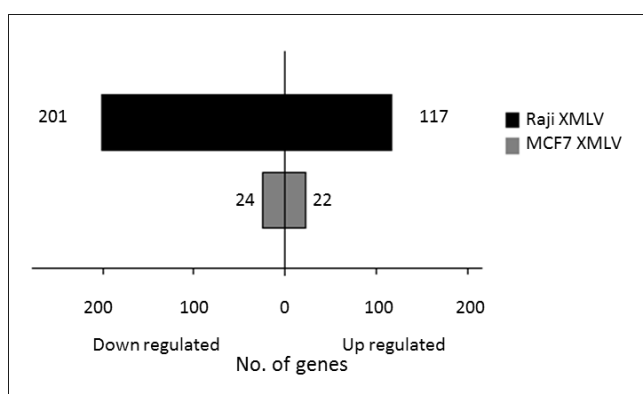


Figure 8.3 117 well-annotated genes were up regulated and 201 well-annotated genes were down regulated with a fold change of 1.5 or more in XMLV infected Raji cells. In XMLV infected MCF7 cells, 22 well-annotated genes were up regulated and 24 well-annotated genes were down regulated with a FC of 1.5 or more.

The heat map for the top 50 genes with $FC \geq 1.5$ and p value < 0.05 is given in the Figure 8.4.

Figure 8.4 Heat map for signal intensity of top 50 individual gene entities

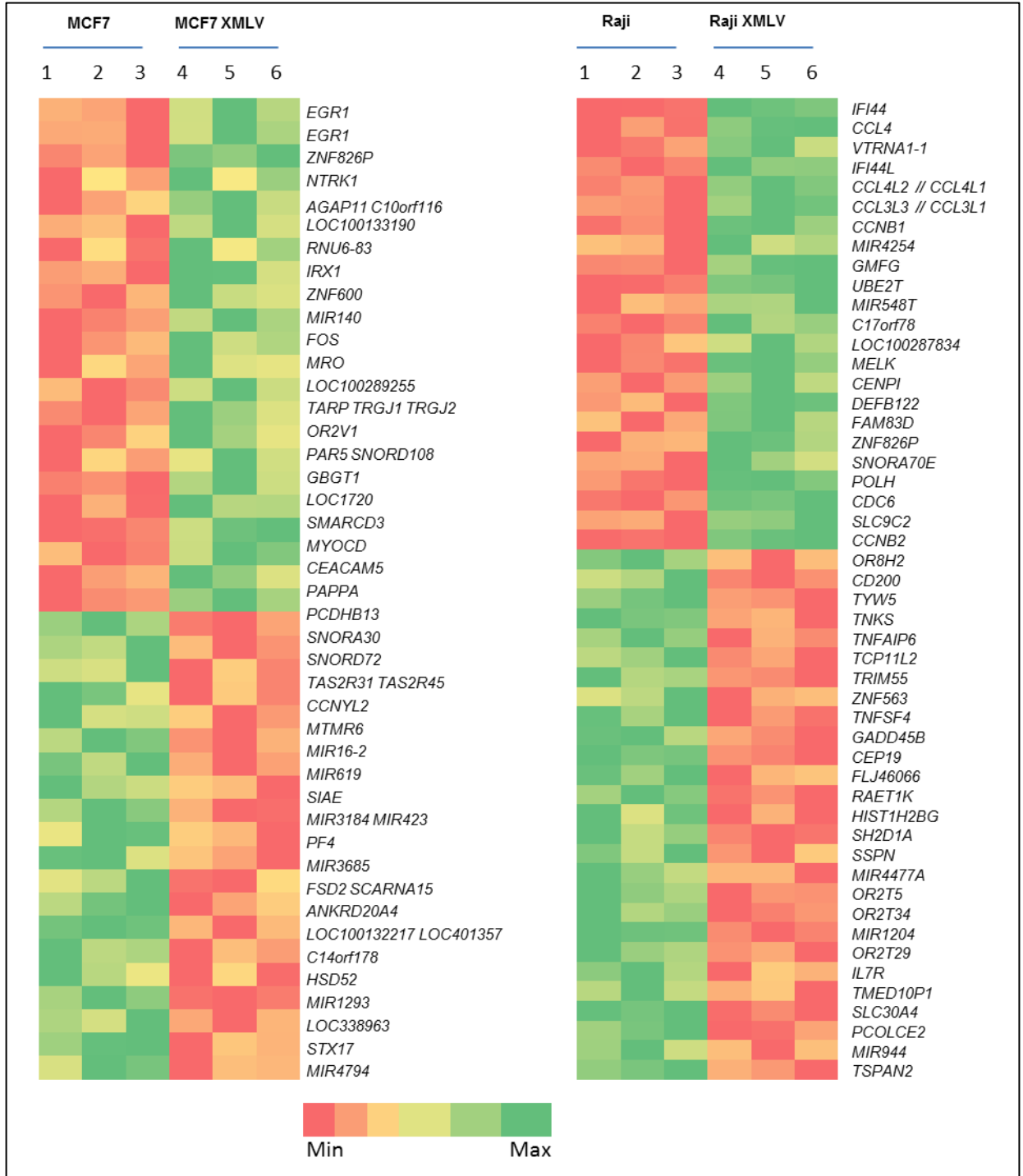


Figure 8.4 Relative signal intensities of top 50 gene entities, differentially expressed in XMLV infected MCF7 and Raji cells versus the respective uninfected ones. All the entities have been assigned a colour based on their expression relative to the baseline. The green and red colours indicate the maximum and minimum expression values respectively with yellow colour indicating a borderline expression.

The complete list of these genes is given in the Appendix 5 along with functional annotations in the IPA listings. The results are summarized briefly in the Table 8.2.

Table 8.2 Functional summary of entities with ≥ 1.5 fold change expression

Categories on basis of function	Up regulated Entities		Down regulated Entities	
	Raji	MCF7	Raji	MCF7
Cytokine	2	0	3	1
Enzyme	19	1	23	1
G protein coupled receptor	4	1	6	2
Growth factor	2	0	0	0
Ion channel	1	0	5	0
Kinase	7	0	8	0
Ligand dependent nuclear receptor	1	0	1	0
miRNA	7	1	4	7
Other	65	12	121	11
Peptidase	5	1	2	0
Phosphatase	2	0	0	1
Transcription regulator	0	6	14	0
Translation regulator	0	0	0	0
Transmembrane receptor	0	0	6	0
Transporter	2	0	8	1
Total Genes	117	22	201	24

Table 8.2 Different categories in which the differentially expressed genes can be grouped by function.

As can be seen, most of the changes affect entities of unknown function (“Other”). Enzymes was the next most frequent category in the Raji cells with kinases as an abundant subset.

The only differentially expressed gene common to both XMLV infected Raji and MCF7 cells was zinc finger protein 826, pseudogene (ZNF826P) which was up-regulated in Raji cells (1.87 FC, $p= 0.007$) and in MCF7 cells (1.76 FC, $p= 0.002$).

The differentially expressed well-annotated genes in the XMLV infected Raji and XMLV infected MCF7 cells with a $FC \geq 1.5$ were further analysed using the IPA software. The IPA analyses include assessments of the relationship between the proteins encoded by the list of genes on the basis of their annotated functions and interactions. This analysis is based on reports in the scientific literature. The IPA software then groups the genes into networks according to host

functions affected. Fisher's exact test is used to determine statistical significance of any associations discovered. The different host functions altered in XMLV infected Raji and MCF7 cells as determined by IPA are summarized in the Figure 8.5.

Figure 8.5 Host functions affected in XMLV infected Raji and MCF7 cells

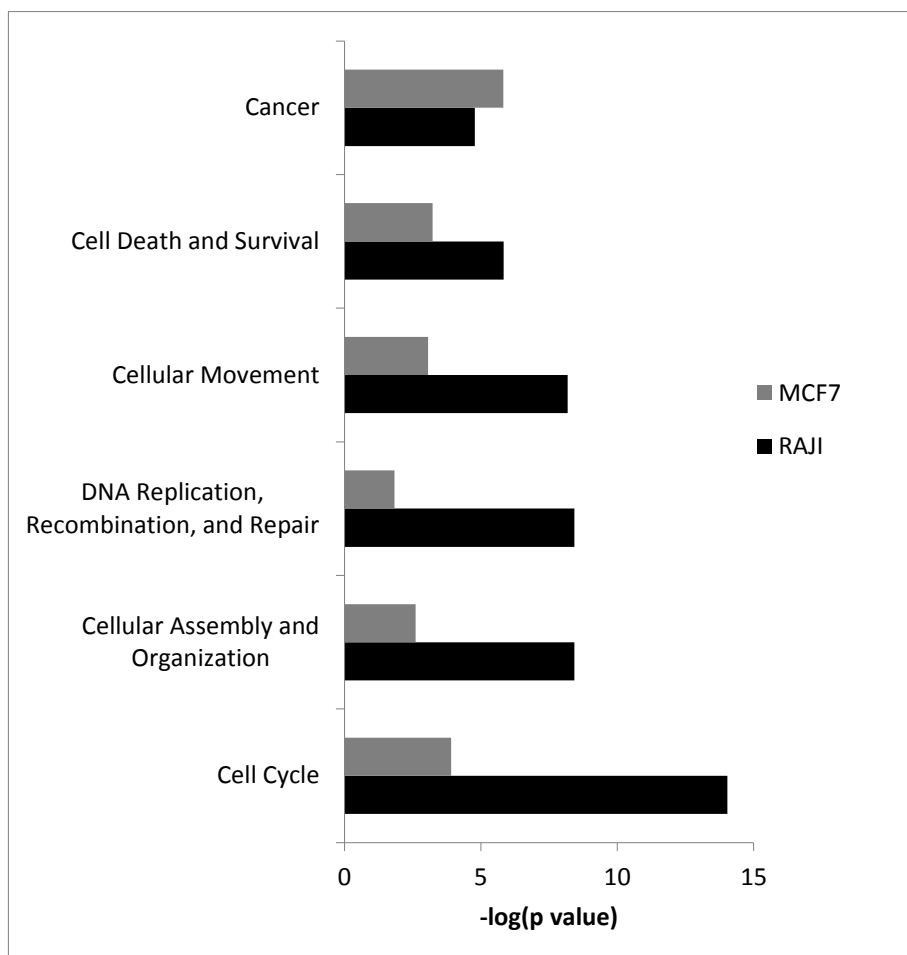


Figure 8.5 Host functions affected in XMLV infected Raji cells and XMLV infected MCF7 cells as compared to the respective uninfected cells. The horizontal axis shows $-\log$ of p value of overlap of the differentially expressed genes related to host functions affected.

It should be noted that the functional grouping of genes by IPA software is based on the current literature related to the genes and cannot be regarded with the same rigour as, for example, biochemical pathway analysis. However, it can be useful in formulating hypotheses. IPA mapping of the differentially expressed genes to canonical pathways showed a number of interesting associations. Fisher's exact test was used to determine significance. No canonical pathway with a gene overlap having a significance of less 10^{-5} was observed in MCF7 cells

but in Raji cells two canonical pathways were found to be significant. These are illustrated in Figure 8.6.

Figure 8.6 Significant canonical pathways

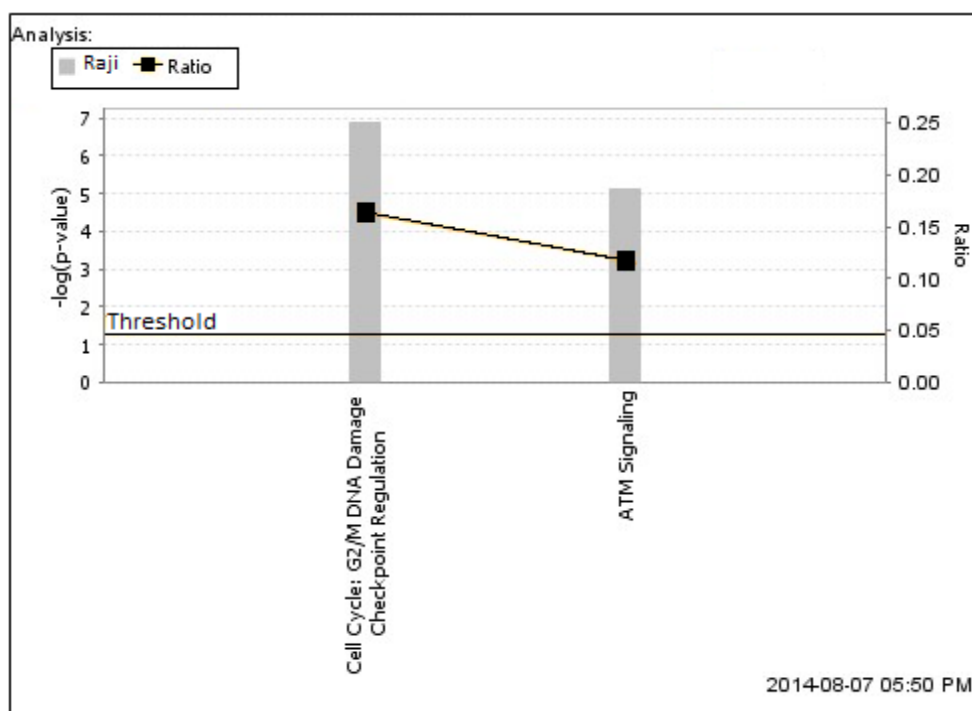


Figure 8.6 Two canonical pathways with genes overlapping with that of the differentially expressed genes in Raji cells infected with XMLV with a significance of p value $<10^{-5}$. Black line with dots represents ratio of differentially expressed genes in XMLV Raji cells that belong to the respective pathway to total number of genes in the respective pathway.

The first pathway affected (Figure 8.6) was the G2/M DNA damage checkpoint regulation pathway. A total number of 8 genes out of 49 genes (16.3%) of this pathway was differentially expressed in XMLV infected Raji cells. The p value of overlap for this pathway was 1.28×10^{-7} . The second significant observation was for the ATM signalling pathway. The p value of overlap for this pathway was 7.35×10^{-6} , with seven out of 59 pathway genes (11.9%) differentially expressed in XMLV infected Raji cells. The ATM signalling pathway is normally activated as a result of double strand DNA damage and in turn activates the G2/M DNA damage check point, to arrest the cell cycle and repair the damaged DNA ²⁶⁴. This analysis did not take into account the direction of change in expression. Therefore the next step was to determine whether the genes mapped to the pathway were would be predicted to stimulate or inhibit. The following genes were mapped to the canonical pathways: Cyclin dependent kinase 1(CDK1), Cyclin B1 (CCNB1), Cyclin B2 (CCNB2), Growth arrest and DNA-damage-inducible alpha (GADD45A), Cell division cycle 25C (CDC25C), CDC28 protein kinase

regulatory subunit 2 (CKS2), Polo-like kinase 1 (PLK1), Aurora kinase A (AURKA), Growth arrest and DNA-damage-inducible beta (GADD45B) and Fanconi anaemia complementation group D2 (FANCD2). The first 5 genes were common to both pathways. The G2/M DNA damage checkpoint regulation pathway included the first 8 genes, while the ATM signalling pathway included the first 5 and the last two genes. Among these genes, CDK1, CCNB1, CCNB2, CDC25C, PLK1, CKS2, FANCD2 and AURKA were up regulated in Raji cells infected with XMLV (see Appendix 5 for further details), while only GADD45A and GADD45B were down regulated. The pattern of gene expression in Raji cells favours cell cycle progression, and not cell cycle arrest. In fact up regulation of CCNB1, CDK1, PLK1 and CDC25C all favour the entry of cells into mitosis²⁶⁵. The effect of these differentially expressed genes in Raji cells need to be confirmed experimentally. For this purpose, the expression of genes should be compared with the respective translated proteins and then the functional effects of any differentially expressed proteins on Raji cell behaviour should be investigated.

8.3.2 Validation of microarray by qRT-PCR

The microarray gene data were validated to ensure that expression changes were not due to false discovery in the large dataset. A panel of 7 genes of biological interest, including both up regulated and down regulated genes was selected for validation by qRT-PCR. The results are summarised in Figure 8.7.

Figure 8.7 Validation of microarray results by qRT-PCR

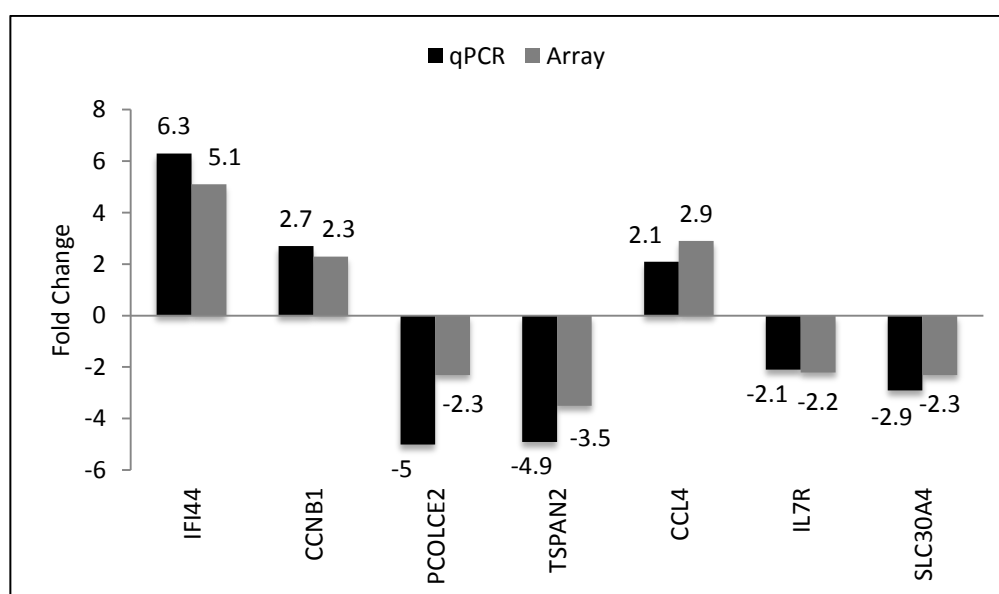


Figure 8.7 Comparison between the results of validation by qRT-PCR and the results of the Raji microarray.

Figure 8.7 shows that each of the differentially expressed genes on the microarray was validated by qRT-PCR, reinforcing the results of the microarray. This shows that the changes in gene expression predicted by the microarray are genuine.

8.3.2.1 Validation of Early Growth response-1 (EGR1) gene expression in MCF7 XMLV by qRT-PCR

In the MCF7 XMLV microarray, the expression of two different EGR1 gene probe sets was found to be up regulated in the XMLV infected MCF7 cells with 2.2 and 2.16 fold change and with p values of 0.0211 and 0.0218 respectively. The expression of EGR1 was validated in MCF7 cells infected with XMLV by qRT-PCR. The result is shown in the Figure 8.8.

Figure 8.8 Validation of EGR1 gene

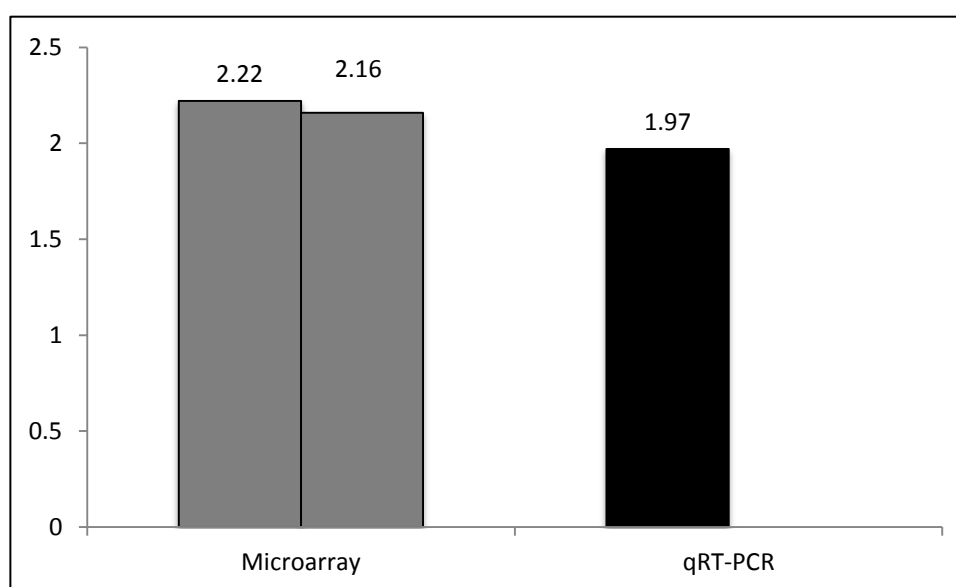


Figure 8.8 EGR1 shows a fold change of 1.97 by qRT-PCR. This validates the gene expression of EGR1 in MCF7 XMLV microarray, which shows a fold change of 2.2 and 2.16.

The differential expression of EGR1 predicted by the microarray analysis is therefore a genuine change that may be of biological significance in MCF7 cells infected with XMLV.

8.3.3 Comparison of change in miRNA expression

Visual inspection of the microarray lists showed an interesting phenomenon as many of the small changes observed in XMLV infected MCF7 cells affected miRNAs. I explored this further and all of the miRNAs which showed differential

expression at significance of $p < 0.05$ are listed in Table 8.3 and illustrated in Figure 8.9 (The cut-off of $FC \geq 1.5$ was not applied here).

Figure 8.9 Differentially expressed miRNAs

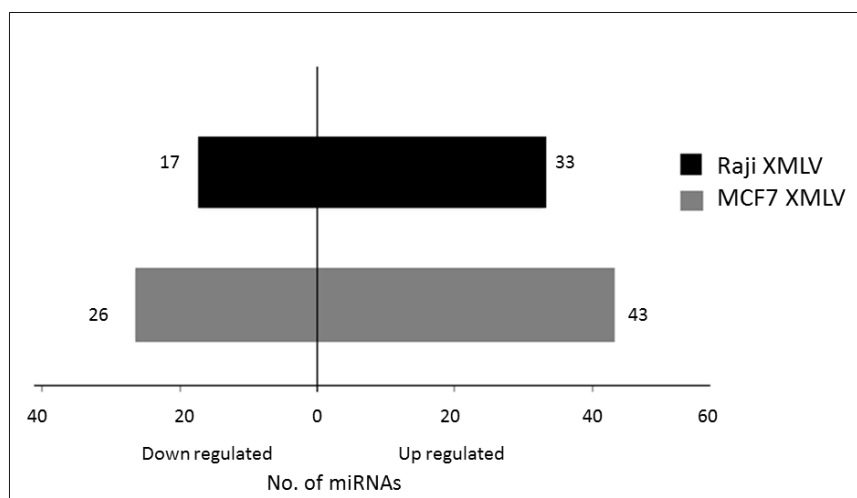


Figure 8.9 In contrast to the coding gene changes, the numbers of miRNAs displaying differential expression was greater in XMLV infected MCF7 cells than Raji cells.

Table 8.3 Differentially expressed miRNAs

	Down regulated miRNA	Up regulated miRNA
MCF7 cells	MIR16-2, MIR619, MIR3184, MIR423, MIR3685, MIR1293, MIR4794, MIR554, MIR584, MIR3911, MIR1289-1, <u>MIR1253</u> , MIR3684, <u>MIR15B</u> , MIR631, MIR3148, MIR4718, MIR31, MIR4705, MIR4433, MIR4280, MIR4680, MIR1304, MIR627, MIR454, MIR632	MIR1236, MIR3672, <u>MIR613</u> , MIR1324, MIR1324, MIR1184-1, MIR1184-2, MIR1184-3, MIR3661, MIR518F, MIR4765, MIR4744, MIR3910-1, MIR3910-2, MIR4803, MIR153-1, MIR106B, MIR4776-1, MIR4776-2, MIR1234, MIR939, MIR3606, MIR132, MIR1976, MIR214, MIR3120, MIR4689, MIR4770, MIR1185-2, MIR4638, MIR431, MIR4791, MIR511-1, MIR511-2, MIR3116-1, MIR3116-2, MIR4752, MIR934, MIR744, MIR1322, MIR3150A, MIR3150B, MIR548M, MIR770, MIR140
Raji cells	MIR944, MIR1204, MIR4477A, MIR1302-3, MIR23C, MIR103A2, MIR103A2, MIR320B2, <u>MIR15B</u> , MIR378I, MIR376C, MIR155, MIR3146, MIR411, MIR1913, MIR329-2, MIR1245A	MIR4495, MIR193A, MIR4288, MIR1295A, MIR148A, MIR24-2, MIR574, MIR574, MIR4640, MIR576, MIR943, MIR130B, <u>MIR1253</u> , MIR3689F, MIR1205, MIR193B, <u>MIR613</u> , MIR4732, MIR181C, MIR661, <u>MIR4442</u> , MIR346, MIR372, MIR548I3, MIR4478, MIR3972, MIR345, MIR150, MIR603, MIR382, MIR2909, MIR548T, MIR4254

Table 8.3 Differentially expressed miRNAs in MCF7 and Raji cells infected with XMLV. Three miRNAs were common between MCF7 and Raji cells (underlined).

Very few miRNA changes were common between MCF7 and Raji cells and only two (MIR15B, MIR613) showed regulation in the same direction in both cell lines. Nevertheless, the miRNAs were analysed by IPA to see if they could be clustered into groups according to host functions altered. The host functions which correlated with the miRNA clustering with significance included developmental disorders, hereditary disorders, skeletal and muscle disorders, dermatological diseases, inflammatory diseases, cellular development, cellular growth and proliferation, cancer, cell death and survival. While the biological significance of these changes has not been established, it would be interesting to explore further to establish whether the marked differences between Raji and MCF7 miRNA changes represent tissue-specific responses to XMLV. It will also be important to learn whether it represents a general effect of gammaretrovirus infection or a more specific response due, for example, to occupation of the XPR1 receptor by XMLV *env* gene products.

8.3.4 Comparison of FeLV B versus XMLV gene expression

In order to see if the differential expression of selected genes in Raji cells was specific for XMLV or a general response to gammaretroviruses, the expression of validated genes was also checked by qRT-PCR in Raji cells infected with FeLV B in triplicates. The results are summarized in Figure 8.10.

Figure 8.10 Gene expression in XMLV vs FeLV B infected Raji cells

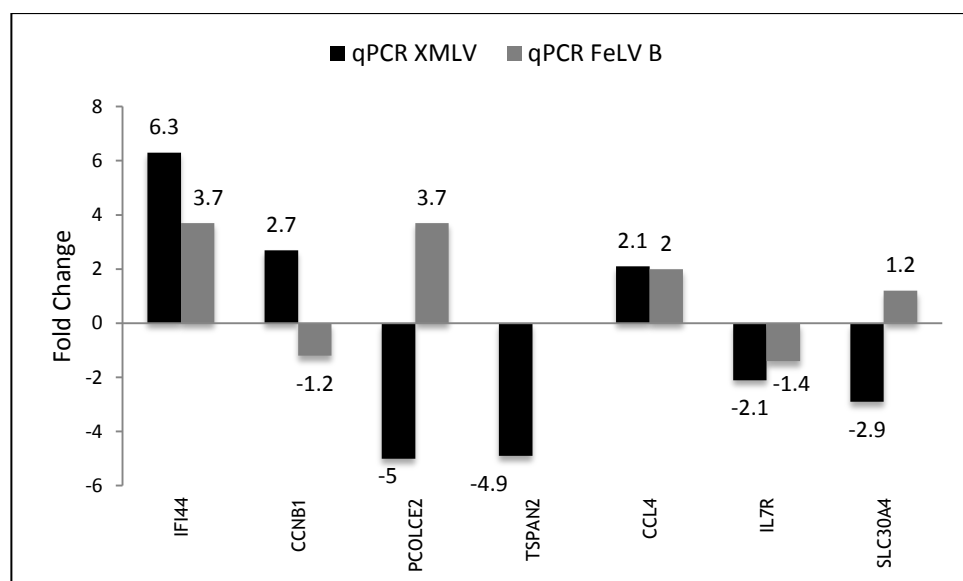


Figure 8.10 Comparison of differential expression of genes in Raji cells infected with XMLV with that in Raji cells infected with FeLV B determined by qRT-PCR.

Figure 8.10 shows that changes in the expression of IFI44, CCL4 and IL7R were comparable for FeLV B and XMLV infected Raji cells. However the expression of

PCOLCE2, CCNB1, and SLC30A4 were oppositely regulated in the XMLV and FeLV B infected Raji cells.

8.4 Discussion

In this chapter I have demonstrated that XMLV infection of cells can result in differential expression of genes, with a more pronounced effect in Raji cells as compared to MCF7 cells. I also demonstrated that a panel of genes selected for functional interest and validated using qRT-PCR showed changes consistent with the microarray results. The effect of FeLV B on some of these genes was also tested in Raji cells and in other cell lines. Notably, FeLV B infection up regulated IFI44 and CCL4 in a similar manner to XMLV suggesting that this might be part of a cellular response to chronic retroviral infection.

Using IPA software, I found that the differentially expressed genes in Raji cells infected with XMLV were significantly enriched for two canonical pathways: the G2/M DNA damage checkpoint regulation pathway and the Ataxia Telangiectasia Mutated (ATM) signalling pathway. Both of these pathways regulate cell cycle arrest following any DNA damage²⁶⁴. The gene expression changes I observed suggested that these pathways were altered in a manner that would favour cell cycle progression. Among these genes, CCNB1 gene, known to play a crucial role in regulating cell cycle^{266,267} was validated by qRT-PCR. The other genes involved in these pathways (CDK1, CDC25C, PLK1, AURKA) also showed a change in gene expression indicative of progression of cell cycle in Raji cells infected with XMLV^{265,268,269}. The expression of CCNB1 has been reported to be up regulated in malignancies, especially those with aggressive behaviour and poor outcome^{270,271}. In contrast, down regulation of CCNB1 causes cell cycle to arrest at G2 phase, inhibiting cell proliferation and induces apoptosis^{267,272}. I did not have time to explore the effects of viral infection on growth of Raji cells, but these changes in gene expression suggest that growth stimulation is the likely outcome.

The expression of CCL4, also known as macrophage inflammatory protein-1 β (MIP-1 β), was also validated by qRT-PCR. CCL4 forms a complex with CLL3 (MIP-1 α) which serves as a chemoattractant for natural killer cells and monocytes²⁷³.

Notably, multiple orthologues of these genes (CCL3L1, CCL3L3, CCL4L1, CCL4L2) were upregulated in Raji cells (validated by A. Terry), and would be expected to act synergistically to evoke biological responses. Raji cells are known to express up regulated levels of the chemokine CCL4 due to infection with Epstein-Barr virus (EBV)²⁷⁴. CCL4 (in complex with CCL3) attracts helper T cell type 1 (Th-1 cells) via the CCR5 receptor, a G-protein coupled cell surface receptor²⁷⁵. Th-1 cells play a very important role in antiviral activity by recruiting cytotoxic T cells to remove the virus-infected cells. Raji cells are also known to express high levels of CCL17 and CCL20 induced by EBV latent proteins²⁷⁴. Due to expression of CCL17 and CCL20, helper T cell type 2 (Th-2 cell) recruitment is favoured as compared to Th-1 cells²⁷⁴. Th-2 cells are responsible for humoral or antibody mediated immunity. Th-2 recruitment theoretically favours Raji cell-survival *in vivo*²⁷⁴. The XMLV infected Raji cells express 2.9 fold higher levels of CCL4 as compared to the uninfected Raji cells. However, I noted no effect on CCL17 and CCL20 expression. These findings imply that XMLV infected Raji cells may be more potent in attracting Th-1 cells via CCL4 and thus are potential targets of cytotoxic T cell mediated removal. However this hypothesis needs to be verified experimentally. As described in Chapter 3, when I xenografted Raji cells into BALB/c nude mice, Raji tumour nodules were initially formed in the mice but they regressed soon thereafter. It is conceivable that the Raji cells xenografted into nude mice acquired XMLV from the BALB/c, which could have resulted in higher expression levels of CCL4 and their subsequent removal by host immune system. BJAB cell line is an EBV-negative human Burkitt's lymphoma cell line. Up regulation of CCL3 and CCL4 by treatment with rituximab is known to cause the rejection of xenografted BJAB cell tumours in mice²⁷⁶ showing how these chemokines can play a functional role in xenograft rejection. Though BALB/c nude mice are depleted in T cells, they are not totally deficient³⁴ and moreover harbour natural killer (NK) cells²⁷⁷ that express high levels of CCR5²⁷⁸ and may play a role in the Raji cell rejection phenomenon.

The interferon- α inducible protein 44, IFI44 is an interferon stimulated gene (ISG)^{279,280}. While ISGs form an important part of the innate immune response²⁸¹ IFI44 and IFI44L were the only representatives of this functional group that were up regulated in Raji cells. IFI44 has antiviral activity against HIV-1²⁸² and also against other viruses e.g. hepatitis C virus²⁸⁰. IFI44 is known to have an

antiproliferative activity and has been described to bind to intracellular GTP and thus prevent cyclic AMP (cAMP) mediated signalling²⁸⁰. It would be interesting to test the status of these pathways in infected cells, but this was beyond the scope of my studies. IFI44 was also found to be up regulated 15-fold in FeLV-infected Kyo1 cells but not in a series of other leukaemia cells lines (A. Terry, unpublished results).

The interleukin 7 receptor (IL7R) was found to be modestly down-regulated in Raji cells infected with either XMLV or FeLV B. The effects of this change on responses to IL7 have not been tested.

Solute carrier family 30 gene member 4 (SLC30A4) also known as Zinc Transporter-4 (ZnT-4) encodes a zinc transporting protein²⁸³. I found that the expression of SLC30A4 was down regulated in Raji cells infected with XMLV while it was slightly up regulated in Raji cells infected with FeLV B. This variation in the expression of SLC30A4 is quite interesting because XPR1, the receptor used by XMLV, is a phosphate exporter³⁷, while PiT1, the receptor used by FeLV B, is a phosphate transporter²⁴⁶ and it is responsible for uptake of phosphate into the cells from the surroundings. A phenomenon of Zinc-Phosphate homeostasis is known in plants, where a deficiency of one can lead to the excess of the other²⁸⁴. On the other hand in bacteria, phosphate transporters also play a role as zinc co-transporters²⁸⁵, thus suggesting there can be a possible connection between ligation of receptors by FeLV B and XMLV, and the subsequent effect on SLC30A4 expression.

Differential expression of genes due to gammaretroviral infection has previously been noted in the 22Rv1 prostate cancer cell line which is chronically infected with XMRV. Suppression of XMRV transcription in 22Rv1 results in reduced expression of osteopontin, CXCL14, IL13, and TIMP2¹⁸⁹ and leads to altered xenograft behaviour, with reduced angiogenesis and tumour size and increased necrosis *in vivo*¹⁸⁹. XMRV infection of primary prostatic stromal fibroblasts was reported to cause differential expression of cytokines which can increase the migratory ability of LNCaP cells and also increase tube formation in human mammary epithelial (HMEC) cells *in vitro*¹⁸⁹. Similarly, XMRV was reported to increase the proliferation rate of LNCaP but not PC3 cells by p27^{kip1} down regulation²⁵⁸. Thus the differential expression of genes as a result of XMRV

infection can vary from cell to cell. As some of these phenomena were reported in cells with long established infection, a role for insertional mutagenesis followed by clonal selection could not be excluded.

I found the expression of EGR1 to be up regulated in MCF7 cells infected with XMLV with a fold change of approximately 2. This finding was validated using qRT-PCR. EGR1 is a zinc finger transcription factor and is known to regulate genes for growth factors, hormones, cytokines and adhesion molecules etc.²⁸⁶. EGR1 may act as a tumour suppressor or as an oncogene depending on the cell type^{287,288}. The expression of EGR1 also varies in different cell types. EGR1 is over expressed in prostate cancer cells²⁸⁹ and is considered to be important in regulating the transition of prostatic *in situ* tumours into invasive prostatic cancers^{288,290}. EGR1 is down regulated in oestrogen receptor negative breast cancers where it acts as a tumour suppressor^{289,291} but its expression is up regulated in oestrogen receptor positive breast cancer cells²⁹². MCF7 is a breast cancer cell line positive for oestrogen receptor^{293,294}. Oestrogen is considered to be responsible for the increased EGR1 expression in MCF7 cells²⁹⁵. Erythropoietin treatment of MCF7 cells also increases cell proliferation by up regulating EGR1 expression²⁹⁶. Down regulation of EGR1 in MCF7 cells negatively affects the migratory ability of cells *in vitro*²⁹⁷. Thus the ability of XMLV infected MCF7 cells to show a mild acceleration in wound healing as described in Chapter 7 may be at least partially due to EGR1 up regulation in XMLV infected MCF7 cells.

miRNA are small RNA molecules comprising 18-25 nucleotides that are known to play a role in the post-transcriptional regulation of gene expression²⁹⁸. They may also play a role in viral infections by facilitating or inhibiting replication or by mediating cellular responses to infection^{299,300}. It was found that 69 miRNAs were differentially expressed in XMLV infected MCF7 cells while 50 miRNAs were differentially expressed in XMLV infected Raji cells as compared to uninfected cells with a significance of $p < 0.05$. The larger number of altered mRNAs in MCF7 cells compared to Raji cells was surprising in light of the much smaller number of changes to coding genes. It appears unlikely that this was due to a global change in the miRNA processing machinery in MCF7 cells, as similar numbers of miRNAs were up and down regulated, and no significant changes were noted in the expression of relevant genes (DICER, DROSHA). Some of the miRNAs (e.g. MIR150, MIR372 and MIR106ba) known for their role in controlling or responding

to other viruses^{301,302,303} were differentially expressed in MCF7 and Raji cells infected with XMLV. However, other miRNAs (e.g. MIR222 and 221) known to be significantly up regulated as a result of XMRV infection of LNCaP prostate cancer cells and known to be associated with an increase in cell proliferation, cell invasion and transformation activity²⁵⁸ did not show a differential expression in Raji cells or MCF7 cells as a result of XMLV infection.

9 General discussion

The main aims of this project were to examine the significance of gammaretrovirus infection as a confounding factor for xenograft related experiments and as a potential source of zoonosis. I also considered the mechanisms of resistance of human cells to gammaretroviral infection, and the ways in which persistent infection can affect host cell behaviour including global effects on host transcription.

There have been reports that human cancer cells xenografted into mice may acquire XMLV, but these previous reports were unable to exclude *in vitro* cross contamination as the source of most infections with XMLV¹⁷³. I have studied this phenomenon prospectively and have shown that when MCF7 cells are xenografted in BALB/c mice, a mouse strain positive for the *Bxv1* locus, a significant proportion (>40%) of tumour explants released infectious XMLV. I have also shown that the newly isolated XMLV was replication competent and on sequencing was found to match almost completely (99.96%) to the *Bxv1* locus. Thus XMLV can not only act as a potential confounding factor for the xenograft related experiments but also as source of XMLV contamination in the laboratory. Xenograft experiment models are used by researchers throughout the world without apparent awareness of the potential presence of infectious XMLV as a confounding factor.

It is recognised that my experiments were conducted under conditions that were highly conducive to activation of XMLV and infection of the xenografts. I used the BALB/c strain that harbours a replication-competent XMLV provirus at the *Bxv1* locus which is readily inducible^{30,304,305}. I also used MCF7 cells which are unusually susceptible to gammaretroviral infection as like 293 cells, they lack a functional APOBEC barrier to spreading infection (Anne Terry, personal communication). My findings are reminiscent of early studies that showed a high frequency of retroviral activation in xenografts of urogenital tumours¹⁷¹. Moreover, some prostate cancer cell lines have been shown to express low levels of APOBEC3G and to be non-restrictive to MLVs⁷⁹ in a similar manner to MCF7 cells. To gain a fuller understanding of the risks of acquiring replicating XMLV in xenografts, it would be necessary to repeat these studies on a larger scale in other commonly used mouse strains that are used for xenograft studies.

Another aspect of my thesis work that merits further study is the stage at which xenograft cells become infected with XMLV. By cell fractionation I was able to confirm that the MCF7 cells within primary explant cultures were infected with XMLV, but the presence of actively replicating XMLV in the xenograft *in vivo* was not addressed here. Again, early studies that showed virus production from epithelial cells in some xenografts *in vivo*¹⁷¹ suggesting that at least in some cases infection was initiated *in vivo* and not merely after explanting.

I also showed that *Bxv1* locus was not carried by NOD/SCID/ γ_c^{null} (NSG) mice, despite the fact that NSG mice have a breeding history that includes the *Bxv1* positive C57BL/6 strain²³¹. The *Bxv1* locus was presumably lost due to repeated inbreeding with NOD/Shi-scid mice. When NSG mice were used for xenografting, no replication competent virus was detected. I was able to clone and sequence a defective virus from the explants that was clearly distinct from XMLV but related to endogenous polytropic MLVs. A defective virus capable of even abortive infection of xenografts could have direct effects on cell properties even if it does not present a risk for horizontal spread. A recent study by Trivaii *et al*²³⁵ showed that NSG mice are not entirely risk-free as they harbour replication competent EMLV that can be activated from the endogenous provirus *Emv30*. Trivaii *et al*²³⁵ also showed that the EMLV contributed as a mutagenic cofactor in the development of mouse myeloid neoplasms that were in part driven by paracrine stimulation from the human xenograft cells. This finding also raises the possibility that EMLV could undergo further recombination with endogenous retroviruses to generate polytropic murine leukaemia virus (PMLV) capable of infecting human cells. For example C57BL/6 is a strain of mice that lacks replication competent EMLV, but it was found that EMLV was generated in immune deficient C57BL/6 mice as a result of recombination³⁰⁶. The recombinant EMLV was capable of infecting mouse cells and capable of giving rise to lymphomas³⁰⁶. It will be important to continue to investigate laboratory mouse strains for their capacity to activate MLV of all types that may act as confounding factors in xenografts and in other experimental settings.

I found that cultured human cells varied in their susceptibility to infection with XMLV and FeLV B. The susceptibility presented by most cell lines was very similar for both viruses suggesting that factors affecting gammaretroviruses in

general predominated over virus-specific factors such as receptor expression. On the basis of susceptibility, we were able to classify human cell lines/primary cells into highly susceptible, partially susceptible and resistant. Most human cells showed evidence of APOBEC-mediated mutation of FeLV, but this activity was found to be deficient in 293 cells, and presumably MCF7 cells also, where rapidly spreading infection was observed. As no primary cells displayed the APOBEC-deficient, rapidly-spreading phenotype, it seems likely that this is an aberrant property of transformed or established cell lines. It would be interesting to extend my observations to a wider panel of cancer cell lines to establish how many display this phenotype. Loss of APOBEC activity may be a late event affecting immortalised cell lines or an earlier event in the development of some tumours. A recent report showed that more than half of all human cancers show mobilisation and reinsertions of LINE1 retrotransposons³⁰⁷. LINE1 elements constitute ~20% of the human genome and while most are now inactive, a small subset remains capable of retrotransposition. They can also mediate reinsertion of other repetitive elements such as the Alu family that lack independent mobility and can even transduce cellular coding sequences in cancer cells. Although most of these new insertions are in heterochromatin and become transcriptionally inactive³⁰⁷, the scale of this process suggest that cancer driver mutations may arise in some cases. APOBEC3 family members have been reported to inhibit LINE1 activity³⁰⁸ suggesting that my observations on the low FeLV restricting activity in transformed human cells may be indicative of a cancer-specific aberration.

While the APOBEC gene family are obviously important in preventing cross-species spread, the ways in which the gammaretroviruses evade this resistance mechanism in their natural hosts are not clearly understood. HIV carries an accessory gene product, Vif, that mediates the degradation of APOBEC3 proteins and it has been suggested that the glycoGag may play a role in resistance of murine leukaemia viruses by preventing encapsidation of APOBEC3 proteins⁹¹. However, a recent exhaustive study concluded that control of encapsidation was not involved in MLV resistance to murine APOBEC3 and acknowledged that there is currently no clear explanation for the phenomenon³⁰⁹. My studies showed that deletion of FeLV glycoGag does not affect the rate of replication in human cells. However, it would be interesting to test whether FeLV glycoGag has an

analogous role when the virus is grown in the cells of its natural host, the domestic cat.

Another potentially important aspect of my findings is the resistance of primary human blood cells (PBMCs) and some leukemic cell lines (e.g. Reh) to infection with FeLV and XMLV at an early stage of the replication cycle. In these cells proviral DNA is synthesised and persists, but with little evidence of G->A mutations, showing that neither APOBEC nor any of the known retroviral restriction factors can readily explain my observations. It will be interesting to identify the factor(s) responsible as these are likely to have a role as a major barrier to cross-species spread by the gammaretroviruses and the lack of evidence for sero-conversion in domestically or occupationally exposed individuals¹⁴⁹.

Retroviruses are known to be capable of changing the behaviour of cells by insertional mutagenesis, or by expression of viral proteins, which may subsequently suppress the immune system or may affect the interaction between different tissues²⁵⁸. I have shown that XMLV can infect susceptible cells such as the MCF7 mammary carcinoma cell line and result in a high proviral copy number. I have not examined XMLV insertion sites, but based on the reported preference of MLV and XMRV for insertion at transcription start sites and active chromatin features^{182,245} it seems very likely that XMLV will share the same preference. XMLV insertion may therefore play an important role in activation of genes that can possibly impart a selective advantage to the infected cell. This means that there is a high possibility of insertional mutagenesis and clonal selection if such infected cells are grown for a long period. Due to the non-cytopathic nature of XMLV infection in most cells, it is possible that operators will not be even aware that their cells are infected, either as a result of xenografting or by *in vitro* contamination. Chronically infected MCF7 cells also show a difference in wound healing, though a minor one, as compared to the uninfected cells. As the differences were not evident in freshly infected cells, a role for insertional mutagenesis in this minor difference has not been excluded.

The effects of a closely similar gammaretrovirus (XMRV) on host cells and cell lines^{189,258,222} have been explored widely due to interest generated by its presumed association with human diseases. It has also been claimed that Raji

cells, a Burkitt's lymphoma cell line, form syncytia when infected with XMRV²⁵⁷. However I did not observe any such effect of XMLV on Raji cells and my observations on the effects of *Mycoplasma* on THP-1 cells suggest the possibility that this report might have been due to a similar contamination artefact. XMLV uses the XPR1 receptor to enter cells. As XPR1 is a G protein receptor³⁵ with a reported role in phosphate transport³⁷, binding of viral Env protein in persistently infected cells represents another mechanism by which viral infection may alter xenograft properties and experimental outcomes^{310,311}.

The retroviruses have generally been regarded as weak inducers of host innate immune responses, but recent careful studies have shown that gammaretroviruses can initiate responses that may be significant for host resistance^{45,46}. I have shown that the differential expression of genes is much more pronounced in Raji cells (a hematopoietic cell line) infected with XMLV as compared to that seen in the MCF7 breast cancer cell line infected with XMLV. Whether this reflects a general capacity of haematopoietic cells, the sentinel cells of the immune system, to respond more actively to gammaretroviral infection will require more extensive studies. A further complicating factor is the EBV infected status of Raji Burkitt's lymphoma cells. While these cells display only the minimal 'latency I' pattern of EBV with expression of EBNA-1 and non-coding RNAs (EBER), they can be induced to express immediate early lytic cycle genes³¹². It would be interesting to test whether non-EBV infected Burkitt's lymphoma cell lines display a similar response to gammaretroviral infection, and whether EBV functions are affected in Raji cells. Changes in EBV gene expression would not have been detected in my microarray analysis which contained only cellular gene probes, but could in future studies be detected by alternative methods of analysis such as RNA-Seq³¹³.

The differentially expressed genes in Raji cells infected with XMLV included the interferon stimulated genes IFI44 and IFI44L, and a series of chemokines that play effective roles in the host immune response. Similar results were obtained when gene expression of IFI44 and CCL4 was checked in Raji cells infected with FeLV B, showing that this is a generic response to gammaretroviral infection. Analysis carried out on other leukaemia cell lines e.g. Kyo1 cells showed an up regulation of IFI44 up to 15 fold in the cells infected with FeLV B as compared to

the uninfected Kyo1 cells. This observation shows that these response pathways are intact in other leukaemias, and raises the possibility of harnessing these responses for immunotherapy of leukaemia. It is interesting in this regard that I observed the regression of Raji tumour nodules formed in BALB/c mice (Chapter 3), which could conceivably be due to mobilisation and infection of the cells with XMLV and subsequent changes in the gene expression resulting in immune recognition and removal by the host system. This response should be investigated further as it may provide a novel route to cancer therapy.

Appendices

Appendix 1: Primers and their thermal cycling conditions.

XMLV and NSG defective virus sequencing primers

	Name	5' to 3' Sequence	Origin
1	Fn1	GCGCCAGTCATCCGATAG	0-18*
2	Rn1	GTTACGGTCTGTCCCATATTTTAA	630-650*
3	Fn2	CAATTGCCCAATGAGATCGAG	1541-1561*
4	Rn2	TGCTCATCCTCTGCCCTAC	1997-2016*
5	Fn3**	GGATCTGAGAGAAGTCAACAAGC	2950-2975*
6	Rn3**	TCTTTTGT CAGAACGGCAATG	3856-3877*
7	Fn4	CATTGCCGTTCTGACAAAAGA	3856-3877*
8	Rn4	CAAAC TGATCGGGCATCAC	4751-4769*
9	Fn5	GTGATGCCCGATCAGTTTG	4751-4769*
10	Rn5	GTCCTTTCCAGCGAGGTTC	5654-5672*
11	Fn6	GAACCTCGCTGGAAGGAC	5654-5672*
12	Rn6	CGTTGTACCGAGGCTCCTG	5867-5885*
13	Fn7	TACCTCTGCCCCAGCTAAC	6783-6803*
14	Rn7	CTGGATCTATTGATTTGAGTTGG	7671-7693*
15	Fn8**	CAAAC TCAAATCAATAGATCCAG	7671-7693*
16	Rn8**	GCTTTATTGGGAACACGGGTA	8166-8186*

All primers were used for sequencing BALB/c XMLV.

* Primers based on N417 XMLV (accession number HQ246218).

** Primers used for sequencing both XMLV and NSG defective virus.

Primers for detecting XMLV and NSG defective sequences

	Name	5' to 3' Sequence	Origin
1	XMLV LTR- <i>gag</i> <i>F</i>	GCGCCAGTCATCCGATAG	0-18*
2	XMLV LTR- <i>gag</i> <i>R</i>	GTTACGGTCTGTCCCATATTTTAA	630-650*
3	XMLV LTR <i>F</i> **	CAAAC TCAAATCAATAGATCCAG	7671-7693*
4	XMLV LTR <i>R</i> **	GCTTTATTGGGAACACGGGTA	8166-8186*
5	XMLV <i>env</i> <i>F</i>	GGCAGGAGCCTCGGTACAA	
6	XMLV <i>env</i> <i>R</i>	TGTCATTAGGTTGGTAACTCTCCAAGT	XMLV <i>env</i> ¹⁷³

All primers were used for detecting BALB/c XMLV.

* Primers based on N417 XMLV (accession number HQ246218)

** Primers used for detecting both XMLV and NSG defective virus.

Primers for detecting XMRV

	Name	5' to 3' Sequence	Origin
1	XMRV <i>gag</i> <i>F</i>	AACCGTTTGTCTCTCCTAAACCC	XMRV <i>gag</i> ¹⁷³
2	XMRV <i>gag</i> <i>R</i>	GCAGGGTAAAGGGCAGATCG	

Primers for detecting endogenous *Bxv1* in mouse genome

	Name	5' to 3' Sequence	Origin
1	<i>Bxv1</i> -tail2F	G G C C T C G C T G T T C C T T G	<i>Bxv1</i> LTR-flanking
2	<i>Bxv1</i> -tail2R	G A G A G A G C G T G G C A A A C C T T	mouse genome on mouse chr 1

Primers for detecting BALB/c *Emv1* endogenous ecotropic virus

	Name	5' to 3' Sequence	Origin
1	<i>Emv1</i> F1	C A T G G A G A G T A C A A C G C T C T C A A	<i>Emv1 env</i> (accession no. dq366147)
2	<i>Emv1</i> R1	T G G T G G G G G C T G T T T C C	
3	<i>Emv1</i> F2	C C A C G G G C C G T C C T A T T	
4	<i>Emv1</i> R2	C T C C T C A C A A T C T C T G G A A C A	

Primers for designing XMLV probe

	Name	5' to 3' Sequence	Origin
1	XMLV Probe F	G A T G G T A C T C A G A T A A A G C G A A A C T	196-220*
2	XMLV Probe R	C T G G G T A G T C A A T C A C T C T G A G G	488-510*

* Primers based on N417 XMLV (accession number HQ246218)

Primers for XMLV *env* cloning

	Name	5' to 3' Sequence	Origin
1	F4	G G A G C A G C A T G G A A G G T C	5774-5791*
2	R1	A A C T T C C T T G T G A C T T T T G A G A A C	7830-7853*
3	F4-BamHI	C C T C C G G G A T C C G C A G C A T G G A A G G T C	XMLV <i>env</i> *
4	R1-SalI	C T T C C T T G C A G C T G T T G A G A A C T C A G C T C	XMLV <i>env</i> *

* Primers based on N417 XMLV (accession number HQ246218)

Primers for detecting FeLV B

	Name	5' to 3' Sequence	Origin
1	FeLV <i>gag</i> F	C G A C C A T A C C T G T T G T C C T T	FeLV B <i>gag</i>
2	FeLV <i>gag</i> R	T T C A A C C T G G G A A A T G C T A T	
3	FeLV LTR F	C G G C C C A T G C A T C C T T A A C	FeLV B LTR
4	FeLV LTR R	A A C A C C G A G A C C A C G A G T C A G	

Primers for sequencing FeLV B

	Name	5' to 3' Sequence	Origin
1	FeLV hyper F	G C A A C C G G T A A G G T G A C T C	FeLV B <i>pol</i>
2	FeLV hyper R	T T C A A A G G G T T T G G T G A T A T C T G	

Primers for detecting *Mycoplasma*

	Name	5' to 3' Sequence	Origin
1	Myco 280 F	G G G A G C A A A C A G G A T T A G A T A C C C T	Zakharova <i>et al</i> ²⁵⁶
2	Myco 280 R	T G C A C C A T C T G T C A C T C T G T T A A C C T C	

Human CD14 primers

	Name	5' to 3' Sequence	Origin
	CD14 F	C G A G G A C C T A A G A T A A C C G G C	Park <i>et al</i> ²⁵⁴
	CD14 R	G T T G C A G C T G A G A T C G A G C A C	

Human internal control primers

	Name	5' to 3' Sequence	Origin
1	Human GAPDH F	C C C C A C A C A C A T G C A C T T A C C	Human GAPDH ¹⁷³
2	Human GAPDH R	C C T A G T C C C A G G G C T T T G A T T	
3	Human MYC F	G A G C G G G C G G C C G G C T A G G G T	Human MYC
4	Human MYC R	C T C G G G T G T T G T A A G T T C C A G T G C	
5	β Actin F	T G A A G T C T G A C G T G G A C A T C	Park <i>et al</i> ²⁵⁴
6	β Actin R	A C T C G T C A T A C T C C T G C T T G	

Mouse internal control primers

	Name	5' to 3' Sequence	Origin
1	Mouse GAPDH F	A G T A T G A T G A C A T C A A G A A G G	Mouse GAPDH ¹⁷³
2	Mouse GAPDH R	A T G G T A T T C A A G A G A G T A G G G	

Thermal cycling conditions

Thermal cycling conditions for XMLV, XMRV, *Bxv1*, mouse and human internal control primers, and *Emv1*

Cycle Step	Temperature	Time	Number of cycles
Initial Denaturation	95°C	3 minutes	1
Denaturation	95°C	30 seconds	35
Annealing	60°C	30 seconds	
Extension	72°C	3 minutes	
Final Extension	72°C	7 minutes	1
Hold	4°C	∞	

Thermal cycling conditions for FeLV B LTR primers

Cycle Step	Temperature	Time	Number of cycles
Initial Denaturation	95°C	3 minutes	1
Denaturation	95°C	30 seconds	35
Annealing	50°C	30 seconds	
Extension	72°C	3 minutes	
Final Extension	72°C	7 minutes	1
Hold	4°C	∞	

Thermal cycling conditions for XMLV *env* cloning primers

Cycle Step	Temperature	Time	Number of cycles
Initial Denaturation	95°C	2 minutes	1
Denaturation	95°C	20 seconds	30
Annealing	55°C	20 seconds	
Extension	72°C	30 seconds	
Final Extension	72°C	3 minutes	1
Hold	4°C	∞	

Thermal cycling conditions for Pfu PCR for sequencing of XMLV

Cycle Step	Temperature	Time	Number of cycles
Initial Denaturation	95°C	2 minutes	1
Denaturation	95°C	20 seconds	40
Annealing	60°C	20 seconds	
Extension	72°C	45 seconds	
Final Extension	72°C	3 minutes	1
Hold	4°C	∞	

Thermal cycling conditions for FeLV B *env* and *gag* primers

Cycle Step	Temperature	Time	Number of cycles
Initial Denaturation	95°C	3 minutes	1
Denaturation	95°C	30 seconds	35
Annealing	50°C	30 seconds	
Extension	72°C	30 seconds	
Final Extension	72°C	7 minutes	1
Hold	4°C	∞	

Thermal cycling conditions for XMLV probe

Cycle Step	Temperature	Time	Number of cycles
Initial Denaturation	95°C	3 minutes	1
Denaturation	95°C	30 seconds	35
Annealing	60°C	30 seconds	
Extension	72°C	3 minutes	
Final Extension	72°C	7 minutes	1
Hold	4°C	∞	

Thermal cycling conditions for CD14 expression

Cycle Step	Temperature	Time	Number of cycles
Initial Denaturation	95°C	3 minutes	1
Denaturation	95°C	1 seconds	35
Annealing	60°C	1 seconds	
Extension	72°C	1 minutes	
Final Extension	72°C	7 minutes	1
Hold	4°C	∞	

Thermal cycling conditions for β Actin expression

Cycle Step	Temperature	Time	Number of cycles
Initial Denaturation	95°C	3 minutes	1
Denaturation	95°C	1 seconds	25
Annealing	60°C	1 seconds	
Extension	72°C	1 minutes	
Final Extension	72°C	7 minutes	1
Hold	4°C	∞	

Thermal cycling conditions for Pfu PCR for sequencing FeLV B *pol*

Cycle Step	Temperature	Time	Number of cycles
Initial Denaturation	95°C	2 minutes	1
Denaturation	95°C	20 seconds	30
Annealing	62°C	20 seconds	
Extension	72°C	30 seconds	
Final Extension	72°C	3 minutes	1
Hold	4°C	∞	

Appendix 2: Alignment of *Bxv1* (accession no.AC115959.17) and BALB/c XMLV rescued from MCF7 explants.

```

Bxv1          GCGCCAGTCATCCGATAGACTGAGTCGCCCCGGGTACCCGTGTTCCCAATA
BALB/c XMLV    GCGCCAGTCATCCGATAGACTGAGTCGCCCCGGGTACCCGTGTTCCCAATA
*****

Bxv1          AAGCCTTTTGCTGTTTGCATCCGAAACGTGGCCTCGCTGTTCCCTGGGAG
BALB/c XMLV    AAGCCTTTTGCTGTTTGCATCCGAAACGTGGCCTCGCTGTTCCCTGGGAG
*****

Bxv1          GGTCTCCTCAGAGTGATTGACTACCCAGCTCGGGGGTCTTTCATTTGGGG
BALB/c XMLV    GGTCTCCTCAGAGTGATTGACTACCCAGCTCGGGGGTCTTTCATTTGGGG
*****

Bxv1          GCTCGTCCGGGATTTGGAGACCCCCGCCAGGGACCACCGACCCACCGTC
BALB/c XMLV    GCTCGTCCGGGATTTGGAGACCCCCGCCAGGGACCACCGACCCACCGTC
*****

Bxv1          GGGAGGTAAGCTGGCCAGCGATCGTTTTGTCTCCGTCTCTGTCTTTGTGC
BALB/c XMLV    GGGAGGTAAGCTGGCCAGCGATCGTTTTGTCTCCGTCTCTGTCTTTGTGC
*****

Bxv1          GTGTGTGTGTGTGCCGGCATCTACTTTTTGCGCCTGCGTCTGAATCTGTA
BALB/c XMLV    GTGTGTGTGTGTGCCGGCATCTACTTTTTGCGCCTGCGTCTGAATCTGTA
*****

Bxv1          CTAGTTAGCTAACTAGATCTGTATCTGGCGGTTCCGTGGAAGAACTGACG
BALB/c XMLV    CTAGTTAGCTAACTAGATCTGTATCTGGCGGTTCCGTGGAAGAACTGACG
*****

Bxv1          AGTTTCGTATTCCCGACCGCAGCCCTGGGAGACGTCTCAGAGGCATCAGGG
BALB/c XMLV    AGTTTCGTATTCCCGACCGCAGCCCTGGGAGACGTCTCAGAGGCATCAGGG
*****

Bxv1          GCCCGCTGGGTGGCCCAATCAGTAAGTCCGAGTCCGACCGATTCCGGACT
BALB/c XMLV    GCCCGCTGGGTGGCCCAATCAGTAAGTCCGAGTCCGACCGATTCCGGACT
*****

Bxv1          ATTTGGAGCCCCTCCTTTGTGCGAGGGGTACGTGGTTCTTTTAGGAGACG
BALB/c XMLV    ATTTGGAGCCCCTCCTTTGTGCGAGGGGTACGTGGTTCTTTTAGGAGACG
*****

Bxv1          AGAGGTCCAAGCCCTCGCCGCCTCCATCTGAATTTTTGCTTTCGGTTTTT
BALB/c XMLV    AGAGGTCCAAGCCCTCGCCGCCTCCATCTGAATTTTTGCTTTCGGTTTTT
*****

Bxv1          CGCCGAAACCGCGCCGCGCTCTTGTCTGTCTCAGTGTGTTTTGTCATT
BALB/c XMLV    CGCCGAAACCGCGCCGCGCTCTTGTCTGTCTCAGTGTGTTTTGTCATT
*****

Bxv1          TGTCTGTTTCGTTATTGTTTTGGACCGTTTCTAAAAATATGGGACAGACCG
BALB/c XMLV    TGTCTGTTTCGTTATTGTTTTGGACCGTTTCTAAAAATATGGGACAGACCG
*****

Bxv1          TAACCACCCCTCTGAGTCTGACCCTAGAACAAGTGGGGAGACGTCCAGCGC
BALB/c XMLV    TAACCACCCCTCTGAGTCTGACCCTAGAACAAGTGGGGAGACGTCCAGCGC
*****

Bxv1          ATCGCGTCCAACCAGTCCGTGGACGTCAAGAAGAGACGTGGGTCACCTT
BALB/c XMLV    ATCGCGTCCAACCAGTCCGTGGACGTCAAGAAGAGACGTGGGTCACCTT
*****

```

Bxv1
 BALB/c XMLV
 CTGCTCTGCCGAGTGGCCAACTTTCGGTGTAGGGTGGCCGCAAGATGGTA
 CTGCTCTGCCGAGTGGCCAACTTTCGGTGTAGGGTGGCCGCAAGATGGTA

Bxv1
 BALB/c XMLV
 CTTTTAATTTGGACATTATTTTACAGGTAAATCTAAGGTGTTCTCTCCC
 CTTTTAATTTGGACATTATTTTACAGGTAAATCTAAGGTGTTCTCTCCC

Bxv1
 BALB/c XMLV
 GGTCCCCACGGACACCCGGATCAGGTCCCATAACATTGTCACCTGGGAGGC
 GGTCCCCACGGACACCCGGATCAGGTCCCATAACATTGTCACCTGGGAGGC

Bxv1
 BALB/c XMLV
 TATTGCCTATGAACCCCTCCGTGGGTCAAACCTTTTGTCTCTCCCAAAC
 TATTGCCTATGAACCCCTCCGTGGGTCAAACCTTTTGTCTCTCCCAAAC

Bxv1
 BALB/c XMLV
 TCTCCCTCTCTCCAACCGCTCCCATCCTCCCATCCGGTCTTCGACCCAA
 TCTCCCTCTCTCCAACCGCTCCCATCCTCCCATCCGGTCTTCGACCCAA

Bxv1
 BALB/c XMLV
 CCTCCGCCCCGATCTGCCCTTACCCTGCTCTTACCCCTCTATAAAACC
 CCTCCGCCCCGATCTGCCCTTACCCTGCTCTTACCCCTCTATAAAACC

Bxv1
 BALB/c XMLV
 CAGACCTTCTAAACCTCAGGTTCTCTCCGATAATGGCGGACCTCTCATTG
 CAGACCTTCTAAACCTCAGGTTCTCTCCGATAATGGCGGACCTCTCATTG

Bxv1
 BALB/c XMLV
 ACCTTCTCACAGAAGACCCCTCCGCCGTACGGAGAACAGGGACCGTCTCTCC
 ACCTTCTCACAGAAGACCCCTCCGCCGTACGGAGAACAGGGACCGTCTCTCC

Bxv1
 BALB/c XMLV
 TCTGACGGAGATGGCGACAGAGAAGAGGCCACCTCCACTCCTGAGATTCC
 TCTGACGGAGATGGCGACAGAGAAGAGGCCACCTCCACTCCTGAGATTCC

Bxv1
 BALB/c XMLV
 TGCCCCCTCTCCCATGGTGTCTCGCTTGCGGGGCAAAAAGAGACCCCCCG
 TGCCCCCTCTCCCATGGTGTCTCGCTTGCGGGGCAAAAAGAGACCCCCCG

Bxv1
 BALB/c XMLV
 CGGCAGTTTCCACCACCTCTCGGGCTTTCCTACTCCGTTTGGGGGGTAAT
 CGGCAGTTTCCACCACCTCTCGGGCTTTCCTACTCCGTTTGGGGGGTAAT

Bxv1
 BALB/c XMLV
 GGTCAGTTGCAGTACTGGCCGTTTTCCTCCTCGGATCTATATAACTGGAA
 GGTCAGTTGCAGTACTGGCCGTTTTCCTCCTCGGATCTATATAACTGGAA

Bxv1
 BALB/c XMLV
 AAATAATAACCCTTCCTTCTCTGAAGATCCAGGTAATTGACTGCCTTAA
 AAATAATAACCCTTCCTTCTCTGAAGATCCAGGTAATTGACTGCCTTAA

Bxv1
 BALB/c XMLV
 TCGAGTCTGTCTCACCACCCACCAGCCTACTTGGGATGACTGTCAACAG
 TCGAGTCTGTCTCACCACCCACCAGCCTACTTGGGATGACTGTCAACAG

Bxv1
 BALB/c XMLV
 TTGCTGGGGACTCTGCTGACAGGAGAAGAAAAGCAGCGGGTGTCTCTGGA
 TTGCTGGGGACTCTGCTGACAGGAGAAGAAAAGCAGCGGGTGTCTCTGGA

Bxv1
 BALB/c XMLV
 AGCCAGAAAGGCAGTCCGGGGCGACGATGGCCGCCCCACCCAATTGCCCA
 AGCCAGAAAGGCAGTCCGGGGCGACGATGGCCGCCCCACCCAATTGCCCA

Bxv1
 BALB/c XMLV
 ATGAGATCGAGGCTGCCTTTCCCCTCGAACGTCCCAGCTGGGACTACACC
 ATGAGATCGAGGCTGCCTTTCCCCTCGAACGTCCCAGCTGGGACTACACC

Bxv1
 BALB/c XMLV
 ACCCTTAGAGGTAGGAACCACCTAGTTCTCTATCGCCAGCTGCTCTTGCC
 ACCCTTAGAGGTAGGAACCACCTAGTTCTCTATCGCCAGCTGCTCTTGCC

Bxv1
 BALB/c XMLV
 GGGTCTCCAAAATGCGGGCAGGAGCCCCACCAATTTGGCTAAGGTAAAAG
 GGGTCTCCAAAATGCGGGCAGGAGCCCCACCAATTTGGCTAAGGTAAAAG

Bxv1
 BALB/c XMLV
 GAATAACCCAGGGGTCCAACGAGTCGCCCTCGGCCTTTCTAGAGAGACTC
 GAATAACCCAGGGGTCCAACGAGTCGCCCTCGGCCTTTCTAGAGAGACTC

Bxv1
 BALB/c XMLV
 AAAGAGGCCTATCGCAGATACTCCTTATGACCCTGAGGACCCTGGGCA
 AAAGAGGCCTATCGCAGATACTCCTTATAACCCTGAGGACCCTGGGCA

Bxv1
 BALB/c XMLV
 AGAAACCAATGTATCCATGTCGTTTCATCTGGCAGTCTGCTCCAGACATTG
 AGAAACCAATGTATCCATGTCGTTTCATCTGGCAGTCTGCTCCAGACATTG

Bxv1
 BALB/c XMLV
 GTCGAAAAGTTAGAGCGGTTAGAAGACTTAAAAAATAAGACCTTAGGGGAC
 GTCGAAAAGTTAGAGCGGTTAGAAGACTTAAAAAATAAGACCTTAGGGGAC

Bxv1
 BALB/c XMLV
 TTAGTGAGAGAAGCAGAAAGGATCTTTAATAAGAGAGAGACCCAGAAAGA
 TTAGTGAGAGAAGCAGAAAGGATCTTTAATAAGAGAGAGACCCAGAAAGA

Bxv1
 BALB/c XMLV
 GAGAGAAGAACGTATTAAGAGAGAAACAGAGGAAAAAGAGGAGCGCCGTA
 GAGAGAAGAACGTATTAAGAGAGAAACAGAGGAAAAAGAGGAGCGCCGTA

Bxv1
 BALB/c XMLV
 GGGCAGAGGATGAGCAGAAAGAGAAAGAGAGGGACCGCAGAAGACAGAGA
 GGGCAGAGGATGAGCAGAAAGAGAAAGAGAGGGACCGCAGAAGACAGAGA

Bxv1
 BALB/c XMLV
 GAAATGAGCAAACCTCTTGCCACCGTAGTTACAGGTCAGAGACAGGATAG
 GAAATGAGCAAACCTCTTGCCACCGTAGTTACAGGTCAGAGACAGGATAG

Bxv1
 BALB/c XMLV
 ACAGGGGGGAGAGCGAAGGAGGCCCAACTCGATAAGGACCAATGCGCCT
 ACAGGGGGGAGAGCGAAGGAGGCCCAACTCGATAAGGACCAATGCGCCT

Bxv1
 BALB/c XMLV
 ACTGCAAAGAAAAGGGACACTGGGCTAGGGATTGCCCAAAGAAGCCACGG
 ACTGCAAAGAAAAGGGACACTGGGCTAGGGATTGCCCAAAGAAGCCACGG

Bxv1
 BALB/c XMLV
 GGGCCCCGAGGACCGAGGCCCCAGACCTCCCTCCTGACCCTAGATGACTA
 GGGCCCCGAGGACCGAGGCCCCAGACCTCCCTCCTGACCCTAGATGACTA

Bxv1
 BALB/c XMLV
 GGGAGGTCAGGGTCAGGAGCCCCCCCCCTGAACCCAGGATAACCCTTACTG
 GGGAGGTCAGGGTCAGGAGCCCCCCCCCTGAACCCAGGATAACCCTTACTG

Bxv1
 BALB/c XMLV
 TCGGGGGCAACCAGTCACCTTCCTGGTGGATACTGGGGCCCAACACTCC
 TCGGGGGCAACCAGTCACCTTCCTGGTGGATACTGGGGCCCAACACTCC

Bxv1
 BALB/c XMLV
 GTGCTGACCCAGAACCCTGGACCCCTAAGTGACAGGTCTGCCTGGGTCCA
 GTGCTGACCCAGAACCCTGGACCCCTAAGTGACAGGTCTGCCTGGGTCCA

Bxv1
 BALB/c XMLV
 AGGGGCTACTGGAGGAAAGCGGTATCACTGGACCACAGATCGCAAGGTGC
 AGGGGCTACTGGAGGAAAGCGGTATCACTGGACCACAGATCGCAAGGTGC

Bxv1
 BALB/c XMLV
 ACCTGGCTACCGGTAAGGTCACCTCACTCTTTCTCCATGTGCCGGACTGC
 ACCTGGCTACCGGTAAGGTCACCTCACTCTTTCTCCATGTGCCGGACTGC

Bxv1
 BALB/c XMLV
 CCTTATCCTTTGCTAGGAAGGGACTTGTTGACTAAGTTAAAGGCCAGAT
 CCTTATCCTTTGCTAGGAAGGGACTTGTTGACTAAGTTAAAGGCCAGAT

Bxv1
 BALB/c XMLV
 CCACTTCGAGGGATCGGGAGCTCAGGTTGTGGGACCAAAGGACAGCCCC
 CCACTTCGAGGGATCGGGAGCTCAGGTTGTGGGACCAAAGGACAGCCCC

Bxv1
 BALB/c XMLV
 TGCAGGTGTTGACCCCTTGGCATAGAGGATGAGTATCGGCTACATGAGACC
 TGCAGGTGTTGACCCCTTGGCATAGAGGATGAGTATCGGCTACATGAGACC

Bxv1
 BALB/c XMLV
 TCAACAGAGCCGGATGTTTTCTCTAGGGTCCACCTGGCTTTCTGACTTTCC
 TCAACAGAGCCGGATGTTTTCTCTAGGGTCCACCTGGCTTTCTGACTTTCC

Bxv1
 BALB/c XMLV
 CCAGGCCTGGGCAGAAACCGGGGGCATGGGACTGGCAGTTCGCCAAGCGC
 CCAGGCCTGGGCAGAAACCGGGGGCATGGGACTGGCAGTTCGCCAAGCGC

Bxv1
 BALB/c XMLV
 CTCTGATTATACCTCTAAAGGCAACCTCCACCCCTGTGTCCATCAAACAG
 CTCTGATTATACCTCTAAAGGCAACCTCCACCCCTGTGTCCATCAAACAG

Bxv1
 BALB/c XMLV
 TACCCCATGTCACACGAAGCCAGACTGGGGATCAAGCCCCACATACAGAG
 TACCCCATGTCACACGAAGCCAGACTGGGGATCAAGCCCCACATACAGAG

Bxv1
 BALB/c XMLV
 ACTGTTGGACCAGGGAATATTGGTACCTTGCCAGTCCCCCTGGAACACAC
 ACTGTTGGACCAGGGAATATTGGTACCTTGCCAGTCCCCCTGGAACACAC

Bxv1
 BALB/c XMLV
 CCCTGCTGCCCGTTAAGAAACCAGGGACTAATGATTACAGGCCTGTCCAG
 CCCTGCTGCCCGTTAAGAAACCAGGGACTAATGATTACAGGCCTGTCCAG

Bxv1
 BALB/c XMLV
 GATCTGAGAGAAGTCAACAAGCGGGTGGAAGATATCCACCCCACCGTGCC
 GATCTGAGAGAAGTCAACAAGCGGGTGGAAGATATCCACCCCACCGTGCC

Bxv1
 BALB/c XMLV
 CAATCCTTACAACCTCTTAAGTGACTCCCTCCGTCCCACCAGTGGTACA
 CAATCCTTACAACCTCTTAAGTGACTCCCTCCGTCCCACCAGTGGTACA

Bxv1
 BALB/c XMLV
 CTGTGCTTGATTTAAAAGATGCCTTTTTCTGCCTGAGACTCCACCCACC
 CTGTGCTTGATTTAAAAGATGCCTTTTTCTGCCTGAGACTCCACCCACC

Bxv1
 BALB/c XMLV
 AGTCAGCCTCTCTTTGCCTTTGAGTGGAGAGATCCAGAAATGGGAATCTC
 AGTCAGCCTCTCTTTGCCTTTGAGTGGAGAGATCCAGAAATGGGAATCTC

Bxv1
 BALB/c XMLV
 TGGACAATTGACCTGGACCAGACTCCCACAGGGTTTCAAAAAACAGTCCCA
 TGGACAATTGACCTGGACCAGACTCCCACAGGGTTTCAAAAAACAGTCCCA

Bxv1
 BALB/c XMLV
 CCCTGTTTGATGAGGCATTGCACAGAGACCTAGCAGACTTCCGGATCCAG
 CCCTGTTTGATGAGGCATTGCACAGAGACCTAGCAGACTTCCGGATCCAG

Bxv1
 BALB/c XMLV
 CACCCAGACTTGATCCTGCTACAGTACGTGGATGACTTACTGCTGGCCGC
 CACCCAGACTTGATCCTGCTACAGTACGTGGATGACTTACTGCTGGCCGC

Bxv1
 BALB/c XMLV
 TACTTCCGAAGTACTGACCAACAAGGTACTCGGGCCCTTCTACAAACCC
 TACTTCCGAAGTACTGACCAACAAGGTACTCGGGCCCTTCTACAAACCC

Bxv1
 BALB/c XMLV
 TAGGGGACCTCGGATACCGGGCCCTCGGCCAAGAAAAGCCCAAATCTGCCAG
 TAGGGGACCTCGGATACCGGGCCCTCGGCCAAGAAAAGCCCAAATCTGCCAG

Bxv1
 BALB/c XMLV
 AAACAGGTTAAATACCTGGGGTACCTTCTGAGGGAGGGTCAGAGATGGCT
 AAACAGGTTAAATACCTGGGGTACCTTCTGAGGGAGGGTCAGAGATGGCT

Bxv1
 BALB/c XMLV
 GACTGAGGCTAGAAAAGAGACTGTGATGGGGCAACCCGTTCCAAAGACTC
 GACTGAGGCTAGAAAAGAGACTGTGATGGGGCAACCCGTTCCAAAGACTC

Bxv1
 BALB/c XMLV
 CTCGACAACCTAAGGGAGTTCTTAGGGACGGCAGGCTTCTGCCGCCTCTGG
 CTCGACAACCTAAGGGAGTTCTTAGGGACGGCAGGCTTCTGCCGCCTCTGG

Bxv1
 BALB/c XMLV
 ATCCCTGGGTTTGCGGAAATGGCGGCCCCCTTGTATCCTCTTACCAAAC
 ATCCCTGGGTTTGCGGAAATGGCGGCCCCCTTGTATCCTCTTACCAAAC

Bxv1
 BALB/c XMLV
 GGGGACTCTGTTTAATTGGGGCCAGACCAGCAAAGGCCTATCAAGAAA
 GGGGACTCTGTTTAATTGGGGCCAGACCAGCAAAGGCCTATCAAGAAA

Bxv1
 BALB/c XMLV
 TCAAACAGGCCCTTCTAACTGCCCCGCCCTGGGATTGCCAGATTTGACT
 TCAAACAGGCCCTTCTAACTGCCCCGCCCTGGGATTGCCAGATTTGACT

Bxv1
 BALB/c XMLV
 AAGCCCTTTGAACTCTTTGTGTCGACGAGAAGCAGGGCTACGCCAAAGGCGT
 AAGCCCTTTGAACTCTTTGTGTCGACGAGAAGCAGGGCTACGCCAAAGGCGT

Bxv1
 BALB/c XMLV
 CCTAACGCAAAAACCTGGGACCTTGGCGTCGGCCTGTGGCTACCTGTCCA
 CCTAACGCAAAAACCTGGGACCTTGGCGTCGGCCTGTGGCTACCTGTCCA

Bxv1
 BALB/c XMLV
 AAAAGCTAGACCCAGTGGCAGCCGGGTGGCCCCCTTGCCCTACGGATGGTA
 AAAAGCTAGACCCAGTGGCAGCCGGGTGGCCCCCTTGCCCTACGGATGGTA

Bxv1
 BALB/c XMLV
 GCAGCCATTGCCGTTCTGACAAAAGATGCAGGCAAGCTAACTATGGGACA
 GCAGCCATTGCCGTTCTGACAAAAGATGCAGGCAAGCTAACTATGGGACA

Bxv1
 BALB/c XMLV
 GCCGCTAGTCATCCTGGCCCCCATGCAGTAGAGGCACTGGTCAAGCAAC
 GCCGCTAGTCATCCTGGCCCCCATGCAGTAGAGGCACTGGTCAAGCAAC

Bxv1
 BALB/c XMLV
 CCCCTGACCGCTGGCTATCCAACGCCCGCATGACCCACTACCAGGCAATG
 CCCCTGACCGCTGGCTATCCAACGCCCGCATGACCCACTACCAGGCAATG

Bxv1
 BALB/c XMLV
 CTCCTAGACACTGACCGAGTTCAGTTCGGACCAGTGGTGGCCCTCAATCC
 CTCCTAGACACTGACCGAGTTCAGTTCGGACCAGTGGTGGCCCTCAATCC

Bxv1
 BALB/c XMLV
 TGCCACCTTGCTCCCTCTACCGGAAAAAGGAGCCCCCATGATTGCCTCG
 TGCCACCTTGCTCCCTCTACCGGAAAAAGGAGCCCCCATGATTGCCTCG

Bxv1
 BALB/c XMLV
 AGATCTTGGCTGAAACGCATGGAACCAGACCGGATCTCACCGACCAGCCC
 AGATCTTGGCTGAAACGCATGGAACCAGACCGGATCTCACCGACCAGCCC

Bxv1
 BALB/c XMLV
 ATCCCAGACGCCGACCACACCTGGTATAACCGATGGGAGCAGCTTCTGCA
 ATCCCAGACGCCGACCACACCTGGTATAACCGATGGGAGCAGCTTCTGCA

Bxv1
 BALB/c XMLV
 AGAAGGACAGCGAAAGGCTGGGGCAGCAGTGACGACTGAAACCGAGGTAA
 AGAAGGACAGCGAAAGGCTGGGGCAGCAGTGACGACTGAAACCGAGGTAA

Bxv1
 BALB/c XMLV
 TCTGGGCGAGGGCCCTGCCAGCTGGAACGTCAGCCCAGCGAGCCGAACTG
 TCTGGGCGAGGGCCCTGCCAGCTGGAACGTCAGCCCAGCGAGCCGAACTG

Bxv1
 BALB/c XMLV
 ATCGCACTCACCCAAGCCCTGAAAAATGGCAGAAGGTAAGAAGCTAAATGT
 ATCGCACTCACCCAAGCCCTGAAAAATGGCAGAAGGTAAGAAGCTAAATGT

Bxv1
 BALB/c XMLV
 TTACACTGATAGCCGCTATGCCTTCGCTACGGCCCATGTTCATGGGGAAA
 TTACACTGATAGCCGCTATGCCTTCGCTACGGCCCATGTTCATGGGGAAA

Bxv1
 BALB/c XMLV
 TATATAGGAGACGGGGTTGCTGACCTCAGAAGGCAAGGAAATCAAGAAC
 TATATAGGAGACGGGGTTGCTGACCTCAGAAGGCAAGGAAATCAAGAAC

Bxv1
 BALB/c XMLV
 AAAAGCGAGATCCTAGCCTTGCTGAAAGCCCTCTTTTGGCCAAAGAGACT
 AAAAGCGAGATCCTAGCCTTGCTGAAAGCCCTCTTTTGGCCAAAGAGACT

Bxv1
 BALB/c XMLV
 CAGTATTATCCATTGCCCAGGACATCAGAAAGGAGACAGTGCCGAAGCCA
 CAGTATTATCCATTGCCCAGGACATCAGAAAGGAGACAGTGCCGAAGCCA

Bxv1
 BALB/c XMLV
 GAGGCAACCGTATGGCAGACCAGGCGGCCGAGAGGCAGCCACAAAAACA
 GAGGCAACCGTATGGCAGACCAGGCGGCCGAGAGGCAGCCACAAAAACA

Bxv1
 BALB/c XMLV
 GTTCCAGAAGCCTCTACACTCCTTATAGAGGACTCGACCCCGTACACGCC
 GTTCCAGAAGCCTCTACACTCCTTATAGAGGACTCGACCCCGTACACGCC

Bxv1
 BALB/c XMLV
 TGCCTATCTCCATTACACCGAAACAGATCTAAAAAGATTGCGAGAACTGG
 TGCCTATCTCCATTACACCGAAACAGATCTAAAAAGATTGCGAGAACTGG

Bxv1
 BALB/c XMLV
 GGGCCACCTATAATCAGATAAAAGGATATTGGGTCTTACAAGGCAAGCCG
 GGGCCACCTATAATCAGATAAAAGGATATTGGGTCTTACAAGGCAAGCCG

Bxv1
 BALB/c XMLV GTGATGCCCGATCAGTTTGTGTTTGAATTATTAGACTCCCTTCATAGACT
 GTGATGCCCGATCAGTTTGTGTTTGAATTATTAGACTCCCTTCATAGACT

Bxv1
 BALB/c XMLV CACCCATCTCAGCCCTCAAAAGATGAAGGCGCTCCTTGACAGAGAAGAAA
 CACCCATCTCAGCCCTCAAAAGATGAAGGCGCTCCTTGACAGAGAAGAAA

Bxv1
 BALB/c XMLV GCCCCTACTACATGTTAAACAGGGACAGAACTCTTCAGTATGTGGCAGAA
 GCCCCTACTACATGTTAAACAGGGACAGAACTCTTCAGTATGTGGCAGAA

Bxv1
 BALB/c XMLV TCCTGCACAGTCTGTGCTCAAGTAAATGCTAGTAAAGCCAAAATCGGGGC
 TCCTGCACAGTCTGTGCTCAAGTAAATGCTAGTAAAGCCAAAATCGGGGC

Bxv1
 BALB/c XMLV AGGGGTACGAGTACGCGGACATCGACCAGGTACCCATTGGGAAATTGACT
 AGGGGTACGAGTACGCGGACATCGACCAGGTACCCATTGGGAAATTGACT

Bxv1
 BALB/c XMLV TCACTGAAGTTAAACCAGGGCTGTACGGGTACAAGTACCTCCTGGTGTTT
 TCACTGAAGTTAAACCAGGGCTGTACGGGTACAAGTACCTCCTGGTGTTT

Bxv1
 BALB/c XMLV GTAGACACCTTCTCTGGCTGGGTGGAAGCCTTCCCAACTAAACGTGAAAC
 GTAGACACCTTCTCTGGCTGGGTGGAAGCCTTCCCAACTAAACGTGAAAC

Bxv1
 BALB/c XMLV TGCCAAGGTTGTGACCAAGAAGCTATTAGAAGAAATATCCCAAGATTCCG
 TGCCAAGGTTGTGACCAAGAAGCTATTAGAAGAAATATCCCAAGATTCCG

Bxv1
 BALB/c XMLV GGATGCCACAGGTATTGGGTTCCGATAATGGGCCTGCCTTCGTCTCCCAG
 GGATGCCACAGGTATTGGGTTCCGATAATGGGCCTGCCTTCGTCTCCCAG

Bxv1
 BALB/c XMLV GTAAGTCAGTCGGTGGCCGATTTACTGGGGATCGATTGGAAATTACATTG
 GTAAGTCAGTCGGTGGCCGATTTACTGGGGATCGATTGGAAATTACATTG

Bxv1
 BALB/c XMLV TGCTTATAGACCCAGAGTTCAGGTCAGGTAGAAAAGATGAATAGAACCA
 TGCTTATAGACCCAGAGTTCAGGTCAGGTAGAAAAGATGAATAGAACCA

Bxv1
 BALB/c XMLV TCAAGGAGACTCTAACTAAATTAACGCTTGCAGCTGGCACTAGAGACTGG
 TCAAGGAGACTCTAACTAAATTAACGCTTGCAGCTGGCACTAGAGACTGG

Bxv1
 BALB/c XMLV GTRACTCTACTCCCCTTAGCCCTCTACCGAGCCCGGAACACTCCGGGCC
 GTRACTCTACTCCCCTTAGCCCTCTACCGAGCCCGGAACACTCCGGGCC

Bxv1
 BALB/c XMLV CCATGGACTGACTCCGTATGAAATTTCTGTATGGGGCACCCCGCCCTTG
 CCATGGACTGACTCCGTATGAAATTTCTGTATGGGGCACCCCGCCCTTG

Bxv1
 BALB/c XMLV TCAATTTTCATGATCCTGAAATGTCAAAGTTAACTAATAGTCCCTCTCTC
 TCAATTTTCATGATCCTGAAATGTCAAAGTTAACTAATAGTCCCTCTCTC

Bxv1
 BALB/c XMLV CAAGTCACTTACAGGCCCTCCAAGCAGTACAACGAGAGGTCTGGAAGCC
 CAAGTCACTTACAGGCCCTCCAAGCAGTACAACGAGAGGTCTGGAAGCC

Bxv1
 BALB/c XMLV GCTGGCCGCTGCTTATCAGGACCAGCTAGATCAGCCAGTGATACCACACC
 GCTGGCCGCTGCTTATCAGGACCAGCTAGATCAGCCAGTGATACCACACC

Bxv1
 BALB/c XMLV CCTTCCGTGTCGGTGACGCCGTGTGGGTACGCCGGCACCAGACTAAGAAC
 CCTTCCGTGTCGGTGACGCCGTGTGGGTACGCCGGCACCAGACTAAGAAC

Bxv1
 BALB/c XMLV TTGGAACCTCGCTGGAAAGGACCCTACACCGTCCTGCTGACCACCCCCAC
 TTGGAACCTCGCTGGAAAGGACCCTACACCGTCCTGCTGACCACCCCCAC

Bxv1
 BALB/c XMLV CGCTCTCAAAGTTGACGGCATCTCTGCGTGGATAACACGCCGCTCACGTAA
 CGCTCTCAAAGTTGACGGCATCTCTGCGTGAATACACGCCGCTCACGTAA

Bxv1
 BALB/c XMLV AGGCGGCGACAACCTCCTCCGGCCGGAGCAGCATGGAAGGTCCAGCGTTCT
 AGGCGGCGACAACCTCCTCCGGCCGGAGCAGCATGGAAGGTCCAGCGTTCT

Bxv1
 BALB/c XMLV CAAAACCCCTTAAAGATAAGATTAAACCGTGGGGCCCCCTAATAGTTATA
 CAAAACCCCTTAAAGATAAGATTAGCCCGTGGGGCCCCCTAATAGTTATA

Bxv1
 BALB/c XMLV GGGATCTTGGTGAGGGCAGGAGCCTCGGTACAACGTGACAGCCCTCACCA
 GGGATCTTGGTGAGGGCAGGAGCCTCGGTACAACGTGACAGCCCTCACCA

Bxv1
 BALB/c XMLV GGTCTTCAATGTCACTTGGAGAGTTACCAACCTAATGACAGGACAAACAG
 GGTCTTCAATGTCACTTGGAGAGTTACCAACCTAATGACAGGACAAACAG

Bxv1
 BALB/c XMLV CTAACGCTACCTCCCTCCTGGGGACGATGACAGACACCTTCCCTAAACTA
 CTAACGCTACCTCCCTCCTGGGGACGATGACAGACACCTTCCCTAAACTA

Bxv1
 BALB/c XMLV TATTTTGA CT TGTGTGATTTAGTTGGAGACCATTGGGATGACCCAGAACC
 TATTTTGA CT TGTGTGATTTAGTTGGAGACCATTGGGATGACCCAGAACC

Bxv1
 BALB/c XMLV CGATATTGGAGATGGTTGCCGCTCTCCGGGGGAAGAAAAGGACAAGAC
 CGATATTGGAGATGGTTGCCGCTCTCCGGGGGAAGAAAAGGACAAGAC

Bxv1
 BALB/c XMLV TGTATGACTTCTATGTTTGCCCCGGTCATACTGTACCAATAGGGTGTGGA
 TGTATGACTTCTATGTTTGCCCCGGTCATACTGTACCAATAGGGTGTGGA

Bxv1
 BALB/c XMLV GGGCCGGGAGAGGGCTACTGTGGCAAATGGGGATGTGAGACCACTGGACA
 GGGCCGGGAGAGGGCTACTGTGGCAAATGGGGATGTGAGACCACTGGACA

Bxv1
 BALB/c XMLV GGCATACTGGAAGCCATCATCATCATGGGACCTAATTTCCCTTAAGCGAG
 GGCATACTGGAAGCCATCATCATCATGGGACCTAATTTCCCTTAAGCGAG

Bxv1
 BALB/c XMLV GAAACACTCCTAAGGATCAGGGCCCCCTGTTATGATTCTCGGTCTCCAGT
 GAAACACTCCTAAGGATCAGGGCCCCCTGTTATGATTCTCGGTCTCCAGT

Bxv1
 BALB/c XMLV GGCGTCCAGGGTGCCACACCGGGGGTTCGATGCAACCCCTAGTCTTAGA
 GGCGTCCAGGGTGCCACACCGGGGGTTCGATGCAACCCCTAGTCTTAGA

Bxv1
 BALB/c XMLV
 ATTCAGTACGCGGGTAAAAAGGCCAGCTGGGATGCCCCAAAAGTTTGGG
 ATTCAGTACGCGGGTAAAAAGGCCAGCTGGGATGCCCCAAAAGTTTGGG

Bxv1
 BALB/c XMLV
 GACTAAGACTCTACCGATCCACGGGGCCGACCCGGTGACCCGGTTCTCT
 GACTAAGACTCTACCGATCCACGGGGCCGACCCGGTGACCCGGTTCTCT

Bxv1
 BALB/c XMLV
 TTGACCCGCCAGGTCTCAATGTAGGACCCCGCGTCCCCATTGGGCCTAA
 TTGACCCGCCAGGTCTCAATGTAGGACCCCGCGTCCCCATTGGGCCTAA

Bxv1
 BALB/c XMLV
 TCCCGTGATCACTGAACAGCTACCCCCCTCCAACCCGTGCAGATCATGC
 TCCCGTGATCACTGAACAGCTACCCCCCTCCAACCCGTGCAGATCATGC

Bxv1
 BALB/c XMLV
 TCCCCAGGCCTCCTCATCTCCTCCTTCAGGCGGGCCTCTATGGTGCCT
 TCCCCAGGCCTCCTCATCTCCTCCTTCAGGCGGGCCTCTATGGTGCCT

Bxv1
 BALB/c XMLV
 GGGGCTCCCCCGCCTTCTCAACAACCTGGGACGGGGGACAGGCTGCTAAA
 GGGGCTCCCCCGCCTTCTCAACAACCTGGGACGGGGGACAGGCTGCTAAA

Bxv1
 BALB/c XMLV
 CCTAGTAAAAGGAGCCTATCAAGCACTCAACCTCACCAGTCCCGACAGAA
 CCTAGTAAAAGGAGCCTATCAAGCACTCAACCTCACCAGTCCCGACAGAA

Bxv1
 BALB/c XMLV
 CCCAAGAGTGCTGGCTGTGTCTGGTATCGGGACCCCCCTACTACGAAGGG
 CCCAAGAGTGCTGGCTGTGTCTGGTATCGGGACCCCCCTACTACGAAGGG

Bxv1
 BALB/c XMLV
 GTTGCCGTCTAGGTACCTACTCCAACCATACTCTGCCCCAGCTAACTG
 GTTGCCGTCTAGGTACCTACTCCAACCATACTCTGCCCCAGCTAACTG

Bxv1
 BALB/c XMLV
 CTCCGTGGCCTCCCAACACAAGCTGACCCTGTCCGAAGTGACCGGGCAGG
 CTCCGTGGCCTCCCAACACAAGCTGACCCTGTCCGAAGTGACCGGGCAGG

Bxv1
 BALB/c XMLV
 GACTCTGCGTAGGAGCAGTTCCCAAAAACCCATCAGGCCCTGTGTAATACC
 GACTCTGCGTAGGAGCAGTTCCCAAAAACCCATCAGGCCCTGTGTAATACC

Bxv1
 BALB/c XMLV
 ACCCAGAAGGCGAGCGACGGGTCTACTATCTGGCTGCTCCCGCCGGGAC
 ACCCAGAAGGCGAGCGACGGGTCTACTATCTGGCTGCTCCCGCCGGGAC

Bxv1
 BALB/c XMLV
 CATCTGGGCTTGCAACACCGGGCTCACTCCCTGCCATCTACCCTGTAC
 CATCTGGGCTTGCAACACCGGGCTCACTCCCTGCCATCTACCCTGTAC

Bxv1
 BALB/c XMLV
 TCAACCTCACCACCGATTACTGTGTCTGGTTGAGCTCTGGCCAAAGGTG
 TCAACCTCACCACCGATTACTGTGTCTGGTTGAGCTCTGGCCAAAGGTG

Bxv1
 BALB/c XMLV
 ACCTACCACTCCCCTGGTTATGTTTATGACCAGTTTGAGAGAAAAACCAA
 ACCTACCACTCCCCTGGTTATGTTTATGACCAGTTTGAGAGAAAAACCAA

Bxv1
 BALB/c XMLV
 ATATAAAAGAGAGCCGGTGTCACTAACTCTGGCCCTGCTGTTGGGAGGAC
 ATATAAAAGAGAGCCGGTGTCACTAACTCTGGCCCTGCTGTTGGGAGGAC

Bxv1
 BALB/c XMLV
 TTACTATGGGCGGCATAGCTGCAGGAGTAGGAACAGGGACTACAGCCCTA
 TTACTATGGGCGGCATAGCTGCAGGAGTAGGAACAGGGACTACAGCCCTA

Bxv1
 BALB/c XMLV
 GTGGCCACCAAACAATTTCGAGCAGCTCCAGGCAGCCATACATACAGACCT
 GTGGCCACCAAACAATTTCGAGCAGCTCCAGGCAGCCATACATACAGACCT

Bxv1
 BALB/c XMLV
 TGGGGCCTTAGAAAAATCAGTCAGTGCCCTAGAAAAGTCTCTGACCTCGT
 TGGGGCCTTAGAAAAATCAGTCAGTGCCCTAGAAAAGTCTCTGACCTCGT

Bxv1
 BALB/c XMLV
 TGTCTGAGGTGGTCCCTACAGAACCGGAGAGGATTAGATCTGCTGTTCCCTA
 TGTCTGAGGTGGTCCCTACAGAACCGGAGAGGATTAGATCTGCTGTTCCCTA

Bxv1
 BALB/c XMLV
 AAAGAAGGAGGATTATGTGCTGCCCTAAAAGAAGAATGCTGTTTCTATGC
 AAAGAAGGAGGATTATGTGCTGCCCTAAAAGAAGAATGCTGTTTCTATGC

Bxv1
 BALB/c XMLV
 AGACCACACTGGCGTAGTAAGGGATAGCATGGCTAAGCTAAGAGAAAGGC
 AGACCACACTGGCGTAGTAAGGGATAGCATGGCTAAGCTAAGAGAAAGGC

Bxv1
 BALB/c XMLV
 TAAACCAGAGGCCAAAAATTGTTTCGAATCAGGACAAGGGTGGTTTGAGGGA
 TAAACCAGAGGCCAAAAATTGTTTCGAATCAGGACAAGGGTGGTTTGAGGGA

Bxv1
 BALB/c XMLV
 CTGTTTAAACAGGTCCCCATGGTTCACGACCCTGATATCCACCATATGGG
 CTGTTTAAACAGGTCCCCATGGTTCACGACCCTGATATCCACCATATGGG

Bxv1
 BALB/c XMLV
 CCCTCTGATAGTACTTTTATTAATCCTACTCCTCGGACCCTGCATTCTCA
 CCCTCTGATAGTACTTTTATTAATCCTACTCCTCGGACCCTGCATTCTCA

Bxv1
 BALB/c XMLV
 ACCGCTTGGTCCAGTTTGTAAAAGACAGAATTTTCGGTGGTGCAGGCCCTG
 ACCGCTTGGTCCAGTTTGTAAAAGACAGAATTTTCGGTGGTGCAGGCCCTG

Bxv1
 BALB/c XMLV
 GTTCTGACCCAACAGTATCACCAACTCAAATCAATAGATCCAGAAGAAGT
 GTTCTGACCCAACAGTATCACCAACTCAAATCAATAGATCCAGAAGAAGT

Bxv1
 BALB/c XMLV
 AGAATCGCGTGAATAAAAAGATTTTATTCAGTTTCCAGAAAGAGGGGGGAA
 AGAATCGCGTGAATAAAAAGATTTTATTCAGTTTCCAGAAAGAGGGGGGAA

Bxv1
 BALB/c XMLV
 TGAAAGACCCCACCATAAAGGCTTAGCAAGCTAGCTGCAGTAACGCCATTT
 TGAAAGACCCCACCATAAAGGCTTAGCAAGCTAGCTGCAGTAACGCCATTT

Bxv1
 BALB/c XMLV
 TGCAAGGCATGAAAAAGTACCAGAGCTGAGTTCTCAAAGTCAACAAGGAA
 TGCAAGGCATGAAAAAGTACCAGAGCTGAGTTCTCAAAGTCAACAAGGAA

Bxv1
 BALB/c XMLV
 GTTTAGTTAAAGAATAAAGGCTGAACAAAACCTGGGACAGGGGCCAAACAGG
 GTTTAGTTAAAGAATAAAGGCTGAACAAAACCTGGGACAGGGGCCAAACAGG

Bxv1
 BALB/c XMLV
 ATATCTGTGGTTCGAGCACCTGGGCCCCGGCTCAGGGCCAAGAACAGATGG
 ATATCTGTGGTTCGAGCACCTGGGCCCCGGCTCAGGGCCAAGAACAGATGG

Bxv1
 BALB/c XMLV
 TACTCAGATAAAAGCGAAACTAGCAACAGTTTCTGGAAAGTCCCACCTCAG
 TACTCAGATAAAAGCGAAACTAGCAACAGTTTCTGGAAAGTCCCACCTCAG

Bxv1
 BALB/c XMLV
 TTTCAAGTTCCCCAAAAGACCGGGAAAAACCCAAGCCTTATTTAAACTA
 TTTCAAGTTCCCCAAAAGACCGGGAAAAACCCAAGCCTTATTTAAACTA

Bxv1
 BALB/c XMLV
 ACCAATCAGCTCGCTTCTCGCTTCTGTAAACCGCGCTTTTTGCTCCCCAGC
 ACCAATCAGCTCGCTTCTCGCTTCTGTAAACCGCGCTTTTTGCTCCCCAGC

Bxv1
 BALB/c XMLV
 CCTATAAAAAGGGTAAAAACCCCACTCGGTGCGCCAGTCATCCGATAG
 CCTATAAAAAGGGTAAAAACCCCACTCGGTGCGCCAGTCATCCGATAG

Bxv1
 BALB/c XMLV
 ACTGAGTCGCCCGGGTACCCGTGTTCCCAATAAAGC
 ACTGAGTCGCCCGGGTACCCGTGTTCCCAATAAAGC

Appendix 3: Virus Sequence from NSG explants (*gag/pol* region) compared with endogenous PMLV like MLV (murine chromosome 13, accession no. 154849.2) *Bxv1* (accession no.AC115959.17) and Mo MLV (accession no. JO2255.1).

NSG *gag/pol*
 PMLV
Bxv1
 Mo MLV
 TCTTTTGTGTCAGAACGGCAATGGCTGCTACCATCCGTAGGCAAGGGGGCCA
 TCTTTTGTGTCAGAACGGCAATGGCTGCTACCATCCGTAGGCAAGGGGGCCA
 TCTTTTGTGTCAGAACGGCAATGGCTGCTACCATCCGTAGGCAAGGGGGCCA
 TCCTTTGTGTCAGTACGGCAATGGCTGCTACCATCCGTAGGCAAGGGGGCCA
 ** *****

NSG *gag/pol*
 PMLV
Bxv1
 Mo MLV
 CCCAGCTGCCACTGGGTCTAGCTTTTTGGACAGGTAGGCCACCGGCCGAC
 CCCAGCTGCCACTGGGTCTAGCTTTTTGGACAGGTAGGCCACCGGCCGAC
 CCCGGCTGCCACTGGGTCTAGCTTTTTGGACAGGTAGGCCACAGGCCGAC
 CCCAGCTGCTACTGGGTCTAGCTTTTTGGACAGGTAGGCCACCGGCCGAC
 *** *****

NSG *gag/pol*
 PMLV
Bxv1
 Mo MLV
 GCCAAGGTCCCAGTTTTTTGCGTTAGGACGCCTTTGGCGTAGCCCTGCCTTC
 GCCAAGGTCCCAGTTTTTTGCGTTAGGACGCCTTTGGCGTAGCCCTGCCTTC
 GCCAAGGTCCCAGTTTTTTGCGTTAGGACGCCTTTGGCGTAGCCCTGCCTTC
 GCCAAGGTCCCAGTTTTTTGCGTTAGGACACCTTTGGCGTAGCCCTGCCTTC

NSG *gag/pol*
 PMLV
Bxv1
 Mo MLV
 TCGTCGACAAAGAGTTCAAAGGGCTTAGTCAAATCTGGCAATCCCAGGGC
 TCGTCGACAAAGAGTTCAAAGGGCTTAGTCAAATCTGGCAATCCCAGGGC
 TCGTCGACAAAGAGTTCAAAGGGCTTAGTCAAATCTGGCAATCCCAGGGC
 TCGTCGACAAAGAGTTCAAAGGGCTTAGTCAAATCTGGCAACCCCAGGGC

NSG *gag/pol*
 PMLV
Bxv1
 Mo MLV
 TGGGGCAGTTAGAAGAGCCTGTTTGATTTCTTGATAGGCCTTTTGCTGGT
 TGGGGCAGTTAGAAGAGCCTGTTTGATTTCTTGATAGGCCTTTTGCTGGT
 GGGGGCAGTTAGAAGGGCCTGTTTGATTTCTTGATAGGCCTTTTGCTGGT
 TGGGGCAGTTAGAAGAGCCTGCTTGATTTCTTGATAGGCCTTTTGTTGGT
 ***** **

NSG *gag/pol*
 PMLV
Bxv1
 Mo MLV
 CTGGGCCCCAATTAAACAGAGTCCCCGTTTTGGTGAGAGGGTACAAGGGG
 CTGGGCCCCAATTAAACAGAGTCCCCGTTTTGGTGAGAGGGTACAAGGGG
 CTGGGCCCCAATTAAACAGAGTCCCCGTTTTGGTAAGAGGATACAAGGGG
 CTGGGCCCCAATTAAACAGAGTCCCCGTTTTGGTGAGAGGGTACAAGGGG

NSG *gag/pol* GCTGCCATTTCTGCAAACCCAGGGATCCAGAGGCGACAGAAGCCTGCCGT
 PMLV GCTGCCATTTCTGCAAACCCAGGGATCCAGAGGCGACAGAAGCCTGCCGT
 Bxv1 GCCGCCATTTCCGCAAACCCAGGGATCCAGAGGCGGCAGAAGCCTGCCGT
 Mo MLV GCTGCCATTTCTGCAAACCCAGGGATCCAGAGGCGACAGAAGCCTGCCGT
 ** *****

NSG *gag/pol* CTCTAGGAACTCCCTTAGTTGTCGAGGGGTCTTCGGAGTAGGCTGCCCCA
 PMLV CCCTAGGAACTCCCTTAGTTGTCGAGGGGTCTTCGGAGTAGGCTGCCCCA
 Bxv1 CCCTAGGAACTCCCTTAGTTGTCGAGGAGTCTTTGGAACGGGTGCCCCA
 Mo MLV CCCTAGGAACTCCCTTAGTTGTCGAGGGGTCTTCGGAGTAGGCTGCCCCA
 * ***** **

NSG *gag/pol* TCACAGTCTCTTTTCTGGCCTCAGTCAGCCATCTCTGACCCTCTTTTAGA
 PMLV TCACAGTCTCTTTTCTGGCCTCAGTCAGCCATCTCTGACCCTCTTTTAGA
 Bxv1 TCACAGTCTCTTTTCTAGCCTCAGTCAGCCATCTCTGACCCTCCCTCAGA
 Mo MLV TCACAGTCTCTTTTCTGGCCTCAGTCAGCCATCTCTGACCCTCTTTTAGA
 ***** *

NSG *gag/pol* AGATACCCAGATACTTGACCTGTTTCTGGCAAATTTGGGCTTTCTTGCC
 PMLV AGATACCCAGATACTTGACCTGTTTCTGGCAAATTTGGGCTTTCTTGCC
 Bxv1 AGGTACCCAGGTATTTAACCTGTTTCTGGCAGATTTGGGCTTTCTTGCC
 Mo MLV AGATACCCAGATACTTGACCTGTTTCTGGCAAATTTGGGCTTTCTTGCC
 ** ***** **

NSG *gag/pol* CGAGGCCCGATACCCGAGGTCCCCTAGGGTTTGTAACAGGGCCCGAGTAC
 PMLV CGAGGCCCGATACCCGAGGTCCCCTAGGGTTTGTAACAGGGCCCGAGTAC
 Bxv1 CGAGGCCCGGTATCCGAGGTCCCCTAGGGTTTGTAAGGGCCCGAGTAC
 Mo MLV CGAGGCCCGATACCCGAGGTCCCCTAGGGTTTGTAACAGGGCCCGAGTAC
 ***** **

NSG *gag/pol* CTTGTTGGCAGTCGAGTCAGAAGTGGCGCCAGCAGTAAGTCATCCACG
 PMLV CTTGTTGGCAGTCGAGTCAGAAGTGGCGCCAGCAGTAAGTCATCCACG
 Bxv1 CTTGTTGGCAGTCTAGTTCGGAAGTAGCGGCCAGCAGTAAGTCATCCACG
 Mo MLV CTTGTTGGCAGTCTAGTTCAGAAGTGGCGCCAGCAGTAAGTCATCCACG
 ***** **

NSG *gag/pol* TACTGTAGCAGGATCAAGTCTGGGTGCTGGATCCGGAAGCTGCTAGGTC
 PMLV TACTGTAGCAGGATCAAGTCTGGGTGCTGGATCCGGAAGCTGCTAGGTC
 Bxv1 TACTGTAGCAGGATCAAGTCTGGGTGCTGGATCCGGAAGCTGCTAGGTC
 Mo MLV TACTGTAGCAGGATCAAGTCTGGGTGCTGGATCCGGAAGCTGCTAGGTC

NSG *gag/pol* TCTGTGCAGTGCCTCATCAAACAGGGTGGGACTGTTTTGAAACCCGTG
 PMLV TCTGTGCAGTGCCTCATCAAACAGGGTGGGACTGTTTTGAAACCCGTG
 Bxv1 TCTGTGCAATGCCTCATCAAACAGGGTGGGACTGTTTTGAAACCCGTG
 Mo MLV TCTGTGCAGTGCCTCATCAAACAGGGTGGGACTGTTTTGAAACCCGTG

NSG *gag/pol* GGAGTCTGGTCCAGGTTAATTGTCTGAGATTCCCATCTCTGGGTCTCTC
 PMLV GGAGTCTGGTCCAGGTTAATTGTCTGAGATTCCCATCTCTGGGTCTCTC
 Bxv1 GGAGTCTGGTCCAGGTTAATTGTCCAGAGATTCCCATTTCTGGATCTCTC
 Mo MLV GGAGTCTGGTCCAGGTTAATTGTCTGAGATTCCCATCTCTGGATCTCTC

NSG *gag/pol* CACTCAAAGGCGAAGAGAGGCTGACTGGTGGGGTGGAGTCTCAGGCAGAA
 PMLV CACTCAAAGGCGAAGAGAGGCTGACTGGTGGGGTGGAGTCTCAGGCAGAA
 Bxv1 CACTCAAAGGCGAAGAGAGGCTGACTGGTGGGGTGGAGTCTCAGGCAGAA
 Mo MLV CACTCAAAGGCGAAGAGAGGCTGACTGGTGGGGTGGAGTCTCAGGCAGAA

NSG *gag/pol* AAAGGCATCCTTTAAGTCAAGCACAGTGTACCCTGGTGGGACGGTGGGA
 PMLV AAAGGCATCCTTTAAGTCAAGCACAGTGTACCCTGGTGGGACGGTGGGA
 Bxv1 AAAGGCATCTTTTAAATCAAGCACAGTGTACCCTGGTGGGACGGAGGGA
 Mo MLV AAAGGCATCCTTTAATCAAGCACAGTGTACCCTGGTGGGACGGTGGGA

```
NSG gag/pol      GCCCGCTCAAGAGGTTGTAAGGGTTGGGCACGGTGGGGTGGATGTCTTCC
PMLV             GCCCGCTCAAGAGGTTGTAAGGGTTGGGCACGGTGGGGTGGATGTCTTCC
Bxv1            GTCCACTTAAGAGGTTGTAAGGATTGGGCACGGTGGGGTGGATATCTTCC
Mo MLV          GCCCGCTCAAGAGGTTGTAAGGGTTGGGCACGGTGGGGTGGATGTCTTCC
* * * * *      *****
```

```
NSG gag/pol      ACCCGCTTGTTGACTTCTCTCAGATCC
PMLV             ACCCGCTTGTTGACTTCTCTCAGATCC
Bxv1            ACCCGCTTGTTGACTTCTCTCAGATCC
Mo MLV          ACCCGCTTGTTGACTTCTCTCAGATCC
*****
```


Appendix 4: Virus Sequence from NSG explants (LTR region) compared with endogenous PMLV like MLV (murine chromosome 13, accession no. 154849.2) *Bxv1* (accession no.AC115959.17) and Mo MLV (accession no. JO2255.1).

```

NSG LTR      CCAAC----TCAAATCAATAGATCCAGAAGAAGTGGAATCACGTGAATAA
PMLV         CCAAC----TCAAATCAATAGATCCAGAAGAAGTGGAATCACGTGAATAA
Bxv1       CCAAC----TCAAATCAATAGATCCAGAAGAAGTAGAATCGCGTGAATAA
Mo MLV       ATCACCAGCTGAAGCCTATAGA-----GTACGAGCCATAGATAAAAATAA
              **      * ** * *****          * *      **          *****

NSG LTR      AAGATTTTATTTCAGTTTCCAGAAAAGAGGGGGGAATGAAAAGACCCCACCAT
PMLV         AAGATTTTATTTCAGTTTCCAGAAAAGAGGGGGGAATGAAAAGACCCCACCAT
Bxv1       AAGATTTTATTTCAGTTTCCAGAAAAGAGGGGGGAATGAAAAGACCCCACCAT
Mo MLV       AAGATTTTATTTCAGTTTCCAGAAAAGAGGGGGGAATGAAAAGACCCCACCTG
              ***** ** * ***** *****

NSG LTR      CAGGCTTAGCAAGCTAGCTGCAGTAACGCCATTTTGCAAGGCATGAAAAA
PMLV         CAGGCTTAGCAAGCTAGCTGCAGTAACGCCATTTTGCAAGGCATGAAAAA
Bxv1       AAGGCTTAGCAAGCTAGCTGCAGTAACGCCATTTTGCAAGGCATGAAAAA
Mo MLV       TAGGTTTGGCAAGCTAGCTTAAGTAACGCCATTTTGCAAGGCATGGAAAA
              *** * ***** *****

NSG LTR      GTACCAGAGCTGAGTTCTCAAAAAGTTACAAGAAAGTTCAGTTAAAAATTA
PMLV         GTACCAGAGCTGAGTTCTCAAAAAGTTACAAGAAAGTTCAGTTAAAGATTA
Bxv1       GTACCAGAGCTGAGTTCTCAAAAAGTACAAGGAAGTTTAGTTAA-----
Mo MLV       ATAC-ATAACTGAGAATAGAG-----AAGTTCAGATCAAGGTCA
              *** * * *****          *          ***** * * *

NSG LTR      ACAGTTAAAGATT--AAGGCTGAATAATACTGGGACAGGGGCCAA-----
PMLV         ACAGTTAAAGATT--AAGGCTGAATAATACTGGGACAGGGGCCAA-----
Bxv1       -----AGAAT--AAGGCTGAACAAAACCTGGGACAGGGGCCAAACAGG
Mo MLV       GGAAC---AGATGGAACAGCTGAATA----TGGGCCAA--ACAGG-----
              ***      * ***** *          *** **      *

NSG LTR      ATATCGGTGGTCAAGCACCT--GGGCCCCGGCTCAGGGCCAAGAACAGATG
PMLV         ATATCGGTGGTCAAGCACCT--GGGCCCCGGCTCAGGGCCAAGAACAGATG
Bxv1       ATATCTGTGGTTCGAGCACCT--GGGCCCCGGCTCAGGGCCAAGAACAGATG
Mo MLV       ATATCTGTGGT--AAGCAGTTCTGCCCCGGCTCAGGGCCAAGAACAGATG
              ***** ***** ***** * *****

NSG LTR      GCTCTCAGACGTCAGTGTTAGCAGAACTAGCTTCACTGATTTAGAAAAAT
PMLV         GCTCTCAGACGTCAGTGTTAGCAGAACTAGCTTCACTGATTTAGAAAAAT
Bxv1       GTACTIONAGATA-----AAGCGAAACTAGCA-----
Mo MLV       GAAC--AGCT--GAATATGGGCCAAACA--GGA-----TATC
              * * **          ** *** *

NSG LTR      AGAGGTGCACAGTGCTCTGGCCACTCCTTGAACCTGTGTGTCTGCCAATG
PMLV         AGAGGTGCACAGTGCTCTGGCCACTCCTTGAACCTGTGTGTCTGCCAATG
Bxv1       -----ACAG-----
Mo MLV       TGTGGTAAGCAGTTC-C-TGCCCCGGCTC-----AGGGCCAA--
              ***

NSG LTR      TTCTGACCAGGTGTGTGCCCATTTGTTGAACCTTCATTAGACCCCTTTCCTC
PMLV         TTCTGACCAGGTGTGTGCCCATTTGTTGAACCTTCATTAGACCCCTTTCCTC
Bxv1       -----
Mo MLV       ----GAACAGATG-GTCCCA-----GATGCGGTCC--

NSG LTR      GTACCCCTCCCATAACCCATTTCTTGAAAATAGACATTTGTTTAAACTAAA
PMLV         GTACCCCTCCCATAACCCATTTCTTGAAAATAGACATTTGTTTAAACTAAA
Bxv1       -----TTTCTGGAAAG-TCCACC-----TC
Mo MLV       --AGCCCT----CAGCAGTTTCTAGAGAAC---CAT----CAG-----
              ***** ** *          **

```

```

NSG LTR      AAGTCCCACCTCAGTTTCCCCAAATGACCGAGAAATACCCCAAGCCTTAT
PMLV         AAGTCCCACCTCAGTTTCCCCAAATGACCGAGAAATACCCCAAGCCTTAT
Bxv1        A-GTTT-----CAAGTTCCCCAAAAGACCGGGAAAAACCCCAAGCCTTAT
Mo MLV       ATGTTT----CCAGGGTGCCCCAAGGACCTGAAATGACCTGTGCCTTAT
*  * *           * *   *  * * * * * * * * * * * * * * * *

```

```

NSG LTR      TCGAACTAACCAACCAGCTCGCTTCTCGCTTCTGTAACCGCGCTTTTTGC
PMLV         TCGAACTAACCAACCAGCTCGCTTCTCGCTTCTGTAACCGCGCTTTTTGC
Bxv1        TTAAACTAACCAATCAGCTCGCTTCTCGCTTCTGTAACC-----
Mo MLV       TTGAACTAACCAATCAGTTCGCTTCTCGCTTCTGTTTCGCGCGCTTC-TGC
*  * * * * * * * * * * * * * * * * * * * * * * * * * * * *

```

```

NSG LTR      TCCC-CAG
PMLV         TCCC-CAG
Bxv1        -----GC
Mo MLV       TCCCCGAG

```

Appendix 5: List of differentially expressed genes

Raji cells up regulated FC ≥1.5					
SYMBOL	ENTREZ GENE NAME	LOCATION	TYPE(S)	P-VALUE	FOLD CHANGE
IFI44	interferon-induced protein 44	Cytoplasm	other	1.12E-04	5.13
CCL4	chemokine (C-C motif) ligand 4	Extracellular Space	cytokine	1.59E-03	2.99
VTRNA1-1	vault RNA 1-1	Other	other	1.27E-02	2.86
IFI44L	interferon-induced protein 44-like	Other	other	2.66E-04	2.58
CCL4L1/CCL4L2	chemokine (C-C motif) ligand 4-like 1	Plasma Membrane	other	5.30E-04	2.47
CCL3L1/CCL3L3	chemokine (C-C motif) ligand 3-like 1	Plasma Membrane	other	8.33E-04	2.40
CCNB1	cyclin B1	Cytoplasm	kinase	5.25E-04	2.37
MIR4254	microRNA 4254	Cytoplasm	microRNA	1.57E-02	2.22
GMFG	glia maturation factor, gamma	Cytoplasm	growth factor	2.25E-03	2.11
UBE2T	ubiquitin-conjugating enzyme E2T (putative)	Nucleus	enzyme	1.90E-05	2.09
MIR548	microRNA 548c	Cytoplasm	microRNA	1.64E-02	2.07
C17orf78	chromosome 17 open reading frame 78	Other	other	9.21E-03	2.01
LOC100287704/LOC100287834	uncharacterized LOC100287704	Other	other	1.26E-02	1.95
MELK	maternal embryonic leucine zipper kinase	Cytoplasm	kinase	3.55E-04	1.92
CENPI	centromere protein I	Nucleus	other	7.55E-03	1.89
DEFB122	defensin, beta 122 (pseudogene)	Other	other	2.63E-02	1.89
FAM83D	family with sequence similarity 83, member D	Other	other	1.68E-02	1.89
ZNF826P	zinc finger protein 826, pseudogene	Other	other	7.35E-03	1.87
SNORA70E	small nucleolar RNA, H/ACA box 70E	Other	other	2.28E-02	1.87
POLH	polymerase (DNA directed), eta	Nucleus	enzyme	1.66E-03	1.85
CDC6	cell division cycle 6	Nucleus	other	2.45E-03	1.84
SLC9C2	solute carrier family 9, member C2 (putative)	Other	other	7.08E-03	1.83
CCNB2	cyclin B2	Cytoplasm	other	1.92E-04	1.83
PLK1	polo-like kinase 1	Nucleus	kinase	1.63E-02	1.82
SPAG5	sperm associated antigen 5	Nucleus	peptidase	2.58E-03	1.82
CDC25C	cell division cycle 25C	Nucleus	phosphatase	3.11E-02	1.81
GINS2	GINS complex subunit 2 (Psf2 homolog)	Nucleus	other	8.26E-03	1.81
HSD17B7	hydroxysteroid (17-beta) dehydrogenase 7	Cytoplasm	enzyme	4.71E-03	1.78
ERH	enhancer of rudimentary homolog (Drosophila)	Nucleus	other	8.77E-04	1.77
TNF	tumor necrosis factor	Extracellular Space	cytokine	6.19E-03	1.74
KIF20A	kinesin family member 20A	Cytoplasm	transporter	3.10E-03	1.74
PSMB6	proteasome (prosome, macropain) subunit, beta type, 6	Other	peptidase	7.69E-03	1.74
OR4D11	olfactory receptor, family 4, subfamily D, member 11	Plasma Membrane	G-protein coupled receptor	2.10E-02	1.73
DEFB119	defensin, beta 119	Extracellular Space	other	1.07E-02	1.72
AURKB	aurora kinase B	Nucleus	kinase	2.01E-02	1.72
CKS2	CDC28 protein kinase regulatory subunit 2	Other	kinase	2.10E-03	1.72
FANCD2	Fanconi anemia, complementation group D2	Nucleus	other	4.75E-04	1.72
MIR2909	microRNA 2909	Cytoplasm	microRNA	1.72E-02	1.72
MIR154/MIR382	microRNA 494	Cytoplasm	microRNA	4.17E-02	1.71
GINS1	GINS complex subunit 1 (Psf1 homolog)	Nucleus	other	1.56E-03	1.70
IGLL3P	immunoglobulin lambda-like polypeptide 3, pseudogene	Other	other	2.00E-02	1.69
CDK1	cyclin-dependent kinase 1	Nucleus	kinase	1.87E-04	1.69

DEFB121	defensin, beta 121	Extracellular Space	other	6.91E-03	1.69
OR1A2	olfactory receptor, family 1, subfamily A, member 2	Plasma Membrane	G-protein coupled receptor	1.45E-02	1.69
NCAPH	non-SMC condensin I complex, subunit H	Nucleus	other	3.98E-03	1.69
AURKA	aurora kinase A	Nucleus	kinase	6.73E-03	1.68
DEPDC1B	DEP domain containing 1B	Cytoplasm	other	1.07E-03	1.68
SPC25	SPC25, NDC80 kinetochore complex component	Cytoplasm	other	1.76E-03	1.68
PSMB3	proteasome (prosome, macropain) subunit, beta type, 3	Cytoplasm	peptidase	4.04E-03	1.68
DEFB123	defensin, beta 123	Extracellular Space	other	8.13E-03	1.65
MIR548/MIR603	microRNA 548c	Cytoplasm	microRNA	1.94E-03	1.65
EME1	essential meiotic structure-specific endonuclease 1	Nucleus	other	2.30E-02	1.65
DIAPH3	diaphanous-related formin 3	Cytoplasm	enzyme	1.59E-02	1.65
FBXL7	F-box and leucine-rich repeat protein 7	Cytoplasm	enzyme	3.03E-02	1.64
CDC20	cell division cycle 20	Nucleus	other	1.00E-02	1.64
USP51	ubiquitin specific peptidase 51	Other	peptidase	3.42E-02	1.64
KNSTRN/C15orf23	kinetochore-localized astrin/SPAG5 binding protein	Cytoplasm	other	3.11E-02	1.63
UBE2C	ubiquitin-conjugating enzyme E2C	Cytoplasm	enzyme	1.96E-03	1.63
KIAA0101	KIAA0101	Nucleus	other	1.42E-03	1.63
TPX2	TPX2, microtubule-associated	Nucleus	other	1.84E-04	1.62
PSMD8	proteasome (prosome, macropain) 26S subunit, non-ATPase, 8	Cytoplasm	other	1.85E-02	1.62
TROAP	trophinin associated protein	Cytoplasm	peptidase	2.53E-03	1.62
CEP55	centrosomal protein 55kDa	Cytoplasm	other	8.45E-03	1.62
CDCA8	cell division cycle associated 8	Nucleus	other	8.47E-03	1.62
MANF	mesencephalic astrocyte-derived neurotrophic factor	Extracellular Space	other	4.55E-04	1.62
PRC1	protein regulator of cytokinesis 1	Nucleus	other	1.24E-03	1.61
KRT76	keratin 76	Cytoplasm	other	3.62E-02	1.60
SNORD53	small nucleolar RNA, C/D box 53	Other	other	3.97E-03	1.60
NUSAP1	nucleolar and spindle associated protein 1	Nucleus	other	9.39E-04	1.60
ANXA2P2	annexin A2 pseudogene 2	Other	other	2.88E-02	1.60
BNIP2	BCL2/adenovirus E1B 19kDa interacting protein 2	Cytoplasm	other	1.80E-02	1.59
RGR	retinal G protein coupled receptor	Plasma Membrane	G-protein coupled receptor	3.12E-02	1.59
BCAS4	breast carcinoma amplified sequence 4	Cytoplasm	other	3.03E-02	1.59
RAPGEF4-AS1	RAPGEF4 antisense RNA 1	Other	other	2.56E-04	1.59
SGOL2	shugoshin-like 2 (S. pombe)	Nucleus	other	5.59E-03	1.59
SNORA49	small nucleolar RNA, H/ACA box 49	Other	other	4.45E-02	1.58
THSD1	thrombospondin, type I, domain containing 1	Extracellular Space	other	3.33E-02	1.58
NUF2	NUF2, NDC80 kinetochore complex component	Nucleus	other	2.75E-03	1.58
MIR150	microRNA 150	Other	microRNA	3.18E-03	1.58
NQO2	NAD(P)H dehydrogenase, quinone 2	Cytoplasm	enzyme	1.65E-02	1.57
NDUFB10	NADH dehydrogenase (ubiquinone) 1 beta subcomplex, 10, 22kDa	Cytoplasm	enzyme	6.81E-03	1.57
CENPW	centromere protein W	Nucleus	other	1.92E-02	1.57
ORC6	origin recognition complex, subunit 6	Nucleus	other	5.68E-04	1.57
SNORD78	small nucleolar RNA, C/D box 78	Other	other	1.89E-03	1.57
CEP128	centrosomal protein 128kDa	Cytoplasm	other	4.60E-03	1.57
DLGAP5	discs, large (Drosophila) homolog-associated protein 5	Nucleus	phosphatase	2.66E-04	1.56

LRRCC1	leucine rich repeat and coiled-coil centrosomal protein 1	Nucleus	transporter	4.55E-02	1.56
MAPT-IT1	MAPT intronic transcript 1 (non-protein coding)	Other	other	3.07E-02	1.56
C3orf36	chromosome 3 open reading frame 36	Other	other	2.23E-04	1.55
GLA	galactosidase, alpha	Cytoplasm	enzyme	4.15E-02	1.55
OR5B21	olfactory receptor, family 5, subfamily B, member 21	Plasma Membrane	G-protein coupled receptor	4.67E-02	1.55
HMGCR	3-hydroxy-3-methylglutaryl-CoA reductase	Cytoplasm	enzyme	2.18E-03	1.55
LOC81691	exonuclease NEF-sp	Nucleus	enzyme	1.01E-02	1.55
LOC400682	zinc finger protein 100-like	Other	other	3.59E-02	1.55
F8A1 (includes others)	coagulation factor VIII-associated 1	Nucleus	other	1.04E-02	1.54
AUNIP	aurora kinase A and ninein interacting protein	Cytoplasm	other	6.28E-03	1.53
CLIC1	chloride intracellular channel 1	Nucleus	ion channel	2.45E-03	1.53
SOX2-OT	SOX2 overlapping transcript (non-protein coding)	Other	other	1.87E-02	1.53
TPRX1	tetra-peptide repeat homeobox 1	Other	other	2.78E-02	1.52
PRDX1	peroxiredoxin 1	Cytoplasm	enzyme	9.85E-03	1.52
RAB4B	RAB4B, member RAS oncogene family	Plasma Membrane	enzyme	1.15E-02	1.52
ESRRA	estrogen-related receptor alpha	Nucleus	ligand-dependent nuclear receptor	8.96E-03	1.52
ODF2	outer dense fiber of sperm tails 2	Cytoplasm	other	1.25E-02	1.52
MCM8	minichromosome maintenance complex component 8	Nucleus	enzyme	3.40E-03	1.51
MIR345	microRNA 345	Cytoplasm	microRNA	4.01E-02	1.51
KIFC1	kinesin family member C1	Nucleus	enzyme	1.86E-02	1.51
GBP3	guanylate binding protein 3	Other	enzyme	1.79E-02	1.51
LACTBL1	lactamase, beta-like 1	Other	other	1.14E-02	1.51
GDF7	growth differentiation factor 7	Extracellular Space	growth factor	2.38E-02	1.51
WNT9B	wingless-type MMTV integration site family, member 9B	Extracellular Space	other	4.67E-02	1.51
KIF20B	kinesin family member 20B	Nucleus	enzyme	1.52E-03	1.51
ACOT1	acyl-CoA thioesterase 1	Cytoplasm	enzyme	2.80E-02	1.51
TUBBP5	tubulin, beta pseudogene 5	Other	other	5.28E-03	1.50
ORC1	origin recognition complex, subunit 1	Nucleus	other	3.04E-02	1.50
FSIP2	fibrous sheath interacting protein 2	Cytoplasm	other	2.74E-02	1.50
HIST2H2BA	histone cluster 2, H2ba (pseudogene)	Other	other	2.37E-02	1.50
COX8A	cytochrome c oxidase subunit VIIIa (ubiquitous)	Cytoplasm	enzyme	1.38E-03	1.50
Raji cells down regulated FC ≥1.5					
SYMBOL	ENTREZ GENE NAME	LOCATION	TYPE(S)	P-VALUE	FOLD CHANGE
TSPAN2	tetraspanin 2	Extracellular Space	other	9.92E-03	-3.57
MIR944	microRNA 944	Cytoplasm	microRNA	1.51E-02	-2.77
PCOLCE2	procollagen C-endopeptidase enhancer 2	Extracellular Space	other	1.31E-03	-2.72
SLC30A4	solute carrier family 30 (zinc transporter), member 4	Cytoplasm	transporter	7.27E-04	-2.32
TMED10P1	transmembrane emp24-like trafficking protein 10 (yeast) pseudogene 1	Other	other	2.62E-02	-2.27
IL7R	interleukin 7 receptor	Plasma Membrane	transmembrane receptor	4.38E-02	-2.26
OR2T29/OR2T5	olfactory receptor, family 2, subfamily T, member 5	Plasma Membrane	G-protein coupled receptor	2.25E-03	-2.24
MIR1204	microRNA 1204	Cytoplasm	microRNA	1.67E-03	-2.18

OR2T3/OR2T34	olfactory receptor, family 2, subfamily T, member 34	Plasma Membrane	other	4.26E-03	-2.12
OR2T29/OR2T5	olfactory receptor, family 2, subfamily T, member 5	Plasma Membrane	G-protein coupled receptor	2.05E-03	-2.12
MIR4477A	microRNA 4477b	Cytoplasm	microRNA	9.00E-03	-2.11
SSPN	sarcospan	Plasma Membrane	other	1.84E-02	-2.03
SH2D1A	SH2 domain containing 1A	Cytoplasm	other	2.25E-02	-2.01
HIST1H2BG	histone cluster 1, H2bg	Nucleus	other	3.08E-02	-2.01
RAET1K	retinoic acid early transcript 1K pseudogene	Other	other	7.99E-04	-2.00
FLJ46066	uncharacterized LOC401103	Other	other	3.81E-02	-1.98
CEP19	centrosomal protein 19kDa	Cytoplasm	other	9.74E-04	-1.97
GADD45B	growth arrest and DNA-damage-inducible, beta	Cytoplasm	other	3.71E-03	-1.97
TNFSF4	tumor necrosis factor (ligand) superfamily, member 4	Extracellular Space	cytokine	1.06E-03	-1.95
ZNF563	zinc finger protein 563	Nucleus	other	3.36E-02	-1.95
TRIM55	tripartite motif containing 55	Cytoplasm	other	6.95E-03	-1.95
TCP11L2	t-complex 11, testis-specific-like 2	Other	other	4.79E-03	-1.93
TNFAIP6	tumor necrosis factor, alpha-induced protein 6	Extracellular Space	other	4.77E-03	-1.92
TNKS	tankyrase, TRF1-interacting ankyrin-related ADP-ribose polymerase	Nucleus	enzyme	2.32E-02	-1.91
TYW5	tRNA-yW synthesizing protein 5	Other	enzyme	9.32E-04	-1.91
CD200	CD200 molecule	Plasma Membrane	other	3.30E-02	-1.91
OR8H2	olfactory receptor, family 8, subfamily H, member 2	Plasma Membrane	G-protein coupled receptor	3.31E-02	-1.88
LINC-ROR	long intergenic non-protein coding RNA, regulator of reprogramming	Other	other	1.33E-02	-1.85
CYP39A1	cytochrome P450, family 39, subfamily A, polypeptide 1	Cytoplasm	enzyme	5.97E-03	-1.83
VCAM1	vascular cell adhesion molecule 1	Plasma Membrane	transmembrane receptor	1.22E-03	-1.83
IKZF3	IKAROS family zinc finger 3 (Aiolos)	Nucleus	transcription regulator	4.12E-03	-1.81
RNF144B	ring finger protein 144B	Other	enzyme	2.13E-04	-1.79
ATP5S	ATP synthase, H ⁺ transporting, mitochondrial Fo complex, subunit s (factor B)	Cytoplasm	transporter	1.61E-02	-1.79
TMEM242	transmembrane protein 242	Other	other	1.94E-02	-1.78
POPDC2	popeye domain containing 2	Other	other	4.04E-02	-1.77
ZMYM5	zinc finger, MYM-type 5	Nucleus	other	5.25E-04	-1.77
ZNF441	zinc finger protein 441	Nucleus	other	2.08E-02	-1.77
ZNF253	zinc finger protein 253	Nucleus	transcription regulator	9.39E-03	-1.77
HUNK	hormonally up-regulated Neu-associated kinase	Cytoplasm	kinase	7.50E-03	-1.77
ADPRH	ADP-ribosylarginine hydrolase	Other	enzyme	5.62E-04	-1.77
ABCD2	ATP-binding cassette, sub-family D (ALD), member 2	Cytoplasm	transporter	3.95E-02	-1.76
PRTFDC1	phosphoribosyl transferase domain containing 1	Cytoplasm	enzyme	1.42E-02	-1.75
TP53BP2	tumor protein p53 binding protein, 2	Nucleus	other	1.13E-02	-1.75
OLAH	oleoyl-ACP hydrolase	Other	enzyme	1.76E-03	-1.75
OR10R2	olfactory receptor, family 10, subfamily R, member 2	Plasma Membrane	other	1.68E-03	-1.75
MYB	v-myb avian myeloblastosis viral oncogene homolog	Nucleus	transcription regulator	2.27E-02	-1.74
LOC100133050	glucuronidase, beta pseudogene	Other	other	3.41E-02	-1.73
RASSF6	Ras association (RalGDS/AF-6) domain family member 6	Other	other	8.03E-04	-1.73
RSPH1	radial spoke head 1 homolog (Chlamydomonas)	Nucleus	other	2.14E-02	-1.72
RAB23	RAB23, member RAS oncogene family	Cytoplasm	enzyme	1.04E-02	-1.71

SLC41A2	solute carrier family 41 (magnesium transporter), member 2	Plasma Membrane	transporter	2.80E-04	-1.71
CHIC2	cysteine-rich hydrophobic domain 2	Plasma Membrane	other	9.76E-05	-1.70
ZNF322	zinc finger protein 322	Cytoplasm	other	2.86E-02	-1.69
TAS2R46	taste receptor, type 2, member 46	Plasma Membrane	G-protein coupled receptor	4.85E-02	-1.69
WNT5A	wingless-type MMTV integration site family, member 5A	Extracellular Space	cytokine	5.31E-03	-1.69
DCAF8	DDB1 and CUL4 associated factor 8	Other	other	1.47E-03	-1.68
SGCB	sarcoglycan, beta (43kDa dystrophin-associated glycoprotein)	Plasma Membrane	other	4.01E-03	-1.68
FBXO3	F-box protein 3	Other	enzyme	1.45E-02	-1.68
SPATA17	spermatogenesis associated 17	Other	other	6.39E-03	-1.68
SNX11	sorting nexin 11	Cytoplasm	transporter	1.79E-02	-1.67
ZNF815P	zinc finger protein 815, pseudogene	Other	other	2.43E-02	-1.67
CCT6P1	chaperonin containing TCP1, subunit 6 (zeta) pseudogene 1	Other	other	1.12E-03	-1.67
TRAT1	T cell receptor associated transmembrane adaptor 1	Plasma Membrane	kinase	1.95E-02	-1.66
CALCRL	calcitonin receptor-like	Plasma Membrane	G-protein coupled receptor	1.70E-02	-1.66
ZNF260	zinc finger protein 260	Nucleus	other	1.37E-02	-1.66
ZNF429	zinc finger protein 429	Nucleus	other	2.35E-02	-1.65
RYBP	RING1 and YY1 binding protein	Nucleus	transcription regulator	1.99E-02	-1.65
ADPRM	ADP-ribose/CDP-alcohol diphosphatase, manganese-dependent	Other	other	9.88E-03	-1.65
ZNF253	zinc finger protein 253	Nucleus	transcription regulator	3.16E-02	-1.65
MTUS2-AS2	MTUS2 antisense RNA 2	Other	other	5.24E-03	-1.65
LOC374443	C-type lectin domain family 2, member D pseudogene	Other	other	1.09E-03	-1.65
NPL	N-acetylneuraminate pyruvate lyase (dihydrodipicolinate synthase)	Other	enzyme	4.68E-04	-1.65
TXNIP	thioredoxin interacting protein	Cytoplasm	other	7.35E-03	-1.65
NR1D2	nuclear receptor subfamily 1, group D, member 2	Nucleus	ligand-dependent nuclear receptor	6.00E-03	-1.65
RANBP3L	RAN binding protein 3-like	Other	other	1.17E-02	-1.64
BAZ2B	bromodomain adjacent to zinc finger domain, 2B	Extracellular Space	other	4.51E-04	-1.64
FAM206A	family with sequence similarity 206, member A	Extracellular Space	other	2.05E-02	-1.64
HTR3B	5-hydroxytryptamine (serotonin) receptor 3B, ionotropic	Plasma Membrane	ion channel	3.46E-02	-1.64
NT5DC1	5'-nucleotidase domain containing 1	Other	other	1.19E-02	-1.64
TPRG1-AS2	TPRG1 antisense RNA 2	Other	other	1.65E-02	-1.64
FOXP1	forkhead box P1	Nucleus	other	7.13E-04	-1.63
ALPK2	alpha-kinase 2	Nucleus	kinase	4.87E-02	-1.63
TBC1D9	TBC1 domain family, member 9 (with GRAM domain)	Plasma Membrane	other	3.55E-02	-1.63
ATP2B1	ATPase, Ca ⁺⁺ transporting, plasma membrane 1	Plasma Membrane	transporter	2.86E-03	-1.63
ACBD7	acyl-CoA binding domain containing 7	Other	other	1.11E-02	-1.63
LPP-AS2	LPP antisense RNA 2	Other	other	2.68E-02	-1.63
PRDM1	PR domain containing 1, with ZNF domain	Nucleus	transcription regulator	1.87E-02	-1.63
LOC100132057	phosphodiesterase 4D interacting protein pseudogene	Other	other	3.90E-02	-1.62
COX19	cytochrome c oxidase assembly homolog 19 (S. cerevisiae)	Cytoplasm	other	9.98E-03	-1.61

RBM18	RNA binding motif protein 18	Other	other	2.52E-04	-1.61
DEFB114	defensin, beta 114	Extracellular Space	other	3.47E-02	-1.61
AURKA	aurora kinase A	Nucleus	kinase	9.86E-03	-1.61
CPEB4	cytoplasmic polyadenylation element binding protein 4	Plasma Membrane	other	1.15E-02	-1.61
PIM1	pim-1 oncogene	Cytoplasm	kinase	1.62E-02	-1.61
PCDHB8	protocadherin beta 8	Other	other	3.25E-02	-1.61
TXNL4B	thioredoxin-like 4B	Nucleus	enzyme	7.27E-04	-1.61
EPB41L5	erythrocyte membrane protein band 4.1 like 5	Plasma Membrane	other	5.28E-03	-1.60
TBC1D3P2	TBC1 domain family, member 3 pseudogene 2	Other	other	6.26E-03	-1.60
TTC32	tetratricopeptide repeat domain 32	Other	other	6.89E-03	-1.60
FAM105B/OTULIN	OTU deubiquitinase with linear linkage specificity	Cytoplasm	peptidase	1.39E-04	-1.60
TXNIP	thioredoxin interacting protein	Cytoplasm	other	2.04E-02	-1.60
SLAMF6	SLAM family member 6	Plasma Membrane	transmembrane receptor	4.03E-03	-1.60
CRYZ	crystallin, zeta (quinone reductase)	Cytoplasm	enzyme	5.54E-03	-1.60
FBXO8	F-box protein 8	Cytoplasm	other	3.73E-03	-1.60
PIEZO2	piezo-type mechanosensitive ion channel component 2	Other	ion channel	2.03E-02	-1.60
ZNF347	zinc finger protein 347	Nucleus	other	3.02E-02	-1.59
UNQ6494	uncharacterized LOC100129066	Other	other	3.61E-02	-1.59
CD59	CD59 molecule, complement regulatory protein	Plasma Membrane	other	1.84E-03	-1.59
FRRS1	ferric-chelate reductase 1	Plasma Membrane	transmembrane receptor	8.27E-03	-1.59
CLN5	ceroid-lipofuscinosis, neuronal 5	Cytoplasm	other	2.73E-03	-1.59
GDAP1	ganglioside induced differentiation associated protein 1	Cytoplasm	other	2.53E-03	-1.59
DPH3P1	diphthamide biosynthesis 3 pseudogene 1	Other	other	1.29E-02	-1.59
FCRL3	Fc receptor-like 3	Other	other	6.17E-06	-1.59
CDH12	cadherin 12, type 2 (N-cadherin 2)	Plasma Membrane	other	5.90E-04	-1.59
CREBRF	CREB3 regulatory factor	Other	other	7.37E-04	-1.59
REPS2	RALBP1 associated Eps domain containing 2	Cytoplasm	other	2.61E-02	-1.58
LOC284930	uncharacterized LOC284930	Other	other	1.28E-02	-1.58
OR7E12P	olfactory receptor, family 7, subfamily E, member 12 pseudogene	Other	other	1.06E-02	-1.58
HIST2H4B // HIST4H4 // HIST2H4A // HIST1H4L // HIST1H4E // HIST1H4B // HIST1H4H // HIST1H4C // HIST1H4J // HIST1H4K // HIST1H4F // HIST1H4D // HIST1H4A // HIST1H4I	histone cluster 1, H4a H4b H4c H4d H4e H4f H4h H4i H4j H4k H4l histone cluster 2, H4a H4b histone cluster 4, H4	Nucleus	Other	2.06E-03	-1.58
HIST2H4B // HIST4H4 // HIST2H4A // HIST1H4L // HIST1H4E // HIST1H4B // HIST1H4H // HIST1H4C // HIST1H4J // HIST1H4K // HIST1H4F // HIST1H4D // HIST1H4A // HIST1H4I	histone cluster 1, H4a H4b H4c H4d H4e H4f H4h H4i H4j H4k H4l histone cluster 2, H4a H4b histone cluster 4, H5	Nucleus	Other	2.06E-03	-1.58
KLHL42	kelch-like family member 42	Nucleus	other	2.26E-02	-1.58
KCTD3	potassium channel tetramerization domain containing 3	Other	ion channel	1.39E-02	-1.58
PHLDA1	pleckstrin homology-like domain, family A, member 1	Cytoplasm	other	4.58E-03	-1.58
DMXL2	Dmx-like 2	Cytoplasm	other	4.02E-03	-1.58
GNG2	guanine nucleotide binding protein (G protein), gamma 2	Plasma Membrane	enzyme	4.11E-02	-1.58

C16orf87	chromosome 16 open reading frame 87	Other	other	9.23E-03	-1.58
FCRL3	Fc receptor-like 3	Other	other	1.18E-02	-1.58
IL7	interleukin 7	Extracellular Space	cytokine	1.95E-02	-1.58
IKZF3	IKAROS family zinc finger 3 (Aiolos)	Nucleus	transcription regulator	5.37E-03	-1.58
CDK17	cyclin-dependent kinase 17	Cytoplasm	kinase	3.63E-02	-1.58
NUDT4P1	nudix (nucleoside diphosphate linked moiety X)-type motif 4 pseudogene 1	Other	other	4.56E-02	-1.57
ZNF480	zinc finger protein 480	Nucleus	other	2.25E-02	-1.57
ARID4A	AT rich interactive domain 4A (RBP1-like)	Nucleus	transcription regulator	1.14E-03	-1.57
SOX5	SRY (sex determining region Y)-box 5	Nucleus	transcription regulator	2.12E-02	-1.57
SQRDL	sulfide quinone reductase-like (yeast)	Cytoplasm	enzyme	4.27E-03	-1.57
MXD1	MAX dimerization protein 1	Nucleus	transcription regulator	3.69E-02	-1.57
ZDHC21	zinc finger, DHHC-type containing 21	Plasma Membrane	enzyme	3.50E-02	-1.57
ZNF724P	zinc finger protein 724, pseudogene	Other	other	7.94E-03	-1.57
GNL3	guanine nucleotide binding protein-like 3 (nucleolar)	Nucleus	other	9.86E-04	-1.57
SNORD19B	small nucleolar RNA, C/D box 19B	Other	other	9.86E-04	-1.57
FAS-AS1	FAS antisense RNA 1	Other	other	2.14E-02	-1.57
MSR1	macrophage scavenger receptor 1	Plasma Membrane	transmembrane receptor	1.89E-02	-1.56
GIN1	gypsy retrotransposon integrase 1	Other	other	4.00E-04	-1.56
FLJ38576	uncharacterized LOC651430	Other	other	4.08E-02	-1.56
LOC729291	uncharacterized LOC729291	Other	other	3.32E-02	-1.56
ZFAT	zinc finger and AT hook domain containing	Nucleus	other	3.55E-02	-1.56
RPL23AP53	ribosomal protein L23a pseudogene 53	Other	other	4.95E-02	-1.56
FBXL3	F-box and leucine-rich repeat protein 3	Nucleus	enzyme	1.20E-02	-1.55
ATAD2B	ATPase family, AAA domain containing 2B	Nucleus	other	1.49E-03	-1.55
SMG1	SMG1 phosphatidylinositol 3-kinase-related kinase	Cytoplasm	kinase	1.00E-03	-1.55
FANK1	fibronectin type III and ankyrin repeat domains 1	Nucleus	transcription regulator	1.47E-02	-1.55
PPIL4	peptidylprolyl isomerase (cyclophilin)-like 4	Nucleus	enzyme	7.61E-04	-1.55
ISCU	iron-sulfur cluster assembly enzyme	Cytoplasm	other	3.72E-03	-1.55
MIR1302	microRNA 1302-5	Cytoplasm	microRNA	4.01E-02	-1.55
C6orf62	chromosome 6 open reading frame 62	Other	other	8.24E-04	-1.54
VPS54	vacuolar protein sorting 54 homolog (S. cerevisiae)	Extracellular Space	other	2.02E-03	-1.54
CWC22	CWC22 spliceosome-associated protein homolog (S. cerevisiae)	Nucleus	other	6.42E-03	-1.54
HES1	hes family bHLH transcription factor 1	Nucleus	transcription regulator	1.50E-02	-1.54
HYDIN	HYDIN, axonemal central pair apparatus protein	Other	other	4.63E-02	-1.54
LINC00339	long intergenic non-protein coding RNA 339	Other	other	2.94E-02	-1.54
POF1B	premature ovarian failure, 1B	Plasma Membrane	other	4.08E-03	-1.54
PCMTD2	protein-L-isoaspartate (D-aspartate) O-methyltransferase domain containing 2	Cytoplasm	enzyme	5.94E-03	-1.54
KCTD7	potassium channel tetramerization domain containing 7	Other	ion channel	1.59E-02	-1.54
FLJ43681	ribosomal protein L23a pseudogene	Other	other	2.17E-02	-1.54
HS3ST3B1	heparan sulfate (glucosamine) 3-O-sulfotransferase 3B1	Cytoplasm	enzyme	8.99E-03	-1.54
FAM127B	family with sequence similarity 127, member B	Other	other	4.90E-03	-1.53
KIR2DS4 (includes others)	killer cell immunoglobulin-like receptor, two domains, short cytoplasmic tail, 4	Plasma Membrane	transmembrane receptor	4.20E-02	-1.53
BCL7A	B cell CLL/lymphoma 7A	Other	other	1.39E-02	-1.53

TRMT10B	tRNA methyltransferase 10 homolog B (S. cerevisiae)	Other	other	1.92E-02	-1.53
LOC442132	golgin A6 family-like 1 pseudogene	Other	other	4.20E-02	-1.53
ZNF639	zinc finger protein 639	Nucleus	transcription regulator	3.59E-03	-1.53
C1orf186	chromosome 1 open reading frame 186	Other	other	7.08E-04	-1.53
NEK7	NIMA-related kinase 7	Nucleus	kinase	7.22E-03	-1.53
SYCP3	synaptonemal complex protein 3	Nucleus	other	7.11E-03	-1.53
RGCC	regulator of cell cycle	Cytoplasm	other	2.97E-03	-1.53
GADD45A	growth arrest and DNA-damage-inducible, alpha	Nucleus	other	4.80E-03	-1.52
FKBP14	FK506 binding protein 14, 22 kDa	Cytoplasm	enzyme	1.16E-02	-1.52
ZNF740	zinc finger protein 740	Other	other	1.77E-02	-1.52
LOC441461	uncharacterized LOC441461	Other	other	2.00E-02	-1.52
SLC12A6	solute carrier family 12 (potassium/chloride transporter), member 6	Plasma Membrane	transporter	2.85E-02	-1.52
TYW3	tRNA-yW synthesizing protein 3 homolog (S. cerevisiae)	Other	other	6.09E-04	-1.52
ABCA1	ATP-binding cassette, sub-family A (ABC1), member 1	Plasma Membrane	transporter	2.36E-03	-1.52
SAMSN1	SAM domain, SH3 domain and nuclear localization signals 1	Nucleus	other	1.87E-02	-1.52
CYP2E1	cytochrome P450, family 2, subfamily E, polypeptide 1	Cytoplasm	enzyme	1.01E-03	-1.52
TBC1D3P1-DHX40P1	TBC1D3P1-DHX40P1 readthrough transcribed pseudogene	Other	other	2.71E-02	-1.52
SNORA46	small nucleolar RNA, H/ACA box 46	Other	other	1.10E-02	-1.52
TBCEL	tubulin folding cofactor E-like	Other	other	1.11E-03	-1.52
FAM179B	family with sequence similarity 179, member B	Extracellular Space	other	1.16E-02	-1.52
KCNJ1	potassium inwardly-rectifying channel, subfamily J, member 1	Plasma Membrane	ion channel	8.08E-03	-1.52
FAM108C1/ABHD17C	abhydrolase domain containing 17C	Other	enzyme	5.26E-03	-1.51
LRRC70	leucine rich repeat containing 70	Other	other	2.95E-02	-1.51
TAGAP	T cell activation RhoGTPase activating protein	Cytoplasm	other	4.16E-03	-1.51
CSGALNACT2	chondroitin sulfate N-acetylgalactosaminyltransferase 2	Cytoplasm	enzyme	3.89E-04	-1.51
SMAD4	SMAD family member 4	Nucleus	transcription regulator	8.83E-03	-1.51
BACE2	beta-site APP-cleaving enzyme 2	Cytoplasm	peptidase	3.26E-02	-1.51
KRTAP6-3	keratin associated protein 6-3	Other	other	1.31E-02	-1.51
R3HCC1L	R3H domain and coiled-coil containing 1-like	Other	other	2.98E-02	-1.51
OR4D5	olfactory receptor, family 4, subfamily D, member 5	Plasma Membrane	G-protein coupled receptor	1.57E-02	-1.51
PILRA	paired immunoglobulin-like type 2 receptor alpha	Plasma Membrane	other	5.81E-03	-1.50
TRA2B	transformer 2 beta homolog (Drosophila)	Nucleus	other	8.61E-03	-1.50
MICU3	mitochondrial calcium uptake family, member 3	Other	other	4.64E-02	-1.50
MCF7 cells up regulated FC ≥1.5					
SYMBOL	ENTREZ GENE NAME	LOCATION	TYPE(S)	P-VALUE	FOLD CHANGE
EGR1	early growth response 1	Nucleus	transcription regulator	2.11E-02	2.22
EGR1	early growth response 1	Nucleus	transcription regulator	2.18E-02	2.16
ZNF826P	zinc finger protein 826, pseudogene	Other	other	2.22E-03	1.76
NTRK1	neurotrophic tyrosine kinase, receptor, type 1	Plasma Membrane	kinase	5.00E-02	1.71
AGAP6 (includes others)	ArfGAP with GTPase domain, ankyrin repeat and PH domain 6	Other	other	4.98E-02	1.67
ADIRF	adipogenesis regulatory factor	Nucleus	other	4.98E-02	1.67

RNU6-83P	RNA, U6 small nuclear 83, pseudogene	Other	other	2.24E-02	1.66
IRX1	iroquois homeobox 1	Nucleus	transcription regulator	4.05E-02	1.64
ZNF600	zinc finger protein 600	Other	other	2.89E-02	1.64
MIR140	microRNA 140	Cytoplasm	microRNA	4.21E-02	1.63
FOS	FBJ murine osteosarcoma viral oncogene homolog	Nucleus	transcription regulator	1.11E-02	1.63
MRO	maestro	Nucleus	other	1.17E-02	1.57
LOC100130964	ADAM metallopeptidase domain 3A-like	Other	other	3.11E-02	1.55
TARP	TCR gamma alternate reading frame protein	Cytoplasm	other	1.51E-02	1.55
OR2V1	olfactory receptor, family 2, subfamily V, member 1	Plasma Membrane	G-protein coupled receptor	4.40E-02	1.54
SNORD108	small nucleolar RNA, C/D box 108	Other	other	2.36E-02	1.54
GBGT1	globoside alpha-1,3-N-acetylgalactosaminyltransferase 1	Other	enzyme	3.96E-02	1.54
LOC1720	dihydrofolate reductase pseudogene	Other	other	3.29E-02	1.53
SMARCD3	SWI/SNF related, matrix associated, actin dependent regulator of chromatin, subfamily d, member 3	Nucleus	transcription regulator	4.69E-03	1.53
MYOCD	myocardin	Nucleus	transcription regulator	3.17E-02	1.53
CEACAM5	carcinoembryonic antigen-related cell adhesion molecule 5	Plasma Membrane	other	6.54E-03	1.51
PAPPA	pregnancy-associated plasma protein A, pappalysin 1	Extracellular Space	peptidase	3.28E-02	1.50
PCDHB13	protocadherin beta 13	Extracellular Space	other	1.37E-03	1.50
MCF7 cells down regulated FC ≥1.5					
SYMBOL	ENTREZ GENE NAME	LOCATION	TYPE(S)	P-VALUE	FOLD CHANGE
SNORA30	small nucleolar RNA, H/ACA box 30	Other	other	1.48E-03	-2.08
SNORD72	small nucleolar RNA, C/D box 72	Other	other	7.37E-03	-2.02
TAS2R31	taste receptor, type 2, member 31	Plasma Membrane	G-protein coupled receptor	2.26E-02	-2.01
TAS2R45	taste receptor, type 2, member 45	Plasma Membrane	G-protein coupled receptor	2.26E-02	-2.01
CCNYL2	cyclin Y-like 2	Other	other	3.18E-02	-1.94
MTMR6	myotubularin related protein 6	Cytoplasm	phosphatase	2.42E-02	-1.87
MIR15/MIR16-2	microRNA 15a	Cytoplasm	microRNA	3.39E-03	-1.85
MIR619	microRNA 619	Cytoplasm	microRNA	4.86E-03	-1.84
SIAE	sialic acid acetyltransferase	Cytoplasm	enzyme	3.64E-02	-1.83
MIR3184	microRNA 3184	Cytoplasm	microRNA	3.98E-03	-1.82
MIR423	microRNA 423	Cytoplasm	microRNA	3.98E-03	-1.82
TVP23B	trans-golgi network vesicle protein 23 homolog B (<i>S. cerevisiae</i>)	Other	other	1.33E-02	-1.79
PF4	platelet factor 4	Extracellular Space	cytokine	4.88E-02	-1.75
MIR3685	microRNA 3685	Cytoplasm	microRNA	2.13E-02	-1.71
FSD2	fibronectin type III and SPRY domain containing 2	Other	other	4.43E-02	-1.68
SCARNA15	small Cajal body-specific RNA 15	Other	other	4.43E-02	-1.68
ANKRD20A4 (includes others)	ankyrin repeat domain 20 family, member A3	Plasma Membrane	other	3.02E-02	-1.68
LOC401357	uncharacterized LOC401357	Other	other	3.99E-02	-1.65
C14orf178	chromosome 14 open reading frame 178	Other	other	1.01E-02	-1.64
HSD52	uncharacterized LOC729467	Other	other	3.22E-02	-1.58
MIR1293	microRNA 1293	Cytoplasm	microRNA	6.60E-03	-1.56

LOC338963	epididymal protein pseudogene	Other	other	2.16E-02	-1.53
STX17	syntaxin 17	Plasma Membrane	transporter	4.09E-02	-1.52
MIR4794	microRNA 4794	Cytoplasm	microRNA	1.90E-02	-1.52

References

1. Vogt, P. in *Retroviruses* 1–25 (Cold spring harbour laboratory press, NY, 1997). at <<http://www.ncbi.nlm.nih.gov/books/NBK19388/>>
2. Lindemann, D., Steffen, I. & Pöhlmann, S. Cellular entry of retroviruses. *Adv. Exp. Med. Biol.* **790**, 128–49 (2013).
3. Neil, J. C., Smart, J. E., Hayman, M. J. & Jarret, O. Polypeptides of feline leukemia virus: a glycosylated gag-related protein is released into culture fluids. *Virology* **150**, 250–253 (1980).
4. Corbin, A. *et al.* A nonstructural gag-encoded glycoprotein precursor is necessary for efficient spreading and pathogenesis of murine leukemia viruses. *J. Virol.* **68**, 3857 (1994).
5. Prats, A. C., De Billy, G., Wang, P. & Darlix, J. L. CUG initiation codon used for the synthesis of a cell surface antigen coded by the murine leukemia virus. *J. Mol. Biol.* **205**, 363–72 (1989).
6. Laprevotte, I., Hampe, A., Sherr, C. J. & Galibert, F. Nucleotide sequence of the gag gene and gag-pol junction of feline leukemia virus. *J. Virol.* **50**, 884 (1984).
7. Edwards, S. A. & Fan, H. gag-Related polyproteins of Moloney murine leukemia virus: evidence for independent synthesis of glycosylated and unglycosylated forms. *J. Virol.* **30**, 551–63 (1979).
8. Cole, G. E., Stacy-hipps, S. & Nunberg, J. H. Recombinant feline herpesviruses expressing feline leukemia virus envelope and gag proteins. *J. Virol.* **64**, 4930 (1990).
9. Nash, M. A., Meyer, M. K., Decker, G. L. & Arlinghaus, R. B. A subset of Pr65gag is nucleus associated in murine leukemia virus-infected cells. *J. Virol.* **67**, 1350–6 (1993).
10. Swanstrom, R. & Wills, J. in *Retroviruses*. 263–334 (Cold Spring Harbor Laboratory Press, 1997). at <<http://www.ncbi.nlm.nih.gov/books/NBK19418/>>
11. Linial, M. *et al.* Index of Viruses-Retroviridae. In: *ICTVdB - The Universal Virus Database, version 4. Büchen-Osmond, C (Ed), Columbia University, New York, USA* (2006). at <http://www.ncbi.nlm.nih.gov/ICTVdb/Ictv/fs_index.htm>
12. Vogt, V. in *Retroviruses*. 27–70 (Cold Spring Harbor Laboratory Press, 1997). at <<http://www.ncbi.nlm.nih.gov/books/NBK19361/>>
13. Hunter, E. in *Retroviruses*. 71–119 (Cold Spring Harbor Laboratory Press, 1997). at <<http://www.ncbi.nlm.nih.gov/books/NBK19440/>>
14. Telesnitsky, A. & Goff, S. in *Retroviruses*. 121–160 (Cold Spring Harbor Laboratory Press, 1997). at <<http://www.ncbi.nlm.nih.gov/books/NBK19383/>>
15. Neil, J. C. & Stewart, M. A. in *Retroviruses and Insights into Cancer* (ed. Dudley, J.) 285–305 (Springer New York, 2011). doi:10.1007/978-0-387-09581-3
16. Brown, P. O. in *Retroviruses*. 161–203. (Cold Spring Harbor Laboratory Press, Cold Spring Harbor, NY, 1997). at <<http://www.ncbi.nlm.nih.gov/books/NBK19392/>>
17. Gifford, R. & Tristem, M. The Evolution , Distribution and Diversity of Endogenous Retroviruses. *Virus Genes* **26**, 291–315 (2003).
18. Stoye, J. P. Studies of endogenous retroviruses reveal a continuing evolutionary saga. *Nat. Rev. Microbiol.* **10**, 395–406 (2012).

19. Rabson, A. & Graves, B. in *Retroviruses*. 205–262 (Cold Spring Harbor Laboratory Press, 1997). at <<http://www.ncbi.nlm.nih.gov/books/NBK19367/>>
20. Kozak, C. A. The mouse 'xenotropic' gammaretroviruses and their XPR1 receptor. *Retrovirology* **7**, 101 (2010).
21. Cingöz, O. & Coffin, J. M. Endogenous murine leukemia viruses: Relationship to XMRV and related sequences detected in human DNA samples. *Adv. Virol.* **2011**, 10 (2011).
22. Baliji, S., Liu, Q. & Kozak, C. A. Common inbred strains of the laboratory mouse that are susceptible to infection by mouse xenotropic gammaretroviruses and the human-derived retrovirus XMRV. *J. Virol.* **84**, 12841–9 (2010).
23. Bhardwaj, N. & Coffin, J. M. Endogenous retroviruses and human cancer: is there anything to the rumors? *Cell Host Microbe* **15**, 255–9 (2014).
24. Coffin, J. M., Stoye, J. P. & Frankel, W. N. Genetics of endogenous murine leukemia viruses. *Ann. N. Y. Acad. Sci.* **567**, 39–49 (1989).
25. Frankel, W. N., Stoye, J. P., Taylor, B. A. & Coffin, J. M. A linkage map of endogenous murine leukemia proviruses. *Genetics* **124**, 221–36 (1990).
26. Fischinger, P., Blevins, C. & Dunlop, N. Genomic masking of nondefective recombinant murine leukemia virus in Moloney virus stocks. *Science* **201**, 457–459 (1978).
27. Levy, J. & Pincus, T. Demonstration of biological activity of a murine leukemia virus of New Zealand Black mice. *Science* **170**, 326–327 (1970).
28. Hoggan, M. D., O'Neill, R. R. & Kozak, C. A. Noncotropic murine leukemia viruses in BALB/c and NFS/N mice: characterization of the BALB/c Bxv-1 provirus and the single NFS endogenous xenotrope. *J. Virol.* **60**, 980 (1986).
29. Sherr, C. J., Lieber, M. M. & Todaro, G. J. Mixed splenocyte cultures and graft versus host reactions selectively induce an 'S-tropic' murine type C virus. *Cell* **1**, 55–58 (1974).
30. Christine, K. & Wallace, R. Genetic mapping of xenotropic leukemia virus-inducing loci in two mouse strains. *Science* **199**, 1448–1449 (1978).
31. Datta, S. K. & Schwartz, R. S. Mendelian segregation of loci controlling xenotropic virus production in NZB crosses. *Virology* **83**, 449–52 (1977).
32. Kozak, C. A., Hartley, J. W. & Morse, H. C. Laboratory and wild-derived mice with multiple loci for production of xenotropic murine leukemia virus. *J. Virol.* **51**, 77–80 (1984).
33. Achong, B., Trumper, P. & Giovanella, B. C-Type virus particles in human tumours transplanted into nude mice. *Br. J. Cancer* **34**, 203–206 (1976).
34. Ikehara, S., Pahwa, R. N., Fernandes, G., Hansen, C. T. & Good, R. A. Functional T cells in athymic nude mice. *Proc. Natl. Acad. Sci. U. S. A.* **81**, 886–888 (1984).
35. Battini, J. L., Rasko, J. E. & Miller, A. D. A human cell-surface receptor for xenotropic and polytropic murine leukemia viruses: possible role in G protein-coupled signal transduction. *Proc. Natl. Acad. Sci. U. S. A.* **96**, 1385–90 (1999).
36. Marin, M., Taylor, C. S., Nouri, A., Kozak, S. L. & Kabat, D. Polymorphisms of the cell surface receptor control mouse susceptibilities to xenotropic and polytropic leukemia viruses. *J. Virol.* **73**, 9362–8 (1999).
37. Giovannini, D., Touhami, J., Charnet, P., Sitbon, M. & Battini, J. Inorganic phosphate export by the retrovirus receptor XPR1 in Metazoans. *CellReports* **3**, 1866–1873 (2013).

38. Yang, H., Bell, T. A., Churchill, G. A. & Pardo-Manuel de Villena, F. On the subspecific origin of the laboratory mouse. *Nat. Genet.* **39**, 1100–7 (2007).
39. Yan, Y. *et al.* Evolution of functional and sequence variants of the mammalian XPR1 receptor for mouse xenotropic gammaretroviruses and the human-derived retrovirus XMRV. *J. Virol.* **84**, 11970–80 (2010).
40. Martin, C., Buckler-White, A., Wollenberg, K. & Kozak, C. A. The avian XPR1 gammaretrovirus receptor is under positive selection and is disabled in bird species in contact with virus-infected wild mice. *J. Virol.* **87**, 10094–104 (2013).
41. Perera, S. S. & Saksena, N. K. Innate, Adaptive and Intrinsic Immunity in Human Immunodeficiency Virus Infection. *Am. J. Infect. Dis.* **8**, 132–148 (2012).
42. Akira, S., Uematsu, S. & Takeuchi, O. Pathogen recognition and innate immunity. *Cell* **124**, 783–801 (2006).
43. Iwasaki, A. A virological view of innate immune recognition. *Annu. Rev. Microbiol.* **66**, 177–96 (2012).
44. Stetson, D. B. & Medzhitov, R. Type I interferons in host defense. *Immunity* **25**, 373–81 (2006).
45. Farrell, A. Innate immunity: Innate sensing of retroviruses. *Nat. Med.* **19**, 1102–1102 (2013).
46. Liberatore, R. A. & Bieniasz, P. D. Sensing retroviruses. *Immunity* **35**, 8–10 (2011).
47. Savina, A. & Amigorena, S. Phagocytosis and antigen presentation in dendritic cells. *Immunol. Rev.* **219**, 143–56 (2007).
48. Hume, D. A. Macrophages as APC and the Dendritic Cell Myth. *J. Immunol.* **181**, 5829–5835 (2008).
49. Heufler, C. *et al.* Interleukin-12 is produced by dendritic cells and mediates T helper 1 development as well as interferon-gamma production by T helper 1 cells. *Eur. J. Immunol.* **26**, 659–68 (1996).
50. Seder, R. A. & Paul, W. E. Acquisition of lymphokine-producing phenotype by CD4+ T cells. *Annu. Rev. Immunol.* **12**, 635–73 (1994).
51. Spellberg, B. & Edwards, J. E. Type 1/Type 2 immunity in infectious diseases. *Clin. Infect. Dis.* **32**, 76–102 (2001).
52. Abbas, A. K., Murphy, K. M. & Sher, A. Functional diversity of helper T lymphocytes. *Nature* **383**, 787–93 (1996).
53. Rinaldo, C. *et al.* High levels of anti-human immunodeficiency virus type 1 (HIV-1) memory cytotoxic T-lymphocyte activity and low viral load are associated with lack of disease in HIV-1-infected long-term nonprogressors. *J. Virol.* **69**, 5838–5842 (1995).
54. Schenkel, J. M. *et al.* T cell memory. Resident memory CD8 T cells trigger protective innate and adaptive immune responses. *Science* **346**, 98–101 (2014).
55. Bieniasz, P. D. Intrinsic immunity: a front-line defense against viral attack. *Nat. Immunol.* **5**, 1109–15 (2004).
56. Neil, S. & Bieniasz, P. Human immunodeficiency virus, restriction factors, and interferon. *J. Interf. cytokine Res.* **29**, 569–580 (2009).
57. Yan, N. & Chen, Z. J. Intrinsic antiviral immunity. *Nat. Immunol.* **13**, 214–22 (2012).

58. Wang, Z. *et al.* APOBEC3 deaminases induce hypermutation in human papillomavirus 16 DNA upon beta interferon stimulation. *J. Virol.* **88**, 1308–17 (2014).
59. Tanaka, Y. *et al.* Anti-viral protein APOBEC3G is induced by interferon-alpha stimulation in human hepatocytes. *Biochem. Biophys. Res. Commun.* **341**, 314–9 (2006).
60. Koning, F. A. *et al.* Defining APOBEC3 expression patterns in human tissues and hematopoietic cell subsets. *J. Virol.* **83**, 9474–85 (2009).
61. Refsland, E. W. *et al.* Quantitative profiling of the full APOBEC3 mRNA repertoire in lymphocytes and tissues: implications for HIV-1 restriction. *Nucleic Acids Res.* **38**, 4274–84 (2010).
62. Conticello, S. G., Thomas, C. J., Petersen-Mahrt, S. K. & Neuberger, M. S. Evolution of the AID/APOBEC family of polynucleotide (deoxy)cytidine deaminases. *Mol. Biol. Evol.* **22**, 367–77 (2005).
63. Zennou, V., Perez-Caballero, D., Göttlinger, H. & Bieniasz, P. D. APOBEC3G incorporation into human immunodeficiency virus type 1 particles. *J. Virol.* **78**, 12058–61 (2004).
64. Wolf, D. & Goff, S. P. Host restriction factors blocking retroviral replication. *Annu. Rev. Genet.* **42**, 143–163 (2008).
65. Bishop, K. N., Holmes, R. K., Sheehy, A. M. & Malim, M. H. APOBEC-mediated editing of viral RNA. *Science* **305**, 645 (2004).
66. Beale, R. C. *et al.* Comparison of the differential context-dependence of DNA deamination by APOBEC enzymes: correlation with mutation spectra in vivo. *J. Mol. Biol.* **337**, 585–96 (2004).
67. Mangeat, B. *et al.* Broad antiretroviral defence by human APOBEC3G through lethal editing of nascent reverse transcripts. *Nature* **424**, 99–103 (2003).
68. Armitage, A. E. *et al.* Conserved footprints of APOBEC3G on Hypermutated human immunodeficiency virus type 1 and human endogenous retrovirus HERV-K(HML2) sequences. *J. Virol.* **82**, 8743–61 (2008).
69. Bourara, K., Liegler, T. J. & Grant, R. M. Target cell APOBEC3C can induce limited G-to-A mutation in HIV-1. *PLoS Pathog.* **3**, 1477–85 (2007).
70. Bishop, K. N. *et al.* Cytidine deamination of retroviral DNA by diverse APOBEC proteins. *Curr. Biol.* **14**, 1392–1396 (2004).
71. Hultquist, J. F. *et al.* Human and rhesus APOBEC3D, APOBEC3F, APOBEC3G, and APOBEC3H demonstrate a conserved capacity to restrict Vif-deficient HIV-1. *J. Virol.* **85**, 11220–34 (2011).
72. Yang, B., Chen, K., Zhang, C., Huang, S. & Zhang, H. Virion-associated uracil DNA glycosylase-2 and apurinic/apyrimidinic endonuclease are involved in the degradation of APOBEC3G-edited nascent HIV-1 DNA. *J. Biol. Chem.* **282**, 11667–75 (2007).
73. Aguiar, R. S. & Peterlin, B. M. APOBEC3 proteins and reverse transcription. *Virus Res.* **134**, 74–85 (2008).
74. Bishop, K. N., Verma, M., Kim, E. Y., Wolinsky, S. M. & Malim, M. H. APOBEC3G inhibits elongation of HIV-1 reverse transcripts. *PLoS Pathog.* **4**, e1000231 (2008).
75. Mbisa, J. L., Bu, W. & Pathak, V. K. APOBEC3F and APOBEC3G inhibit HIV-1 DNA integration by different mechanisms. *J. Virol.* **84**, 5250–9 (2010).

76. Anderson, J. L. & Hope, T. J. APOBEC3G restricts early HIV-1 replication in the cytoplasm of target cells. *Virology* **375**, 1–12 (2008).
77. Newman, E. N. *et al.* Antiviral function of APOBEC3G can be dissociated from cytidine deaminase activity. *Curr. Biol.* **15**, 166–70 (2005).
78. Boi, S. *et al.* Incorporation of mouse APOBEC3 into murine leukemia virus virions decreases the activity and fidelity of reverse transcriptase. *J. Virol.* **88**, 7659–62 (2014).
79. Bogerd, H. P., Zhang, F., Bieniasz, P. D. & Cullen, B. R. Human APOBEC3 proteins can inhibit xenotropic murine leukemia virus-related virus infectivity. *Virology* **410**, 234–9 (2011).
80. Stieler, K. & Fischer, N. Apobec 3G efficiently reduces infectivity of the human exogenous gammaretrovirus XMRV. *PLoS One* **5**, e11738 (2010).
81. Chaipan, C. *et al.* Severe restriction of xenotropic murine leukemia virus-related virus replication and spread in cultured human peripheral blood mononuclear cells. *J. Virol.* **85**, 4888–97 (2011).
82. Jónsson, S. R. *et al.* The restriction of zoonotic PERV transmission by human APOBEC3G. *PLoS One* **2**, e893 (2007).
83. Okeoma, C. M., Huegel, A. L., Lingappa, J., Feldman, M. D. & Ross, S. R. APOBEC3 proteins expressed in mammary epithelial cells are packaged into retroviruses and can restrict transmission of milk-borne virions. *Cell Host Microbe* **8**, 534–43 (2010).
84. Nowarski, R. & Kotler, M. APOBEC3 cytidine deaminases in double-strand DNA break repair and cancer promotion. *Cancer Res.* **73**, 3494–8 (2013).
85. Roberts, S. A. *et al.* An APOBEC cytidine deaminase mutagenesis pattern is widespread in human cancers. *Nat. Genet.* **45**, 970–6 (2013).
86. Sheehy, A. M., Gaddis, N. C., Choi, J. D. & Malim, M. H. Isolation of a human gene that inhibits HIV-1 infection and is suppressed by the viral Vif protein. *Nature* **418**, 646–50 (2002).
87. Sheehy, A. M., Gaddis, N. C. & Malim, M. H. The antiretroviral enzyme APOBEC3G is degraded by the proteasome in response to HIV-1 Vif. *Nat. Med.* **9**, 1404–7 (2003).
88. Doehle, B. P., Schäfer, A. & Cullen, B. R. Human APOBEC3B is a potent inhibitor of HIV-1 infectivity and is resistant to HIV-1 Vif. *Virology* **339**, 281–8 (2005).
89. Rulli, S. J. *et al.* Interactions of murine APOBEC3 and human APOBEC3G with murine leukemia viruses. *J. Virol.* **82**, 6566–75 (2008).
90. Kobayashi, M. *et al.* APOBEC3G targets specific virus species. *J. Virol.* **78**, 8238–8244 (2004).
91. Kolokithas, A. *et al.* The glycosylated Gag protein of a murine leukemia virus inhibits the antiretroviral function of APOBEC3. *J. Virol.* **84**, 10933–6 (2010).
92. Nitta, T. *et al.* Moloney murine leukemia virus glyco-gag facilitates xenotropic murine leukemia virus-related virus replication through human APOBEC3-independent mechanisms. *Retrovirology* **9**, 58 (2012).
93. Low, A. *et al.* Mutation in the glycosylated gag protein of murine leukemia virus results in reduced in vivo infectivity and a novel defect in viral budding or release. *J. Virol.* **81**, 3685–92 (2007).

94. Stremlau, M. *et al.* The cytoplasmic body component TRIM5alpha restricts HIV-1 infection in Old World monkeys. *Nature* **427**, 848–53 (2004).
95. Reymond, A. *et al.* The tripartite motif family identifies cell compartments. *EMBO J.* **20**, 2140–51 (2001).
96. Stremlau, M. *et al.* Specific recognition and accelerated uncoating of retroviral capsids by the TRIM5alpha restriction factor. *Proc. Natl. Acad. Sci. U. S. A.* **103**, 5514–9 (2006).
97. Xu, L. *et al.* BTBD1 and BTBD2 colocalize to cytoplasmic bodies with the RBCC/tripartite motif protein, TRIM5delta. *Exp. Cell Res.* **288**, 84–93 (2003).
98. Li, X. & Sodroski, J. The TRIM5alpha B-box 2 domain promotes cooperative binding to the retroviral capsid by mediating higher-order self-association. *J. Virol.* **82**, 11495–502 (2008).
99. Javanbakht, H. *et al.* Characterization of TRIM5alpha trimerization and its contribution to human immunodeficiency virus capsid binding. *Virology* **353**, 234–46 (2006).
100. Neil, S. J. D., Zang, T. & Bieniasz, P. D. Tetherin inhibits retrovirus release and is antagonized by HIV-1 Vpu. *Nature* **451**, 425–30 (2008).
101. Kupzig, S. *et al.* Bst-2/HM1.24 is a raft-associated apical membrane protein with an unusual topology. *Traffic* **4**, 694–709 (2003).
102. Hinz, A. *et al.* Structural basis of HIV-1 tethering to membranes by the BST-2/tetherin ectodomain. *Cell Host Microbe* **7**, 314–23 (2010).
103. Perez-Caballero, D. *et al.* Tetherin inhibits HIV-1 release by directly tethering virions to cells. *Cell* **139**, 499–511 (2009).
104. Van Damme, N. *et al.* The interferon-induced protein BST-2/CD317 restricts release of virions from infected cells and is down-regulated from the cell surface by HIV-1 Vpu. *Cell Host Microbe* **3**, 245–52 (2008).
105. McNatt, M. W., Zang, T. & Bieniasz, P. D. Vpu binds directly to tetherin and displaces it from nascent virions. *PLoS Pathog.* **9**, e1003299 (2013).
106. McNatt, M. W. *et al.* Species-specific activity of HIV-1 Vpu and positive selection of tetherin transmembrane domain variants. *PLoS Pathog.* **5**, e1000300 (2009).
107. Douglas, J. L. *et al.* Vpu directs the degradation of the human immunodeficiency virus restriction factor BST-2/Tetherin via a {beta}TrCP-dependent mechanism. *J. Virol.* **83**, 7931–47 (2009).
108. Iwabu, Y. *et al.* HIV-1 accessory protein Vpu internalizes cell-surface BST-2/tetherin through transmembrane interactions leading to lysosomes. *J. Biol. Chem.* **284**, 35060–72 (2009).
109. Zhang, R., Bloch, N., Nguyen, L. A., Kim, B. & Landau, N. R. SAMHD1 restricts HIV-1 replication and regulates interferon production in mouse myeloid cells. *PLoS One* **9**, e89558 (2014).
110. Lahouassa, H. *et al.* SAMHD1 restricts the replication of human immunodeficiency virus type 1 by depleting the intracellular pool of deoxynucleoside triphosphates. *Nat. Immunol.* **13**, 223–8 (2012).
111. Laguette, N. *et al.* SAMHD1 is the dendritic- and myeloid-cell-specific HIV-1 restriction factor counteracted by Vpx. *Nature* **474**, 654–7 (2011).

112. Hrecka, K. *et al.* Vpx relieves inhibition of HIV-1 infection of macrophages mediated by the SAMHD1 protein. *Nature* **474**, 658–61 (2011).
113. Sommerfelt, M. A. Retrovirus receptors. *J. Gen. Virol.* **80**, 3049–3064 (1999).
114. Ikeda, H., Laigret, F., Martin, M. A. & Repaske, R. Characterization of a molecularly cloned retroviral sequence associated with Fv-4 resistance. *J. Virol.* **55**, 768–77 (1985).
115. Ikeda, H. & Sugimura, H. Fv-4 resistance gene: A truncated endogenous murine leukemia virus with ecotropic interference properties. *J. Virol.* **63**, 5405–12 (1989).
116. Kool, J. & Berns, A. High-throughput insertional mutagenesis screens in mice to identify oncogenic networks. *Nat. Rev. Cancer* **9**, 389–99 (2009).
117. Lander, E. S. *et al.* Initial sequencing and analysis of the human genome. *Nature* **409**, 860–921 (2001).
118. Ryan, F. P. Human endogenous retroviruses in health and disease: a symbiotic perspective. *J. R. Soc. Med.* **97**, 560–5 (2004).
119. Griffiths, D. J. Endogenous retroviruses in the human genome sequence. *Genome Biol.* **2**, 1–5 (2001).
120. Nelson, P. N. *et al.* Demystified. Human endogenous retroviruses. *Mol. Pathol.* **56**, 11–8 (2003).
121. Oliveira, N. M., Farrell, K. B. & Eiden, M. V. In vitro characterization of a Koala retrovirus. *J. Virol.* **80**, 3104–3107 (2006).
122. Lieber, M. M. *et al.* Isolation from the asian mouse *Mus caroli* of an endogenous type C virus related to infectious primate type C viruses. *Proc. Natl. Acad. Sci. U. S. A.* **72**, 2315–9 (1975).
123. Avila-Arcos, M. C. *et al.* One hundred twenty years of koala retrovirus evolution determined from museum skins. *Mol. Biol. Evol.* **30**, 299–304 (2013).
124. Ishida, Y., Zhao, K., Greenwood, A. D. & Roca, A. L. Proliferation of endogenous retroviruses in the early stages of a host germ line invasion. *Mol. Biol. Evol.* **32**, 109–20 (2015).
125. Denner, J. Transspecies transmissions of retroviruses: new cases. *Virology* **369**, 229–33 (2007).
126. Simmons, G. S. *et al.* Prevalence of koala retrovirus in geographically diverse populations in Australia. *Aust. Vet. J.* **90**, 404–9 (2012).
127. Armstrong, J. A., Porterfield, J. S. & De Madrid, A. T. C-type virus particles in pig kidney cell lines. *J. Gen. Virol.* **10**, 195–8 (1971).
128. Bouillant, A. M. & Greig, A. S. Type C virus production by a continuous line of pig oviduct cells (PFT). *J. Gen. Virol.* **27**, 173–80 (1975).
129. Blusch, J. H., Patience, C. & Martin, U. Pig endogenous retroviruses and xenotransplantation. *Xenotransplantation* **9**, 242–251 (2002).
130. Martin, U. *et al.* Expression of pig endogenous retrovirus by primary porcine endothelial cells and infection of human cells. *Lancet* **352**, 692–4 (1998).
131. Wilson, C. A. *et al.* Type C retrovirus released from porcine primary peripheral blood mononuclear cells infects human Cells. *J. Virol.* **72**, 3082–3087 (1998).

132. Seow, J. & Chew, F. T. Clinical xenotransplantation. *Lancet* **362**, 1421–2 (2003).
133. Van der Laan, L. J. *et al.* Infection by porcine endogenous retrovirus after islet xenotransplantation in SCID mice. *Nature* **407**, 90–4 (2000).
134. Patience, C., Takeuchi, Y. & Weiss, R. A. Infection of human cells by an endogenous retrovirus of pigs. *Nat. Med.* **3**, 282–6 (1997).
135. Ericsson, T. A. *et al.* Identification of receptors for pig endogenous retrovirus. *Proc. Natl. Acad. Sci. U. S. A.* **100**, 6759–64 (2003).
136. Heneine, W. *et al.* No evidence of infection with porcine endogenous retrovirus in recipients of porcine islet-cell xenografts. *Lancet* **352**, 695–9 (1998).
137. Paradis, K. *et al.* Search for cross-species transmission of porcine endogenous retrovirus in patients treated with living pig tissue. *Science* **285**, 1236–41 (1999).
138. Bolin, L. L. & Levy, L. S. Viral determinants of FeLV infection and pathogenesis: lessons learned from analysis of a natural cohort. *Viruses* **3**, 1681–98 (2011).
139. Mendoza, R., Anderson, M. M. & Overbaugh, J. A putative Thiamine transport protein is a receptor for feline leukemia virus subgroup A. *J. Virol.* **80**, 3378–3385 (2006).
140. Nakata, R. *et al.* Reevaluation of host ranges of feline leukemia virus subgroups. *Microbes Infect.* **5**, 947–950 (2003).
141. Stewart, M. *et al.* Nucleotide sequences of a feline leukemia virus subgroup A envelope gene and long terminal repeat and evidence for the recombinational origin of subgroup B viruses. *J. Virol.* **58**, 825–34 (1986).
142. Boomer, S., Eiden, M., Burns, C. C. & Overbaugh, J. Three distinct envelope domains, variably present in subgroup B feline leukemia virus recombinants, mediate Pit1 and Pit2 receptor recognition. *J. Virol.* **71**, 8116–23 (1997).
143. Riedel, N., Hoover, E. A., Dornsife, R. E. & Mullins, J. I. Pathogenic and host range determinants of the feline aplastic anemia retrovirus. *Proc. Natl. Acad. Sci. U. S. A.* **85**, 2758–62 (1988).
144. Quigley, J. G. *et al.* Cloning of the cellular receptor for feline leukemia virus subgroup C (FeLV-C), a retrovirus that induces red cell aplasia. *Blood* **95**, 1093–9 (2000).
145. Onions, D., Jarret, O., Testa, N., Frassoni, F. & Toth, S. Selective effect of feline leukaemia virus on early erythroid precursors. *Nature* **296**, 156–158 (1982).
146. Shalev, Z. *et al.* Identification of a feline leukemia virus variant that can use THTR1, FLVCR1, and FLVCR2 for infection. *J. Virol.* **83**, 6706–16 (2009).
147. Jarrett, O., Hardy, W. D., Golder, M. C. & Hay, D. The frequency of occurrence of feline leukaemia virus subgroups in cats. *Int. J. Cancer* **21**, 334–7 (1978).
148. Hartmann, K. Clinical aspects of feline retroviruses: a review. *Viruses* **4**, 2684–710 (2012).
149. Hardy, W. D. *et al.* Biology of feline leukemia virus in the natural environment. *Cancer Res.* **36**, 582–8 (1976).
150. Levy, J. *et al.* 2008 American Association of Feline Practitioners' feline retrovirus management guidelines. *J. Feline Med. Surg.* **10**, 300–16 (2008).
151. Paprotka, T. *et al.* Recombinant origin of the retrovirus XMRV. *Science* **333**, 97–101 (2011).

152. Yan, Y., Liu, Q. & Kozak, C. A. Six host range variants of the xenotropic/polytropic gammaretroviruses define determinants for entry in the XPR1 cell surface receptor. *Retrovirology* **6**, 87 (2009).
153. Schlager, R., Choe, D. J., Brown, K. R., Thaker, H. M. & Singh, I. R. XMRV is present in malignant prostatic epithelium and is associated with prostate cancer, especially high-grade tumors. *Proc. Natl. Acad. Sci. U. S. A.* **106**, 16351–6 (2009).
154. Arnold, R. S. *et al.* XMRV infection in patients with prostate cancer: novel serologic assay and correlation with PCR and FISH. *Urology* **75**, 755–61 (2010).
155. Urisman, A. *et al.* Identification of a novel Gammaretrovirus in prostate tumors of patients homozygous for R462Q RNASEL variant. *PLoS Pathog.* **2**, e25 (2006).
156. Lombardi, V. C. *et al.* Detection of an infectious retrovirus, XMRV, in blood cells of patients with chronic fatigue syndrome. *Science* **326**, 585–9 (2009).
157. McCormick, A. L., Brown, R. H., Cudkovic, M. E., Al-Chalabi, A. & Garson, J. A. Quantification of reverse transcriptase in ALS and elimination of a novel retroviral candidate. *Neurology* **70**, 278–83 (2008).
158. Delviks-Frankenberry, K., Cingoz, O., Coffin, J. M. & Pathak, V. K. Recombinant Origin, Contamination, and De-discovery of XMRV. *Curr. Opin. Virol.* **19**, 72–81 (2013).
159. Lo, S. C. *et al.* Detection of MLV-related virus gene sequences in blood of patients with chronic fatigue syndrome and healthy blood donors. *Proc. Natl. Acad. Sci. U. S. A.* **107**, 15874–9 (2010).
160. Oakes, B. *et al.* Contamination of human DNA samples with mouse DNA can lead to false detection of XMRV-like sequences. *Retrovirology* **7**, 109 (2010).
161. Erlwein, O. *et al.* DNA extraction columns contaminated with murine sequences. *PLoS One* **6**, e23484 (2011).
162. Simmons, G. *et al.* Failure to confirm XMRV/MLVs in the blood of patients with Chronic Fatigue Syndrome: A multi-laboratory Study. *Science* **334**, 814–817 (2011).
163. Knouf, E. C. *et al.* Multiple integrated copies and high-level production of the human retrovirus XMRV (xenotropic murine leukemia virus-related virus) from 22Rv1 prostate carcinoma cells. *J. Virol.* **83**, 7353–6 (2009).
164. Huntly, B. J. & Gilliland, D. G. Leukaemia stem cells and the evolution of cancer-stem-cell research. *Nat. Rev. Cancer* **5**, 311–21 (2005).
165. Shultz, L. D., Ishikawa, F. & Greiner, D. L. Humanized mice in translational biomedical research. *Nat. Rev. Immunol.* **7**, 118–30 (2007).
166. McAllister, R. *et al.* C-Type Virus released from cultured human Rhabdomyosarcoma cells. *Nature* **235**, 3–6 (1972).
167. Okabe, H., Gilden, R. V. & Hatanaka, M. RD 114 virus-specific sequences in feline cellular RNA: Detection and Characterization. *J. Virol.* **12**, 984–994 (1973).
168. Yoshikawa, R., Sato, E., Igarashi, T. & Miyazawa, T. Characterization of RD-114 virus isolated from a commercial canine vaccine manufactured using CRFK cells. *J. Clin. Microbiol.* **48**, 3366–9 (2010).
169. Yoshikawa, R., Shimode, S., Sakaguchi, S. & Miyazawa, T. Contamination of live attenuated vaccines with an infectious feline endogenous retrovirus (RD-114 virus). *Arch. Virol.* **159**, 399–404 (2014).

170. Todaro, G. J., Arnstein, P., Parks, W. P., Lennette, E. H. & Huebner, R. J. A type-C virus in human rhabdomyosarcoma cells after inoculation into NIH Swiss mice treated with antithymocyte serum. *Proc. Natl. Acad. Sci. U. S. A.* **70**, 859–62 (1973).
171. Wunderli, H., Mickey, D. & Paulson, D. C Type virus particles in human urogenital tumours after heterotransplantation into nude mice. *Br. J. Cancer* **39**, 35–42 (1979).
172. Gautsch, J. W., Knowles, A. F., Jensen, F. C. & Kaplan, N. O. Highly efficient induction of type C retroviruses by a human tumor in athymic mice. *Proc. Natl. Acad. Sci. U. S. A.* **77**, 2247–50 (1980).
173. Zhang, Y. *et al.* Frequent detection of infectious xenotropic murine leukemia virus (XMLV) in human cultures established from mouse xenografts. *Cancer Biol. Ther.* **12**, 617–628 (2011).
174. Antoine, M., Wegmann, B. & Kiefer, P. Envelope and long terminal repeat sequences of an infectious murine leukemia virus from a human SCLC cell line: implications for gene transfer. *Virus Genes* **17**, 157–68 (1998).
175. Hué, S. *et al.* Disease-associated XMRV sequences are consistent with laboratory contamination. *Retrovirology* **7**, 111 (2010).
176. Sfanos, K. S. *et al.* Identification of replication competent murine gammaretroviruses in commonly used prostate cancer cell lines. *PLoS One* **6**, e20874 (2011).
177. Deichmann, M. *et al.* Detection of reverse transcriptase activity in human melanoma cell lines and identification of a murine leukemia virus contaminant. *Arch. Dermatol. Res.* **296**, 345–52 (2005).
178. Takeuchi, Y., McClure, M. O. & Pizzato, M. Identification of gammaretroviruses constitutively released from cell lines used for human immunodeficiency virus research. *J. Virol.* **82**, 12585–8 (2008).
179. Huuse, E. M. *et al.* Monitoring the effect of Docetaxel treatment in MCF7 xenografts using multimodal in vivo and ex vivo magnetic resonance methods, histopathology, and gene expression. *Transl. Oncol.* **3**, 252–63 (2010).
180. Warrington, J. M. *et al.* Selenized milk casein in the diet of BALB/c nude mice reduces growth of intramammary MCF-7 tumors. *BMC Cancer* **13**, 492 (2013).
181. Hayward, W. S., Neel, B. G. & Astrin, S. M. Activation of a cellular onc gene by promoter insertion in ALV-induced lymphoid leukosis. *Nature* **290**, 475–480 (1981).
182. Kim, S. *et al.* Integration site preference of xenotropic murine leukemia virus-related virus, a new human retrovirus associated with prostate cancer. *J. Virol.* **82**, 9964–77 (2008).
183. Schröder, A. R. *et al.* HIV-1 integration in the human genome favors active genes and local hotspots. *Cell* **110**, 521–529 (2002).
184. Mitchell, R. S. *et al.* Retroviral DNA integration: ASLV, HIV, and MLV show distinct target site preferences. *PLoS Biol.* **2**, E234 (2004).
185. Noguchi, M. *et al.* Interleukin-2 receptor gamma chain mutation results in X-linked severe combined immunodeficiency in humans. *Cell* **73**, 147–57 (1993).
186. Grunebaum, E. *et al.* Bone marrow transplantation for severe combined immune deficiency. *JAMA* **295**, 508–18 (2006).
187. Hacein-Bey-Abina, S. *et al.* A serious adverse event after successful gene therapy for X-Linked Severe Combined Immunodeficiency. *N. Engl. J. Med.* **348**, 255–266 (2003).

188. Kohn, D. B., Sadelain, M. & Glorioso, J. C. Occurrence of leukaemia following gene therapy of X-linked SCID. *Nat. Rev. Cancer* **3**, 477–88 (2003).
189. Stieler, K., Schumacher, U., Horst, A. K. & Fischer, N. XMRV induces cell migration, cytokine expression and tumor angiogenesis: Are 22Rv1 cells a suitable prostate cancer model? *PLoS One* **7**, e42321 (2012).
190. Murgai, M. *et al.* Xenotropic MLV envelope proteins induce tumor cells to secrete factors that promote the formation of immature blood vessels. *Retrovirology* **10**, 34 (2013).
191. Rosenberg, N. & Jolicoeur, P. in *Retroviruses* 475–585 (Cold spring harbour laboratory press, NY, 1997). at <<http://www.ncbi.nlm.nih.gov/books/NBK19378/>>
192. Alian, A., Sela-Donenfeld, D., Panet, A. & Eldor, A. Avian hemangioma retrovirus induces cell proliferation via the envelope (env) gene. *Virology* **276**, 161–8 (2000).
193. Liu, S. L. & Miller, A. D. Oncogenic transformation by the jaagsiekte sheep retrovirus envelope protein. *Oncogene* **26**, 789–801 (2007).
194. Maeda, N., Fan, H. & Yoshikai, Y. Oncogenesis by retroviruses : old and new paradigms. *Rev. Med. Virol.* **18**, 387–405 (2008).
195. Katz, E. *et al.* MMTV Env encodes an ITAM responsible for transformation of mammary epithelial cells in three-dimensional culture. *J. Exp. Med.* **201**, 431–9 (2005).
196. Li, Y., Cardona, S. M., Traister, R. S. & Lynch, W. P. Retrovirus-induced spongiform neurodegeneration is mediated by unique central nervous system viral targeting and expression of env alone. *J. Virol.* **85**, 2060–78 (2011).
197. Zhao, X. & Yoshimura, F. K. Expression of murine leukemia virus envelope protein is sufficient for the induction of apoptosis. *J. Virol.* **82**, 2586–9 (2008).
198. Soule, H. D., Vazquez, J., Long, A., Albert, S. & Brennan, M. A human cell line from a pleural effusion derived from a breast carcinoma. *J. Natl. Cancer Inst.* **51**, 1409–16 (1973).
199. Brandes, L. J. & Hermonat, M. W. Receptor status and subsequent sensitivity of subclones of MCF-7 human breast cancer cells surviving exposure to diethylstilbestrol. *Cancer Res.* **43**, 2831–5 (1983).
200. Foley, G. E. *et al.* Continuous culture of human lymphoblasts from blood of a child with acute leukaemia. *Cancer* **18**, 522–9 (1965).
201. Nara, P. L. *et al.* Simple, rapid, quantitative, syncytium-forming microassay for the detection of human immunodeficiency virus neutralizing antibody. *AIDS Res. Hum. Retroviruses* **3**, 283–302 (1987).
202. Ohkubo, T. *et al.* A novel Ph1 chromosome positive cell line established from a patient with chronic myelogenous leukemia in blastic crisis. *Leuk. Res.* **9**, 921–926 (1985).
203. Andersson, L. C., Nilsson, K. & Gahmberg, C. G. K562: A human erythroleukemic cell line. *Int. J. cancer.* **23**, 143–7 (1979).
204. Kang, C. D. *et al.* Signaling mechanism of PMA-induced differentiation of K562 cells. *Biochem. Biophys. Res. Commun.* **221**, 95–100 (1996).
205. Sundström, C. & Nilsson, K. Establishment and characterization of a human histiocytic lymphoma cell line (U-937). *Int. J. Cancer* **17**, 565–77 (1976).

206. Weiss, A., Wiskocil, R. L. & Stobo, J. D. The role of T3 surface molecules in the activation of human T cells: a two-stimulus requirement for IL 2 production reflects events occurring at a pre-translational level. *J. Immunol.* **133**, 123–8 (1984).
207. Rosenfeld, C. *et al.* An effective human leukaemic cell line: Reh. *Eur. J. Cancer* **13**, 377–379 (1977).
208. Han, T., Dadey, B. & Minowada, J. Cultured human leukemic non-T/non-B lymphoblasts and their stimulating capacity in 'one-way' mixed lymphocyte reaction: suggestive evidence for early T-cell or B-cell precursors. *Cancer* **44**, 136–40 (1979).
209. Tsuchiya, S. *et al.* Establishment and characterization of a human acute monocytic leukemia cell line (THP-1). *Int. J. Cancer* **26**, 171–6 (1980).
210. Auwerx, J. The human leukemia cell line, THP-1: a multifaceted model for the study of monocyte-macrophage differentiation. *Experientia* **47**, 22–31 (1991).
211. Daigneault, M., Preston, J. A., Marriott, H. M., Whyte, M. K. B. & Dockrell, D. H. The identification of markers of macrophage differentiation in PMA-stimulated THP-1 cells and monocyte-derived macrophages. *PLoS One* **5**, e8668 (2010).
212. Chen, Q. & Ross, A. C. Retinoic acid regulates cell cycle progression and cell differentiation in human monocytic THP-1 cells. *Exp. Cell Res.* **297**, 1–24 (2013).
213. Graham, F. L., Smiley, J., Russell, W. C. & Nairn, R. Characteristics of a human cell line transformed by DNA from human adenovirus type 5. *J. Gen. Virol.* **36**, 59–74 (1977).
214. Cailleau, R., Young, R., Olivé, M. & Reeves, W. J. Breast tumor cell lines from pleural effusions. *J. Natl. Cancer Inst.* **53**, 661–74 (1974).
215. Bates, S. E. *et al.* Expression of the transforming growth factor- α /epidermal growth factor receptor pathway in normal human breast epithelial cells. *Endocrinology* **126**, 596–607 (1990).
216. Giassi, L. J. *et al.* Expanded CD34+ human umbilical cord blood cells generate multiple lymphohematopoietic lineages in NOD-scid IL2rgamma(null) mice. *Exp. Biol. Med.* **233**, 997–1012 (2008).
217. Marin, M. *et al.* Antiviral activity of an intracellularly expressed single-chain antibody fragment directed against the murine leukemia virus capsid protein. *Hum. Gene Ther.* **11**, 389–401 (2000).
218. Rose, P. P. & Korber, B. T. Detecting hypermutations in viral sequences with an emphasis on G \rightarrow A hypermutation. *Bioinformatics* **16**, 400–401 (2000).
219. Dobbin, Z. C. *et al.* Using heterogeneity of the patient-derived xenograft model to identify the chemoresistant population in ovarian cancer. *Oncotarget.* **5**, 8750–64 (2014).
220. Coulson-Thomas, V. J., Gesteira, T. F., Hascall, V. & Kao, W. Umbilical cord mesenchymal stem cells suppress host rejection: the role of the glycocalyx. *J. Biol. Chem.* **289**, 23465–81 (2014).
221. Marusyk, A. *et al.* Non-cell-autonomous driving of tumour growth supports sub-clonal heterogeneity. *Nature* **514**, 54–58 (2014).
222. Metzger, M. J., Holguin, C. J., Mendoza, R. & Miller, A. D. The prostate cancer-associated human retrovirus XMRV lacks direct transforming activity but can induce low rates of transformation in cultured cells. *J. Virol.* **84**, 1874–80 (2010).

223. Silverman, R. H., Nguyen, C., Weight, C. J. & Klein, E. A. The human retrovirus XMRV in prostate cancer and chronic fatigue syndrome. *Nat. Rev. Urol.* **7**, 392–402 (2010).
224. Tang, S. *et al.* Absence of detectable XMRV and other MLV-related viruses in healthy blood donors in the United States. *PLoS One* **6**, e27391 (2011).
225. Stoye, J. P. & Moroni, C. Endogenous retrovirus expression in stimulated murine lymphocytes. Identification of a new locus controlling mitogen induction of a defective virus. *J. Exp. Med.* **157**, 1660–74 (1983).
226. VanWeelden, K., Flanagan, L., Binderup, L., Tenniswood, M. & Welsh, J. Apoptotic regression of MCF-7 xenografts in nude mice treated with the vitamin D3 analog, EB1089. *Endocrinology* **139**, 2102–10 (1998).
227. Kozak, C. A. & Rowe, W. P. Genetic mapping of the ecotropic murine leukemia virus-inducing locus of BALB/c mouse to chromosome 5. *Science* **204**, 69–71 (1979).
228. Hook, L. M. *et al.* Characterization of a novel murine retrovirus mixture that facilitates hematopoiesis. *J. Virol.* **76**, 12112–22 (2002).
229. Shultz, L. D. *et al.* Multiple defects in innate and adaptive immunologic function in NOD/LtSz-scid mice. *J. Immunol.* **154**, 180–91 (1995).
230. Shultz, L. D. *et al.* Human lymphoid and myeloid cell development in NOD/LtSz-scid IL2R gamma null mice engrafted with mobilized human hemopoietic stem cells. *J. Immunol.* **174**, 6477–89 (2005).
231. Ito, M. *et al.* NOD/SCID /gamma null c mouse: an excellent recipient mouse model for engraftment of human cells. *Blood* **100**, 3175–3182 (2002).
232. Yi, B., Williams, P. J., Niewolna, M., Wang, Y. & Yoneda, T. Tumor-derived platelet-derived growth factor-BB plays a critical role in osteosclerotic bone metastasis in an animal model of human breast cancer. *Cancer Res.* **62**, 917–923 (2002).
233. Evans, S. M. *et al.* Tamoxifen Induces Hypoxia in MCF-7 Xenografts. *Cancer Res.* **57**, 5155–5161 (1997).
234. Harris, R. S. *et al.* DNA deamination mediates innate immunity to retroviral infection. *Cell* **113**, 803–9 (2003).
235. Trivai, I. *et al.* Endogenous retrovirus induces leukemia in a xenograft mouse model for primary myelofibrosis. *Proc. Natl. Acad. Sci. U. S. A.* **111**, 8595–600 (2014).
236. Michel, R. B., Ochakovskaya, R. & Mattes, M. J. Antibody localization to B-Cell lymphoma xenografts in immunodeficient mice: Importance of using residualizing radiolabels. *Clin. Cancer Res.* **8**, 2632–2639 (2002).
237. Chao, M. P. *et al.* Anti-CD47 antibody synergizes with rituximab to promote phagocytosis and eradicate non-Hodgkin lymphoma. *Cell* **142**, 699–713 (2010).
238. Stieler, K. *et al.* Host range and cellular tropism of the human exogenous gammaretrovirus XMRV. *Virology* **399**, 23–30 (2010).
239. Laurent, F., Tchénio, T., Buckle, M., Hazan, U. & Bury-Moné, S. XMRV low level of expression in human cells delays superinfection interference and allows proviral copies to accumulate. *Virology* **456-457**, 28–38 (2014).
240. Fan, H. & Johnson, C. Insertional oncogenesis by non-acute retroviruses: implications for gene therapy. *Viruses* **3**, 398–422 (2011).

241. Suzuki, T. *et al.* New genes involved in cancer identified by retroviral tagging. *Nat. Genet.* **32**, 166–74 (2002).
242. Uren, A. G., Kool, J., Berns, A. & van Lohuizen, M. Retroviral insertional mutagenesis: past, present and future. *Oncogene* **24**, 7656–72 (2005).
243. Aloia, A. L. *et al.* A reporter system for replication-competent gammaretroviruses: the inGluc-MLV-DERSE assay. *Gene Ther.* **20**, 169–76 (2013).
244. Martin, K. L., Johnson, M. & D'Aquila, R. T. APOBEC3G complexes decrease human immunodeficiency virus type 1 production. *J. Virol.* **85**, 9314–26 (2011).
245. Wu, X., Li, Y., Crise, B. & Burgess, S. M. Transcription start regions in the human genome are favored targets for MLV integration. *Science* **300**, 1749–51 (2003).
246. Bottger, P. & Pedersen, L. Two highly conserved glutamate residues critical for type III sodium-dependent phosphate transport revealed by uncoupling transport function from retroviral receptor function. *J. Biol. Chem.* **277**, 42741–7 (2002).
247. Uckert, W., Willmsky, G., Pedersen, F. S., Blankenstein, T. & Pedersen, L. RNA levels of human retrovirus receptors Pit1 and Pit2 do not correlate with infectibility by three retroviral vector pseudotypes. *Hum. Gene Ther.* **9**, 2619–2627 (1998).
248. Fogarty, K. H. *et al.* Interrelationship between cytoplasmic retroviral Gag concentration and Gag–membrane association. *J. Mol. Biol.* **426**, 1611–1624 (2014).
249. Doehle, B. P. *et al.* Differential sensitivity of murine leukemia virus to APOBEC3-mediated inhibition is governed by virion exclusion. *J. Virol.* **79**, 8201–7 (2005).
250. Apolonia, L. *et al.* Promiscuous RNA Binding Ensures Effective Encapsidation of APOBEC3 Proteins by HIV-1. *PLOS Pathog.* **11**, e1004609 (2015).
251. Sayah, D. M., Sokolskaja, E., Berthoux, L. & Luban, J. Cyclophilin A retrotransposition into TRIM5 explains owl monkey resistance to HIV-1. *Nature* **430**, 569–73 (2004).
252. Maillard, P. V, Reynard, S., Serhan, F., Turelli, P. & Trono, D. Interfering residues narrow the spectrum of MLV restriction by human TRIM5alpha. *PLoS Pathog.* **3**, e200 (2007).
253. Del Prete, G. Q. *et al.* Restricted replication of xenotropic murine leukemia virus-related virus in pigtailed macaques. *J. Virol.* **86**, 3152–66 (2012).
254. Park, E. K. *et al.* Optimized THP-1 differentiation is required for the detection of responses to weak stimuli. *Inflamm. Res.* **56**, 45–50 (2007).
255. Ruetten, H., Thiemermann, C. & Perretti, M. Upregulation of ICAM-1 expression on J774.2 macrophages by endotoxin involves activation of NF-kappaB but not protein tyrosine kinase: comparison to induction of iNOS. *Mediators Inflamm.* **8**, 77–84 (1999).
256. Zakharova, E., Grandhi, J., Wewers, M. D. & Gavrilin, M. A. Mycoplasma suppression of THP-1 cell TLR responses is corrected with antibiotics. *PLoS One* **5**, e9900 (2010).
257. Stürzel, C. M. *et al.* Utilization of replication-competent XMRV reporter-viruses reveals severe viral restriction in primary human cells. *PLoS One* **8**, e74427 (2013).
258. Pandhare-Dash, J., Mantri, C. K., Gong, Y., Chen, Z. & Dash, C. XMRV accelerates cellular proliferation, transformational activity, and invasiveness of prostate cancer cells by downregulating p27(Kip1). *Prostate* **72**, 886–897 (2012).

259. Gallily, R., Salman, M., Tarshis, M. & Rottem, S. Mycoplasma fermentans (incognitus strain) induces TNF alpha and IL-1 production by human monocytes and murine macrophages. *Immunol. Lett.* **34**, 27–30 (1992).
260. Reyes, L., Davidson, M. K., Thomas, L. C. & Davis, J. K. Effects of Mycoplasma fermentans incognitus on differentiation of THP-1 cells. *Infect. Immun.* **67**, 3188–3192 (1999).
261. Carroll, K. & O’Kennedy, R. The elimination of mycoplasma from infected hybridomas by passaging in BALB/c mice. *J. Immunol. Methods* **108**, 189–93 (1988).
262. Benjamini, Y. & Hochberg, Y. Controlling the False Discovery Rate: A practical and powerful approach to multiple testing. *J. R. Stat. Soc.* **57**, 289–300 (1995).
263. Perneger, T. V. What’s wrong with Bonferroni adjustments. *BMJ* **316**, 1236–1238 (1998).
264. Canman, C. E. & Lim, D. S. The role of ATM in DNA damage responses and cancer. *Oncogene* **17**, 3301–8 (1998).
265. Roshak, A. K. *et al.* The human polo-like kinase, PLK, regulates cdc2/cyclin B through phosphorylation and activation of the cdc25C phosphatase. *Cell. Signal.* **12**, 405–411 (2000).
266. Sartor, H., Ehlert, F., Grzeschik, K., Muller, R. & Adolph, S. Assignment of two human cell cycle genes, CDC25C and CCNB1, to 5q31 and 5q12, respectively. *Genomics* **13**, 911–912 (1992).
267. Yuan, J. *et al.* Cyclin B1 depletion inhibits proliferation and induces apoptosis in human tumor cells. *Oncogene* **23**, 5843–52 (2004).
268. Gavet, O. & Pines, J. Progressive activation of CyclinB1-Cdk1 coordinates entry to mitosis. *Dev. Cell* **18**, 533–543 (2010).
269. Lens, S. M. A., Voest, E. E. & Medema, R. H. Shared and separate functions of polo-like kinases and aurora kinases in cancer. *Nat. Rev. Cancer* **10**, 825–41 (2010).
270. Nam, H. J. & van Deursen, J. M. Cyclin B2 and p53 control proper timing of centrosome separation. *Nat. Cell Biol.* **16**, 538–49 (2014).
271. Hoffmann, T. K. *et al.* Cyclin B1 expression and p53 status in squamous cell carcinomas of the head and neck. *Anticancer Res.* **31**, 3151–7 (2011).
272. Yuan, J. *et al.* Stable gene silencing of cyclin B1 in tumor cells increases susceptibility to taxol and leads to growth arrest in vivo. *Oncogene* **25**, 1753–62 (2006).
273. Bystry, R. S., Aluvihare, V., Welch, K. A., Kallikourdis, M. & Betz, A. G. B cells and professional APCs recruit regulatory T cells via CCL4. *Nat. Immunol.* **2**, 1126–1132 (2001).
274. Nakayama, T. *et al.* Selective induction of Th2-attracting chemokines CCL17 and CCL22 in human B Cells by Latent Membrane Protein 1 of Epstein-Barr Virus. *J. Virol.* **78**, 1665–1674 (2004).
275. Maurer, M. & von Stebut, E. Macrophage inflammatory protein-1. *Int. J. Biochem. Cell Biol.* **36**, 1882–6 (2004).
276. Cittera, E. *et al.* The CCL3 family of chemokines and innate immunity cooperate in vivo in the eradication of an established lymphoma xenograft by Rituximab. *J. Immunol.* **178**, 6616–6623 (2007).
277. Welsh, R. M. Mouse natural killer cells: induction specificity, and function. *J. Immunol.* **121**, 1631–5 (1978).

278. Mack, M. *et al.* Expression and characterization of the chemokine receptors CCR2 and CCR5 in mice. *J. Immunol.* **166**, 4697–704 (2001).
279. Kitamura, A., Takahashi, K., Okajima, A. & Kitamura, N. Induction of the human gene for p44, a hepatitis-C-associated microtubular aggregate protein, by interferon-alpha/beta. *Eur. J. Biochem.* **224**, 877–83 (1994).
280. Hallen, L. C. *et al.* Antiproliferative activity of the human IFN-alpha-inducible protein IFI44. *J. Interf. cytokine Res.* **27**, 675–80 (2007).
281. Wong, M. T. & Chen, S. S. L. Emerging roles of interferon-stimulated genes in the innate immune response to hepatitis C virus infection. *Cell. Mol. Immunol.* (2014). doi:10.1038/cmi.2014.127
282. Wie, S. H. *et al.* HIV downregulates interferon-stimulated genes in primary macrophages. *J. Interf. cytokine Res.* **33**, 90–95 (2013).
283. Cousins, R. J. & McMahon, R. J. Integrative aspects of zinc transporters. *J. Nutr.* **130**, 1384S–7S (2000).
284. Bouain, N. *et al.* Phosphate and zinc transport and signalling in plants: toward a better understanding of their homeostasis interaction. *J. Exp. Bot.* **65**, 5725–41 (2014).
285. Jackson, R. J. *et al.* Expression of the PitA phosphate/metal transporter of *Escherichia coli* is responsive to zinc and inorganic phosphate levels. *FEMS Microbiol. Lett.* **289**, 219–24 (2008).
286. Khachigian, L. M. & Collins, T. Early growth response factor 1: a pleiotropic mediator of inducible gene expression. *J. Mol. Med.* **76**, 613–16 (1998).
287. Krones-herzig, A. *et al.* Early Growth Response 1 acts as a tumor suppressor in vivo and in vitro via regulation of p53. *Cancer Res.* **65**, 5133–5143 (2005).
288. Abdulkadir, S. A. Mechanisms of prostate tumorigenesis: roles for transcription factors Nkx3.1 and Egr1. *Ann. N. Y. Acad. Sci.* **1059**, 33–40 (2005).
289. Virolle, T. *et al.* Egr1 promotes growth and survival of prostate cancer cells. Identification of novel Egr1 target genes. *J. Biol. Chem.* **278**, 11802–10 (2003).
290. Abdulkadir, S. A. *et al.* Impaired prostate tumorigenesis in Egr1-deficient mice. *Nat. Med.* **7**, 101–7 (2001).
291. Ronski, K. *et al.* Early growth response gene 1 (EGR1) is deleted in estrogen receptor-negative human breast carcinoma. *Cancer* **104**, 925–30 (2005).
292. Song, H. *et al.* Egr1 acts as a critical mediator of estrogenic actions in mouse uterus. *Fertil. Steril.* **96**, S118–S119 (2011).
293. Subik, K. *et al.* The Expression Patterns of ER, PR, HER2, CK5/6, EGFR, Ki-67 and AR by Immunohistochemical Analysis in Breast Cancer Cell Lines. *Breast Cancer Basic Clin. Res.* **4**, 35–41 (2010).
294. Holliday, D. L. & Speirs, V. Choosing the right cell line for breast cancer research. *Breast Cancer Res.* **13**, 215 (2011).
295. Pratt, M. A., Satkunarathnam, A. & Novosad, D. M. Estrogen activates raf-1 kinase and induces expression of Egr-1 in MCF-7 breast cancer cells. *Mol. Cell. Biochem.* **189**, 119–25 (1998).

296. Trost, N. *et al.* Recombinant human erythropoietin alters gene expression and stimulates proliferation of MCF-7 breast cancer cells. *Radiol. Oncol.* **47**, 382–9 (2013).
297. Mitchell, A., Dass, C. R., Sun, L. Q. & Khachigian, L. M. Inhibition of human breast carcinoma proliferation, migration, chemoinvasion and solid tumour growth by DNazymes targeting the zinc finger transcription factor EGR-1. *Nucleic Acids Res.* **32**, 3065–9 (2004).
298. Bartel, D. P. MicroRNAs: genomics, biogenesis, mechanism, and function. *Cell* **116**, 281–97 (2004).
299. Lecellier, C. H. *et al.* A cellular microRNA mediates antiviral defense in human cells. *Science* **308**, 557–560 (2005).
300. Pedersen, I. M. *et al.* Interferon modulation of cellular microRNAs as an antiviral mechanism. *Nature* **449**, 919–22 (2007).
301. Wang, X. *et al.* Inhibition of anti-HIV microRNA expression: A mechanism for opioid-mediated enhancement of HIV infection of monocytes. *Am. J. Pathol.* **178**, 41–7 (2011).
302. Qi, Y. *et al.* High-throughput sequencing of microRNAs in adenovirus type 3 infected human laryngeal epithelial cells. *J. Biomed. Biotechnol.* **2010**, 8 (2010).
303. Guo, H. *et al.* MicroRNAs-372/373 promote the expression of hepatitis B virus through the targeting of nuclear factor I/B. *Hepatology* **54**, 808–19 (2011).
304. Stoye, J. P. & Moroni, C. Phenotypic mixing of retroviruses in mitogen-stimulated lymphocytes: analysis of xenotropic and defective endogenous mouse viruses. *J. Gen. Virol.* **65**, 317–26 (1984).
305. Todaro, G. J., Sherr, C. J., Benveniste, R. E., Lieber, M. M. & Melnick, J. L. Type C viruses of baboons: isolation from normal cell cultures. *Cell* **2**, 55–61 (1974).
306. Young, G. R. *et al.* Resurrection of endogenous retroviruses in antibody-deficient mice. *Nature* **491**, 774–778 (2012).
307. Tubio, J. M. *et al.* Extensive transduction of nonrepetitive DNA mediated by L1 retrotransposition in cancer genomes. *Science* **345**, 1251343 (2014).
308. Muckenfuss, H. *et al.* APOBEC3 proteins inhibit human LINE-1 retrotransposition. *J. Biol. Chem.* **281**, 22161–72 (2006).
309. Nair, S., Sanchez-Martinez, S., Ji, X. & Rein, A. Biochemical and biological studies of mouse APOBEC3. *J. Virol.* **88**, 3850–60 (2014).
310. Vaughan, A. E., Mendoza, R., Aranda, R., Battini, J. L. & Miller, A. D. Mechanism for XMRV neurotoxicity. *Retrovirology* **8**, (Suppl 2):O18 (2011).
311. Vaughan, A. E., Mendoza, R., Aranda, R., Battini, J. L. & Miller, A. D. Xpr1 is an atypical G-protein-coupled receptor that mediates xenotropic and polytropic murine retrovirus neurotoxicity. *J. Virol.* **86**, 1661–9 (2012).
312. Decaussin, G., Leclerc, V. & Ooka, T. The lytic cycle of Epstein-Barr virus in the nonproducer Raji line can be rescued by the expression of a 135-kilodalton protein encoded by the BALF2 open reading frame. *Journal of Virology* **69**, 7309 (1995).
313. Lin, Z. *et al.* Quantitative and qualitative RNA-Seq-based evaluation of Epstein-Barr virus transcription in type I latency Burkitt's lymphoma cells. *J. Virol.* **84**, 13053–13058 (2010).